Molecular and cellular preconditioning - powerful strategies for neuroprotection

Dissertation

zur

Erlangung des Doktorgrades

der Naturwissenschaften

(Dr. rer. nat.)

dem

Fachbereich Pharmazie (16)

der Philipps-Universität Marburg

vorgelegt von

Eva-Maria Öxler

aus Donauwörth

Marburg/Lahn 2012

Vom Fachbereich Pharmazie der Philipps-Universität Marburg als Dissertation am 18.12.2012 angenommen.

Erstgutachter Prof. Dr. Carsten Culmsee

Zweitgutachter Prof. Dr. Moritz Bünemann

Tag der mündlichen Prüfung am 19. Dezember 2012

Meinen Eltern

In memoriam Josef Karl Öxler
(*1943 - †2007)

ERKLÄRUNG

Ich versichere, dass ich meine Dissertation

„Molecular and cellular preconditioning – powerful strategies for neuroprotection“

selbständig ohne unerlaubte Hilfe angefertigt und mich dabei keiner anderen als der von mir ausdrücklich bezeichneten Quellen bedient habe.

Die Dissertation wurde in der jetzigen oder einer ähnlichen Form noch bei keiner anderen Hochschule eingereicht und hat noch keinen sonstigen Prüfungszwecken gedient.

Marburg, den 08.11.2012

.....

(Eva-Maria Öxler)

Table of Content

1. Introduction 1
   1.1. The phenomenon of preconditioning 1
   1.2. Neuronal cell death 5
   1.3. The role of AIF in neuronal cell death and survival 8
   1.4. Stem cell-based therapy for the treatment of neurodegenerative diseases and acute brain injuries 11
   1.5. Neurogenesis – the potential of neural progenitor cells 15
   1.6. The HT-22 cell model 17
   1.7. Aim of the thesis 19
2. Materials and methods 20
   2.1. Cell culture 20
      2.1.1. Cell culture materials 20
      2.1.2. Cultivation of HT-22 cells 21
      2.1.3. Induction of cell death in HT-22 cells 22
      2.1.4. Cultivation of NPCs 23
      2.1.5. Cultivation of SNL feeder cells 24
      2.1.6. Cultivation of primary MEF 25
      2.1.7. SiRNA transfection 25
      2.1.8. Starvation and production of CM 26
   2.2. Chemicals and reagents 26
      2.2.1. Inhibitors of cell death 27
      2.2.2. Inhibitors of protein synthesis and PI3K 28
      2.2.3. Digestion of RNA and proteins 28
      2.2.4. Primary antibodies 29
      2.2.5. Secondary antibodies 29
      2.2.6. SiRNA sequences 29
      2.2.7. PCR-primer 30
   2.3. Kits 31
   2.4. Cell viability assays 32
      2.4.1. MTT assay 32
      2.4.2. xCELLigence system 32
   2.5. Visualization and characterization of mitochondria 33
   2.6. ATP assay 34
   2.7. Detection of lipid peroxides 34
   2.8. Detection of mitochondrial membrane potential 35

2.9. Protein analysis 36
2.9.1. Buffers for Western blot analysis 36
2.9.2. Protein preparation and mitochondria isolation 38
2.9.3. Gel electrophoresis 39
2.10. RNA analysis 40
2.10.1. RNA preparation 40
2.10.2. RT-PCR 41
2.10.3. Agarose gel electrophoresis 44
2.11. Isolation of apoptotic bodies 45
2.12. ELISA assay 45
2.13. MALDI-TOF analysis 46
2.14. Aceton precipitation 46
2.15. Cut off filtration 47
2.16. Digestion of CM 47
2.17. Preparation of cell lysates 47
2.18. Dialysis and lyophilisation 48
2.19. Gel filtration by Äkta analysis 48
2.20. Statistical analysis 49
3. Results 50
3.1. AIF deficiency mediates neuroprotection through a preconditioning effect 50
3.1.1. AIF gene silencing by siRNA attenuates glutamate toxicity 50
3.1.2. AIF siRNA preserves mitochondrial integrity and function from glutamate damage 52
3.1.3. ROS inhibition has no effect on neuroprotection mediated by AIF gene silencing 56
3.1.4. AMPK is not affected in the AIF deficiency model system of HT-22 cells 57
3.1.5. Silencing of AIF mediates a decrease in mitochondrial complex I expression 61
3.1.6. Low dose rotenone treatment preserves cells from glutamate neurotoxicity 62
3.2. Neuroprotection mediated by NPC-derived conditioned medium 66
3.2.1. NPCs undergoing starvation in a caspase-dependent manner protect neuronal cells against damage by growth factor withdrawal and glutamate toxicity 66
3.2.2. Heating increases the protective effect of CM 68
3.2.3. Identification of the chemical nature of compounds responsible for the neuroprotective effect of CM 69
3.2.4. Inhibition of protein synthesis during starvation 71
3.2.5. Neuroprotective effect of NPC lysate 73
3.2.6. Cell type specifity of CM 74

3.2.7. Mitochondria from NPCs do not provide neuroprotective effects 76
3.2.8. Apoptotic bodies from NPC do not mediate neuroprotective effects 77
3.2.9. Cut off filtrations limit the protein size 77
3.2.10. Coomassie staining of NPC CM 78
3.2.11. MALDI-TOF analyses identify proteins in CM 79
3.2.12. RT-PCR analysis of interesting proteins from the MALDI-TOF results....81
3.2.13. Peroxiredoxin-1 and galectin-1 as protective components of CM 83
3.2.14. Inhibition of PI3K 90
3.2.15. Gel filtration separates CM into several protective fractions 92
3.2.16. Methods for CM concentration 93
3.2.17. Stability of CM and cell lysates 95
3.2.18. Pre- versus post-treatment 96
4. Discussion 97
4.1. Importance of preconditioning and conditioning effects in neuronal cell survival as a therapeutic strategy 98
4.2. Molecular preconditioning – neuroprotection mediated by AIF depletion 101
4.2.1. AIF deficiency mediates mitoprotection 101
4.2.2. Preconditioning mediated by complex I inhibition 102
4.2.3. AMPK is not involved in the HT-22 model system 105
4.2.4. AIF and its modulators as therapeutic targets 108
4.3. Molecular conditioning – life from dying NPCs....110
4.3.1. Life from death: cell death mediates neuroprotection 110
4.3.2. Heat activation of CM 113
4.3.3. Neuroprotective components in the mixture of CM 114
4.3.3.1. Peroxiredoxins 114
4.3.3.2. Galectin-1....118
4.3.3.3. Further possible neuroprotective components in NPC CM 122
4.3.4. Clinical implications of CM....125
5. Summary....128
6. Zusammenfassung....130
7. Abbreviations 132
8. Attachment....137
9. References....151
10. Publications 168
10.1. Original papers 168
10.2. Poster presentations....168

10.3. Patent 168
11. Acknowledgements 169
12. Curriculum vitae 170

1. Introduction

1.1. The phenomenon of preconditioning

Preconditioning describes the phenomenon of small doses of noxious stimuli inducing tolerance towards future injury. In 1943, Richard L. Noble was the first who described that short periods of global hypoxia protect the entire mammalian organism and preserves brain energy metabolism during longer periods of hypoxia (Noble, 1943). The term “preconditioning” was introduced in 1964 (Janoff, 1964), and until today researchers investigate this important concept and the underlying complex mechanisms that mediate cell survival and increase life expectancy.

Tolerance induced by preconditioning occurs by ischemia, low doses of endotoxins, and hypoxia (Cadet and Krasnova, 2009). The tolerance can occur within minutes after the stimulus (rapid preconditioning) involving cellular changes which influence enzymes, secondary messengers, and ion channels. Moreover, the tolerance can be developed after several hours (late preconditioning) (Correia et al., 2010). This late phenomenon of preconditioning is characterized by altered gene expression and de novo protein synthesis (Barone et al., 1998;Gidday, 2006;Kirino, 2002).

However, the exact mechanisms leading to the induction and maintenance of tolerance towards later injury remain largely unknown. Most researchers agree that there is not just one mechanism that is exclusively responsible for preconditioning effects. More likely, the phenomenon of preconditioning requires a concerted action of different cellular and molecular mechanisms (Dirnagl and Meisel, 2008) which are in the focus of this thesis in model systems of neural cell death.

At the molecular level, many mechanisms for preconditioning are described and a lot of them apparently converge at mitochondria. The most prominent mechanisms involve slight increase in reactive oxygen species (ROS) production, opening of mitoK_{ATP} channels, upregulation of uncoupling proteins, and stabilization of the transcription factor hypoxia-inducible factor 1 (HIF-1).

The mitochondria are major sources of ROS, and especially the respiratory chain complexes I and III are considered as the primary sites of ROS production and release (Zhang and Gutterman, 2007). Multiple studies demonstrated that slight increases in ROS levels mediated brain tolerance in paradigms of preconditioning

(Dirnagl et al., 2009;Dirnagl and Meisel, 2008;Ravati et al., 2000;Ravati et al., 2001). Such ROS-mediated preconditioning can be abolished through radical scavengers (Ravati et al., 2000). It was further shown that moderate increases in ROS levels were followed by the activation of the transcription factor nuclear factor-kappa B (NF-κB) and a subsequent increase in NF-κB-regulated gene expression, such as manganese superoxide dismutase (MnSOD) (Ravati et al., 2001). Furthermore, an increase in ROS induced by H_2O_2 mediated neuroprotection, thereby blocking the loss of mitochondrial membrane potential (MMP, $\Delta\Psi_m$) and leading to an increase in expression levels of the pro-survival protein Bcl-2 (Tang et al., 2005).

In addition, a connection between ROS levels and mitoK_{ATP} channels was demonstrated since antagonists of mitoK_{ATP} channels were able to block preconditioning effects whereas mitoK_{ATP} channel openers, such as diazoxide, mediated neuroprotective effects (Simerabet et al., 2008). MitoK_{ATP} channel expression in brain mitochondria is up to seven times higher compared to liver or heart mitochondria (Bajgar et al., 2001). This reflects the particular importance of mitochondria for the regulation of neuronal function and survival. Preconditioning by mitoK_{ATP} channel openers is linked to mitochondrial depolarization and PKC activation which prevents free radical production during neuronal stress (Kis et al., 2004).

Recently, it was shown that inhibition of mitochondrial complex I by NS1619 induces neuronal protection by preconditioning in rat cortical neurons, thereby increasing ROS production and mitochondrial depolarization (Gaspar et al., 2008;Gaspar et al., 2009). Moreover, NS1619 decreased the Ca^{2+} influx through glutamate receptors and increased the activity of superoxide dismutase (SOD) (Gaspar et al., 2009). Thus, mitochondrial ROS apparently play a critical role in mediating preconditioning to the brain.

An important protein that is regulated by ROS is the uncoupling protein 2 (UCP 2) (Echtay and Brand, 2007). UCP 2 is located in the inner mitochondrial membrane and highly expressed in brain neurons (Brand and Esteves, 2005;Duval et al., 2002) where it can uncouple the electron transport from ATP synthesis, thereby regulating the energy balance (Kim-Han and Dugan, 2005) of the cell. In vitro and in vivo experiments demonstrate that an upregulation of UCP 2 mediates neuroprotective effects via preconditioning in response to various cellular stresses (Diano et al.,

2003) which is triggered by enzymes, such as adenosine 5'-monophosphate-activated protein kinase (AMPK) (Xie et al., 2008). Further, it was shown that UCP 2 overexpression in mice prevented neuronal death after stroke and brain traumata by mild uncoupling (Mattiasson et al., 2003).

Another key player in developing brain tolerance is HIF-1. Mitochondria and mitochondrial ROS are critical regulators of HIF-1α, a subunit of HIF-1 involved in angiogenesis, cell metabolism, apoptosis, and cell survival. Under hypoxic conditions HIF-1α is stabilized by the inhibition of prolyl-hydroxylase enzymes that initiate the cascade of HIF-1α degradation under normal conditions. Mitochondrial ROS inhibit the activity of these enzymes, thereby promoting the stabilization of HIF-1α. This crosstalk between mitochondrial ROS and HIF-1α has been suggested to be responsible for neuroprotection mediated by preconditioning (Correia and Moreira, 2010). In fact, it is demonstrated that hypoxic preconditioning is associated with an increase in ROS and a subsequent induction of HIF-1 and its downstream gene erythropoietin (Liu et al., 2005).

All these findings suggest a central role of mitochondria in the regulation of neural survival mediated by preconditioning effects in the brain. The first part of this thesis investigates mechanisms of mitochondrial preconditioning caused by the regulation of mitochondrial complex proteins in a murine neural cell line of hippocampal origin.

Another important aspect in preconditioning is modulation at the cellular level by an interaction between neighboring cells. Such cell-cell communication occurs e.g. through the formation of gap junctions by apposition of two hemichannels, also named connexins, which link two cells across an extracellular space of about 2-4 nm. Through these gap junctions a rapid and direct communication between the cytoplasm of neighboring cells is possible, and molecules up to 1 kDa can diffuse between the cells (Bloomfield and Volgyi, 2009). It has been shown that controlled hypoxic preconditioning increases connexin 43 (cx43) expression in neural stem cells (NSCs) which is essential for many of the functional and beneficial interactions after NSC engraftment between grafted cells and host cells (Jäderstad et al., 2010). An increase in cx43 hemichannels results in ATP release that is hydrolized to adenosine, a potent neuroprotective molecule (Lin et al., 2008).

In addition, it has been demonstrated that glial cells drive a preconditioning-induced protection of the blood brain barrier (BBB) (Gesuete et al., 2011). The main components of the BBB are endothelial cells of the cerebral microvasculature, which are closely associated with astrocyte endfeet, pericytes, and microglia. This association plays an important role for the maintenance of the central nervous system (CNS) microenvironment (Deli et al., 2005). Ischemic preconditioning has been shown to attenuate disruption of the BBB and brain edema in models of ischemic brain injury (Hua et al., 2008;Masada et al., 2001). Gesuete et al. demonstrated that astrocytes are major mediators of the observed protective phenotype assumed by BBB protection after preconditioning (Gesuete et al., 2011).

A further proof for preconditioning effects mediated at the cellular level was reported after heat shock preconditioning. Thermal stress induces glial cells to produce heat shock protein (HSP) 70, which is then transported to the adjacent axonal process (Masada et al., 2001). Such a cell-cell transfer provides a mechanism for fast delivery of neuroprotective substances during stress situations (Brown, 2007). The fact, that glial cells release HSP 70 and neurons can take up HSP 70 resulting in greater tolerance to cell death induced by chemical substances or trophic factor withdrawal was further confirmed in tissue culture experiments (Guzhova et al., 2001).

Such intercellular interactions mediated by preconditioning can be mimicked by the generation of so called conditioned media (CM). Medium from cells cultivated under slightly stressful conditions can be used in other model systems of lethal neuronal stress to mediate neuroprotective effects. For example, CM generated from human adipose stem cells under mild hypoxic conditions shows beneficial therapeutic effects in an in vivo rat model of stroke (Cho et al., 2012). Thus, CM offers new therapeutic potential to use fundamental self-protecting processes of organisms for the treatment of neurological disorders.

The second part of this thesis investigates the neuroprotective effects of CM generated from neural progenitor cells (NPCs) that undergo cell death induced by growth factor withdrawal in a model system of hippocampal HT-22 neurons that are exposed to lethal glutamate concentrations combined with growth factor deprived media.

1.2. Neuronal cell death

Acute brain injury and neurodegenerative diseases, such as Parkinson's disease (PD), Alzheimer's disease (AD), Huntington's disease (HD), and amyotrophic lateral sclerosis (ALS) are characterized by progressive dysfunction and death of neurons leading to the severe neurological impairments characterizing these diseases (Kim and de Vellis, 2009). Although recent advances have improved the management of these diseases there is no curative therapy available. The current treatments are mostly symptomatic and often successful for a limited time only since most of these diseases are progressive in their development. Further, long-term medication is often accelerated to high doses leading to severe side effects (Kim and de Vellis, 2009;Lang and Lozano, 1998a;Lang and Lozano, 1998b;Marshall, 1994). Thus, it is very important to understand the mechanisms causing neuronal cell death that underlie progressive loss of brain function in neurodegenerative diseases or after acute brain injuries.

The two major forms to classify neuronal cell death in pathological contexts are necrosis and apoptosis. In the last few years several additional classifications of neuronal cell death have been introduced based on biochemical and functional considerations, such as regulated necrosis and authophagy (Galluzzi et al., 2012). All these forms of neuronal cell death are described in neurodegenerative diseases and acute brain injuries.

The typical characteristics of necrosis are mitochondrial swelling, depletion of ATP, massive calcium influx, and deregulation of the intracellular ion homeostasis. In later stages, hallmarks of necrosis are cell swelling, membrane lysis, and inflammatory processes (Majno and Joris, 1995). Necrotic cell death is described for several neurodegenerative diseases and for vascular-occlusive diseases, but it has also been suggested to contribute to embryonic development (Yuan et al., 2003;Zong and Thompson, 2006). In contrast to classic necrosis, which is described to occur accidental, recently identified forms of regulated necrosis appear in a programmed manner dependent on RIP1 and/or RIP3 activation (Galluzzi et al., 2012).

The characteristics of apoptotic cell death are DNA fragmentation, nuclear condensation, membrane blebbing, and the formation of apoptotic bodies (Kerr et al., 1972). These apoptotic bodies are phagocytosed by neighboring cells and contain intracellular components. In contrast to necrosis, apoptotic cells are removed without

causing inflammatory response and damage to the surrounding tissue. Therefore, apoptosis plays an important physiological role in the replacement of senescent or excessive cells (Vaux and Korsmeyer, 1999). Furthermore, apoptosis exerts essential functions during the development of the nervous system by controlling synapses and removing excessive and unneeded neural cells (Oppenheim, 1991).

Pathological pathways of apoptosis have been associated with a lot of neurodegenerative diseases, such as AD and PD, and also with acute brain damage, such as after cerebral ischemia or traumatic brain injury (TBI) (Mattson, 2000). Apoptotic cell death may result from two biochemical cascades, described as the intrinsic (also called mitochondrial) pathway and the extrinsic pathway (Figure 1).

The extrinsic pathway of apoptotic cell death is initiated outside a cell, when conditions in the extracellular environment determine cell death. This pathway relies on death receptors, such as the Fas receptor that transmit extracellular signals of danger. The activation of these death receptors leads to the activation of several caspases, including caspase-8 and 3 (Galluzzi et al., 2009). Caspases are proteolytic enzymes that cleave important cellular proteins, e.g. actin or laminin, and activate nucleases like caspase-activated desoxyribonuclease (CAD), which upon proteolytic activation translocates into the nucleus where it cleaves the DNA in the final steps of apoptotic cell death.

The intrinsic apoptosis pathway is initiated within the cell. It is characterized by high levels of ROS as well as the activation of the pro-apoptotic protein Bid which leads to mitochondrial permeabilization followed by the subsequent release of other pro-apoptotic proteins like apoptosis inducing factor (AIF), cytochrome c, Omi/HtrA2 or Smac/DIABLO (Galluzzi et al., 2009). When AIF is released from the mitochondria it translocates to the nucleus where it induces chromatin condensation and large-scale DNA fragmentation resulting in caspase-independent cell death (Susin et al., 1996;Susin et al., 1999).

In addition, cytosolic cytochrome c forms a complex with apoptosis protease-activating factor-1 (Apaf-1) and pro-caspase-9, named apoptosome. The apoptosome catalyzes the activation of execution caspases including caspase-3, 6, and 7 (Mehta et al., 2007). These caspases induce the breakdown of the cellular framework through degradation of substrates like actin or by activation of CAD.

Furthermore, caspase activation is triggered by release of Smac/DIABLO or Omi/HtrA2 from mitochondria. When released into the cytosol, Smac/DIABLO and Omi/HtrA2 can block the anti-apoptotic protein XIAP (x-chromosomal linked inhibitor of apoptosis) and other inhibitors of apoptosis thereby activating caspases in an indirect manner (Mehta et al., 2007).

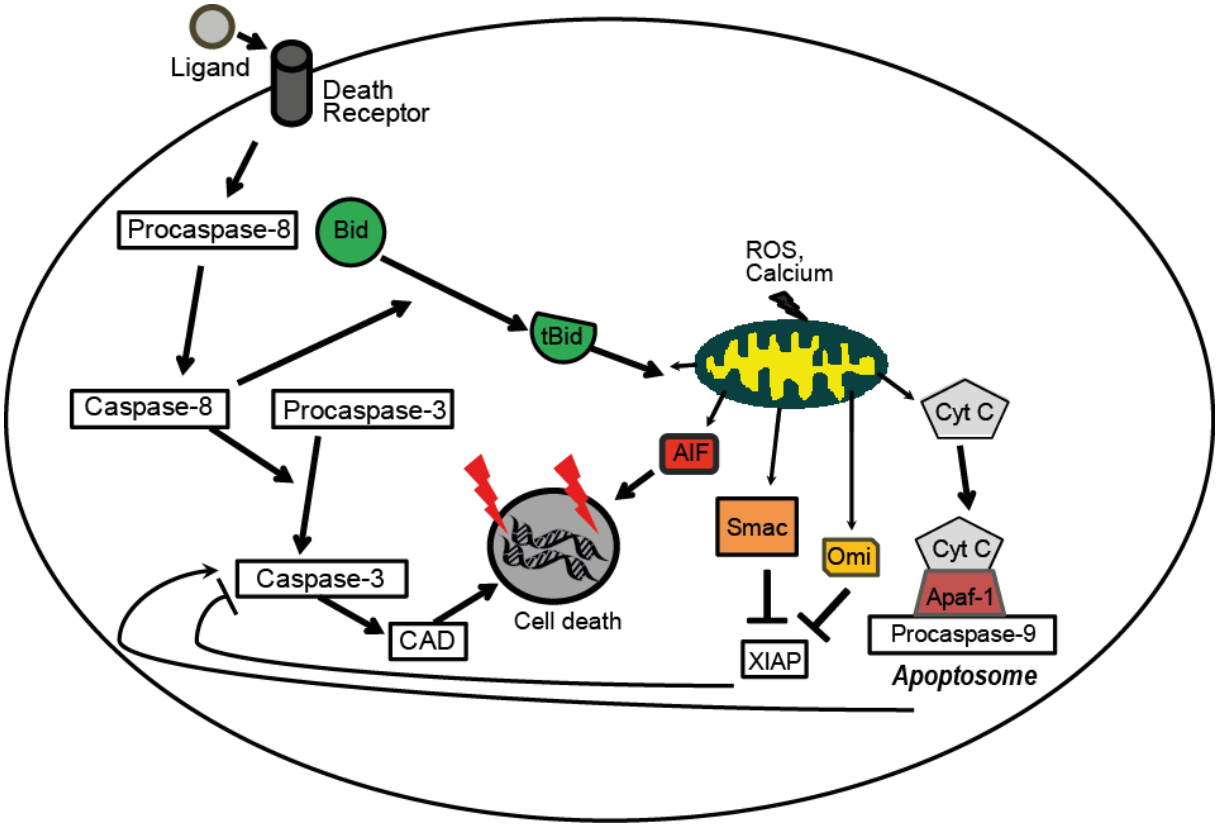

Figure 1: Intrinsic and extrinsic pathways of apoptotic cell death in mammalian cells.

The extrinsic pathway is triggered by members of the death receptor family (e.g. Fas, CD95, necrosis factor receptor I). Ligand binding to these receptors leads to activation of caspases and nucleases that cleave DNA in the nucleus. Activation of caspase-8 also leads to the cleavage of the pro-apoptotic protein Bid into its truncated form (tBid), which links the extrinsic and the intrinsic pathway. The intrinsic pathway triggered by intracellular stress is characterized by the activation of Bid which leads to mitochondrial membrane permeabilization resulting in the release of other pro-apoptotic proteins, such as AIF, Smac, Omi and cytochrome C (cyt c). AIF translocates into the nucleus where it induces chromatin condensation. Smac and Omi inhibit XIAP resulting in a direct activation of caspase-3. Further, the apoptosome consisting of cyt c, Apaf-1, and caspase-9 activates caspase-3 thereby significantly amplifying initial caspase activation upstream of mitochondrial damage.

1.3. The role of AIF in neuronal cell death and survival

AIF is a nuclear encoded ~62 kDa flavoprotein that is located in the inner mitochondrial membrane. It is synthesized as a ~67 kDa precursor protein (pro-AIF) that is imported into mitochondria via its N-terminal prodomain which contains two mitochondrial location sequences (MLS). In the mitochondria the imported pro-AIF is processed into the mature ~62 kDa protein (Otera et al., 2005;Susin et al., 1999). During intrinsic cell death AIF is cleaved into a soluble ~57 kDa form that is released to the cytosol and translocates to the nucleus where it induces chromatin condensation and large-scale DNA fragmentation (~50 kbp) (Susin et al., 1996;Susin et al., 1999). In fact, AIF was the first mitochondrial protein shown to mediate caspase-independent cell death (Susin et al., 1996;Susin et al., 1999). AIF has been shown to bind DNA in a sequence-independent manner (Ye et al., 2002). This interaction is mediated by the positive electrostatic potential at the surface of AIF and leads to chromatin condensation, a fundamental feature of apoptosis (Vahsen et al., 2004). However, AIF does not degrade naked DNA (Susin et al., 1999), and the mechanisms by which AIF leads to DNA fragmentation are not yet clarified. Since AIF lacks nuclease activity it has been proposed that AIF mediates DNA fragmentation through interaction with other nuclear protein factors. In mammalian cells cyclophilin A was identified as a cofactor that directly interacts with AIF (Cande et al., 2004). Cyclophilin A has been reported to have calcium-dependent nuclease activity (Montague et al., 1994), and it has been suggested that AIF and cyclophilin A work synergistically to induce chromatinolysis since the combination of both proteins causes degradation of plasmid DNA in vitro (Cande et al., 2004).

It is now well established that AIF-dependent cell death plays a key role in neuronal death in model systems of cerebral ischemia (Culmsee et al., 2005;Plesnila et al., 2004;Zhu et al., 2003), TBI (Slemmer et al., 2008), and epileptic seizures (Cheung et al., 2005).

Different modulators of mitochondrial AIF release were identified, such as calpain I which can induce cleavage and release of AIF from isolated mitochondria (Polster et al., 2005). The cleavage of AIF is inhibited by Bcl-2 and Bcl-xL overexpression (Otera et al., 2005) suggesting that AIF-cleavage occurs downstream of mitochondrial membrane permeabilization since both proteins exert pro-survival functions by inhibiting mitochondrial membrane pore formation (Galluzzi et al., 2009).

Further, it was demonstrated that the pro-apoptotic protein Bid mediated mitochondrial release of AIF in neural cells (Grohm et al., 2010;Landshamer et al., 2008;Tobaben et al., 2011). In addition, poly(ADP-ribose)polymerase 1 (PARP-1) activity was associated with lethal AIF release and genetic deletion, and pharmacological inhibition of PARP-1 prevented AIF translocation and provided neuroprotection in vitro and in vivo (Wang et al., 2009;Wang et al., 2011;Yu et al., 2002). Activation of PARP-1, a DNA repair enzyme, is triggered by DNA strand breaks as it occurs e.g. after excessive production of free radicals (Wang et al., 2009). Overactivation of PARP-1 leads to utilization of mitochondrial nicotinamide adenine dinucleotide (NAD^+), ATP depletion, and an increase in levels of poly(ADP-ribose) (PAR). Of note, AIF has recently been shown to possess a high-affinity PAR-binding site, and the physical interaction between PAR and AIF seem to be responsible for the resulting cell death after PARP-1 activation. It has been demonstrated that about 20 % of mitochondrial AIF is localized at the cytosolic side of the outer mitochondrial membrane where it is available for binding of PAR (Yu et al., 2009). PAR binding to AIF likely induces a conformation change in AIF that lowers its affinity to the mitochondrial membrane leading to its release (Wang et al., 2011). This kind of caspase-independent form of programmed cell death (PCD) involving PARP-1 activation plays an important role in multiple experimental and physiopathological scenarios, including stroke, inflammation, and neurodegeneration and has been termed parthanatos (David et al., 2009;Galluzzi et al., 2012).

The cumulative evidence for a key role of AIF translocation to the nucleus in paradigms of neuronal cell death led to the conclusion that controlling AIF upstream of mitochondrial release may emerge as a promising therapeutic strategy in neurological diseases, such as cerebral ischemia and neurodegenerative disorders (Delavallee et al., 2011). However, direct inhibition of AIF by small molecules is not available so far and previous neuroprotective effects were achieved using siRNA-mediated gene silencing or in genetic models of reduced AIF expression, such as *harlequin* (*Hq*) mice, which express only 20 % AIF compared to wildtype mice. For example, AIF siRNA attenuated apoptosis in neuronal cells exposed to oxygen-glucose deprivation (OGD) or glutamate (Landshamer et al., 2008). Further, Cheung et al. demonstrated sustained neuronal survival after DNA damage- and excitotoxin-induced cell death in Hq/Apaf1$^{-/-}$ double mutant mice (Cheung et al., 2006). Moreover, AIF deficiency protected brain tissue of Hq mice against hypoxia/ischemia

(Zhu et al., 2003;Zhu et al., 2007), focal cerebral ischemia (Culmsee et al., 2005;Plesnila et al., 2004), or ionizing radiation in vivo (Osato et al., 2010).

To date, the exact mechanism by which AIF depletion sustains neuronal survival is unknown. Reduced translocation of the protein to the nucleus as the underlying mechanism of neuroprotection is controversial since neurons of Hq mice or neurons exposed to AIF siRNA still express considerable amounts of AIF, which should be sufficient for nuclear translocation and induction of apoptosis after its release from the mitochondria. In fact, few amounts of cytosolic AIF are sufficient for translocation to the nucleus and subsequent induction of chromatin condensation and DNA fragmentation. Further, the fast kinetics of AIF release to the nucleus (Landshamer et al., 2008) disagrees with a direct protective effect only mediated by reduced AIF levels. Thus, other effects may be responsible for the neuroprotective effect of AIF depletion, such as metabolic effects at the level of mitochondria.

Since AIF is a flavoprotein containing binding sites for FAD and NADH with putative NADH and NADPH oxidase activities (Joza et al., 2001), loss of AIF may affect the redox balance in mitochondria. Previous studies have shown that AIF-depleted cells like $AIF^{-/-}$ embryonic stem cells (ESCs) and Hq cells with significantly reduced AIF levels exert defects in oxidative phosphorylation and mitochondrial respiratory complex stability (Chinta et al., 2009;Vahsen et al., 2004). As a consequence, AIF depletion may mediate a metabolic impact that could play an important role for the integrity, structure, and function of the mitochondria, including the activity and stability of the respiratory chain (Cheung et al., 2006;Joza et al., 2005). Notably, inhibition of the mitochondrial respiratory chain can provide preconditioning effects thereby protecting cells from a following lethal stress (Wiegand et al., 1999). This study addresses the question whether neuroprotection mediated by AIF silencing is caused through a preconditioning effect thereby stabilizing mitochondrial function and integrity.

1.4. Stem cell-based therapy for the treatment of neurodegenerative diseases and acute brain injuries

Transplantation of stem/progenitor cells to the injured brain is a new potentially powerful strategy for a broad spectrum of neurodegenerative diseases and acute brain injuries (Lindvall et al., 2004;Lindvall and Kokaia, 2006). Stem cells/progenitor cells are known to have self-renewing capacity and are able to differentiate into new neurons (Götz and Huttner, 2005). The fact that these cells are relatively easy to isolate and to expand is an important property for their potential clinical application. Furthermore, stem cells may serve as vehicles for the delivery of therapeutic factors since they have a high tropism for inflamed and injured tissue (Mitrecic et al., 2012). So far, numerous studies showed that transplantation of different kinds of stem/progenitor cells provided beneficial effects in several models of neurodegeneration and acute brain injury. Accordingly, stem cell-based approaches may provide novel therapies especially for the treatment of PD, HD, AD, ALS, spinal cord injury (SCI), and stroke (Lindvall et al., 2004;Lindvall and Kokaia, 2006).

For example, the stem cell-based therapy of stroke is mainly investigated with NSCs, mesenchymal stem cells (MSCs), umbilical cord blood and bone mesenchymal stem cells (BMSCs) (Lindvall and Kokaia, 2011). These cells can be administered by various routes including intravascular injections, or intracerebral and intrathecal applications. Human ESC-derived NSCs that were grafted into the ischemic boundary in rats subjected to stroke, migrated towards the lesion and improved forelimb performance (Daadi et al., 2008). Human MSCs, that were intravenously administered, reduced stroke-induced deficits in rats most likely by inducing angiogenesis and improving cerebral blood flow (Onda et al., 2008). BMSCs, which comprise mesenchymal stem and progenitor cells, can secrete various neurotrophic factors and other protective cytokines (Parr et al., 2007). The delivery of BMSCs from human or animal origin by systemic or intracerebral routes, promoted significant functional recovery after stroke (Li and Chopp, 2009). Umbilical cord blood, containing hematopoietic stem cells and other progenitor cells, showed improved behavioral outcome in animal models after systemic delivery, even when administered 30 days after the insult (Park et al., 2009;Vendrame et al., 2004;Vendrame et al., 2006;Zhang et al., 2011). Notably, functional improvement persisted in rodents for at least one year post-treatment (Shen et al., 2007). Further,

functional benefits after stem cell-based therapy were reported in models of cerebral ischemia applied in male and female, and in young and old animals.

There are also the first clinical trials ongoing in which stem cells are transplanted to stroke patients. For example, a clinical trial performed with intravenous injection of autologous ex vivo cultured MSCs in 30 patients with an ischemic lesion in the territory supplied by the middle cerebral artery was reported in 2005 (Bang et al., 2005). A similar study was described in 2010 with 85 patients as a long-term study followed up to 5 years after i.v. application to evaluate the long-term safety and efficacy (Lee et al., 2010). Both studies provide evidence that application of MSCs is safe and leads to functional recovery.

The first clinical trial with transplanted NSCs in stroke patients was recently started by the UK-based company ReNeuron and includes 12 patients between 6 and 24 months after stroke. Increasing numbers of conditionally immortalized NSCs (CTX cells), isolated from human fetal cortex are implanted into the putamen and tested for safety. Additionally, the trial will evaluate a range of potential efficacy measures, such as cognitive impairment, functional outcome, and overall disability, for future trials. (Mack, 2011). Several other clinical studies using intravenous or intraarterial infusion of stem cells in patients with stroke are currently ongoing or prepared, as well as studies for stem cell transplantation in patients with PD, AD, ALS, or SCI to investigate the efficacy and safety of this new therapeutic approach (www.clinicaltrial.gov).

The exact mechanism of therapeutic effects observed after stem cell/progenitor cell transplantation into the brain, however, still remains unclear. Several mechanisms have been proposed for the beneficial effects of this type of cell therapy in experimental settings of neurodegeneration. A frequently proposed hypothesis is the replacement of injured tissue by the transplanted stem cells/progenitor cells through differentiation of the engrafted cells into new neurons. However, only very few cells survive after transplantation which renders this theory of cell replacement rather unlikely (Menasche, 2005;Silva et al., 2005). For example, it was shown that only 0.02 % of 2 million MSCs injected into the carotid artery were stained for neural markers in the ischemic hemisphere (Chen et al., 2002). In addition, functional improvement after stem cell transplantation occurs rapidly and is often obvious in one week, which is an insufficient time for the transplanted cells to become neurons and integrate successfully into the brain circuity (Chen et al., 2001).

Thus, it is more conceivable that the stem/progenitor cell application provides neuroprotective effects and/or induces repair mechanisms in the injured brain tissue (Carletti et al., 2011). This could be mediated by the release of trophic factors by the transplanted cells or by stimulation of endogenous growth factor synthesis in the host tissue. Further, enhanced angiogenesis, inhibition of apoptosis, and stimulation of recruitment, proliferation, and differentiation of endogenous stem cells residing in the brain tissue are potential effects of protection discussed in the literature (Isele et al., 2007;Joyce et al., 2010;Zhu et al., 2011). It is also known, that NSCs exert antioxidant properties thereby rescuing the surrounding neurons. In particular, the secretion of growth factors, such as vascular endothelial growth fator (VEGF), correlated with antioxidant mechanisms in NSCs themselves and the surrounding host cells (Madhavan et al., 2008).

In addition, an interaction of stem/progenitor cells with immunologic cells located in organ systems distant from the CNS has been observed, thereby altering the systemic responses of the immune system (Walker et al., 2011).

However, before stem cell therapy is established to be a safe and robust strategy for the treatment of neurodegenerative disorders it is indispensable to clarify some fundamental questions regarding the underlying mechanisms and also the clinical application. To date, it remains unknown which type of stem cells is the most suitable for therapeutic approaches in neurodegenerative diseases or after acute brain injury. The spectrum of potentially available stem/progenitor cells is enormous reaching from ESC over NSCs and BMSCs to MSCs, and also induced pluripotent stem cells (iPSCs) reprogrammed from fibroblasts (Takahashi and Yamanaka, 2006) or hair follicle cells (Petit et al., 2012) may offer new strategies for stem cell-based therapy in neurological disorders. Moreover, the optimal number of cells that has to be applied to the patients has to be determined. The timing of treatment and the optimum route of delivery is another question remaining for stem cell-based therapy.

A further unresolved question is the optimal age of a patient for stem/progenitor cell transplantation and the localization and extent of e.g. the ischemic lesion or the progression of the disease. Furthermore, it is unknown which influence complicating factors may exert on regenerative mechanisms that are often found in patients with neurodegenerative disorders, such as, for example, diabetes, hypertension, or

arthereosclerosis. In addition, it is necessary to obtain more knowledge about the safety of stem cell transplantation, especially on the potential for tumorigenicity and immunologic rejections.

Beyond that, control standards and quality assurance must be in place to assure a standardized cell preparation (Banerjee et al., 2011). Thus, long-term and large-scale multicenter clinical studies are required to establish and optimize stem cell-based therapy for neurodegenerative diseases. Such studies require huge efforts since they need to pass through strict authorization and admission procedures e.g. through the European Medicines Agency (EMA) or the Food and Drug Administration (FDA) before the clinical trial can be started.

Overall, these obstacles imply that it is highly important to achieve a better understanding for the mechanisms of stem cell-mediated therapeutic effects. Furthermore, the development of a standardized stem cell-derived composition providing neuroprotective effects to acute and chronic neural injuries is highly relevant.

This study investigates CM generated by NPCs undergoing starvation, which offers a method for the generation of a standardized composition for the treatment with stem/progenitor cells. CM generated by dying cells reflects the properties of the surroundings of the stem cell/progenitor cell transplants since only very few cells survive the transplantation into the brain (Chen et al., 2002). The aim of this study is to investigate the neuroprotective potential of this NPC-derived CM, and more importantly, to identify the mediators of neuroprotection.

1.5. Neurogenesis – the potential of neural progenitor cells

Adult neurogenesis has been shown to occur continuously in discrete regions of the CNS of all mammals, including humans (Gage, 2000;Temple, 2001a;Temple, 2001b). Adult neurogenesis occurs primarily in two regions of the adult brain, the subventricular zone (SVZ) of the lateral ventricles and the subgranular zone (SGZ) of the dentate gyrus in the hippocampus (Bedard and Parent, 2004;Curtis et al., 2007;Eriksson et al., 1998). Neurons born in the adult SVZ migrate over a great distance through the rostral migratory stream and become granule neurons and periglomerular neurons in the olfactory bulb. Neurons born in the adult SGZ migrate into the granule cell layer of the dentate gyrus and become dentate granule cells (Zhao et al., 2008). These neurons are generated from adult NSCs which are cells that can self-renew and differentiate into all types of neural cells, including neurons, astrocytes, and oligodendrocytes. The NSCs differentiate into NPCs, which can only divide a limited number of times. These NPCs develop into mature, non-mitotic neurons (Zhao et al., 2008).

To date, the precise function of adult neurogenesis is still poorly understood. In animals SVZ neurogenesis is regulated by the olfactory experience (Lledo et al., 2006;Lledo and Saghatelyan, 2005). Thus, neurogenesis may be required for special brain functions located in the olfactory bulb and the hippocampus, such as learning and memory.

The generation of new neurons is influenced by many intrinsic and extrinsic signals. For example growth factors, such as epidermal growth factor (EGF) and fibroblast growth factor 2 (FGF 2), are potent mediators for the maintenance of adult NSCs in vitro. In vivo, both factors promote proliferation of NPCs and stem cells in the SVZ, but only FGF 2 increases the number of newborn neurons in the olfactory bulb (Kuhn et al., 1997).

Furthermore, signaling through the sonic hedgehog pathway, the neurotrophin brain-derived neurotrophic factor (BDNF), cytokines and hormones, such as thyroid hormone, respectively, are major regulators of different phases of adult neurogenesis. Additionally, a variety of intrinsic factors, such as miRNAs, cell-cycle regulators, and transcription factors, play critical roles in postnatal neurogenesis (Ming and Song, 2011;Mu et al., 2010).

Interestingly, adult neurogenesis is also affected by pathological conditions of the CNS. For example, seizure activity increases neurogenesis in both regions, the SVZ and the SGZ. However, the role of seizure-associated aberrant neurogenesis in epilepsy has not yet been resolved (Zhao et al., 2008).

Furthermore, neurogenesis in both hippocampus and SVZ was enhanced in models of focal and global ischemia in rodents. After ischemic stroke, newborn cells from the SVZ migrated to the site of injury, which was guided by blood vessels (Zhao et al., 2008).

These findings underline the expectance that neural stem and progenitor cells have the potential to compensate for neuronal dysfunction and death and to recover neural functions in CNS disorders.

For the studies in this thesis, NPCs provided by Prof. Gage were used. This cell line was isolated from 8-10 weeks old C57BL/6 mice using the whole brain without cerebellum and olfactory bulb (Ray and Gage, 2006). Progenitor cells from this cell line grow in a special serum-free medium (described in chapter 2.1.4) as a monolayer, which offers technical advantages compared to neurospheres that are commonly used for research on progenitor cells. Since neurospheres are tightly packed, not all cells are accessible for examining their morphology, proliferation, or differentiation. Progenitor cells cultured as a monolayer enables the evaluation of the cell number, shape, morphology, and other characteristics more accurately. The cells are visible in phase contrast microscopy and show elongated cell bodies with multiple processes (Figure 2). After passaging, just a small number of spheres fail to attach on the uncoated plastic plate. The mouse progenitor cells can be cultivated for several months through multiple passages and even be frozen and re-cultured without any change in their properties (Ray and Gage, 2006).

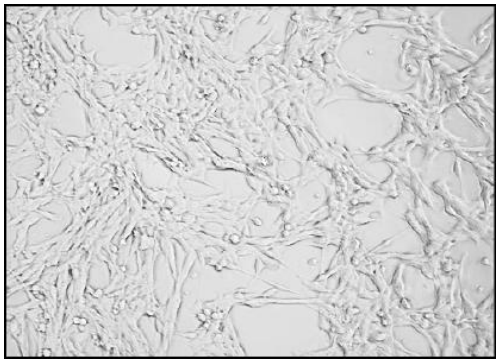

Figure 2: Morphology of neural progenitor cells (NPCs).

NPCs are growing in a monolayer. The cells are phase dark and have elongated cell bodies with multiple processes. 100 x magnitude.

1.6. The HT-22 cell model

To investigate preconditioning effects in vitro HT-22 neurons from an immortalized, hippocampal cell line were used. HT-22 neurons have been generated from HT-4 cells, a cell line originating from primary mouse hippocampal neurons. Immortalization has been achieved using a temperature-sensitive SV-40 T-antigen (Morimoto and Koshland, Jr., 1990). In this cell line, death was induced by exposure to glutamate at millimolar concentrations. The glutamate concentration is quite high compared to concentrations that are used in primary neurons to induce excitotoxicity since the HT-22 cells do not express ionotropic glutamate receptors. Thus, cell death is independent of NMDA-receptor stimulation and mediated through competitive inhibition of the glutamate-cystine antiporter (xCT). This antiporter is a plasma membrane transport protein, which mediates the import of cystine from the extracellular space and the concomitant export of glutamate (Murphy et al., 1989). Blockade of the xCT, e.g. by high extracellular glutamate, results in depletion of cystine and cystein levels, followed by decreased levels of glutathione (GSH). Given the crucial role of GSH as a redox scavenger, reduced GSH plasma levels give rise to excessive ROS formation, mitochondrial damage, release of mitochondrial AIF, DNA damage, and cell death (Sagara et al., 1998;Tan et al., 1998;Tobaben et al., 2011). This kind of cell death has been termed oxytosis (Tan et al., 2001).

In addition, it was observed that cytosolic calcium levels are increased after glutamate treatment in HT-22 cells, despite the absence of NMDA receptors (Tan et al., 1998). Since enhanced ROS formation and increased calcium levels are established features of neuronal death in neurodegenerative disorders, this model system of glutamate-induced oxidative stress in HT-22 cells is a valuable and applicable model to investigate molecular mechanisms of PCD in neurons.

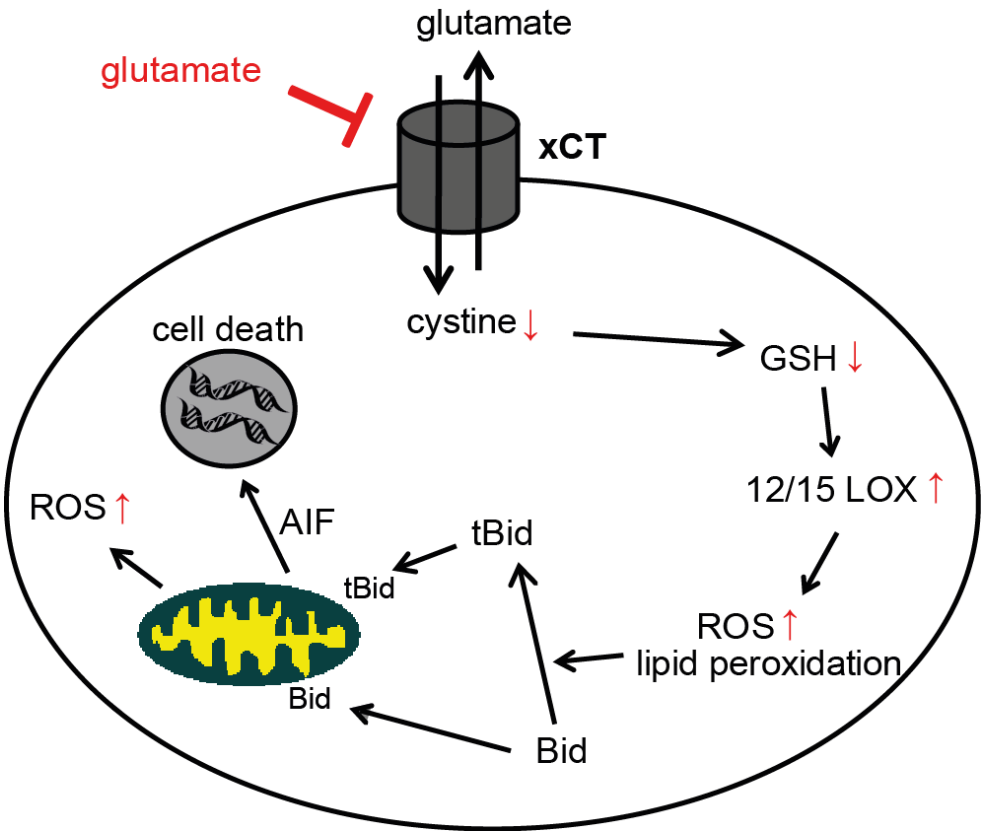

Figure 3: Simplified model of glutamate-induced apoptosis in HT-22 cells.

Exposure to high extracellular glutamate concentrations causes a competitive blockade of the xCT, which results in a depletion of cystine in the cell. This is followed by a decrease in glutathione (GSH) synthesis and causes reduced glutathion peroxidase 4 (Gpx 4) activity. In response to these events 12/15 lipoxygenase (12/15 LOX) is activated and ROS formation and lipid peroxidation increase. Downstream activation and mitochondrial translocation of the BH-3 protein Bid and its truncated form tBid cause mitochondrial dysfunction. Consequently, the pro-apoptotic factor AIF translocates from mitochondria to the nucleus and cleaves DNA, thereby terminating cell death. Red arrows indicate the increases and decreases in cellular molecule levels caused by high glutamate concentrations (modified from Tobaben et al., 2011).

1.7. Aim of the thesis

The aim of this thesis was to investigate mechanisms of molecular and cellular preconditioning that provide neuroprotective effects as exemplified by siRNA-induced AIF depletion and CM obtained from NPCs in a model of glutamate toxicity in HT-22 cells.

AIF has been recognized as an important protein for mediating caspase-independent cell death and also physiological functions in neurons. However, the question how AIF deficiency provides neuroprotection has not been clarified so far.

Thus, the first part of the thesis investigates whether AIF depletion mediates preconditioning in a model system of glutamate toxicity in immortalized hippocampal HT-22 neurons where glutamate induces lethal oxidative stress, mitochondrial fragmentation, and intrinsic pathways of AIF-dependent cell death. The focus of the study was to investigate the protective effects on mitochondrial function and integrity. Furthermore, this neuroprotective effect was investigated for links to ROS generation, AMPK regulation, and complex I inhibition to examine whether the observed preconditioning effect was attributed to a metabolic effect.

The second part of the study deals with cellular conditioning effects mediated by NPCs. Stem cell as well as progenitor cell transplants are potential therapeutics in neurodegenerative diseases and acute brain injuries. However, the optimal application and the mechanisms of protection remain unknown. For that reason the aim of the second part of this thesis was to establish the production of a CM that reflects the conditions after stem/progenitor cell transplantation in the brain. Further, the CM should be suitable for in vivo application. One aim during this research was to investigate the potency and the stability of this CM. Furthermore, the major aim of this study was to identify components of the mixture that mediate the neuroprotective effects of CM. These investigations should be the basis for the development of a composition obtained from the CM for the treatment of neurological disorders.

2. Materials and methods

2.1. Cell culture

2.1.1. Cell culture materials

Sterile plastic ware used in this study is listed in Table 1.

Table 1: Plastic ware

Plastic ware	**Company**
T75 flasks	Greiner, Frickenhausen, Germany
T175 flasks	Greiner, Frickenhausen, Germany
24-well plates	Greiner, Frickenhausen, Germany
96-well plates	Greiner, Frickenhausen, Germany
ibidi slides 8-well plates	Ibidi, Munich, Germany
15 ml tubes	Greiner, Frickenhausen, Germany
50 ml tubes	Greiner, Frickenhausen, Germany
0.5, 1.5, 2 ml tubes	Sarstedt, Nümbrecht, Germany
Cell scraper	Sarstedt, Nümbrecht, Germany
0.22 µm sterile filter	Whatman, Dassel, Germany
5, 10 ml Injekt®	Braun, Melsungen, Germany
3, 10, 50 kDa Amicon® Ultra Centrifugal Filter Units	Millipore, Schwalbach, Germany

2.1.2. Cultivation of HT-22 cells

HT-22 cells were originally generated by David Schubert (Salk Institute, San Diego, USA) and obtained from Gerald Thiel (Homburg/Saar).

For standard cultivation HT-22 cells were kept in 75 cm^2 culture flasks in a standard humidified incubator at 37°C and 5 % CO_2. Cells were split twice per week in a ratio 1:10 - 1:20. For splitting, cells were washed once with phosphate buffered saline (PBS, Table 4) to fully remove the growth media. Afterwards, HT-22 cells were detached from flask with ~2 ml of Trypsin/EDTA solution (Table 5). When cells were detached the protease activity was stopped by adding the 3-fold amount of DMEM growth medium (Table 2). Cell suspension was centrifuged at 1,000 rpm for 5 minutes and resuspended in fresh growth medium. For determination of cell number, a counting chamber (Neubauer Zählkammer, Brand, Wertheim, Germany) was used. Afterwards, the required cell number was seeded into the appropriate culture dishes depending on the respective experiments. The cell densities used in the different culture formats are listed in Table 3.

Table 2: HT-22 growth medium

DMEM-medium with 4.5mg/l glucose and 110 mg/l sodium pyruvate	440 ml
Heat inactivated fetal calf serum (FCS)	50 ml
L-Alanyl-L-glutamine 200 mM	5 ml
Penicillin 10.000 U/ml / Streptomycin 10 mg/ml	5 ml

Table 3: HT-22 cells – cell densities

Cell culture format	**cell density (cells/well)**
96-well plate	~ 8,000 cells/well
24-well plate	~ 60,000 cells/well
ibidi slide 8-well plates	~ 16,000 cells/well
E-plate	~ 8,000 cells/well

Table: 4 Phosphate buffered saline (PBS), pH 7.4

NaCl	9 g
Na_2HPO_4	0.527 g
KH_2PO_4	0.144 g
HCl (0.1M)	q.s. for pH adjustment
Aqua demin.	add to a final volume of 1,000 ml

Table 5: Standard Trypsin/EDTA solution

Trypsin (7.500 U/mg)	100 mg
Ethylenediamine-tetra-acetic acid (EDTA)	40 mg
PBS	Table 4

2.1.3. Induction of cell death in HT-22 cells

Cell death in HT-22 cells was induced when cells reached about 70-80 % confluency. For induction of cell death in HT-22 cells, glutamate solution at a final concentration range of 2-5 mM was used. For glutamate stock solution D,L-glutamic acid monohydrate (Sigma-Aldrich, Taufkirchen, Germany) was dissolved in Earle's balanced salt solution (1x EBSS) or Dulbeccos's modified eagle medium (DMEM; PAA Laboratories GmbH; Cölbe, Germany) to a stock concentration of 1 M. The pH was adjusted to 7.2 with concentrated sodium hydroxide solution (NaOH). The stock solution was stored at -20°C. For inducing cell death, stock solution was diluted with DMEM to final concentrations instantaneously before the treatment and added directly to the cells. In experiments including a pretreatment without washout a 20 mM glutamate solution was prepared and added to the pretreatment solution directly to achieve the final concentration.

2.1.4. Cultivation of NPCs

NPCs, provided by Prof. Dr. Fred H. Gage (Salk Institute, La Jolla, USA) (Ray and Gage, 2006) were cultured in a standard humidified incubator at 37°C and 5 % CO_2. Cells were kept in 75 cm^2 culture flasks and split three times per week in a ratio 1:3 - 1:6. For splitting, media was removed and cells were detached with 1 ml 0.05 % Trypsin/EDTA (GIBCO) within one minute at room temperature. After adding 10 ml DMEM/F12 (PAA, Cölbe, Germany) cells were centrifuged at 1,000 rpm for 3 minutes. The pellet was washed once with 5 ml DMEM/F12 and centrifuged again. The resulting pellet was resuspended in fresh growth medium (Table 6) and seeded out as required. NPC growth medium was freshly prepared and used within 1-2 weeks since stability of the growth factors was limited. For long-term storage the cell pellet was resuspended in 1 ml freezing media (Table 7) and stored at -80°C. After 24 hours the frozen cell suspension was transferred into liquid nitrogen. When thawing the cells culture media contained the double amount of N2 supplement until NPCs reached standard proliferation rates.

Table 6: NPC growth medium

Dulbecco's modified medium Ham's F12 (DMEM/F12)	50 ml
N2 supplement (Invitrogen)	0.5 ml
Penicillin 10.000 U/ml / Streptomycin 10 mg/ml	0.5 ml
L-Alanyl-L-glutamine 200 mM	0.5 ml
Epidermal growth factor 10μg/ml (Invitrogen)	0.1 ml
Basic fibroblast growth factor 10 μg/ml (Invitrogen)	0.1 ml
Heparine 5mg/ml (Sigma-Aldrich)	0.05 ml

Table 7: NPC freezing media

Dulbecco's modified medium Ham's F12 (DMEM/F12)	888 µl
N2 supplement (Invitrogen)	10 µl
DMSO (10 %)	100 µl
Basic fibroblast growth factor 20 ng/ml (Invitrogen)	2 µl

2.1.5. Cultivation of SNL feeder cells

SNL 76/7 feeder cells (Sigma-Aldrich) are a cell line that can be used as a feeder layer to support the growth of mouse ESCs. This cell line was originally generated by a STO cell line transfected with a G418-resistance cassette, RV4.0 (Thomas and Capecchi, 1987), and a leukaemic inhibitory factor (LIF) expression construct (Williams et al., 1988).

The cells were cultured in a standard humidified incubator at 37°C and 5 % CO_2 in 75 cm^2 culture flasks. The cells were split twice a week in a ratio 1:10. Splitting procedure was as described for HT-22 cells. Culture media and freezing media was prepared as listed in Table 8 and 9.

Table 8: SNL culture medium

DMEM-medium with 4.5mg/l glucose and 110 mg/l sodium pyruvate	435 ml
Heat inactivated FCS	50 ml
MEM non-essential amino acids (NEAA) 10mM	5 ml
L-Alanyl-L-glutamine 200 mM	5 ml
Penicillin 10.000 U/ml / Streptomycin 10 mg/ml	5 ml

Table 9: SNL freezing media

DMEM-medium with 4.5mg/l glucose and 110 mg/l sodium pyruvate	70 %
Heat inactivated FCS	20 %
DMSO	10 %

2.1.6. Cultivation of primary MEF

For preparation of primary mouse embryonic fibroblasts (MEFs) embryonic C57black/6 mice (E17-18) were used. Small pieces of embryonic skin were dissected and put into MEF culture media (Table 10). When fibroblasts started to spread out of the skin pieces, the cells were detached using standard trypsin/EDTA solution and seeded into a new culture flask to get a well distributed cell monolayer (Xu, 2005). Cells were split in the same procedure as HT-22 cells when reaching ~80 % confluency on the flask bottom.

Table 10: Primary MEF culture medium

DMEM-medium with 4.5mg/l glucose and 110 mg/l sodium pyruvate	410 ml
Heat inactivated fetal calf serum (FCS)	75 ml
L-Alanyl-L-glutamine 200 mM	10 ml
Penicillin 10.000 U/ml / Streptomycin 10 mg/ml	5 ml

2.1.7. SiRNA transfection

For siRNA transfections, the cationic lipid formulation Lipofectamine RNAiMax (Invitrogen, Karlsruhe, Germany) was used. Transfections were performed in 24-well plates as reverse transfections, i.e. the complexes were prepared within the wells before cells and medium were added. For each well 1.2 µl Lipofectamine RNAiMax were mixed with siRNA and filled up to 100 µl with Optimem I (Invitrogen). The mixture was incubated for 20 minutes at room temperature. Afterwards, 500 µl of an antibiotic free cell suspension (33,333 cells/well) was added. After 48 hours cells were treated in the 24-well format or seeded into another culturing format depending on the respective experiment.

2.1.8. Starvation and production of CM

CM was produced from NPC, MEF, SNL or HT-22 cells. Cells were grown in 75 cm^2 or 175 cm^2 culture flasks until they reached ~70 % confluency. Culture media was removed and cells were washed once with PBS. Afterwards, cells were treated with EBSS with or without phenol red (Table 11 or Sigma-Aldrich). Duration of EBSS treatment was dependent on the cell type: NPCs were treated for at least 24 hours, HT-22 cells for 48 hours and MEFs and SNL cells for about one week until cells underwent starvation. Media were stored at -80°C until further use. Before use the CM was centrifuged (1,000 rpm, 10 minutes) and filtered through a 0.22 μm membrane filter to remove dead cells and cell debris.

For heat activation, CM was heated up to 60°C for at least 10 minutes. CM was used with 6 hours pretreatment in HT-22 cells followed by glutamate treatment if not described otherwise.

Table 11: Earle's balanced salt solution (EBSS 1x) containing phenol red

EBSS 10x (Sigma-Aldrich)	100 ml
$NaHCO_3$	2.2 g
Aqua demin.	add to a final volume of 1,000 ml
HCl (0.1M)	q.s. for pH adjustment

2.2. Chemicals and reagents

All standard chemicals were obtained from Sigma-Aldrich (Taufkirchen, Germany) and Carl Roth (Karlsruhe, Germany), if not described otherwise. All buffers and solutions were prepared using demineralized, ultrapure water supplied by the SG Ultra Clear UV plus Reinstwassersystem (VWR, Darmstadt, Germany).

Demineralized water for aseptic preparation of solutions was sterilized before use by a steam autoclave (Systec V-40, Systec GmbH, Wettenberg, Germany). All media and solutions that were used in cell culture were sterilized by filtration using 0.22 µm filter sets (Sarstedt, Nümbrecht, Germany).

2.2.1. Inhibitors of cell death

Recombinant human peroxiredoxin-1 (prdx-1, Sigma-Aldrich) was dissolved in EBSS resulting in a 250 µg/ml stock and stored at -20°C. It was used at final concentrations of 12.5 µg/ml, 50 µg/ml and 125 µg/ml for applications in HT-22 cells. HT-22 neurons were pretreated with the recombinant protein for 6 hours followed by subsequent glutamate treatment.

Recombinant mouse galectin-1 (gal-1) (R&D Systems, Wiesbaden-Nordenstadt, Germany) was dissolved in EBSS at a stock concentration of 100 µg/ml and stored at -20°C. For applications in HT-22 cells it was used in a final concentration of 10 µg/ml. HT-22 cells were pretreated with prdx-1 for 6 hours before adding glutamate.

Rotenone (Sigma-Aldrich) was dissolved in DMSO in a stock concentration of 1 mM and stored at -20°C until further use protected from light. To achieve protective effects in HT-22 cells rotenone was applied at a final concentration of 20 nM if not described otherwise.

For inhibition of caspases the cell-permeable, irreversible, broad-spectrum caspase inhibitor Q-VD-OPh (Merck KGaA, Darmstadt, Germany) was used. The solution dissolved in DMSO (10 mM) was used at a final concentration of 20-40 µM.

Trolox (6-hydroxy-2,5,7,8-tetramethylchroman-2-carboxylic acid) (Sigma-Aldrich) was dissolved in ethanol in a stock concentration of 100 mM and diluted in culture media to a final working concentration of 100 µM.

AICAR (5-amino-1-β-D-ribofuranosyl-imidazole-4-carboxamide, Sigma-Aldrich), used for activation of AMPK, was dissolved in HT-22 medium at a stock concentration of 100 mM and stored at -20°C until further use. The stock was diluted in culture media to final concentrations as indicated.

For inhibition of AMPK, compound C (6-[4-(2-Piperidin-1-yl-ethoxy)-phenyl)]-3-pyridin-4-yl-pyrrazolo[1,5-a]-pyrimidine) (Merck KGaA, Darmstadt, Germany) was used. The lyophilized powder was dissolved in DMSO at a stock concentration of 10 mM and stored at -20°C until further use. The stock was diluted in media to final concentrations as indicated.

BDNF (R&D Systems) was dissolved in DMSO at a stock concentration of 10 µg/ml and stored at -20°C. For treatment in HT-22 neurons, final concentration in media

ranged from 25-100 ng/ml. Cells were pretreated 6 hours with BDNF followed by subsequent co-treatment of glutamate and BDNF.

2.2.2. Inhibitors of protein synthesis and PI3K

For inhibition of protein synthesis during the production of CM, actinomycin D or cycloheximide (CHX) was added to EBSS that was determined for CM production in NPCs. Actinomycin D (Sigma-Aldrich) was dissolved in DMSO at a stock concentration of 1 mM and stored at -20°C. For treatment of NPCs it was used in final concentrations of 1 µM and 10 µM if not described otherwise. CHX (Sigma-Aldrich) was dissolved in ethanol at a stock concentration of 0.5 mM and stored at -20°C. For application in NPCs it was used at final concentrations of 0.5 µM and 1 µM if not described otherwise. After NPCs underwent starvation the protein synthesis inhibitors were removed from media by a 10 kDa cut off filtration at 4,000 rpm before testing in the HT-22 cell system.

For inhibition of phosphoinositide-3-kinase (PI3K) the cell-permeable, reversible inhibitor LY 294002 (2-(4-morpholinyl)-8-phenyl-4H-1-benzopyran-4-one) was used. LY 294002 was dissolved in DMSO resulting in a 1 mM stock solution. For HT-22 cell treatment a final concentration of 10 µM was used. Cells were pretreated with the inhibitor for 1 hour followed by a pretreatment containing CM and the inhibitor together. Afterwards, the cells were exposed to glutamate.

2.2.3. Digestion of RNA and proteins

For digestion of RNA, ribonuclease A (RNase A) solution (Sigma-Aldrich) was used in a concentration of 70 Kunitz/mg protein. Ribonuclease A targets the 3’phosphate of a pyrimidine nucleotide and cleaves single stranded RNA. Since RNase A exerts its highest activity at 60°C, CM was incubated with for 30 minutes at 60°C before treatment of the cells.

Protease provided by Qiagen (Hilden, Germany) was applied to digest proteins in CM. The lyophilized powder was dissolved in EBSS and 45 mAU/mg protein were used for the digestion. CM and protease were incubated for 30 minutes at 37°C for digestion. Afterwards, the mixture was incubated for 4 hours at 75°C to inactivate the protease. The resulting mixture was then used for cell treatment.

2.2.4. Primary antibodies

All primary antibodies were used at a dilution of 1:1,000 for Western blot analysis in Tris-buffered saline containing 0.05 % Tween 20 and 5 % skim milk powder or Tris-buffered saline containing 5 % BSA (all Sigma-Aldrich) as described in the company's protocol. In this study, the following antibodies have been used: anti-AIF (sc-9416, Santa Cruz), anti-Actin C4 (#691001, ImmunO^{TM}) diluted 1:100,000, anti-AMPK (#2532, Cell Signaling), anti-phospho-AMPK (#2535, Cell Signaling), anti-LGALS1 (#5418, Cell Signaling) diluted in 5 % BSA, 1x TBS and 0.1% Tween 20, anti-MitoProfile® Total OXPHOS Rodent WB Antibody Cocktail (ab110413, abcam), anti-Prdx-1 (#8732, Cell Signaling), and anti-TIM23 (#611223, BD Transduction Laboratories^{TM}). For CM treatment with specific antibodies, the media was incubated with the antibodies for 1-2 hours at room temperature before application to the cells.

2.2.5. Secondary antibodies

For Western blot analysis horseradish peroxidase (HRP) labeled secondary antibodies were used (All Vector Labs, Burlingame, California, USA). Secondary antibodies were diluted 1:4,000 in Western blotting buffer consisting of Tris-buffered saline with 0.05 % tween 20 and 5 % skim milk powder (Sigma-Aldrich).

2.2.6. SiRNA sequences

For the AIF knockdown the following siRNA sequences were used: AAGAGAAA CAGAGAAGAGCCA (AIF siRNA 1), ACAGAGAAGAGCCAUUGCC (AIFsiRNA 12) and AUGUCACAAAGACACUGCA (AIF siRNA 2). As negative control the standard sequence AAGAGAAAAAGCGAAGAGCCA was used (all Eurofins MWG Operon, Ebersberg, Germany).

2.2.7. PCR-primer

For RT-PCR all primers were synthesized at MWG (Eurofins MWG Operon, Ebersberg, Germany). Primer sequences were used as listed in Table 12:

Table 12: Primers used for RT-PCR

AIF fw	5'-GCGTAATACGACTCACTATAGGGAGATCCAGGCAACTTGTTCCAGC-3'
AIF rev	5'-GCGTAATACGACTCACTATAGGGAGACCTCTGCTCCAGCCCTATCG-3'
EEF 2 fw	5'-GCTGCCTTGCGTGTCACCGA-3'
EEF 2 rv	5'-CCCATGGCGGCCTCATCGTC-3'
GAPDH fw	5'-AGGCCGGTGCTGAGTAT-3'
GAPDH rv	5'-TGCCTGCTTCACCACCTTCT-3'
HSP 60 fw	5'-GTCCCTCACTCGCCGCAGAC-3'
HSP 60 rv	5'-GCCTGTTCAAAACCAGCGTGC-3'
HSP 70 fw	5'-ACGCTAGTCGCGCTCGTGGA-3'
HSP 70 rv	5'-TGCGTGGACGAGCTCAGGGT-3'
HSP 90 fw	5'-CTTAGGCTTGCCGTGCGAGT-3'
HSP 90 rv	5'-TGGTCTGCCCGGACGGTGAA-3'
PLA 2 fw	5'-ATGAGGTGCTTGTAGACCCTGATGC-3'
PLA 2 rv	5'-CTTGTGGGGGAGGCGGGACA-3'
Prdx-1 fw	5'-TTCTCACGGCTCTTTCTGTTT-3'
Prdx-1 rv	5'-TTCTGGCTGCTCAATGCTGC-3'
Prdx-2 fw	5'-CCGGCTCTTGCTCACGCAGT-3'

Prdx-2 rv	5’-GTGTCACTGCCGGGCTTCCA-3’
Prdx-5 fw	5’-TGCATCGACGTGCTTGGCAGG-3’
Prdx-5 rv	5’-TCTGGCTCCACGTTCAGTGCC-3’
Prdx-6 fw	5’-GGCATGCTTCCTTCTTGCTGGGA-3’
Prdx-6 rv	5’-TGACCTAGGACCCACCACTGCC-3’

2.3. Kits

Table 13 encompasses all kits used for this study.

Table 13: Kits

Kit	**Company**
BODIPY (581/591 C11)	Invitrogen, Karlsruhe, Germany
Pierce BCA Kit	Perbio Science, Bonn, Germany
NucleoSpin RNA II Kit	Machery & Nagel, Düren, Germany
ELISA Kit	Hölzel Diagnostika GmbH, Cologne, Germany
SuperScript III One Step RT-PCR System with Platinum® Taq	Invitrogen, Karlsruhe, Germany

2.4. Cell viability assays

2.4.1. MTT assay

The MTT assay is a colorimetric assay for measuring the activity of enzymes that reduce 3-(4,5-dimethylthiazol-2-yl)-2,5-diphenyltetrazolium bromide (MTT) to formazan by either a lyosomal/endosomal compartment or mitochondria (Liu et al., 1997), resulting in a purple color. The change in absorption characteristics can be easily detected by absorptive spectroscopy.

Cell viability was evaluated 15-24 hours after growth factor withdrawal or glutamate treatment on the basis of EBSS or 11-18 hours after glutamate treatment on the basis of HT-22 cell culture medium. Quantification of cell viability in NPCs and HT-22 cells by MTT assay was performed in 96-well plates. MTT (Sigma-Aldrich) was dissolved in PBS at a concentration of 2.5 mg/ml. When the morphological changes of the cells indicated cell death, the MTT reagent was added to the media at final concentrations of 0.25-0.5 mg/ml followed by 1 hour incubation at 37°C. The reaction was terminated by removing the media from the cells and freezing the plate at -80°C for at least 1 hour. Absorbance was determined after solving the formazan crystals in dimethyl sulfoxide (DMSO) at 570 nm (FluoStar, BMG Labtech, Offenbach, Germany). Background was detected at 630 nm and substracted accordingly. Cell viability was expressed as absorption level relative to controls, which were set to 100 % viability.

2.4.2. xCELLigence system

The xCELLigence System monitors cellular events in real-time by measuring electrical impedance across interdigitated gold micro-electrodes integrated on the bottom of tissue culture E-plates. Usually, cells have a high electrical resistance. Thus, the more cells are attached to the electrodes, the larger are the increases in impedance.

Consequently, the system is able to detect changes in cell number (proliferating cells), altered attachment properties (cellular death), and especially the kinetics of these processes. The results are provided as a curve containing the cell index as a function of time (Diemert et al., 2012).

For using this system ~8,000 HT-22 cells or 30,000-40,000 NPCs per well were seeded out into 96-well E-plates. Prior to seeding of the cells, background impedance was determined using 100-200 µl of cell culture medium or EBSS. Next, cell suspension was added to a total of 100 µl/well for HT-22 neurons and 200 µl/well for NPCs. Treatment of cells was started when the cell index exceeded a value of about one. Cell index values were recorded using RTCA Software 1.2 (Roche Diagnostics, Penzberg, Germany). After concluding each experiment, E-plates were recycled by removing media, washing the plates twice with demineralised water and adding standard Trypsin/EDTA for 15-20 minutes. Afterwards, 1xTE was removed, the plates were washed a further 3 times and irradiated with UV light for 30 minutes to reassure sterility.

2.5. Visualization and characterization of mitochondria

Mitochondrial morphology in HT-22 cells was visualized using MitoTracker DeepRed (Invitrogen). HT-22 cells were seeded onto ibidi slides at least 24 hours before the treatment (16,000 cells/well). MitoTracker DeepRed was dissolved in DMSO at a final stock concentration of 50 µM and kept protected from light. For applications on cells MitoTracker DeepRed reagent was diluted 1:250 in culture medium (final working concentration 200 nM) together with DAPI (1 µg/ml) for counterstaining of the nuclei. Staining solution was added to the cells for 20 minutes before starting the respective treatment. After completing the experiment, cells were washed with PBS, fixed with 4 % paraformaldehyde (PFA) and washed again twice with PBS. Images were taken using a confocal laser scanning microscope running LSM Image Software (Axiovert 200, Carl Zeiss, Jena, Germany). MitoTracker DeepRed fluorescence was excited at a wavelength of 633 nm (band pass filter) and emissions were detected using a 670 nm long pass filter. Evaluation and classification of mitochondrial morphology was performed as described before (Grohm et al., 2010). Mitochondria were counted manually and categorized in 3 groups, depending on the degree of fragmentation: Category I represents cells with intact tubular network with elongated mitochondria that is found in cells under control conditions. Category II and III indicate an increasing number of fragmented mitochondria. Mitochondrial fragmentation was accompanied by an apoptotic phenotype, showing nuclear condensation and the peri-nuclear accumulation of the mitochondrial fragments. For the quantification of

mitochondrial morphology, at least 500 cells per condition were counted blind to treatment conditions in at least four independent experiments.

2.6. ATP assay

ATP levels can be detected by a method using the luciferase enzyme that catalyzes the following reaction:

$$ATP + Luciferin + O2 \rightarrow Oxyluciferin + AMP + PPi + CO2 + Light.$$

For this assay 8,000 transfected HT-22 cells were seeded in each well of a white 96-well plate (Greiner Bio one, Frickenhausen, Germany) for luminescence measurements 48 hours after the transfection. Twenty-four hours after seeding, cells were treated with glutamate. ATP levels were detected at indicated time points after the onset of glutamate exposure by detection of luminescence using the ViaLight MDA Plus-Kit (Lonza, Verviers, Belgium). The cells were treated with nucleotide releasing reagent and incubated for 5 minutes at room temperature. Afterwards, ATP monitoring reagent was injected into each well and luminescence was detected immediately (FluoStar, BMG Labtech, Offenburg, Germany). The emitted light intensity was measured for quantification of ATP levels. The values are given as relative values in percentage of control levels.

2.7. Detection of lipid peroxides

For detection of cellular lipid peroxidation BODIPY 581/591 C11 (Invitrogen) was used. BODIPY is a sensitive fluorescent reporter for lipid peroxidation, undergoing a shift from red to green fluorescence emission upon oxidation of the phenylbutadiene segment of the fluorophore. This oxidation-dependent emission shift enables fluorescence ratio imaging of lipid peroxidation in living cells. For detection of cellular lipid peroxidation cells were loaded with 2 mM BODIPY solution for 60 minutes in standard medium at indicated time points after glutamate treatment. Cells were harvested, washed and resuspended in PBS. Flow cytometry was performed using 488 nm UV line argon laser for excitation and BODIPY emission was recorded at 530 nm (green) and 585 nm (red) by flow cytometry on a FACScan (BD Bioscience,

Heidelberg, Germany). Data were collected from at least 100,000 cells in three independent experiments.

2.8. Detection of mitochondrial membrane potential

For detection of the MMP in whole cells the Mito PT $\Delta\Psi_m$ kit (Immunochemistry Technologies, Hamburg, Germany) was used. The kit contains tetramethylrhodamin ethal ester (TMRE) which is a lipophilic, cationic fluorescent redistribution dye. This dye has a delocalized positive charge dispersed throughout its molecular structure. Its lipophilic solubility allows TMRE to penetrate into living cells and into mitochondria. Using this kit non-apoptotic cells with healthy mitochondria appear red, whereas apoptotic cells show decreased red fluorescence. HT-22 cells were cultured in 24-well plates and treated with glutamate 48 hours after transfection. When cell death occurs in glutamate-treated controls, the cells were incubated for 20 minutes at 37°C with TMRE. Afterwards, the cells were collected, washed with PBS and suspended in assay buffer. To exclude autofluorescence of the cells a non-treated negative control that was not stained by TMRE was prepared. Flow cytometry was performed using excitation at 550 nm and detecting emission at 570 nm. Data were collected from at least 10,000 cells from at least four independent experiments.

For detection of the MMP in isolated mitochondria DIOC6(3) fluorescence-based assay was performed by Dr. Amalia Dolga. Isolated 25-50 µg mitochondria were incubated with 20 nM DIOC6(3) dye. As a positive control for a complete loss of MMP, CCCP (50 µM) protonophore was applied on intact mitochondria. MMP was analyzed by a FLUOstar Optima fluorescence plate reader using 485 nm excitation and 520 nm emission. Measurements were performed in triplicate and are representative of at least three independent experiments.

2.9. Protein analysis

2.9.1. Buffers for Western blot analysis

Following buffers were used for sodium dodecyl sulfate (SDS) gel electrophoresis and Western blot analysis:

Stacking gel 3.5 %

0.5 M Tris HCl solution pH 8.8	2.5 ml
Acrylamid/bisacrylamide (37.5 : 1) 30 %	1.2 ml
SDS solution 10 %	0.1 ml
Ammoniumpersulfate solution 10 %	0.05 ml
Tetramethylethylenediamine (TEMED)	0.01 ml
Aqua demin.	ad 10 ml

Collection gel 12.5 %

1.5 M Tris HCl solution pH 8.8	2.5 ml
Acrylamid/bisacrylamide (37,5:1) 30 %	3.34 ml
SDS solution 10 %	0.1 ml
Ammoniumpersulfate solution 10 %	0.05 ml
TEMED	0.01 ml
Aqua demin.	ad 10 ml

5x sample buffer Western blot

1M Tris-HCl pH 6.8	70 ml
Glycerol	30 ml
D,L-Dithiotreitol (DTT)	9.3 g
SDS	10 g
β-Mercaptoethanol	1 ml
Bromophenol blue sodium salt	12 mg

1 x Electrophoresis buffer

Tris base	3 g
Glycine	14.4 g
SDS	1 g
Aqua demin.	ad 1000 ml

1x Transfer buffer, pH 8.3

Tris base	3 g
Glycine	14.4 g
Methanol	100 ml
HCl 0.1 M	q.s
Aqua demin.	ad 1000 ml

1x TTBS, pH 7.5

Tris Base	2.4 g
NaCl	29.2 g
HCl 0.1 M	q.s.
Aqua demin.	ad 10 ml

1x Blocking buffer

Skim milk powder	25 g
TBST	ad 500 ml

Stripping buffer, pH 2

Glycine	15 g
SDS	1 g
Tween 20	10 ml
HCl conc.	q.s.
Aqua demin.	ad 1,000 ml

2.9.2. Protein preparation and mitochondria isolation

For obtaining total cell protein extracts HT-22 cells were seeded into 24-well cell culture plates (Greiner Bio one). Cells were washed with PBS, detached with a cell scraper and lysed with 100 ml lysis buffer containing mannitol 0.25 M, Tris 0.05 M, EDTA 1 M, EGTA 1 M, DTT 1 mM, triton-X 1 % (all from Sigma-Aldrich), supplemented with Complete Mini Protease Inhibitor Cocktail (Roche) (1 tablet per 10 ml). The lysate was frozen at -80°C until further use. To remove insoluble membrane fragments, extracts were centrifuged at 13,000 x g for 15 minutes at 4°C after thawing.

For mitochondria isolation and mitochondrial enriched extracts, cells were cultivated in 24-well cell culture plates (Greiner Bio one). Cells were detached using 1x TE and centrifuged at 1,000 rpm for 5 minutes. After washing the cells once with PBS cells were lysed in a buffer containing 250 mM sucrose (Merck, Darmstadt, Germany), 20 mM HEPES (Sigma-Aldrich), 3 mM EDTA (Sigma-Aldrich) supplemented with Complete Mini Protease Inhibitor Cocktail (1 tablet for 10 ml buffer, pH 7.5). Cells were disrupted using a glass douncer (25 passes) followed by 15 passes with a 20G needle. After centrifugation at 900 x g for 10 minutes supernatant was collected and the pellet was disrupted a second time in the same way. After second centrifugation, the collected supernatant was centrifuged at 16,800 x g for 10 minutes and the resulting pellet was suspended in fresh buffer. For pure extracts the pellet was washed three times in buffer or EBSS depending on the experiment.

For determining the amount of protein in the probes the principle of bicinchonic acid (BCA) assay was used. The assay is based on two reactions. First, the peptide bonds in proteins reduce Cu^{2+} ions to Cu^{+} under alkaline conditions. The amount of reduced Cu^{2+} is proportional to the amount of protein present in the solution. This is followed by formation of a purple-colored chelate complex of BCA with Cu^{+} ions. The macromolecular structures of the protein, the amount of peptides, and the four amino acids cysteine, cystine, tryptophan, and tyrosine are responsible for this color reaction of the BCA. This provides a basis to monitor the reduction of alkaline Cu^{2+} by proteins and, thus, determine the protein concentration in biochemical samples and cell extracts (Walker, 1994).

Protein amounts in extracts were determined using the Pierce BCA kit (Perbio Science, Bonn, Germany). To this end, 5 µl of each sample were diluted in 95 µl 1x PBS. A standard curve containing 0 - 150 µg bovine serum albumin (BSA) (Perbio Science, Bonn, Germany) per 100 µl, 5 µl of the respective lysis buffer, and 1x PBS add to 100 µl was prepared. Next, 200 µl of a 1:50 mixture of reagent B : reagent A (Perbio Science, Bonn, Germany) was added to each sample. Samples were incubated for 30 minutes at 60°C. At this temperature, peptide bonds assist in the formation of the reaction product, so the assay sensitivity is increased since the variances caused by unequal amino acid composition are minimized. One hundred µl of each sample were pipetted into a 96-well plate (Nunc, Wiesbaden, Germany). Absorption at 590 nm was determined using a microplate reader (Fluostar OPTIMA, BMG Labtech, Offenburg, Germany) and protein amounts of the test samples were calculated from the standard curve.

2.9.3. Gel electrophoresis

Sodium dodecyl sulfate polyacrylamide gel electrophoresis (SDS-PAGE) has been used to separate proteins according to their different molecular mass. Gels were prepared using BIO-RAD gel casting stand and casting frames. Gels were prepared using a separation gel with a concentration of 12.5 % polyacrylamide and a stacking gel with 3.5 % polyacrylamide. The specific buffers used for the generation of gels and subsequent electrophoresis are provided in 2.9.1.. Prior to electrophoresis, samples were prepared using 20-30 µg of raw protein extract and adding 5 x SDS sample buffer. Samples were heated at 90°C for 10 minutes and loaded to the gel after reaching room temperature. For comparative evaluation of molecular mass, 5 µl of PageRuler^{TM} Plus Prestained Ladder (Fermentas, St. Leon-Rot, Germany) were loaded next to the samples. Electrophoresis was performed initially at 60 V for about 30 minutes to allow for sample collection and increased later to 120 V. Following electrophoretic separation, proteins were blotted on a polyvinylidenfluorid membrane (PVDF, Bio-Rad, Munich, Germany) according to the recommendations by Bio-Rad at 15 V for 60 minutes. PVDF membranes were first activated in methanol and then incubated for 10 minutes in 1 x transfer buffer before blotting. Meanwhile, Whatman blotting paper and the acrylamide gel were incubated for 10 minutes in transfer buffer. Blotting was carried out by stacking one layer of Whatman paper on top of the

anodic plate, followed by the PVDF membrane, the acrylamide gel as the third, and another final layer of Whatman paper on top. Blotting was carried out in a Trans-Blot SD semi-dry transfer cell (Bio-Rad, Munich, Germany) using extra thick Whatman filter paper (Bio-Rad, Munich, Germany) and 1x transfer buffer. After blotting the PVDF membranes were transferred directly into blocking buffer and incubated for 1 hour at room temperature. Afterwards, blots were probed with the primary antibodies (diluted in blocking buffer) overnight at 4°C. The next day, membranes were washed three times with TBST for 5 minutes and probed with the appropriate HRP-conjugated secondary antibody in blocking solution for 1 hour. After washing 3 times with TBST for 15 minutes each, membranes were incubated with chemiluminescent substrate solution HRP-Juice (PJK GmbH, Kleinblittersdorf, Germany). Chemiluminescent signals were recorded and quantified by densitometric analysis using the semi-automated Chemidoc-XRS Imaging System and the dedicated Quantity One software package (both, Bio-Rad, Munich, Germany). Alternatively, towards blotting, some gels were stained by Coomassie Blue R250. Here, the gel was incubated for 1 hour in Coomassie staining solution containing 0.1 % R250, 45 % methanol, 45 % aqua demin. and 10 % pure acetic acid. Afterwards, the gel was discolored overnight in destaining solution containing 30 % methanol, 10 % pure acetic acid and 60 % aqua demin., until single bands were visible.

2.10. RNA analysis

2.10.1. RNA preparation

For RNA extraction HT-22 cells were grown in 24-well plates at an average density of 60,000 cells/well. RNA extracts were prepared using the Nucleo Spin II Kit (Macherey und Nagel, Düren, Germany) according to the manufacturer's instructions. Briefly, HT-22 cells were washed with PBS and harvested in cell lysis buffer R1 supplemented with 1 % β-mercaptoethanol. For each group, 2-4 wells were pooled to gain appropriate amounts of mRNA. Before continuing with the extraction, all samples were shock-frozen in liquid nitrogen and left to thaw slowly on ice. Next, the raw extracts were filtered through Nucleospin-RNA II columns to remove cellular debris. The supernatant was supplemented with ethanol, mixed carefully and loaded on a NucleoSpin RNA II column to extract nucleic acids by adsorption to the silica

matrix of the column. Excessive electrolytes were removed by washing with MDB buffer (supplied with the kit). To remove possible contaminations with genomic DNA recombinant DNAse was added. Further, purification of the column-bound RNA was achieved by subsequent purification, using RA2 and RA3 buffers. RNA was eluted in RNAse free water supplied with the Nucleo Spin Kit II. RNA-concentration was determined by UV-Vis absorption spectroscopy at 260 nm. For intermediate storage RNA-extracts were transferred to the -80°C freezer.

2.10.2. RT-PCR

Following RNA purification, mRNA was amplified using the Super Skript III OneStep PCR kit with Platinum Taq supplied by Invitrogen. Sequence specific primers were used as described in Table 12 in section 2.2.7. Each sample was prepared according to the following scheme given in Table 14-22.

Table 14: ONE STEP PCR sample composition AIF, HSP 60, HSP 70, HSP 90, prdx-1, prdx-2, prdx-5, prdx-6, PLA 2, eEF 2

2x reaction buffer 12.5 µl
Sample (0.1 µg) x µl
fw primer (10 µM) 0.5 µl
rv primer (10 µM) 0.5 µl
SuperScript III enzyme 1 µl
Nuclease free water added to a final volume of 25 µl.

Table 15: ONE STEP PCR sample composition GAPDH

2x reaction buffer 12.5 µl
Sample (0.1 µg) x µl
fw primer (5 µM) 1 µl
rv primer (5 µM) 1 µl
SuperScript III enzyme 0.5 µl
Nuclease free water added to a final volume of 25 µl.

For amplification the following cycler programs were used.

Table 16: ONE-Step PCR cycler program – murine GAPDH

60° C 30 min
95° C 2 min
95° C 30 sec
57° C 1 min } 20-25 cycles
70° C 2 min
70° C 10 min
4° C ∞

Table 17: ONE-Step PCR cycler program – murine AIF

60° C 30 min
95° C 2 min
95° C 30 sec
57° C 1 min } 30 cycles
70° C 2 min
70° C 10 min
4° C ∞

Table 18: ONE Step PCR cycler program - murine prdx-1

60° C 30 min
95° C 2 min
95° C 30 sec
56° C 1 min } 25 cycles
70° C 2 min
70° C 10 min
4° C ∞

Table 19: ONE Step PCR cycler program - murine prdx-2, prdx-5, eEF 2, HSP 90

60° C 30 min

95° C 2 min
95° C 30 sec
63° C 1 min } 20 cycles
70° C 2 min
70° C 10 min
4° C ∞

Table 20: ONE Step PCR cycler program - murine prdx-6, PLA 2

60° C 30 min
95° C 2 min
95° C 30 sec
64.1° C 1 min } 27 cycles
70° C 2 min
70° C 10 min
4° C ∞

Table 21: ONE Step PCR cycler program - murine HSP 60

60° C 30 min
95° C 2 min
95° C 30 sec
61.3° C 1 min } 20 cycles
70° C 2 min
70° C 10 min
4° C ∞

Table 22: ONE Step PCR cycler program - murine HSP 70

60° C 30 min		
95° C 2 min		
95° C 30 sec	}	27 cycles
63° C 1 min		
70° C 2 min		
70° C 10 min		
4° C ∞		

2.10.3. Agarose gel electrophoresis

For visualization PCR products were analyzed by agarose gel electrophoresis and subsequent detection by SYBR Gold (Invitrogen) an intercalating agent that increases its fluorescent emission upon DNA binding. For gel preparation, agarose (1.5 %, Sigma-Aldrich) was suspended in tris/borate/EDTA (TBE) buffer (10 x stock, Invitrogen) and dissolved by heating up the suspension in a microwave oven. After dissolving, 2 µl of SYBR Gold was added into 100 ml suspension, stirred carefully and the solution was filled into the gel cartridge to allow gel formation. For subsequent gel loading, a comb was inserted into the gel, to generate the pockets. Samples were loaded using 1-5 µl of PCR product, 2 µl of Blue Juice sample buffer (Sigma Aldrich) added with nuclease-free water up to a total volume of 7 µl. In addition to the samples 4 µl of a pre-prepared 100 bp reference marker (Fermentas, St. Leon-Roth, Germany) was loaded on the gel. Electrophoresis was conducted at 100 V for about 1 hour. Stained PCR products were detected by UV light excitation and fluorescent emission using the Chemidoc Imaging System (Bio Rad, Munich, Germany). Pictures were taken and analyzed using Quantitiy One software (Bio-Rad, Munich, Germany).

2.11. Isolation of apoptotic bodies

Isolation of apoptotic bodies was performed following a protocol by Hristov et al. (Hristov et al., 2004). CM was collected and clarified from cell debris by centrifugation at 800 x g for 10 minutes. Afterwards, the medium was further centrifuged at 16,000 x g for 20 minutes to isolate the apoptotic bodies and to obtain apoptotic bodies-depleted medium. The pellet was resuspended in EBSS.

2.12. ELISA assay

To determine the concentration of prdx-1 in CM a mouse peroxiredoxin-1 ELISA kit (Hölzel Diagnostika GmbH, Cologne, Germany) was used. This assay employs the quantitative sandwich enzyme immunoassay technique. All reagents were brought to room temperature before using the kit. Prdx-1 standard solution was freshly prepared for every experiment. One hundred µl of samples and standards were added into the microwells of the assay plate, which was pre-coated with a specific prdx-1 antibody. Afterwards, the plate was covered with adhesive stripes and incubated at 37°C for 1 hour. The liquid of each well was removed and 100 µl of biotin antibody was added. After covering the wells the plate was incubated for 1 hour at 37°C. Each well was aspirated and washed three times with 200 µl wash buffer. Next, 100 µl of horseradish peroxidase (HRP)-avidin was pipetted into each well and the plate was incubated for another hour at 37°C. The liquids were removed and wells were washed 5 times with wash buffer. The plate was incubated with 90 µl of TMB substrate for 15-30 minutes protected from light until the blue color developed. The reaction was stopped by adding 50 µl of stop solution to each well. The optical density was determined immediately using a microplate reader (Infinite M200, Tecan Group Ltd., Männedorg, Switzerland) set to 450 nM. Wavelength correction was set to 540 nm and readings at 540 nm were subtracted from the readings at 450 nm. This subtraction corrects the optical imperfections within the plate. Concentrations of prdx-1 in CM were calculated by a linear regression fit of the measurements of the standards.

2.13. MALDI-TOF analysis

MALDI-TOF analysis was performed by Jörg Kahnt from the Max-Planck-Institute, Marburg. Probes were concentrated by Amicon Ultra 10,000 MWCO filtration (Millipore, MA, USA) at 4,300 U/min. Samples were digested with sequencing-grade modified trypsin (Promega) and the resulting peptide mixtures were analyzed by nanoLC (PepMap100 C-18 RP nanocolumn and UltiMate 3,000 liquid chromatography system, Dionex) and automated MSMS (4800 Proteomics Analyzer MDS Sciex). MSMS data were searched against an in-house Mus musculus protein database using Mascot embedded into GPS explorer software (MDS Sciex). For interpretation, focus was on the peptides found with a total ion score higher than 45 and at least 2 peptide counts. Findings with ion scores higher than 45 and lower than two peptide counts are listed for completeness. The ion score for an MSMS match is based on the calculated probability, that the observed match between the experimental data and the database sequence is a random event. The reported score is -10Log(P). So, during a search, if 1,500 peptides fell within the mass tolerance window about the precursor mass, and the significance threshold is chosen to be 0.05, this would translate into a score threshold of 45. For interpretation fragmentation patterns were determined using BLAST search in Pubmed database (www.ncbi.nlm.nih.gov/blast).

2.14. Aceton precipitation

For aceton precipitation fresh CM was mixed with the 4-fold amount of cold aceton (Roth, Karlsruhe, Germany) and kept at -20°C over night. The next day the solution was centrifuged at 13,000 x g, at 4°C for at least 30 minutes. Supernatant was removed and the pellet resuspended in EBSS. For investigation of the supernatant aceton was removed by evaporation at 40°C.

2.15. Cut off filtration

For size exclusion filtration CM or control media was filtrated through a 0.22 µM cellulose filter to remove dead cells and cell debris. Afterwards, media was centrifuged through a 3 kDa, 10 kDa, or 50 kDa cut off filter (Millipore, Schwalbach, Germany) at 4,000 rpm, at 4°C until concentrate volume was below 500 µl. The concentrates were stored at -80°C till further use.

2.16. Digestion of CM

For RNA digestion 70 Kunits Ribonuclease A (Sigma-Aldrich) per mg protein was used. To get an optimal digestion CM and ribonuclease were kept at 60°C for 30 minutes before treating the cells.

For protein digestion, Protease (Qiagen) was used in a concentration of 45 mAU per mg protein. Digestion was performed at 37°C for 30 minutes. Afterwards, the protease was inactivated by heat at 70°C for at least 1 hour.

2.17. Preparation of cell lysates

For cell lysates NPC or SNL feeder cells were washed with PBS and resuspended in 1 ml EBSS. If not described otherwise cells were lysed by a Digital Sonifier® (VWR, Darmstadt, Germany) for 2 minutes in a 1 second sonification 1 second break interval at an amplitude of 20 % on ice. The lysate was diluted to the final volume with EBSS.

2.18. Dialysis and lyophilisation

For dialysis CM, heated at 60°C for 10 minutes was filled into a Spectra/Por® dialysis tube (MWCO 6,000-8,000) (Serva electrophoresis, Mannheim, Germany) and incubated at 4°C overnight in 1 liter aqua demin.

For lyophilization the sample was filled into a vented tube and put into a LDC-1 m Alpha 1-4 freeze dryer (Martin Christ GmbH, Osterode, Germany) under vacuum overnight until volume was constricted to ~ 0.5-1 ml. Further dilutions were done with EBSS.

2.19. Gel filtration by Äkta analysis

For SDS gel filtration of CM ÄKTAprime plus (GE Healthcare, Munich, Germany) was used with PrimeView 5.0 software. Five ml CM were loaded onto a HiLoad™ 16/600 Superdex™ 75 pg column. The column was washed with 120 ml aqua demin. and 120 ml EBSS before loading. The fractions were collected in volumes of 7 ml and stored at -80°C until further use. The applied program is listed in Table 23.

Table 23: Program for ÄKTAprime plus

Action	Breakpoint	Volume [ml]	Flow rate [ml/min]	Fraction size [ml]	Inject valve position
Equilibration	1	0	1	0	Load
Sample injection	2	15	1	0	Inject
Wash	3	20	1	7	Load
Elution	4	45	1	7	Load
Re-equilibration	5	170	1	7	Load

2.20. Statistical analysis

All data are presented as means ± standard deviation (S.D.). For statistical comparison between two groups Mann-Whitney-U-test was used. For statistical comparisons between treatment groups analysis of variance (ANOVA) was performed followed by Scheffé's post hoc test. Calculations were performed with the Winstat standard statistical software package (R. Fitch Software, Bad Krozingen, Germany).

3. Results

3.1. AIF deficiency mediates neuroprotection through a preconditioning effect

3.1.1. AIF gene silencing by siRNA attenuates glutamate toxicity

Downregulation of AIF in HT-22 neurons was achieved using different sequences of AIF-targeting siRNA (AIF siRNA 1, AIF siRNA 12, and AIF siRNA 2). AIF siRNA 12 showed no reduction of AIF expression on mRNA level whereas AIF siRNA 1 and 2 significantly reduced AIF expression at the mRNA level (Figure 4). Thus, AIF siRNA 12 was not used for further experiments. The AIF knockdown achieved with sequences 1 and 2 was further verified by Western blot analysis (Figure 4).

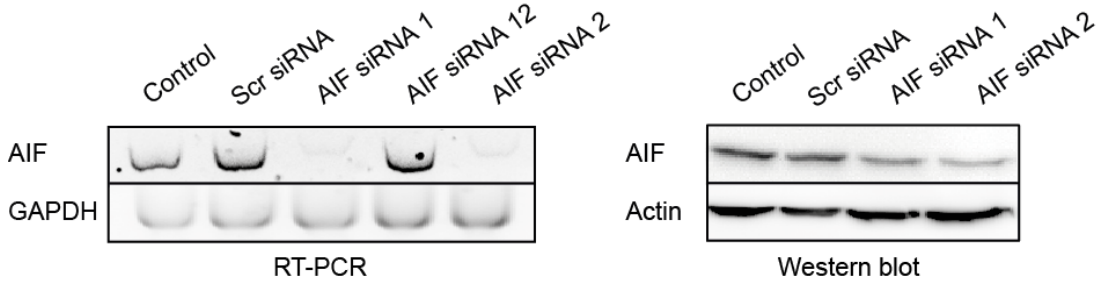

Figure 4: AIF silencing by different AIF siRNA sequences.

AIF knockdown was verified by RT-PCR and Western blot analysis 72 hours after transfection. AIF expression of AIF siRNA (20 nM) transfected cells was compared to non-transfected control cells and cells treated with scrambled (scr) siRNA (20 nM).

AIF silencing significantly attenuated glutamate-induced apoptosis in HT-22 neurons. HT-22 cells exposed to glutamate for 11-18 hours showed typical morphology of cell death: the neuronal cells appear rounded and shrunken, and detached from the culture dish, whereas cells pretreated with AIF siRNA preserved their normal spindle-shaped morphology and were rescued from glutamate-induced apoptosis (Figure 5 A). Cell viability was quantified using the MTT assay, which confirmed the protective effect of AIF siRNA 1 and 2 (Figure 5 B, C). Further, real-time detection of cell death was performed by cell impedance measurements over at least 15 hours with the xCELLigence system, which revealed delayed cell death in AIF-silenced cells. The most pronounced protective effects were achieved with transfection of AIF siRNA 2, which showed sustained protection against cell death and proliferation over time similar to control cells transfected with scrambled siRNA (Figure 5 E). In contrast, AIF siRNA 1 provided only transient protective effects with a delay of cell

death of 1-2 hours compared to controls exposed to glutamate (Figure 5 D). However, time of protection varied in the experiments depending on the sensitivity, passage, and density of the HT-22 cells.

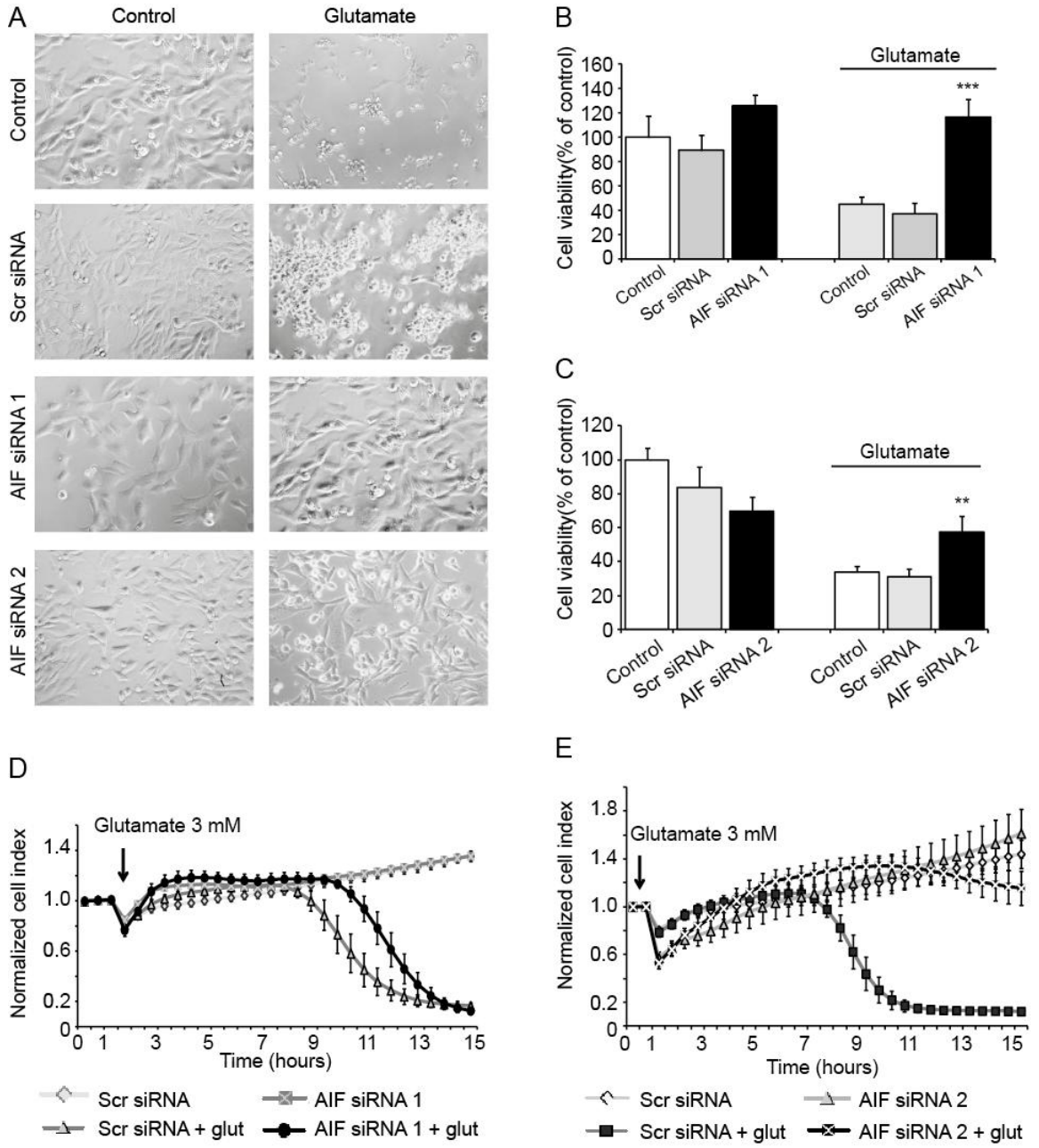

Figure 5: AIF knockdown by different AIFsiRNA sequences attenuates glutamate toxicity.

A: AIF siRNA (20 nM) prevents glutamate-induced (5 mM, 12 h) apoptosis. 100 x magnitude. **B:** MTT assay confirms the protective effect of AIF depletion by AIF siRNA 1 (20 nM) following glutamate exposure (5 mM, 11 h) (n = 7; *** $p < 0.001$, compared to glutamate-treated control and scrambled (scr) siRNA). **C:** MTT assay 72 hours after transfection shows protective effect of AIF siRNA 2 (20 nM) towards glutamate exposure (3 mM, 12 h) (** $p < 0.01$; n = 6, compared to glutamate-treated control and scrambled (scr) siRNA). All statistics were obtained using ANOVA, Scheffé test. **D, E:** xCELLigence real-time impedance measurement: HT-22 cells were treated with glutamate (glut, 3 mM) 72 hours after transfection. **D:** AIF siRNA 1 (20 nM) shows short transient protective effect against glutamate-induced cell death compared to cells transfected with scrambled (scr) siRNA (n = 5). **E:** AIF siRNA 2 (20 nM) shows stronger protection over time (n = 8).

3.1.2. AIF siRNA preserves mitochondrial integrity and function from glutamate damage

In order to investigate if the protective effect of AIF deficiency was attributed to a preconditioning effect at the level of mitochondria, mitochondrial morphology and function were examined. Neurons exposed to glutamate toxicity show disturbed mitochondrial morphology dynamics resulting in detrimental mitochondrial fragmentation (Grohm et al., 2010). Under standard culture conditions, HT-22 cells predominantly expose elongated mitochondria with a tubular network, which are equally distributed throughout the cytosol. This morphology is described as category I. Category II contains cells that are still viable and mitochondria which are already partly fragmented resulting in short tubules and small round fragments. In contrast, cells of category III contain mitochondria which are highly fragmented and accumulate close to the nucleus. In addition, cells of category III show signs of cell death such as pyknotic nuclei.

The increased rate of mitochondrial fission in damaged HT-22 cells as well as peri-nuclear accumulation of the organelles after exposure to glutamate was prevented by AIF siRNA 1 and 2 (Figure 6). AIF-silenced HT-22 cells receiving glutamate showed significantly reduced category III mitochondria compared to control cells and cells transfected with scrambled siRNA treated with glutamate. The amount of category I mitochondria in AIF-depleted cells exposed to glutamate and in untreated controls was similar. This result suggests that the protective mechanism underlying AIF deficiency occurs before the release of AIF from the mitochondria into the cytosol.

To prove this conclusion, the formation of lipid peroxides was investigated, which is associated with irreversible mitochondrial damage and increased ROS production. AIF-silenced cells showed significantly reduced production of lipid peroxides compared to controls exposed to glutamate and significantly attenuated the secondary increase in lipid peroxidation that was associated with mitochondrial damage and cell death in this model system (Cregan et al., 2002) (Figure 7 A). Again, AIF siRNA 2 mediated stronger protective effects compared to AIF siRNA 1, and also showed protective effects after 11 hours of glutamate treatment, whereas cells transfected with AIF siRNA 1 already showed an increase in lipid peroxides 9 hours after glutamate treatment. For that reason AIF siRNA 2 was used for further investigations.

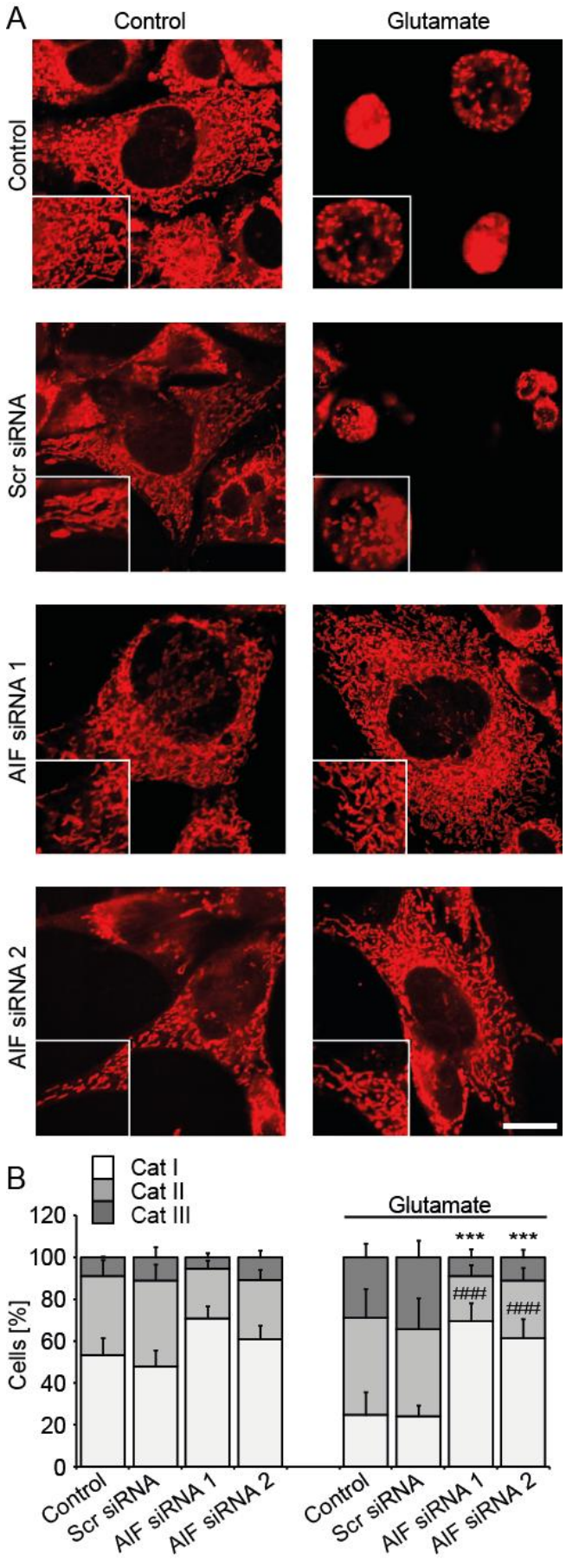

Figure 6: AIF gene silencing provides mitochondrial fission.

A: Fluorescence photomicrographs show that AIF siRNA (20 nM) prevents the fission of mitochondria in glutamate-exposed (3 mM, 14 h) HT-22 neurons. Cells were stained with MitoTracker DeepRed 30 minutes before the glutamate treatment. Bar scale 20 µm. **B:** Quantification of mitochondrial morphology: Category I (Cat I): fused, Category II (Cat II): intermediate, Category III (Cat III): fragmented mitochondria; at least 500 cells were counted per condition blind to treatment conditions. Values are given from six independent experiments (### $p < 0.001$ compared to category I glutamate-treated control and scrambled (scr) siRNA; *** $p < 0.001$ compared to category III glutamate-treated control and scrambled (scr) siRNA). Statistics were obtained using ANOVA, Scheffé test.

Further, ATP levels were examined after glutamate exposure to assess the functional integrity of mitochondria in AIF-depleted cells. Since cell injury results in a rapid decrease in cytoplasmic ATP levels the aim was to find out if the AIF-depleted cells show alterations in ATP levels in the absence or presence of toxic glutamate concentrations. In both cases, ATP levels of AIF-silenced cells were similar to the ATP levels in non-treated control cells and cells transfected with scrambled siRNA (Figure 7 B). The endpoint for the experiment was assessed for the glutamate-treated control cells starting with the onset of cell morphology alteration and culminating in cell detachment and death (Diemert et al., 2012;Tobaben et al., 2011).

In addition, the MMP was investigated in control cells compared to AIF-silenced cells. Under standard culture conditions, AIF-depleted cells showed significantly lower MMP than control cells (Figure 7 C). Further, TMRE staining revealed that glutamate toxicity in non-silenced control cells was associated with pronounced MMP whereas AIF-depleted cells showed significantly higher MMP at the same time point. Carbonyl cyanide chlorophenylhydrazone (CCCP) was applied at the end of the experiment as a positive control for a complete loss of MMP. Further, the slight depolarization under control conditions was verified by DIOC6(3) measurements in isolated mitochondria. These measurements were performed by Dr. Amalia Dolga (Figure 15 D, chapter 3.1.6.).

Taken together, these results suggest a preconditioning effect by AIF depletion which protects HT-22 cells against glutamate toxicity at the level of mitochondria.

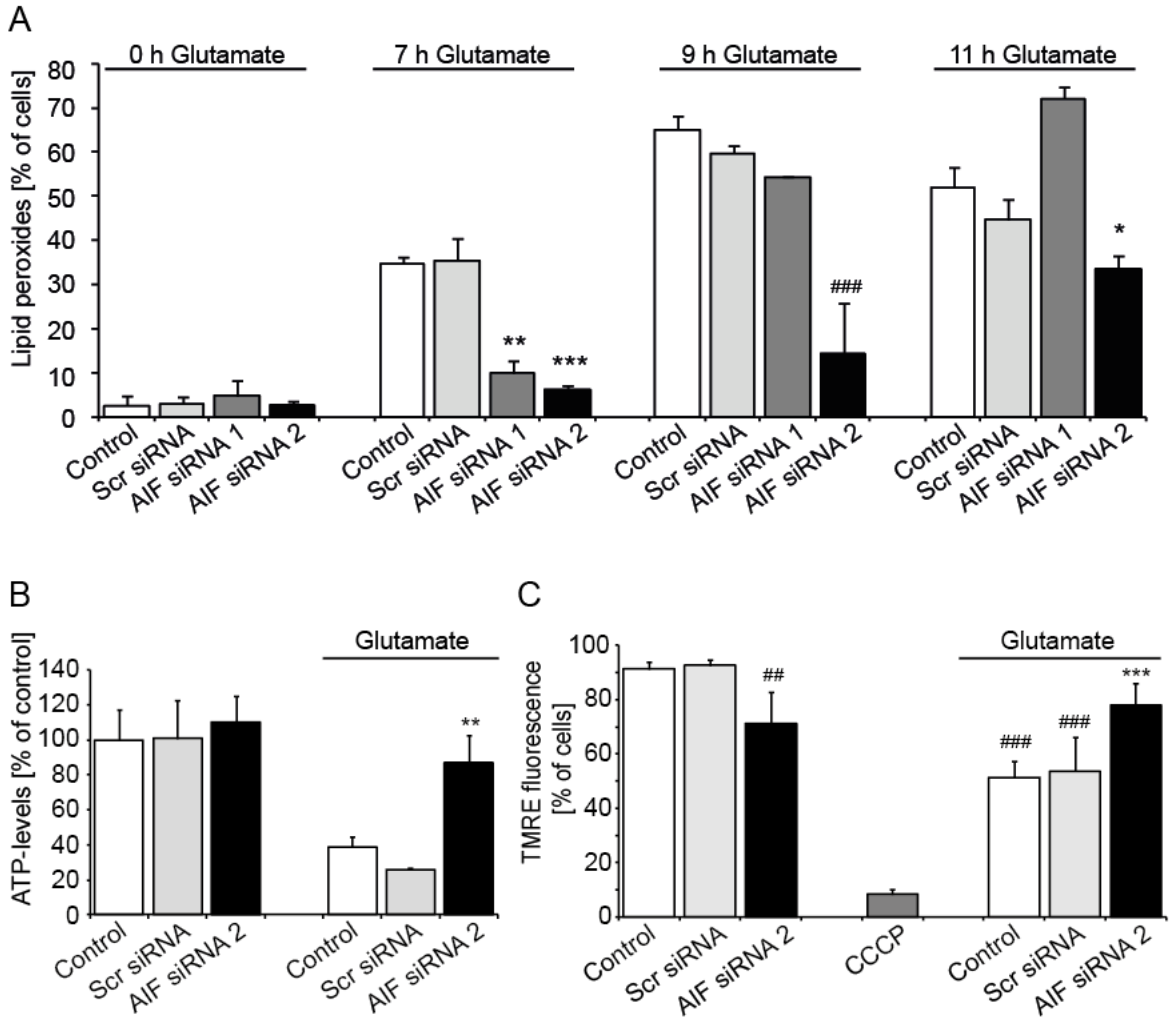

Figure 7: AIF siRNA preserves mitochondrial integrity.

A: Lipid peroxides were measured by BODIPY FACS analysis at indicated time points following glutamate treatment (5 mM). Values are given from three independent experiments; ** $p < 0.01$; *** $p < 0.001$ compared to glutamate-treated (7 h) control and scrambled (scr) siRNA; ### $p < 0.001$, compared to glutamate-treated (9 h) control and scrambled (scr) siRNA; * $p < 0.05$ compared to glutamate-treated control (11 h). **B:** Forty-eight hours after transfection cells were seeded into 96-well plates. Following 24 hours cells were treated with glutamate (3 mM) for 11 hours. ATP levels from AIF-depleted cells (20 nM) were preserved from loss in ATP levels ($n = 6$; ** $p < 0.01$ compared to glutamate-treated control cells and scrambled (scr) siRNA). **C:** MMP, measured by TMRE, is protected from glutamate toxicity (3 mM, 15 h). In AIF-depleted cells MMP is significantly depolarized. Values are given from six independent experiments; ### $p < 0.001$; ## $p < 0.01$ compared to untreated control cells and scrambled (scr) siRNA; *** $p < 0.001$ compared to glutamate-treated control cells and scrambled (scr) siRNA. All statistics were obtained using ANOVA, Scheffé test.

3.1.3. ROS inhibition has no effect on neuroprotection mediated by AIF gene silencing

Preconditioning effects are often described to promote minor decreases in the efficiency of NADH oxidation by the respiratory chain, which increases mitochondrial ROS release followed by activation of mitoK_{ATP} channels (Busija et al., 2008;Dirnagl and Meisel, 2008;Jou, 2008;Ravati et al., 2000;Ravati et al., 2001). To investigate whether this mechanism was also consistent in the applied model system, cells were treated with the antioxidant trolox (6-hydroxy-2,5,7,8-tetramethylchroman-2-carboxylic acid), which should reduce the protective effect of siRNA if resulting from a slight increase in ROS levels. Since trolox alone prevented HT-22 cells from glutamate-induced cell death the experiment was performed with a trolox pretreatment starting with the transfection followed by a washout 24 hours before the glutamate treatment (Figure 8 A). In this way, overlapping protective effects of AIF silencing and trolox were avoided. The trolox pretreatment did not change the protection against glutamate toxicity mediated by AIF siRNA 2 (Figure 8 B). This result was in accordance with the fact that lipid peroxide levels remained unchanged in AIF-silenced HT-22 cells (chapter 3.1.2.).

These results suggest that increased ROS production in AIF-depleted cells is not the major mechanism of the observed preconditioning effect.

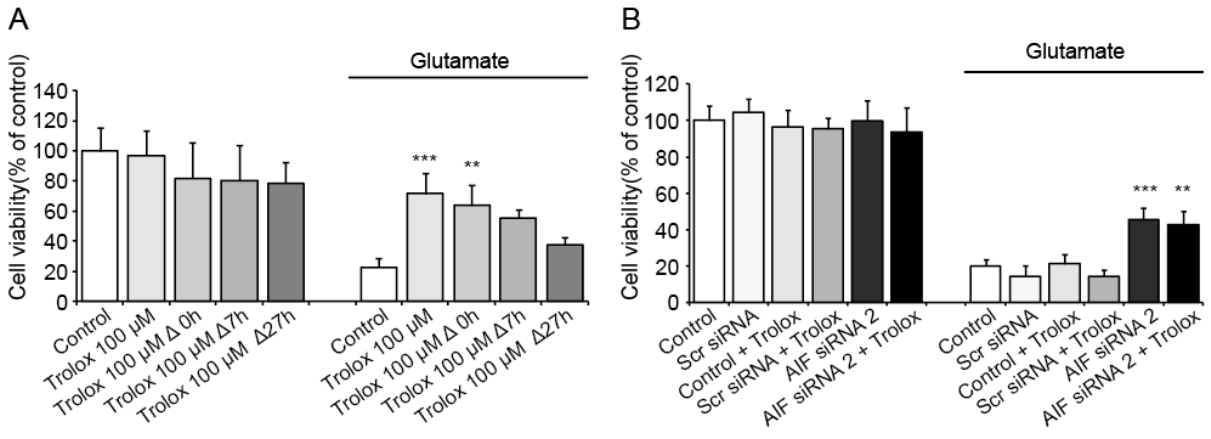

Figure 8: Trolox pretreatment does not affect neuroprotection mediated by AIF deficiency.

A: HT-22 cells were pretreated with trolox (100 µM). Forty-eight hours later the cells were seeded in a 96-well plate. The following day cells were treated with glutamate. Trolox was removed at different time points before glutamate treatment (3 mM; 13 h) (Δ = time between trolox washout and glutamate treatment; n = 8). *** $p < 0.001$, ** $p < 0.01$ compared to glutamate-treated control cells. **B:** Trolox pretreatment (100 µM, 48 h; Δ = 24 h) did not affect neuroprotection mediated by AIF siRNA 2 (n = 8). *** $p < 0.001$, ** $p < 0.01$ compared to glutamate-treated (3 mM, 11 h) control cells and scrambled (scr) siRNA. Statistics were obtained using ANOVA, Scheffé test.

3.1.4. AMPK is not affected in the AIF deficiency model system of HT-22 cells

AMPK is a serine/threonine kinase containing a catalytic α subunit and regulatory β and γ subunits. Under stress conditions energy is consumed and AMPK activation leads to altered cellular metabolism and gene expression to inhibit anabolic processes, stimulate catabolism, and restore ATP levels (Ronnett et al., 2009). In 2007 Pospisilik et al. demonstrated that AMPK is activated in muscle-specific AIF knockout mice without apparent changes in AMPK protein expression (Pospisilik et al., 2007). Thus, it was investigated here, whether AIF gene silencing in HT-22 neurons mediated neuroprotection through AMPK regulation. The AMPK activator AICAR (5-aminoimidazole-4-carboxamide-1-β-D-ribofuranoside) significantly attenuated glutamate toxicity in HT-22 cells in a concentration-dependent manner (Figure 9 A). However, AICAR also exerted slightly toxic effects under control conditions and reduced cell proliferation (Figure 9 A, B). In combination with AIF-silenced neurons AICAR did not affect the protective effect of AIF depletion (Figure 9 C) but the proliferation rate was decreased as detected by the xCELLigence system (Figure 9 B).

Interestingly, AMPK inhibition by compound C also preserved HT-22 cells in a concentration-dependent manner already in the µM range (Figure 10 A). Compound C did not show toxic effects in HT-22 cells, and the neuroprotective effect mediated by AIF-depleted cells was further increased by compound C (Figure 10 B, D).

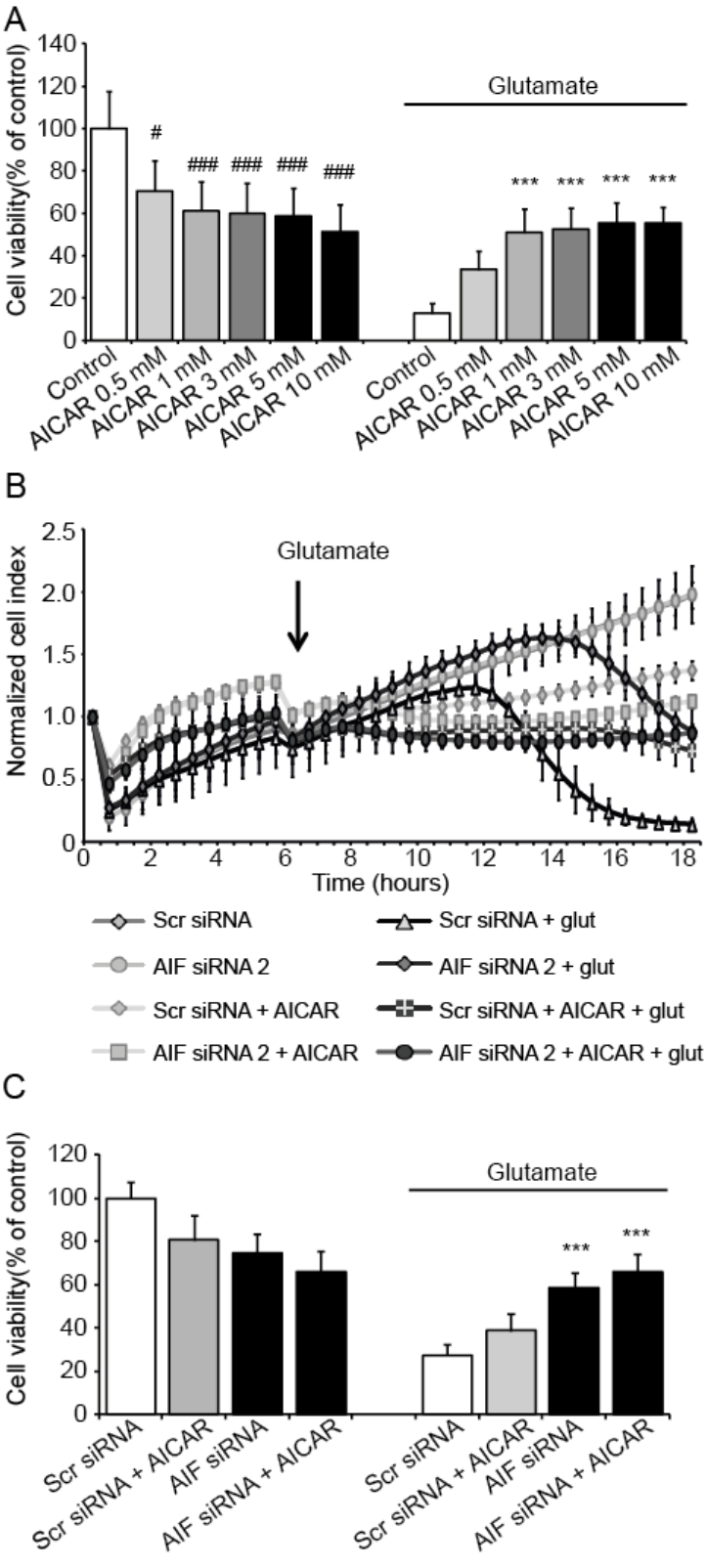

Figure 9: Protective effect of AICAR in HT-22 cells.

A: HT-22 cells were treated with different concentrations of AICAR for 6 hours pretreatment followed by a co-treatment with glutamate (3 mM, 13 h); *** $p < 0.001$ compared to glutamate-treated control cells; # $p < 0.05$, ### $p < 0.001$ compared to untreated control cells; n = 8. **B:** Real-time impedance measurement of HT-22 cells transfected with AIF siRNA 2 (20 nM) and treated with AICAR (5 mM, 6 h pretreatment) and glutamate (3 mM) (n = 5). **C:** Cell viability of AIF-depleted cells treated with AICAR (3 mM, 6 h pretreatment) followed by 10 h exposure to glutamate (4 mM, 10 h) was determined by MTT assay. * $p < 0.05$, *** $p < 0.001$ compared to glutamate-treated scrambled (scr) siRNA; ### $p < 0.001$ compared to glutamate-treated AIF siRNA 2 (n = 6). All statistics were obtained using ANOVA, Scheffé test.

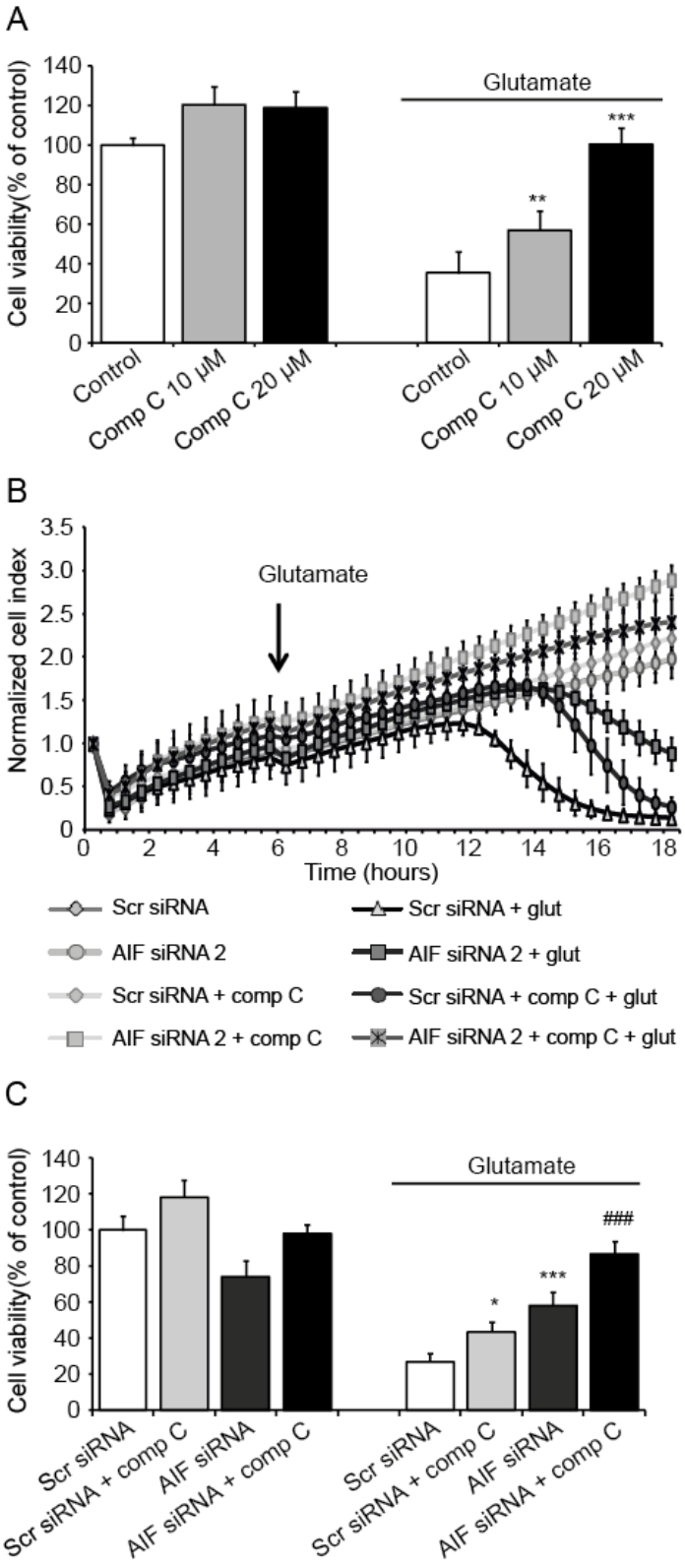

Figure 10: Compound C exerts additive protective effects on AIF-depleted cells in providing neuroprotection against glutamate toxicity.

A: HT-22 cells were treated with different concentrations of compound C (comp C) for 6 h pretreatment followed by a co-treatment with glutamate (2 mM, 11 h). *** $p < 0.001$, ** $p < 0.01$ compared to glutamate-treated control cells (n = 8). **B:** Real-time measurement of HT-22 cells transfected with AIF siRNA 2 (20 nM) and treated with compound C (5 µM, 6 h pretreatment) subsequent glutamate treatment (3 mM) (n = 5). **C:** Cell viability of AIF-depleted cells co-treated with compound C (5 µM, 6 h pretreatment) followed by 10 hours co-treatment with glutamate (4 mM, 10 h) was determined by MTT assay. * $p < 0.05$, *** $p < 0.001$ compared to glutamate-treated scrambled (scr) siRNA; ### $p < 0.001$ compared to glutamate-treated AIF siRNA 2 (n = 6). All statistics were obtained using ANOVA, Scheffé test.

Furthermore, Western blot analyses were performed to investigate effects of AIF depletion on AMPK protein expression levels. After AIF downregulation, however, changes in the levels of p-AMPK, which is the activated form of AMPK, or the basal AMPK levels were not detected (Figure 11 A). As a positive control for the antibodies, cell lysates of HT-22 cells treated with AICAR or compound C were used. The downregulation of AMPK by compound C was confirmed by Western blot. Interestingly, the inhibition of AMPK also mediated decreased AIF expression levels. After exposure to AICAR, a slight increase in p-AMPK could be detected whereas the basal AMPK levels remained unchanged.

These results suggest that AMPK does not play a major role for the neuroprotective effects mediated by AIF depletion in the HT-22 model system.

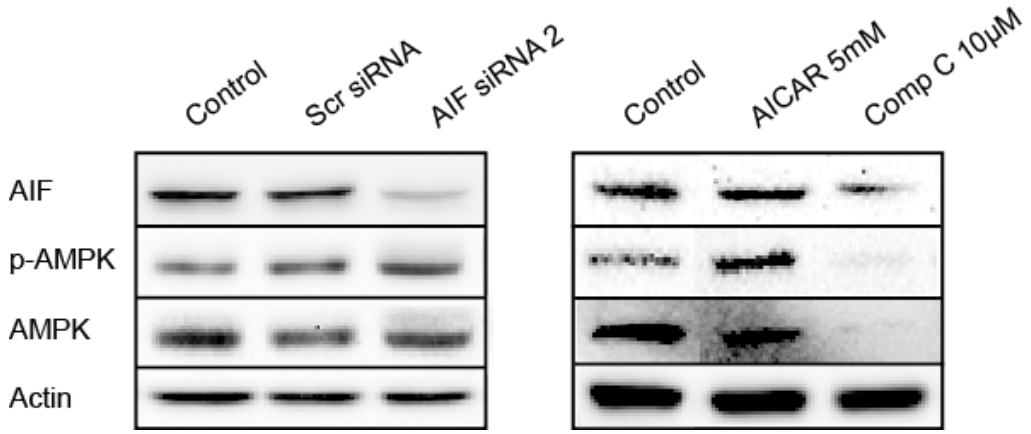

Figure 11: Western blot analysis of AMPK expression levels in HT-22 neurons.

Protein expression levels were determined 72 hours after transfection. No changes in p-AMPK or AMPK levels could be detected. As control for the antibodies cells were treated with compound C (10 µM, 16 h) or AICAR (5 mM, 16 h).

3.1.5. Silencing of AIF mediates a decrease in mitochondrial complex I expression

Previous studies in different model systems implied that AIF-deficiency may reduce levels of mitochondrial complex I (Benit et al., 2008;Vahsen et al., 2004). Thus, the mitochondrial complex protein expressions were detected by Western blot analysis in AIF-silenced HT-22 cells. AIF-depleted cells showed significantly reduced levels of complex I 72 hours after transfection. Other complexes of the respiratory chain were not significantly affected by AIF siRNA in the used cell line compared to control cells and cells transfected with scrambled siRNA. Interestingly, inhibition of mitochondrial complex I by rotenone (20 nM) was associated with slightly decreased expression levels of AIF (Figure 12 A, B). This suggests that mitochondrial complex I and AIF may regulate each other's stability in mitochondria. Furthermore, rotenone treatment did not only affect complex I, but also decreased complex II, IV, and V (Figure 12 A).

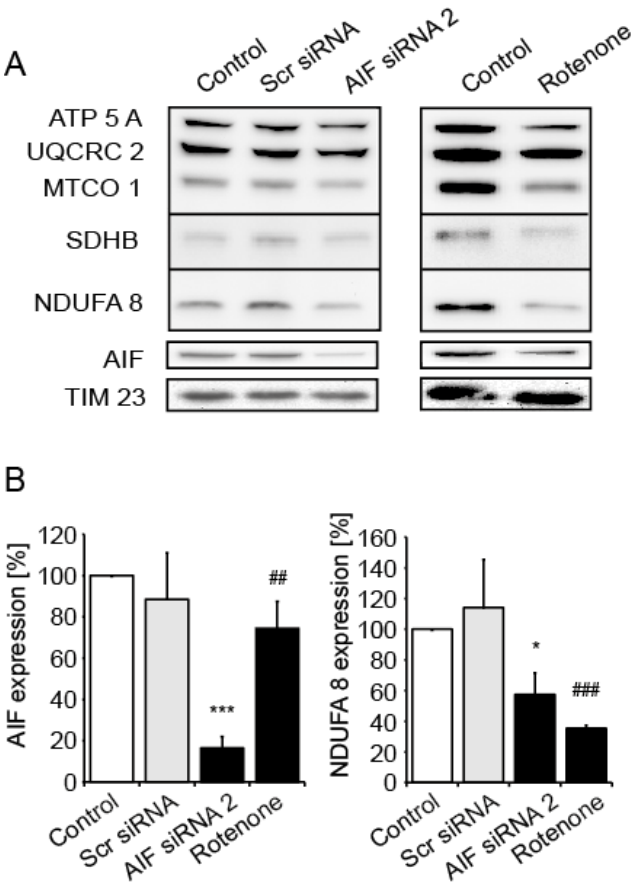

Figure 12: Preconditioning effect mediated by mitochondrial complex I down-regulation.

A: Western blots of mitochondrial enriched cell extracts (30 µg) show that AIF depletion leads to a downregulation of complex I (NDUFA 8: NADH dehydrogenase (ubiquinone) 1 alpha subcomplex 8) 72 hours after transfection. Other complexes showed no significant changes in their expression after AIF depletion (ATP 5A: ATP synthase (complex V); UQCRC 2: ubiquinol-cytochrome c reductase core protein 2 (complex III); MTCO 1: mitochondrially encoded cytochrome c oxidase 1 (complex IV); SDHB: succinate dehydrogenase complex, subunit B (complex II)). Furthermore, rotenone treatment (20 nM, 18 h) leads to a slight decrease of AIF expression. **B:** Quantification of Western blot analysis. AIF and NDUFA 8 specific bands were normalized to TIM 23. Values are given as percentage of control from four independent experiments. *** $p < 0.001$, * $p < 0.05$ compared to scrambled (scr) siRNA; ## $p < 0.01$, ### $p < 0.001$ compared to control .

3.1.6. Low dose rotenone treatment preserves cells from glutamate neurotoxicity

To further link the determined protective effects of AIF-deficient cells with the downregulation of mitochondrial complex I it was tested if inhibition of complex I by rotenone also resulted in a neuroprotective effect in the applied model system. The specific complex I inhibitor rotenone protected HT-22 cells against glutamate toxicity in a concentration-dependent manner as determined by the MTT assay (Figure 13 A). Higher concentrations of rotenone (> 50 nM) induced apoptosis in HT-22 neurons (Figure 13 B).

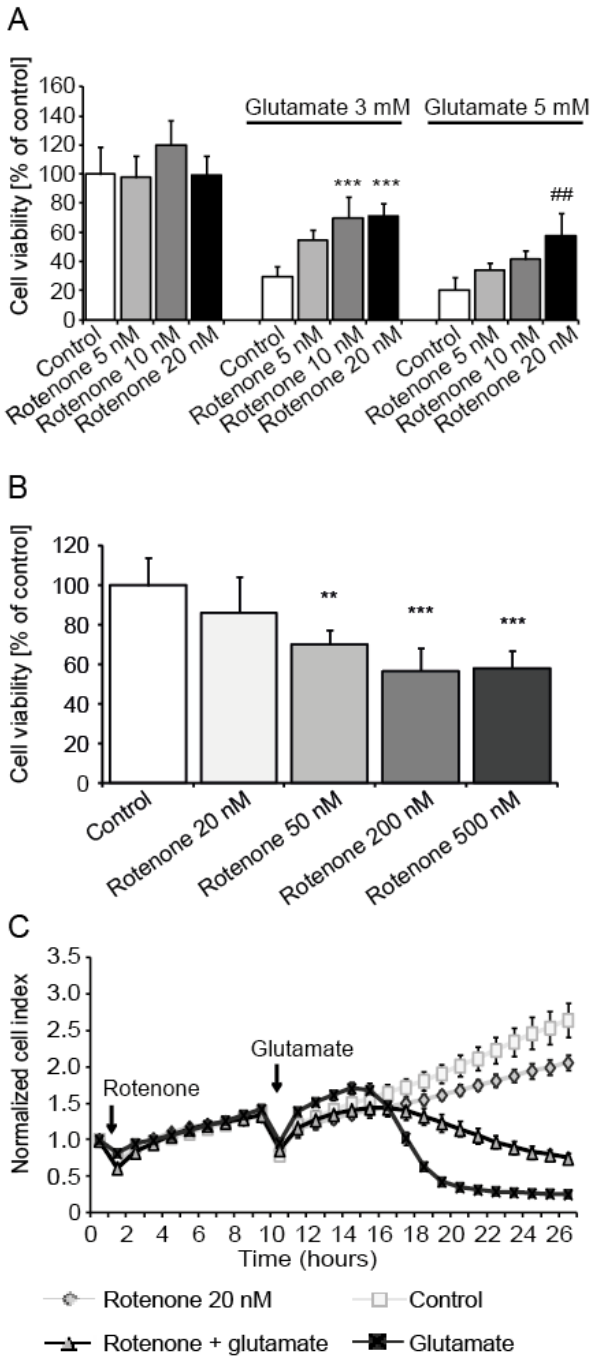

Figure 13: Low dose rotenone leads to transient neuroprotective effects by preconditioning.

A: MTT assays show that rotenone (10 nM and 20 nM) is able to protect HT-22 cells from glutamate-induced (3 and 5 mM, 13 h) cell death (n = 8; *** p < 0.001 compared to glutamate-treated control (3 mM); ## p < 0.01 compared to glutamate-treated control (5 mM); ANOVA, Scheffé test). **B:** Cells treated with higher doses of rotenone (50 nM, 200 nM, and 500 nM, 15 h) undergo apoptosis. (n = 8; **p < 0.01; ***p < 0.001; ANOVA, Scheffé test). **C:** HT-22 cells were plated on a 96-well E-plate and cellular impedance was continuously monitored by the xCELLigence system. Cells were pretreated with rotenone 20 mM for 9 hours. After washout of rotenone pretreated cells showed a transient protective effect against glutamate-induced cell death (3 mM) (n = 6).

Similar to AIF-silencing the neuroprotective effect was just transient when measuring cell viability by impedance measurements (Figure 13 C). The neuroprotective effect was observed in a co-treatment of rotenone and glutamate (Figure 13 A) as well as in a rotenone pretreatment followed by a washout before adding glutamate (Figure 13 C).

Notably, mitochondrial fragmentation as a sign of disturbed mitochondrial morphology dynamics was also attenuated when cells were treated with rotenone (Figure 14 A, B). After glutamate exposure, rotenone receiving cells showed higher amounts of long tubular mitochondria of category I compared to control cells and lower amounts of fragmented mitochondria of category III whereas glutamate-treated controls had mostly fragmented mitochondria that were located around the nucleus.

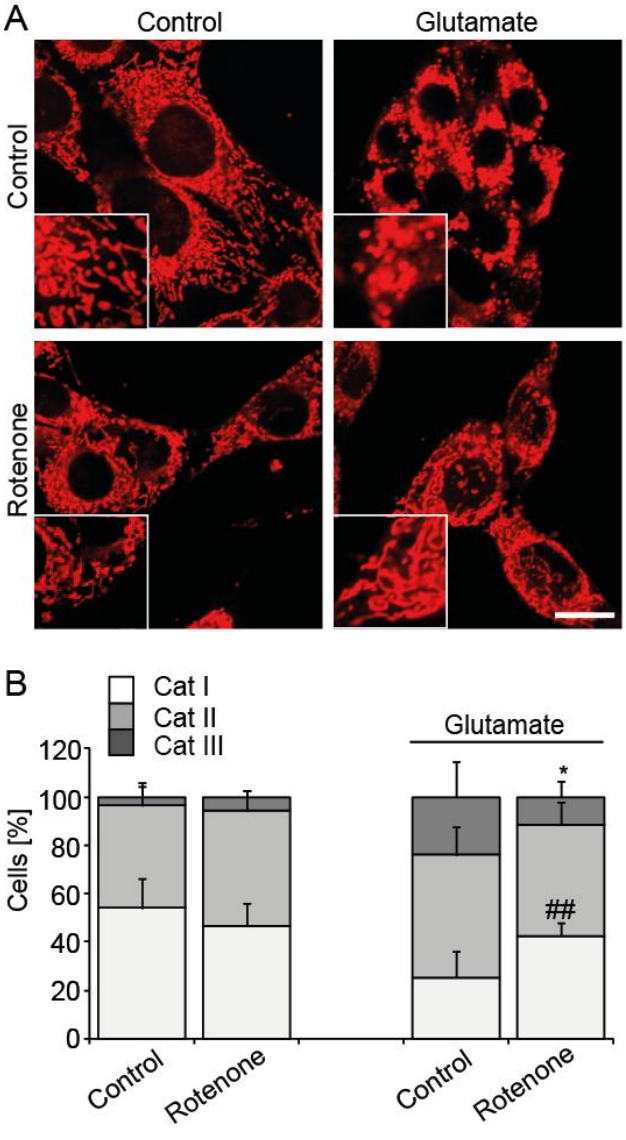

Figure 14: Low doses of rotenone prevent mitochondrial fission.

A: Fluorescence photomicrographs show that rotenone (20 nM) prevents the fission of mitochondria that is apparent in glutamate-exposed (3 mM, 14 h) HT-22 neurons. Cells were stained with MitoTracker DeepRed 30 minutes before glutamate and rotenone treatment. Bar scale 20 µm. **B:** Quantification of mitochondrial morphology: Category I: fused, Category II: intermediate, Category III: fragmented mitochondria; at least 500 cells were counted per condition blinded to treatment conditions (n = 4, * $p < 0.05$; ## $p < 0.01$ compared to glutamate-treated control).

Further, to prove the hypothesis that slight complex I inhibition protected from oxidative stress by a preconditioning effect, levels of lipid peroxides after rotenone treatment were examined. Rotenone alone did not alter lipid peroxide levels under standard culture conditions but it preserved cells from an increase in lipid peroxidation and thus, from further ROS production after the glutamate challenge (Figure 15 A).

Since it is known that strong inhibition of complex I alters cytoplasmic ATP levels (Tretter et al., 2004) HT-22 cells receiving low doses of rotenone were investigated. In a concentration of 20 nM rotenone did not affect basal levels of ATP. However, glutamate-induced loss of ATP levels was prevented by rotenone in the same concentration, which further confirmed rotenone's protective effect at low concentrations (Figure 15 B).

Similar to HT-22 cells transfected with AIF siRNA, next the MMP of rotenone-treated cells was assessed to further test for functional integrity of the organelles. Cells exposed to rotenone-mediated complex I inhibition showed significantly lower MMP than control cells under normal culture conditions. These findings confirmed the conclusion that AIF-silenced cells follow a similar preconditioning effect as rotenone-treated cells, i.e. through reduced activity of mitochondrial complex I. Furthermore, glutamate-induced ultimate mitochondrial depolarization as a late endpoint of mitochondrial damage in this model system of oxytosis was prevented in rotenone-treated cells (Figure 15 C). Again the slight depolarization under culture conditions mediated by rotenone was confirmed by DIOC6(3) staining in isolated mitochondria performed by Dr. Amalia Dolga (Figure 15 D).

Collectively, these results favor the hypothesis that AIF depletion is linked to a decrease in complex I expression levels and respiratory chain activity. These preconditioning effects lead to a stabilization of mitochondria and thus prevent cell death after the glutamate challenge and related induction of oxidative stress (Öxler et al., 2012).

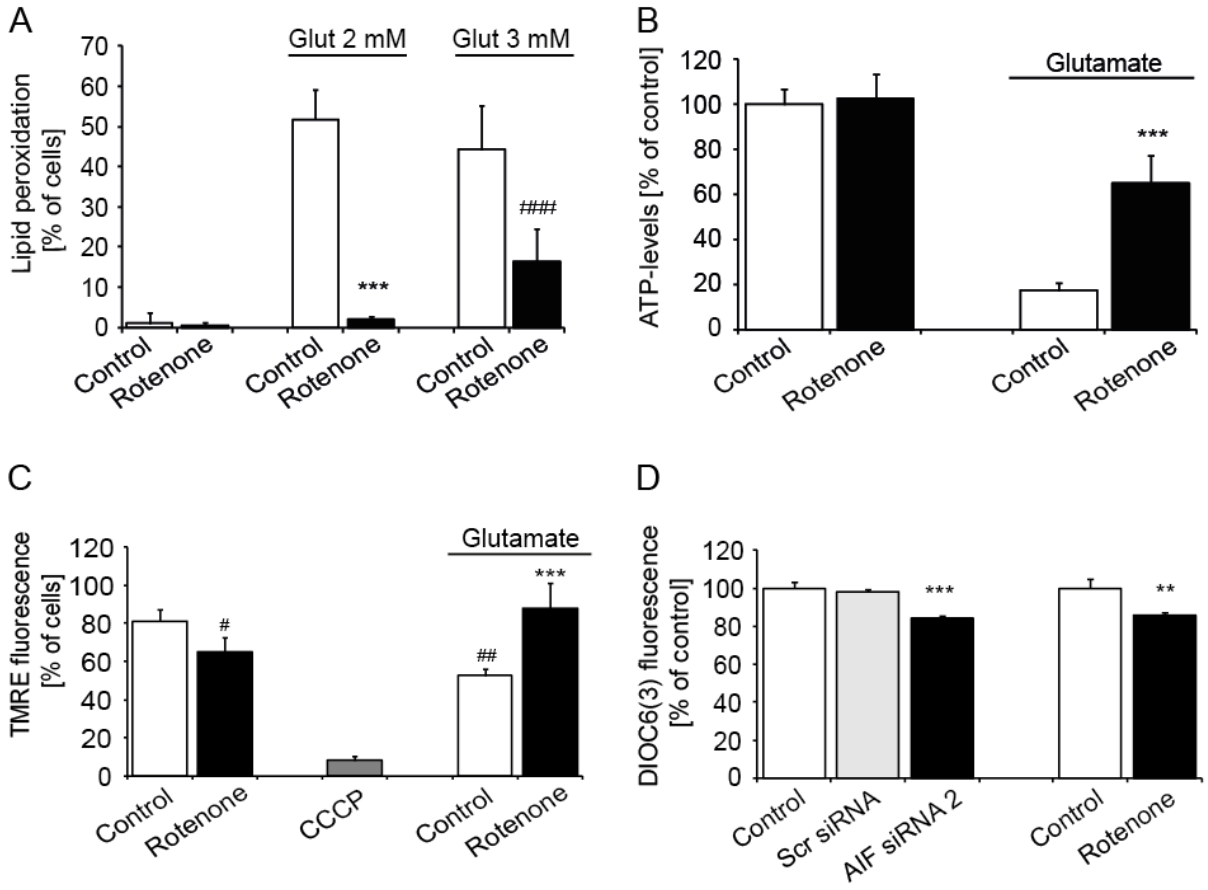

Figure 15: Low doses of rotenone prevent mitochondrial integrity and function.

A: Lipid peroxides were measured by BODIPY FACS analysis 13 hours following glutamate (glut) treatment (2 and 3 mM). Values are given from three independent experiments; *** $p < 0.001$ compared to glutamate-treated control cells (2 mM); ### $p < 0.001$ compared to glutamate-treated control cells (3 mM). **B:** Rotenone receiving cells (20 nM) were preserved from loss in ATP levels 14 hours after glutamate treatment (3 mM). N = 8; *** $p < 0.001$ compared to glutamate-treated control cells. **C:** MMP measured by TMRE is significantly (# $p < 0.05$) decreased by rotenone (20 nM, 15 h) compared to control cells. After glutamate treatment (3 mM, 15 h) MMP is significantly increased by rotenone (20 nM) (*** $p < 0.001$) compared to glutamate-treated control cells (n = 4). ## $p < 0.01$ compared to untreated control. **D:** Seventy-two hours after transfection MMP was measured by DIOC6(3) assay. AIF-depleted mitochondria and rotenone receiving cells (20 nM, 18 h) are depolarized (n = 3; *** $p < 0.001$; ## $p < 0.01$ compared to control).

3.2. Neuroprotection mediated by NPC-derived conditioned medium

3.2.1. NPCs undergoing starvation in a caspase-dependent manner protect neuronal cells against damage by growth factor withdrawal and glutamate toxicity

In this study the aim was to mimic the conditions after NPC transplantation in vivo by withdrawal of growth factor support of cultured NPCs in vitro. To this end, cultured NPCs were deprived of both EGF and bFGF. As expected, such growth factor withdrawal induced apoptotic cell death in the NPCs which rounded up and partly detached from the surface of the culture plate within 24 hours (Figure 16 A) (Diemert et al., 2012). The medium from the dying NPCs was collected and investigated in HT-22 cells for attenuating oxidative stress induced by glutamate and growth factor withdrawal on the basis of EBSS. CM attenuated the glutamate toxicity as detected by MTT cell viability assays. Furthermore, CM prevented cell death induced by EBSS treatment alone which, depending on the sensitivity of HT-22 cells, also induces starvation (Figure 17 A).

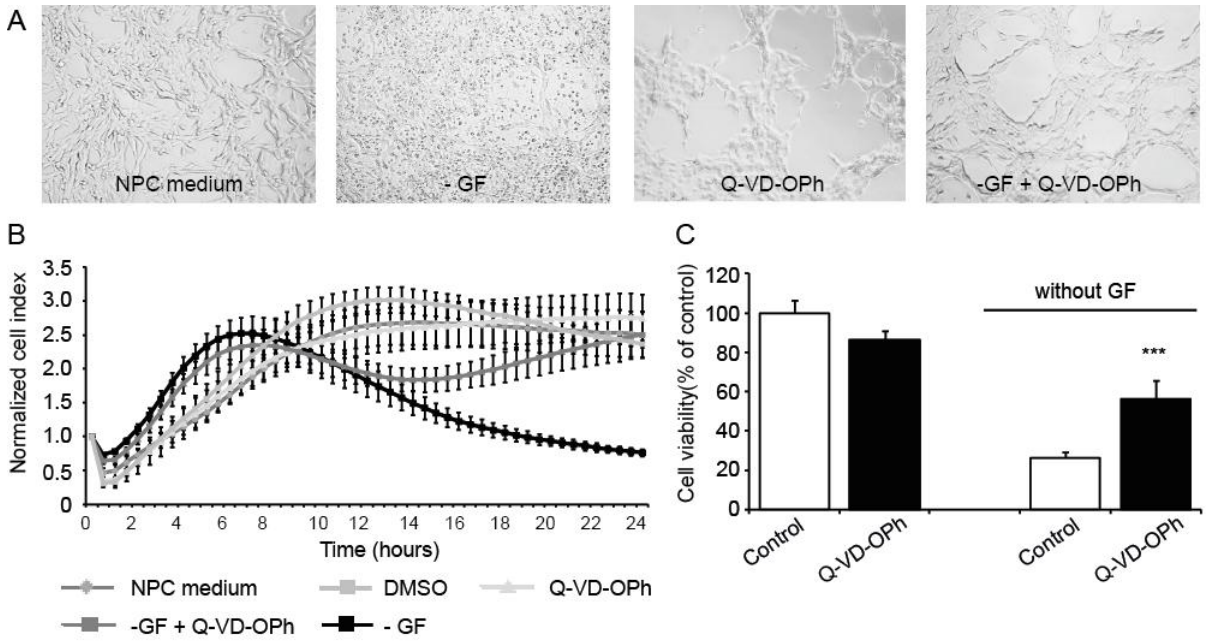

Figure 16: NPCs cultivated without growth factors EGF and bFGF undergo starvation.

A: Representative pictures of the cell morphology of NPCs deprived of growth factors (24 h) +/− Q-VD-OPh co-treatment (40 µM). **B:** Measurement of cellular impedance of NPCs grown with and without growth factors (GF). Co-administration of the pan-caspase inhibitor Q-VD-OPh (40 µM) prevents cell death induced by starvation; n = 5. **C:** Quantification of cell death by MTT assay 24 hours after growth factor withdrawal (n = 12; *** $p < 0.001$ compared to glutamate-treated control; ANOVA, Scheffé test).

To rescue NPCs from EBSS-induced starvation, cells were treated with the broad caspase inhibitor Q-VD-OPh (N-(2-Quinolyl)valyl-aspartyl-(2,6-difluorophenoxy) methyl ketone). Q-VD-OPh is a cell-permeable, irreversible caspase inhibitor that exhibits anti-apoptotic properties against all major caspase-mediated cellular apoptosis pathways. This inhibitor prevented NPCs from EBSS-induced cell death (Figure 16 A-C). DMSO in the same concentration as in the resulting Q-VD-OPh probe was used to exclude damage mediated by the solvent. This is in line with former experiments of Stefanie Neunteibl showing that EBSS-induced starvation in NPCs leads to cleavage of caspase-3 (personal communication).

CM obtained from NPCs rescued by Q-VD-OPh failed to prevent apoptosis induced by glutamate in HT-22 cells (Figure 17 B). Importantly, Q-VD-OPh alone does not protect HT-22 cells from glutamate.

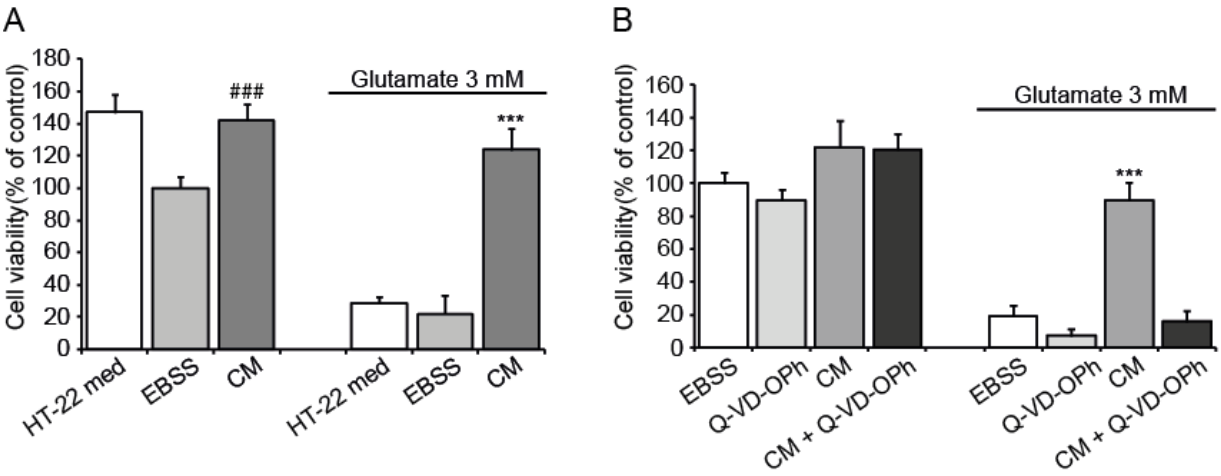

Figure 17: CM from dying NPCs protects HT-22 cells.

A: NPC CM protected HT-22 cells against growth factor withdrawal (–GF) and glutamate-induced toxicity (3 mM, 15 h) demonstrated by MTT assays; (n = 8, *** $p < 0.001$; ANOVA, Scheffé test). **B:** CM produced from NPCs prevented from cell death by the broad caspase inhibitor Q-VD-OPh (40 µM) showed no protective effect from glutamate-induced apoptosis (3 mM, 15 h) in HT-22 cells. CM produced from dying NPCs was used as positive control. The experiment was repeated two times independently (n = 6, *** $p < 0.001$, ANOVA, Scheffé test).

3.2.2. Heating increases the protective effect of CM

To further specify which components were responsible for the protective effect of CM a temperature gradient with diluted CM 1:4 was applied. Diluted CM pre-incubated at room temperature did not show a protective effect against glutamate-induced cell death in HT-22 cells. Surprisingly, significant protection was achieved after heating the medium up to 50-80°C (Figure 18 A), with a maximum protective effect obtained at 60°C. Real-time analyses using impedance measurements confirmed that NPC CM heated at 60°C exerted sustained protective effects compared to native NPC CM that was pre-incubated at room temperature (Figure 18 B). Higher temperatures up to more than 90°C destroyed the protective effect and heating at 100°C even resulted in toxic effects (Figure 18 A). This result can be explained either by an activation of substances at about 60°C or by an inactivation of toxic components or substances and enzymes which antagonized the protective contents. Furthermore, protective substances in CM seem to be heat stable at temperatures up to 80°C.

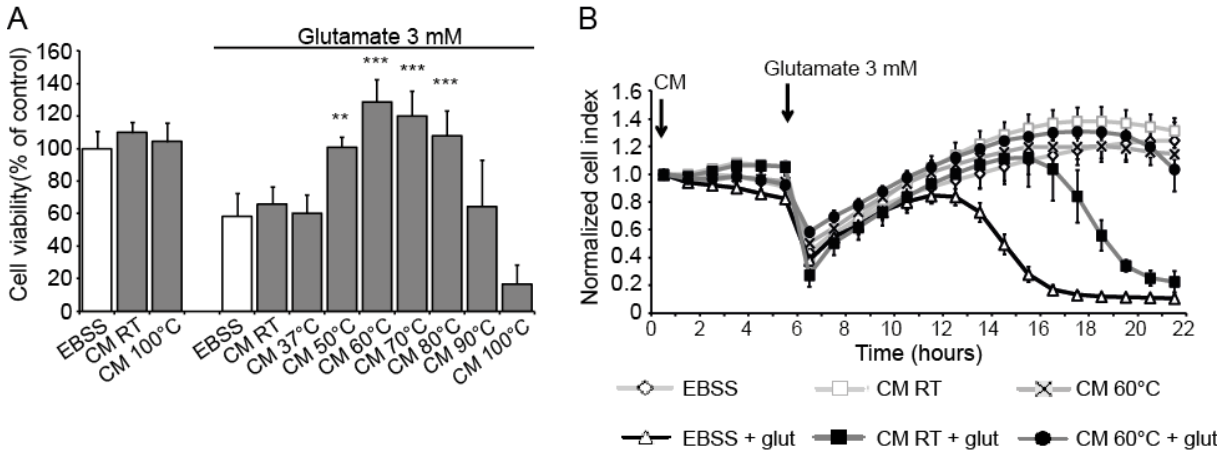

Figure 18: Heat activation of NPC CM.

A: Diluted NPC CM (1:4) was incubated at different temperatures for 30 minutes before pretreatment in HT-22 cells. MTT assay demonstrated a protective effect against glutamate-induced neurotoxicity (3 mM) mediated by NPC CM heated up at 50-80°C but not at 37°C, 90°C, or 100°C (n = 6; ANOVA, Scheffé Test). **B:** HT-22 cells were plated on a 96-well E-plate and cellular impedance was continuously monitored by the xCELLigence system. NPC CM heated up to 60°C for 10 minutes showed significant longer protection against glutamate (glut) toxicity (3 mM) compared to CM kept at room temperature (RT) (n = 3).

3.2.3. Identification of the chemical nature of compounds responsible for the neuroprotective effect of CM

The next step was to identify the chemical nature of the contents mediating the neuroprotective effect of NPC CM. Since it is known that various miRNAs can have protective effects in models of neurodegenerative diseases, such as AD (Wang et al., 2008), CM was treated with RNase, which was inactivated by heat before treating HT-22 cells. However, the RNase treatment did not alter the protective effect of CM (Figure 19 A).

Next, CM was treated with protease to test if proteins are responsible for the neuroprotective effect. Pretreatment of CM with protease showed a very strong reduction in cell viability (Figure 19 B), which is may be explained by toxic degradation products.

Since proteases may have other unspecific effects, including accumulation of toxic degradation products, aceton precipitation with CM was performed. Such precipitation and dilution of precipitate should verify that the protective effect of CM resulted from proteins. Interestingly, the precipitated proteins resulting after centrifugation of the mixture of CM and aceton were still active and also showed strong neuroprotection against glutamate-induced cell death (Figure 19 C). In addition, the neuroprotective activity of the aceton precipitate was further accelerated by heating. As demonstrated in Figure 19 D, heating of the precipitate to 50°C or 60°C for 10 minutes significantly increased the protective effect compared to precipitate that was kept at 37°C.

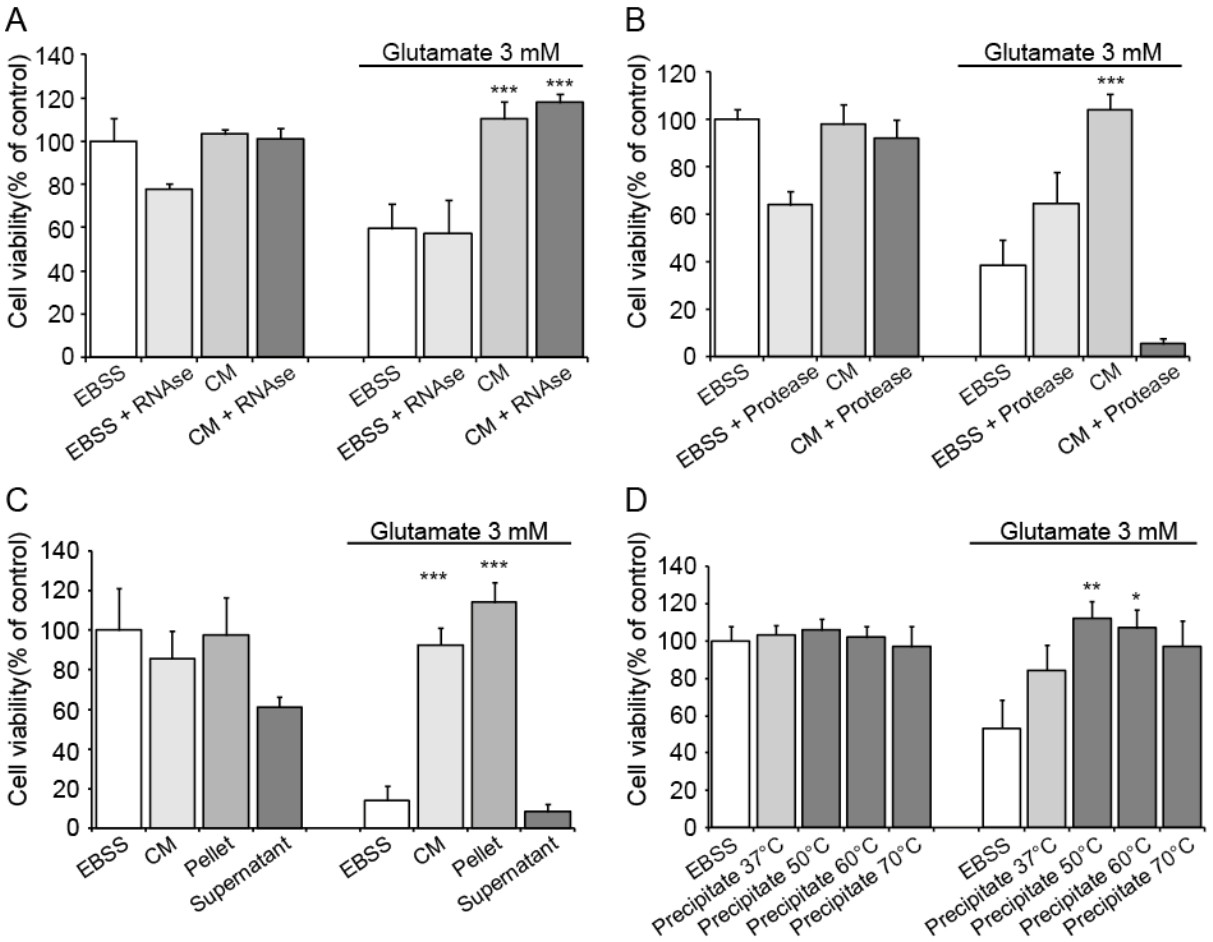

Figure 19: Investigation of the chemical nature of protective components in CM.

A: NPC CM pretreated with RNase showed no reduction in protective effects against glutamate damage (3mM, 15 h) compared to untreated NPC CM in HT-22 cells (n = 5, *** $p < 0.001$). **B:** NPC CM pretreated with protease failed to prevent glutamate-induced toxicity (3 mM, 18 h) in HT-22 cells. CM without protease treatment was used as positive control (n = 8, *** $p < 0.001$). **C:** Proteins in NPC CM were precipitated by aceton. After separation by centrifugation precipitated proteins (pellet) showed significant neuroprotection against glutamate damage (3 mM, 16 h) in HT-22 cells. Supernatant failed to prevent cells from apoptosis (n = 5, *** $p < 0.001$). **D:** Precipitates from NPC CM pretreated with aceton were heated up at 37-70°C for 10 minutes. Precipitates at 50°C and 60°C showed significant stronger protective effects against glutamate toxicity in HT-22 cells as precipitate heated up to 37°C (n = 8, * $p < 0.05$, ** $p < 0.01$). All statictics were obtained with ANOVA, Scheffé test. All results were verified by at least three independent experiments.

3.2.4. Inhibition of protein synthesis during starvation

To further investigate if the protective proteins in CM are already existent in cells under standard culture conditions or if they are produced only during cell death after growth factor withdrawal, CM was produced in the presence of protein synthesis inhibitors. Afterwards, this CM was tested for protective effects in HT-22 cells. The antibiotic actinomycin D and the fungicide cycloheximide (CHX) were used for inhibition of protein synthesis. To first determine at which concentrations these inhibitors were tolerated in NPCs, different concentrations of actinomycin D and CHX were tested under standard culture conditions. As shown in Figure 20 both substances already exert toxic effects at concentrations in the nanomolar range. To ensure that NPCs still undergo starvation in the presence of protein synthesis inhibitors the same concentrations were tested in NPCs treated with EBSS (Figure 20). Neither actinomycin D nor CHX provided any protective effect against growth factor withdrawal.

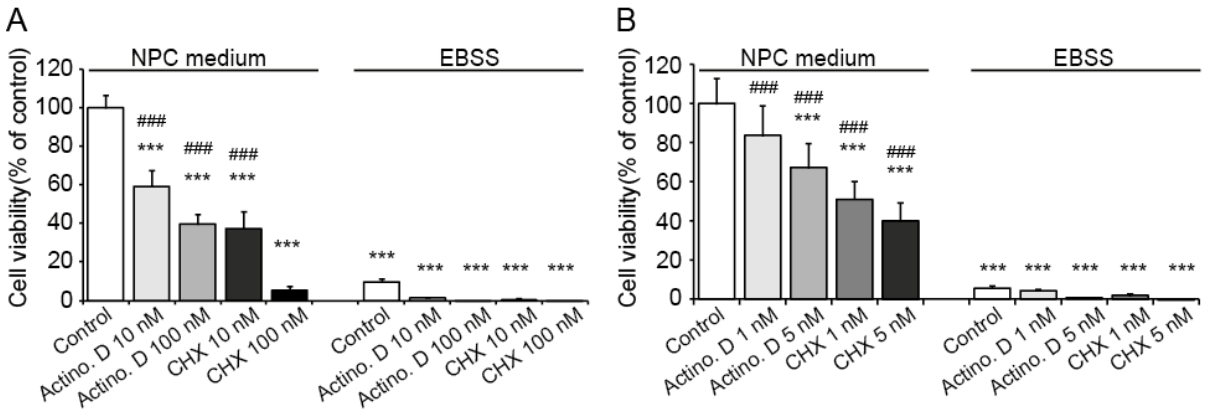

Figure 20: Toxicity of protein synthesis inhibitors in NPCs.

A, B: NPCs were treated with actinomycin D or cycloheximide (CHX) in different concentrations. Both substances provided apoptosis in the nanomolar range. None of the substances affected the cell death induced by growth factor deprivation during EBSS treatment. The experiment was repeated 2 times. *** $p < 0.001$ compared to control in NPC medium, ### $p < 0.001$ compared to EBSS control; n = 6, ANOVA, Scheffé test.

The CM generated by co-treatment of EBSS and either CHX or actinomycin D were tested in the HT-22 model of glutamate toxicity for protective activity. Both inhibitors of protein synthesis did not affect the protective properties of CM (Figure 21 A-D). Actinomycin D and CHX alone did not have any effect on apoptosis induced by

glutamate at low concentrations. In order to avoid additional effects, however, the protein synthesis inhibitors were removed from CM before HT-22 cell treatment.

Thus, the proteins responsible for the neuroprotective effect of CM seem to be already expressed in the NPCs under standard culture conditions.

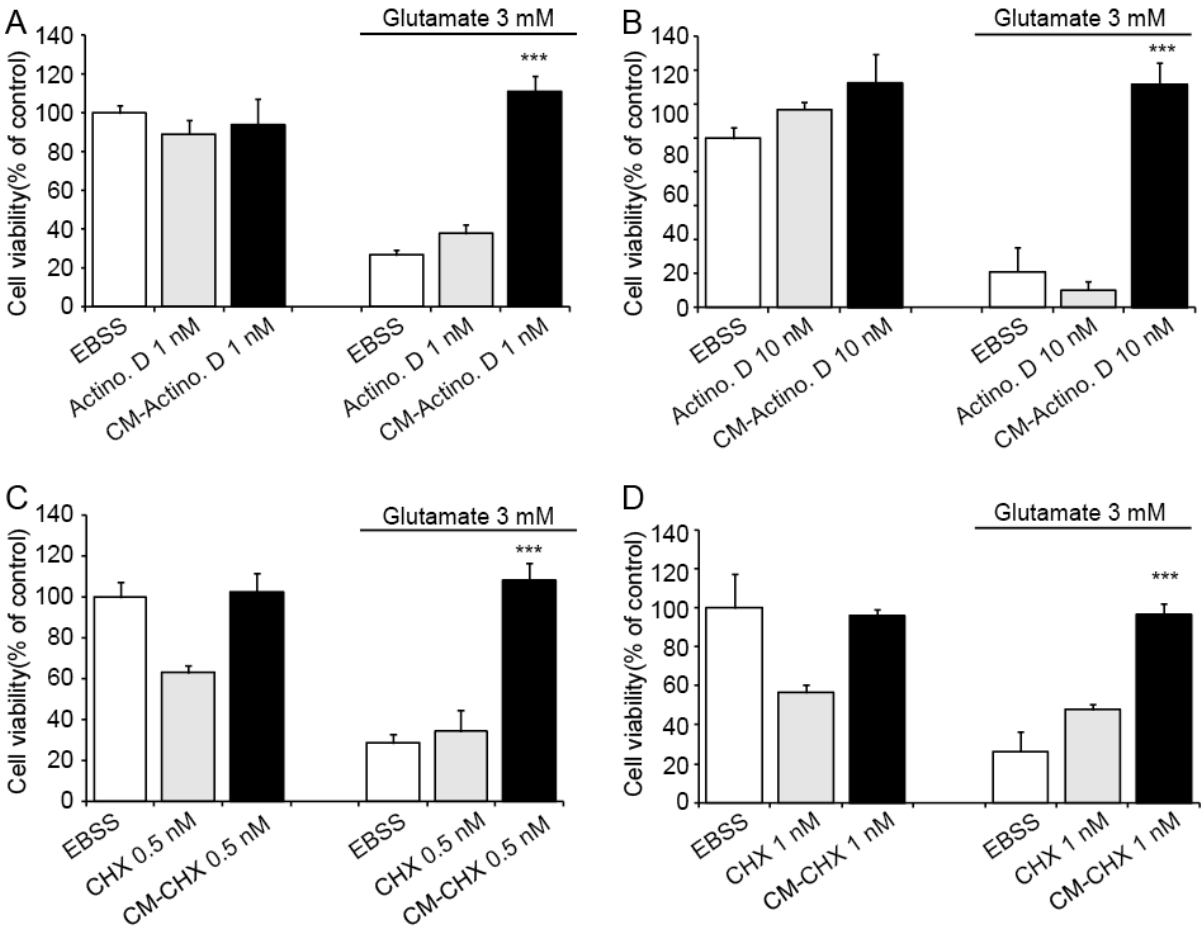

Figure 21: CM generated in the presence of protein synthesis inhibitors protects HT-22 neurons against glutamate-induced cell death.

A, B: HT-22 cells treated with CM produced in the presence of actinomycin D (actino. D, 1 nM and 10 nM) prevent glutamate toxicity (3 mM, 15 h); n = 6. **C,D:** CHX (0.5 nM and 1 nM) had slight toxic effects on HT-22 cells. CM produced in the presence of CHX, however, still provided significant neuroprotective effect; n = 7. *** $p < 0.001$. All statistics were obtained using ANOVA, Scheffé test. Experiments were performed three times independently.

3.2.5. Neuroprotective effect of NPC lysate

For further confirmation that the lysis of the dying cells was the essential step to generate neuroprotective properties in CM, NPCs from standard cultures were lysed by sonication. As shown by MTT assays, also cell lysates were able to protect against glutamate-induced cell death. However, the protective effect of such lysates was only detected when the cells were sonicated less than 5 minutes (Figure 22 A). This is likely due to the amount of proteases released during the sonication. Thus, for further analysis sonication time for the following experiments was restricted to 2 minutes. Heating at 60°C did not have the same strong effect on the neuroprotective effect in the NPC lysate as compared to NPC CM from dying cells. In some experiments, the protective effect of the lysate was even less potent after heating compared to the native lysate (Figure 22 B), in other experiments heating did not alter the protective effect at all.

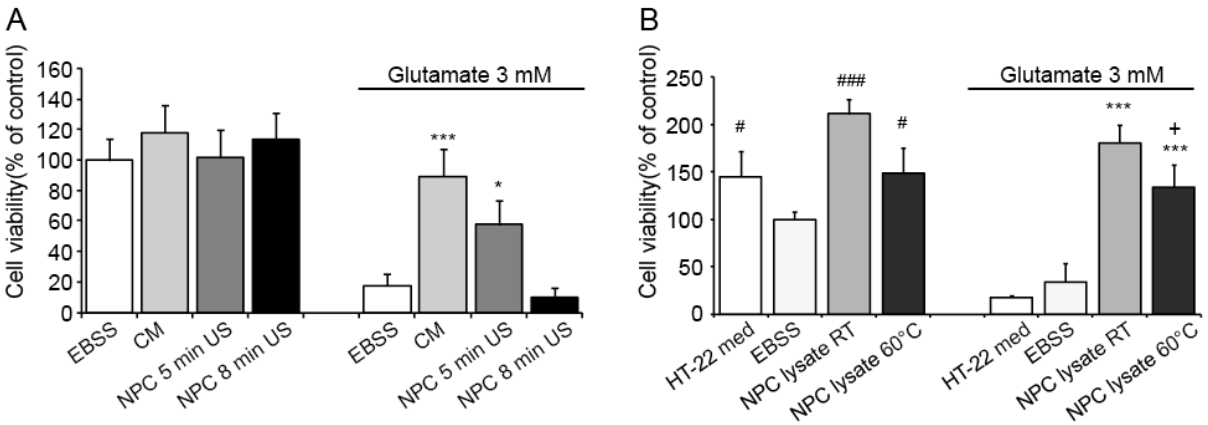

Figure 22: NPC lysate provides neuroprotection.

A: NPCs were sonicated for 5 or 8 minutes (US = ultrasonic). Cells sonicated for 8 minutes failed to prevent cells from glutamate-induced cell death (3 mM, 16 h). CM produced from growth factor deprived NPCs was used as positive control (n = 5, *** $p < 0.001$; * $p < 0.05$, ANOVA, Scheffé test). **B:** NPCs were sonicated for 2 minutes. NPC lysate provided neuroprotection against growth factor withdrawal mediated by EBSS (21 h) and glutamate toxicity (3 mM, 15 h). Heated lysate was less potent in its protective properties compared to non-heated lysate (n = 6; *** $p < 0.001$ compared to glutamate-treated EBSS control; # $p < 0.05$, ### $p < 0.001$ compared to EBSS without glutamate; + $p < 0.05$ compared to glutamate-treated NPC lysate at RT; ANOVA, Scheffé test).

3.2.6. Cell type specifity of CM

To test, if the neuroprotective effect of CM is specific for NPCs, another CM was produced from dying HT-22 cells. HT-22 cells were more resistant to EBSS treatment than NPCs, and they had to be incubated under conditions of starvation for 48 hours to obtain CM from dying cells. This HT-22 CM was able to attenuate glutamate toxicity in the HT-22 cell line and the effect was still observed after heating the CM to 60°C (Figure 23 A). Furthermore, cells treated with HT-22 CM showed higher viability than the control cells treated with EBSS, which indicated a protective effect not only against glutamate treatment but also against EBSS-induced starvation.

Additionally, CM was generated from primary mouse embryonic fibroblasts (MEFs) that underwent starvation. This medium failed to protect HT-22 cells from glutamate-induced apoptosis. Moreover, heating of MEF CM had no effect on the properties of the medium (Figure 23 B). Furthermore, SNL feeder cells from a modified mouse cell line were used as another source for CM. CM from MEFs as well as SNL CM was obtained from incubations of the cells in EBSS for about one week since these cells were less sensitive for starvation than NPCs. Similar to the MEF CM, the SNL CM did not protect against glutamate-induced cell death (Figure 23 C). Surprisingly, when SNL feeder cells were lysed by ultrasonication, significant protective effects were achieved in the glutamate-treated HT-22 cells with and without heating the lysate at 60°C, as quantified in the MTT assay (Figure 23 D). Since this result was in contrast with the findings of CM generated from SNL feeder cells, real-time analysis using the xCELLigence system was performed. This experiment clearly demonstrated that the protective effect of SNL lysate was only transient whereas sustained protective effects over several hours were obtained with the lysate or CM from NPCs (Figure 23 E).

Overall, these data suggest that the neuroprotection of CM is mediated specifically from neural cell lines and is much more potent than CM or cell lysate from fibroblasts.

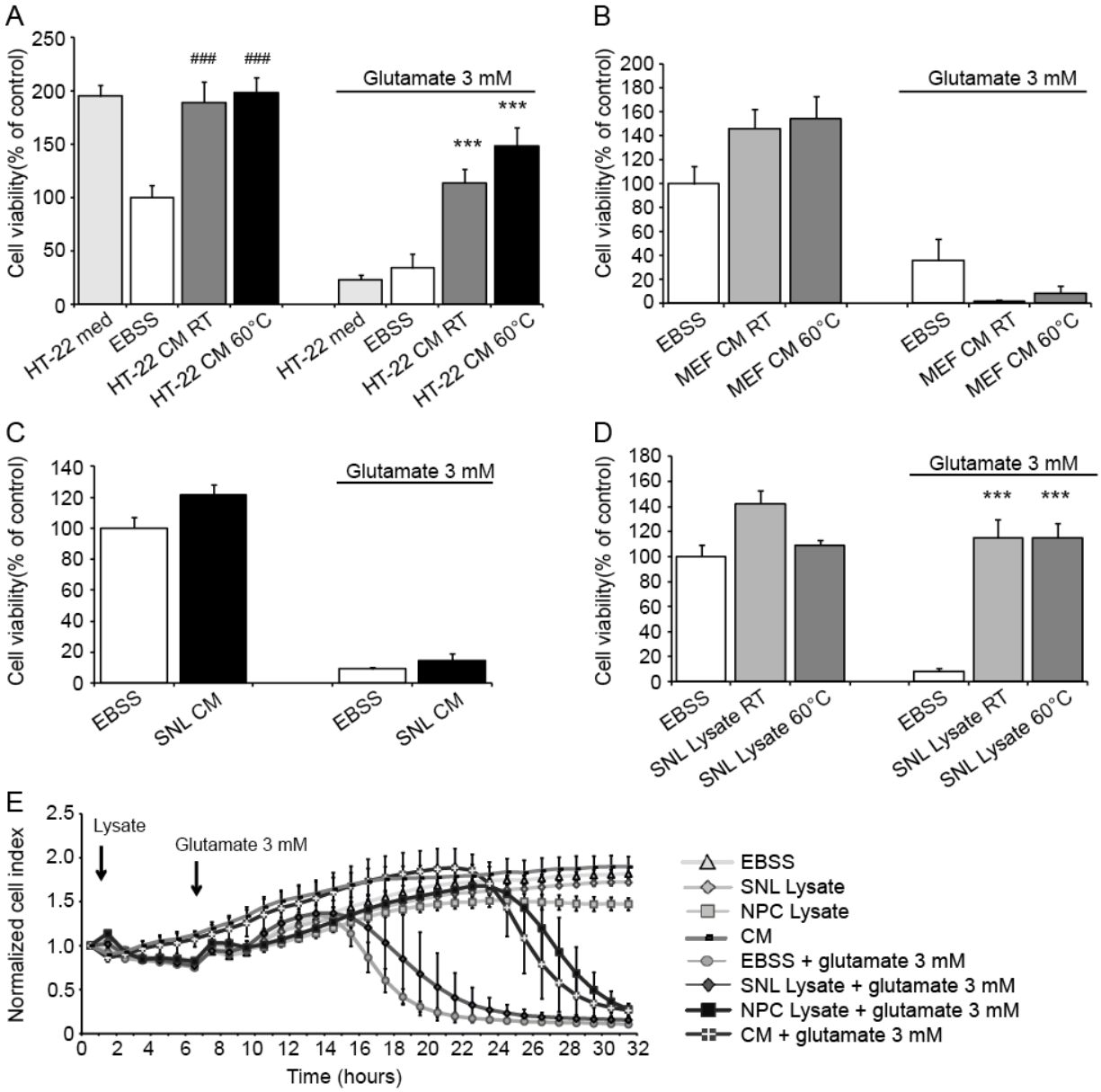

Figure 23: CM and cell lysates from other cell types.

A: HT-22 cells were incubated with EBSS for 2 days. HT-22 CM prevented HT-22 cells against apoptosis mediated by glutamate and growth factor withdrawal with and without heat treatment. (n = 6, ### $p < 0.001$ compared to EBSS, *** $p < 0.001$ compared to glutamate-treated EBSS, ANOVA, Scheffé test). **B, C:** HT-22 cells were pretreated with CM from dying primary MEF (**B**) and dying SNL cells (**C**). Both CM failed to prevent HT-22 cells from glutamate neurotoxicity (3 mM, 15 h) in MTT assay also after heat treatment at 60°C for 10 minutes (n = 7, ANOVA, Scheffé test). **D:** SNL cells lysed by ultrasonic sound protected HT-22 cells against glutamate toxicity (3 mM, 15 h) (n = 6; *** $p < 0.001$; ANOVA, Scheffé test). **E:** SNL and NPC cells (100,000 cells each) were lysed for 120 seconds. Lysed NPCs showed significant stronger protective effect comparable to CM against glutamate toxicity (3 mM) in HT-22 cells.

3.2.7. Mitochondria from NPCs do not provide neuroprotective effects

Recently, it was reported that mitochondrial transfer from BMSCs protect against lung injuries (Prockop, 2012). To examine whether mitochondrial transfer also mediates neuroprotection in NPC CM, isolated mitochondria from NPCs were investigated in the HT-22 model. However, isolated mitochondria failed to prevent glutamate-induced cell death in HT-22 neurons as detected by the MTT assay (Figure 24). Thus, other components of the NPCs have to be responsible for the neuroprotective effects of CM.

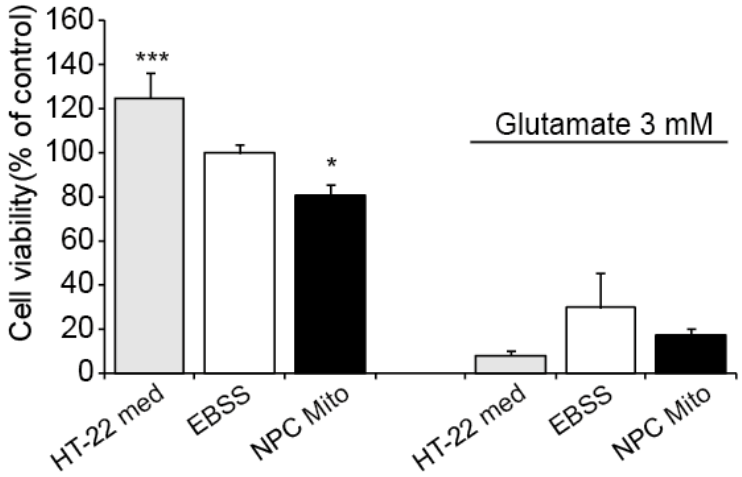

Figure 24: Isolated mitochondria of NPCs do not protect against glutamate-induced toxicity.

Isolated mitochondria from NPCs (NPC Mito) were tested in HT-22 cells towards glutamate toxicity (3 mM, 15 h) and growth factor withdrawal (EBSS, 21 h) (n = 6). *** $p < 0.001$, * $p < 0.05$ compared to EBSS. The experiment was repeated two times independently. Statistics were obtained using ANOVA, Scheffé test.

3.2.8. Apoptotic bodies from NPC do not mediate neuroprotective effects

Apoptotic bodies have been demonstrated to enhance the differentiation of human endothelial progenitor cells in vitro (Hristov et al., 2004). For this reason CM was also investigated for apoptotic bodies to mediate neuroprotection. However, apoptotic bodies isolated from NPCs did not protect against glutamate-induced cell death whereas the remaining compounds of CM still protected HT-22 cells from apoptosis (Figure 25). CM was used as positive control.

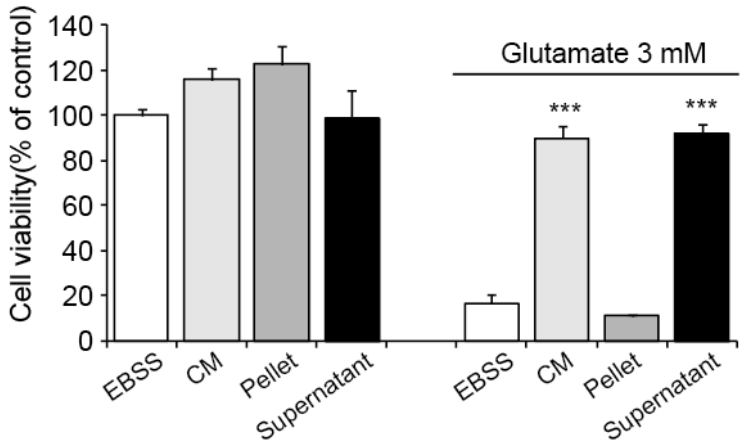

Figure 25: Apoptotic bodies fail to prevent glutamate-induced cell death.

CM was centrifuged at 16,000g for 30 minutes to isolate apoptotic bodies. The pellet containing the apoptotic bodies did not protect HT-22 cells against glutamate toxicity (3 mM, 15 h). The supernatant had still the same protective properties as CM used as control (n = 7). *** $p < 0.01$ compared to glutamate-treated EBSS. Experiment was repeated two times independently. Statistics were obtained using ANOVA, Scheffé test.

3.2.9. Cut off filtrations limit the protein size

To get further insights which proteins were responsible for the neuroprotective effect of CM, size exclusion filtration using a 10 kDa cut off filter (Millipore, Darmstadt, Germany) was performed. After the cut off filtration the CM fractions were heated at 60°C. The filtrate containing proteins smaller than 10 kDa failed to attenuate glutamate toxicity whereas the concentrate with proteins higher than 10 kDa still showed significant protection against glutamate induced damage (Figure 26 A). The fact that this fraction did not reach 100 % of cell viability can be attributed to the protein loss by adsorption to the filter membrane. To further narrow the molecular weight range of the protective protein components in CM, size exclusion with a 50 kDa cut off filter was assessed. The filtrate which contains proteins lower than

50 kDa reached the same protective effect as non-filtered CM that was used as a positive control in this experiment (Figure 26 B). The concentrate containing components higher than 50 kDa did not prevent HT-22 cells from glutamate-induced cell death.

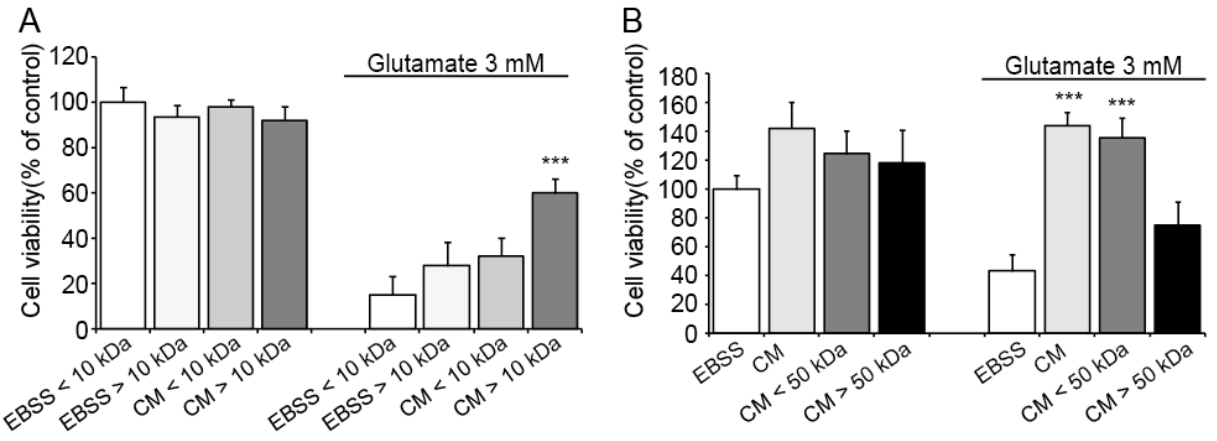

Figure 26: Size exclusion filtration identifies neuroprotective fractions at molecular weights between 10 and 50 kDa.

A: Heated concentrate and filtrate of CM resulting from a 10 kDa cut off filtration were tested for their protective effects in glutamate-treated HT-22 cells (n = 6; *** $p < 0.001$, ANOVA, Scheffé test). Experiment was repeated two times. **B:** After 50 kDa cut off filtration only the filtrate prevented glutamate-induced cell death. Fractions were heated at 60°C for 10 minutes before HT-22 cell treatment (n = 6, *** $p < 0.001$, ANOVA, Scheffé test). The experiment was performed two times independently.

These results indicate that the components of CM mediating the neuroprotective effect have a molecular size ranging between 10 and 50 kDa.

3.2.10. Coomassie staining of NPC CM

In order to visualize the CM proteins at their molecular size, CM was transferred on a SDS gel followed by coomassie blue staining. NPC CM as well as proteins precipitated by aceton, and NPC culture medium deprived of EGF and FGF obtained after 24 hours incubation in NPC showed several strong protein bands (Figure 27). Most proteins had a molecular size between 40 kDa and 70 kDa. As a negative control MEF CM was used. As expected almost no bands were detected in MEF CM and NPC culture media after 24 hours apart from medium additives.

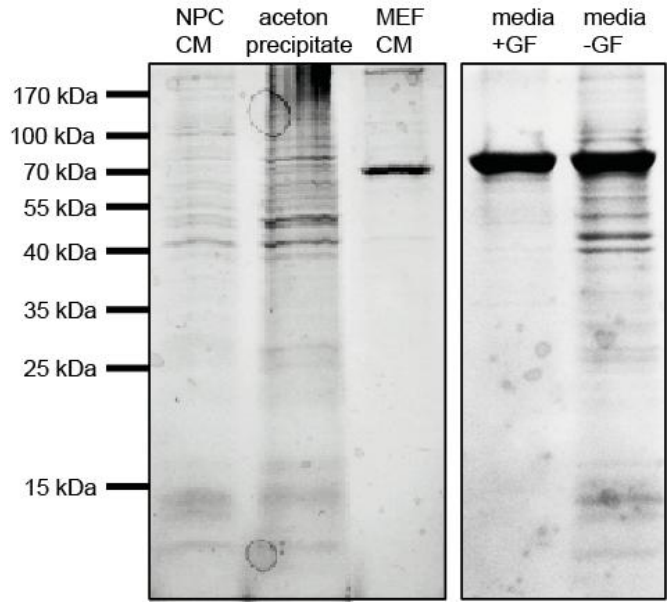

Figure 27: Coomassie staining of CM on a SDS gel.

NPC CM, aceton precipitated proteins of CM, MEF CM, NPC culture medium, and CM produced by growth factor deprived NPC culture medium and was separated on a SDS gel and stained by coomassie blue. From each sample 40 µg of total proteinwere loaded on the gel.

3.2.11. MALDI-TOF analyses identify proteins in CM

To determine the proteins in CM, MALDI-TOF analyses were performed. MALDI-TOF was used to analyze the CM concentrate after 10 kDa cut off filtration, filtrate from 50 kDa cut off filtrations, CM heated at 60°C, CM from NPCs treated with Q-VD-OPh, lysed NPCs, SNL CM, and HT-22 CM. The samples were concentrated by 10 kDa cut off filtration to increase the signal, by default.

Analyses of NPC CM, concentrated by a 10 kDa cut off filter resulted in a broad spectrum of different factors including proteins involved in redox regulation, like peroxiredoxins (prdxs), biosynthesis regulating proteins, like eukaryotic elongation factor 2 (eEF2), and stress response proteins, such as members of the HSP family. In addition, proteins mediating DNA repair were identified in the CM, e.g. histone 2A (Attachment 1). To narrow down this list Q-VD-OPh treated CM was analyzed. However, in the probes of Q-VD-OPh treated CM no proteins could be detected. This confirms the former finding that cell lysis is necessary to obtain neuroprotective effects. As a further attempt to exclude proteins from the list, the filtrate of 50 kDa cut off filtration was analyzed. These probes were also concentrated by a 10 kDa cut off filtration so that the probes should contain mainly proteins with a molecular weight ranging between 10 and 50 kDa. The protein list resulting from these experiments was reduced by half compared to the first list from the 10 kDa cut of filtration.

Proteins that were found in both experiments and that have a molecular weight between 10 and 50 kDa were e.g. members of the prdx family (20-30 kDa) and galectin-1 (gal-1; 14 kDa) (Attachment 2). Furthermore, proteins with higher molecular weight than 50 kDa, such as HSP 70 or 90, which are also interesting candidates for mediating neuroprotective effects were excluded from this list. Analysis of CM after heating to 60°C did not provide different or new findings but confirmed interesting candidate proteins, such as prdx family members, gal-1, and members of the HSP family (Attachment 3). Analysis of NPC lysates did not provide useful data (Attachment 4). Only very few proteins could be identified in the lysate which may result from the fact that the lysate samples contained too many proteins and their signals were overlapping and disturbing each other.

In addition, also the CM generated by HT-22 neurons and SNL feeder cells were analyzed. Interestingly, HT-22 CM, which also showed neuroprotective effects in former analyses, contained peroxiredoxin-1 (prdx-1), which was also consistent in all the other NPC generated probes (Attachment 5). The analysis of SNL CM that is not protective only detected structural proteins, such as vimentin and actin (Attachment 6).

3.2.12. RT-PCR analysis of interesting proteins from the MALDI-TOF results

The MALDI-TOF analyses of the concentrated CM (Attachment 1) identified several proteins that were of interest when examining neuroprotective effects. The first protein family of interest is the prdx family. Prdxs are an ubiquitous family of antioxidant enzymes that also control cytokine-induced peroxide levels and thereby mediate signal transduction in mammalian cells (Wood et al., 2003). It has already been shown that some of these protein family members, including prdx-2, 5, and 6 can mediate neuroprotective effects (Hu et al., 2011;Plaisant et al., 2003;Tulsawani et al., 2010). Since prdx-1 was found in all MALDI-TOF analyses from neuroprotective samples its expression on RNA level in NPCs during treatment with EBSS was further investigated by RT-PCR. Since also prdx-2 and 6 were found in some samples at least with a peptide count-value of 1 and neuroprotective effects of prdx-5 are described in the literature (Plaisant et al., 2003), also these expression levels were determined. Prdx-1 expression level was significantly reduced in NPCs after EBSS treatment whereas prdx-2 and prdx-5 showed no changes in their expression levels during growth factor withdrawal. In contrast, RNA level of prdx-6 was increased after 10 and 20 hours (Figure 28).

Another protein family identified by the MALDI-TOF analyses that may mediate neuroprotective effects is the HSP family. HSPs cope with stress-induced denaturation of other proteins thereby mediating stress tolerance (Romi et al., 2011). There is evidence in the literature that exogenous HSPs, such as HSP 70, are involved in the regulation of neuronal survival (Robinson et al., 2005). Since HSP 60, 70, and 90 were found in the MALDI-TOF analyses of CM their RNA expression levels in NPCs during EBSS treatment was further investigated. HSP 70 expression was strongly downregulated after 6 hours of EBSS treatment but no changes were found after 10 or 20 hours. Thus, this decrease in expression seems to be just a short-time stress reaction. The expression level of HSP 90 was stable over 6, 10, and 20 hours of growth factor withdrawal whereas HSP 60 showed a continuous decrease in RNA expression during EBSS treatment (Figure 28).
In addition, the RNA expression levels of phospholipase A 2 (PLA 2) and eEF 2 were detected at different time points after growth factor withdrawal. PLA 2 was of interest since it is known that several types of PLA 2s are degraded at about 60°C and the

enzyme is also known to have neurotoxic properties (Farooqui et al., 2006;Karray et al., 2012a) which is in accordance with the activation of CM at about 60°C. eEF 2 catalyzes ribosomal translocation during protein synthesis and acts as a biochemical sensor in dendrites (Sutton et al., 2007). For eEF 2 expression levels a continuous increase was detected (Figure 28). A short time increase of PLA 2 expression was observed after 6 hours that diminished again during longer EBSS treatment. GAPDH was used as loading control.

These data already indicate that the protein regulation after growth factor deprivation is very complex and involves a lot of different proteins, and an up- as well as downregulation of these proteins can be observed.

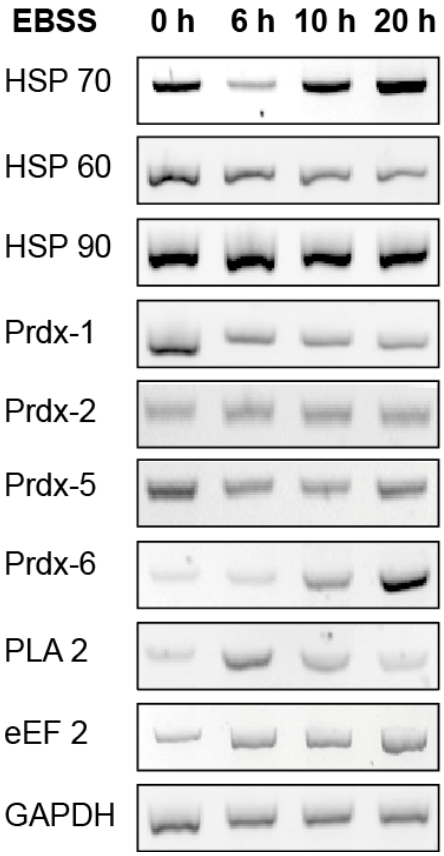

Figure 28: Changes in mRNA mediated by growth factor deprivation.

mRNA expression levels of prdx-1, 2, 5, and 6, HSP 60, 70, and 90, eEF2, and PLA2 were determined 0, 6, 10, and 20 hours after EBSS treatment by RT-PCR. GAPDH was used as loading control. The experiment was repeated independently two times.

3.2.13. Peroxiredoxin-1 and galectin-1 as protective components of CM

Since prdx-1 is described to play a role for neuronal survival in HT-22 cells (Sun et al., 2008) and, furthermore, prdx-1 was identified by MALDI-TOF analyses in all experiments, it was investigated whether prdx-1 is able to mediate protection against oxidative stress in HT-22 cells. The used recombinant protein was of human origin because of availability but human and mouse prdx-1 gene sequences converge in 95 % (Table 24).

Table 24: Gene alignment of human and mouse prdx-1

HUMAN Peroxiredoxin-1	MOUSE Peroxiredoxin-1
MSSGNAKIGHPAPNFKATAVMPDGQFKDIS	MSSGNAKIGYPAPNFKATAVMPDGQFKDIS
LSDYKGKYVVFFFYPLDFTFVCPTEIIAFS	LSEYKGKYVVFFFYPLDFTFVCPTEIIAFS
DRAEEFKKLNCQVIGASVDSHFCHLAWVNT	DRADEFKKLNCQVIGASVDSHFCHLAWINT
PKKQGGLGPMNIPLVSDPKRTIAQDYGVLK	PKKQGGLGPMNIPLISDPKRTIAQDYGVLK
ADEGISFRGLFIIDDKGILRQITVNDLPVG	ADEGISFRGLFIIDDKGILRQITINDLPVG
RSVDETLRLVQAFQFTDKHGEVCPAGWKPG	RSVDEIIRLVQAFQFTDKHGEVCPAGWKPG
SDTIKPDVQKSKEYFSKQK	SDTIKPDVNKSKEYFSKQK
Identities = 190/199 (95%)	

The human recombinant prdx-1 was tested in HT-22 cells at different concentrations using the xCELLigence system for detection of cell viability. Human prdx-1 prevented glutamate-induced cell death in HT-22 cells in a dose-dependent manner (Figure 29 A-C). Interestingly, the protective effect did not vary when the protein was previously heated at 60°C. At a concentration of 125 µg/ml recombinant prdx-1 showed a stable protection against glutamate-induced cell death (Figure 29 A). At a concentration of 25 µg/ml the protective effect of prdx-1 was comparable with the effect of CM that was not previously heated (Figure 29 B). At a concentration of 12.5 µg/ml the recombinant protein still exerted a transient delay in cell death of about 1 hour (Figure 29 C).

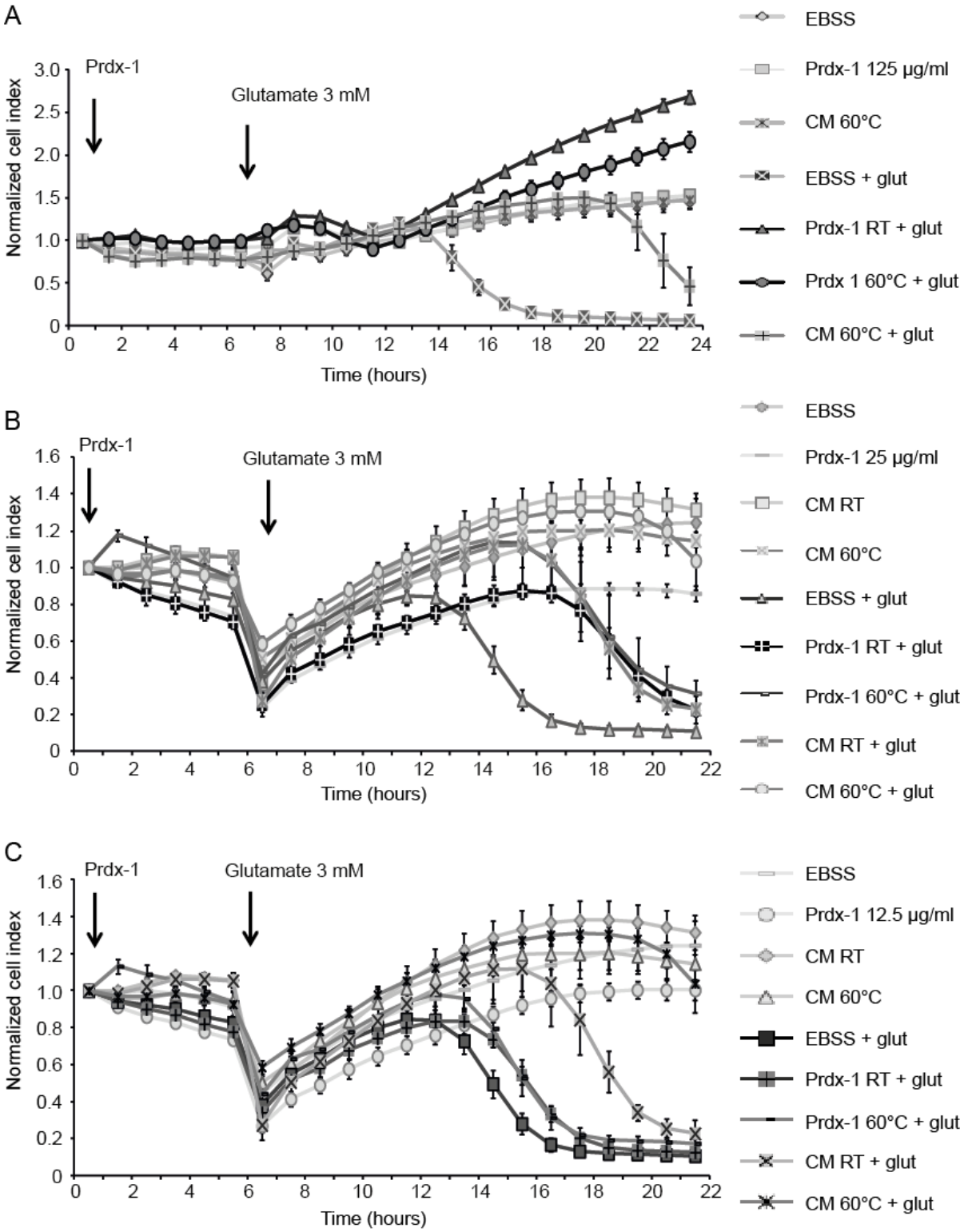

Figure 29: Human recombinant prdx-1 attenuates glutamate toxicity in a concentration-dependent manner.

A-C: HT-22 cells were plated on a 96-well E-plate and cellular impedance was measured continuously. The cells were pretreated with human recombinant prdx-1 in three different concentrations either with or without heating at 60°C for 10 minutes. After 6 hours glutamate (3 mM) was added into the wells. CM was used as a positive control (n = 3).

Western blot analyses demonstrated that HT-22 cells treated with heated as well as non-heated CM showed a significant increase in prdx-1 levels of about 30-40 % (Figure 30). This result suggested that HT-22 cells either take up prdx-1 out of the medium or that CM causes a signal to the cells resulting in an increase in the intracellular expression levels. The increase in endogenous prdx-1 levels detected after incubation with CM was much less compared to treatment with recombinant human prdx-1 at the concentration of 25 µg/ml.

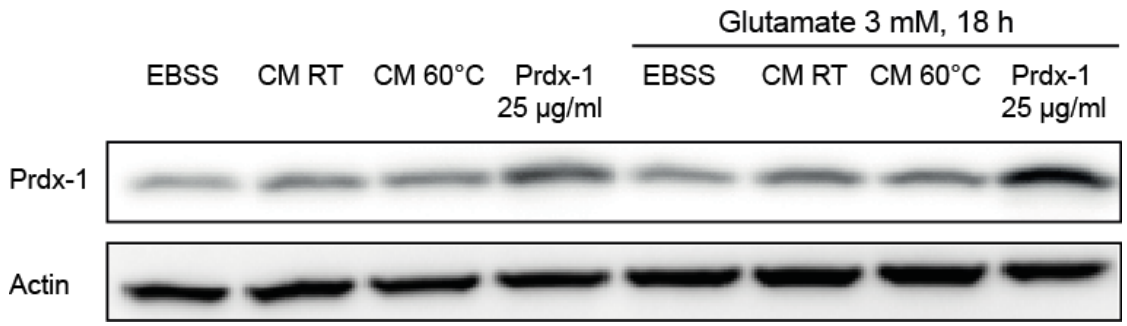

Figure 30: CM increases prdx-1 protein levels in HT-22 cells.

Western blot analysis of HT-22 cells treated with CM or recombinant prdx-1 for 24 hours. HT-22 cells treated with CM showed an increase in prdx-1 levels but not as strong as recombinant prdx-1 in a concentration of 25 µg/ml. The effect was consistent with and without glutamate treatment (3 mM, 18 h). Actin was used as loading control.

In order to evaluate how far prdx-1 contributed to the protective effects of CM, the medium was pretreated with a specific antibody against prdx-1. As demonstrated in Figure 31 B the protective effect of CM was reduced by the anti-prdx-1-antibody but a transient protective effect was still detected over several hours. However, this result was not reproducible all the time. In 5 of overall 8 experiments the antibody attenuated the protective effect of CM. In the remaining 3 experiments the protective effect of CM was not affected which can be due to inefficiency of the antibody. Apparently, even neutralizing prdx-1 using the antibody was insufficient to fully block the protective effect of the CM. This suggests that additional factors significantly contribute to the observed neuroprotection by CM whereas prdx-1 may be dispensable.

To further verify the results obtained with prdx-1 so far, the quantitative amount of prdx-1 in CM was determined by ELISA measurements. ELISA measurements detected prdx-1 amounts of about 3 ng/ml in CM (Table 25). To exclude disturbing interactions between CM and the ELISA also the recovery rate of prdx-1 was

determined in single measurements. No disturbing interactions of CM were detected. Compared to the amount of recombinant human prdx-1 that was required to provide protective effects, the prdx-1 content detected in CM by ELISA was too little to explain neuroprotection of CM through prdx-1 alone. Total protein amount determined by BCA analyses detected protein concentrations in CM around 1 mg/ml. Thus, prdx-1 is likely just a part of a variety of protective proteins in NPC CM. However, it is still possible, that other components in CM activate prdx-1 or that the human recombinant protein has to be added at high concentrations to mediate neuroprotection in the HT-22 cells.

Mouse prdx-1 (ng/ml)	Total protein amount (mg/ml)
2.8	1.1
3.4	1.0
4.3	1.1
3.4	1.4

Table 25: Content of prdx-1 in CM compared to total protein amount
Prdx-1 levels were determined by ELISA measurements and total protein amounts by BCA measurements in 4 independent experiments.

A second interesting candidate protein that was found in all MALDI-TOF analyses and that is also described in the literature to provide neuroprotective effects is gal-1 (Chang-Hong et al., 2005;Lekishvili et al., 2006). For that reason recombinant mouse gal-1 was tested in the system of glutamate toxicity in HT-22 cells. Recombinant gal-1 prevented glutamate-induced toxicity in HT-22 cells as detected by the xCELLigence system (Figure 31 A). This neuroprotective effect was only slightly reduced by heating gal-1 at 60°C. Pretreatment of CM with a specific gal-1 antibody significantly attenuated the protective effect of CM but CM still provided neuroprotection against glutamate toxicity for several hours. However, similar to the experiments with the prdx-1 antibody this result was not reproducible in every experiment. In three of four independent experiments the protective effect of CM was reduced by the anti-gal-1 antibody, whereas in one experiment the antibody failed to attenuate the protection mediated by CM. This suggests that gal-1 partly contributed

to the protective effect of CM, but may as well be dispensable. In one experiment, where both the prdx-1 antibody and the gal-1 antibody affected the potency of CM, a combination of both antibodies showed an additive effect reducing CM protection more effectively than the individual antibodies (Figure 31 B). To exclude that the effects observed with the anti-prdx-1 and the anti-gal-1 antibodies were attributable to unspecific and/or concentration-dependent effects of the antibodies, CM was treated with a specific anti-AMPK antibody at different concentrations. No effect on CM was detected in this control experiment using the xCELLigence system (Figure 31 C).

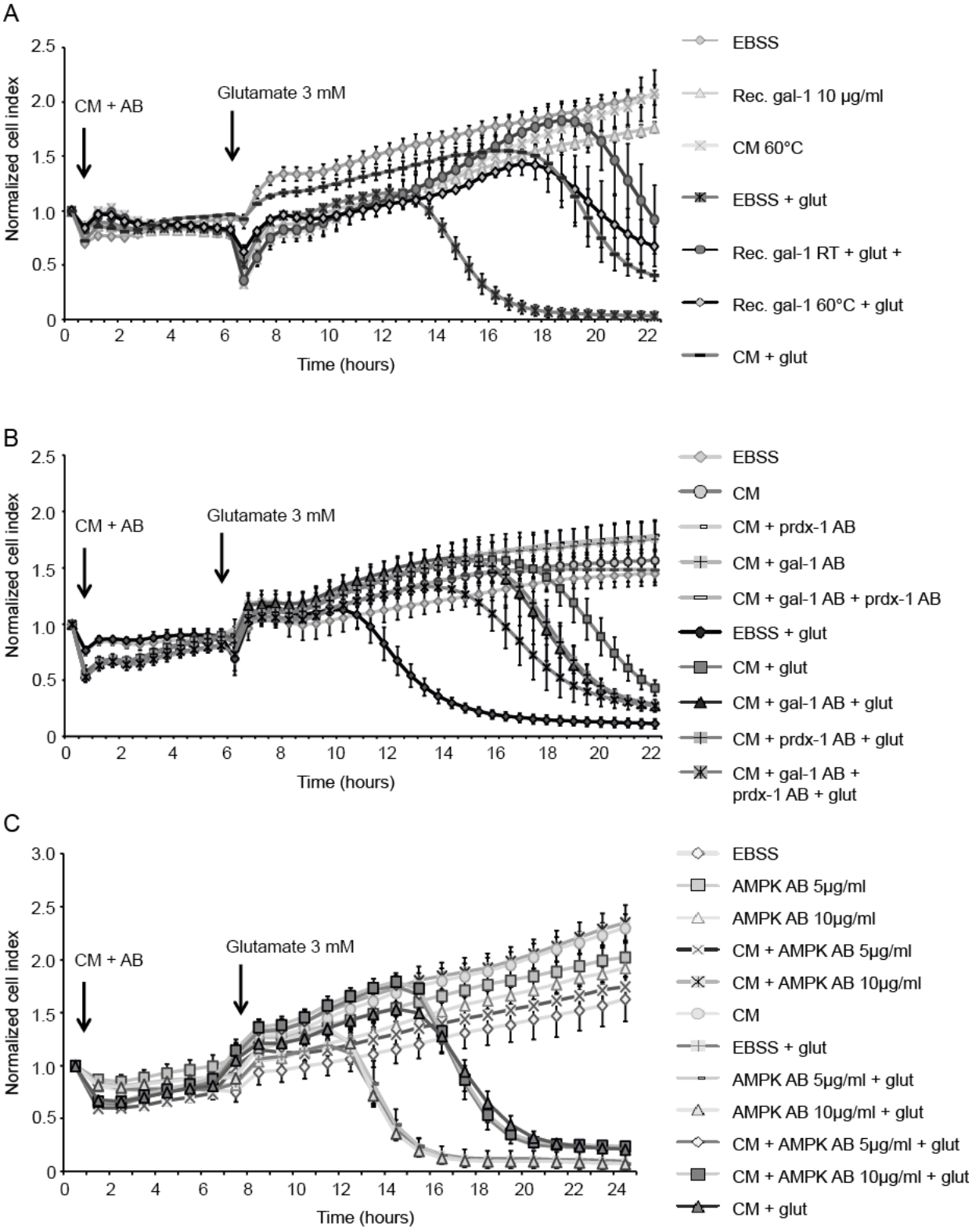

Figure 31: Recombinant gal-1 and prdx-1 may provide additive neuroprotective effect.

A: Real-time measurement of mouse recombinant (rec.) gal-1 (10 µg/ml) indicates a transient protective effect against glutamate toxicity (3 mM) in the HT-22 model system (n = 3). The graph is representative for three independent experiments. **B:** Specific antibodies (AB) against gal-1 and prdx-1 (5 µg/ml each) reduced the potency of CM. Combination of both antibodies showed an additive effect (n = 4). **C:** To exclude unspecific and concentration dependent antibody effects CM was treated with AMPK antibody in two different concentrations (5 and 10 µg/ml) (n = 4).

It has been reported that gal-1 stimulates the secretion of growth factors, such as BDNF (Qu et al., 2010). Growth factors, such as BDNF and VEGF, are lively discussed in several models of stem cell-mediated neuroprotection (Uzun et al., 2010), and they are known to be efficient at very low concentrations (pg/ml; Cho et al., 2012) so that it is conceivable that they are under the detection limit the MALDI-TOF system. To investigate whether BDNF mediates neuroprotection in the applied model system, different concentrations of BDNF were tested in HT-22 neurons treated with glutamate. BDNF failed to rescue cells from glutamate-induced cell death (Figure 32). This is in accordance with former reports showing that HT-22 cells do not express functional TrkB receptors and even after viral infection TrkB expressing HT-22 cells cannot be rescued from oxidative glutamate toxicity by BDNF but only from serum deprived cell death (Rössler et al., 2004). Thus, secretion of BDNF does not affect the neuroprotective effect of CM in the HT-22 cell model system.

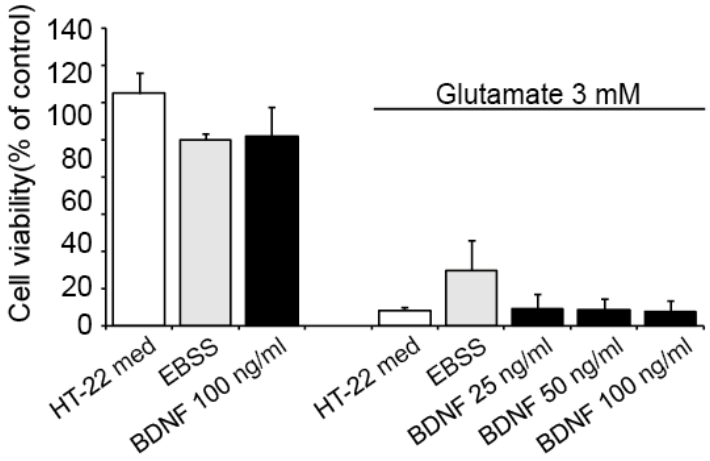

Figure 32: BDNF does not protect HT-22 neurons from glutamate toxicity.

Cells were pretreated with BDNF (6 h) in different concentrations. BDNF failed to prevent glutamate-induced (3 mM, 15 h) cell death in HT-22 cells at all applied concentrations (n = 6).

3.2.14. Inhibition of PI3K

It has been shown in previous studies that BMSC CM mediated protection through stimulation of PI_3K (Isele et al., 2007). In addition, Western blot analyses performed by Dr. Amalia Dolga and Stefanie Neunteibl demonstrated that NPC CM activated Akt within minutes in primary cortical neurons (personal communication), which suggested an involvement of the PI3K/Akt pathway in the neuroprotective effects mediated by CM. For that reason HT-22 cells were pretreated with the PI3K-Inhibitor LY 294002 that acts on the ATP-binding site of the enzyme, before a combination treatment of LY 294002 with either recombinant prdx-1, gal-1, or CM. LY 294002 clearly reduced the protective effect of recombinant prdx-1 (Figure 33 A) as well as of recombinant gal-1 (Figure 33 B) as detected by xCELLigence measurements. Further, the PI3K-inhibitor slightly reduced the protective effect of NPC CM in two independent experiments (Figure 33 C) whereas CM-mediated protection remained unaffected in two other experiments (Figure 33 D). These observations suggest that the protective properties of NPC CM are likely attributed to a mixture of components that may include protective effects mediated by the PI3K pathway, e.g. caused by the proteins prdx-1 and gal-1, however, not exclusively. Thus, the inhibition of one out of several protective pathways may be compensated by other protective components of CM which are yet unknown.

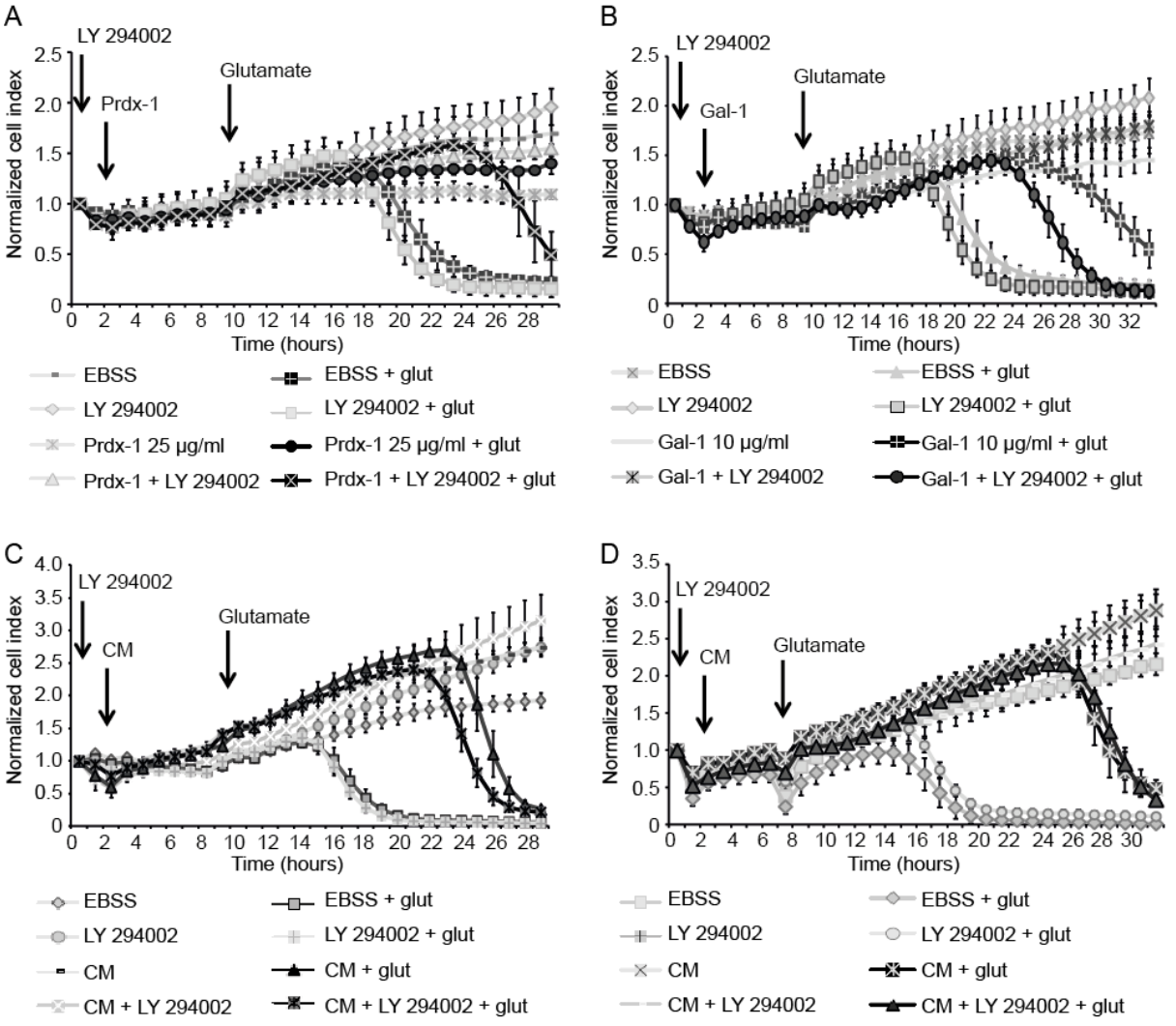

Figure 33: PI_3K inhibition reduces neuroprotection in HT-22 cells.

A: PI_3K inhibitor LY 294002 (10 µM) significantly reduced the protective effect mediated by prdx-1 (25 µg/ml) towards glutamate toxicity (3 mM). The experiment was repeated two times independently (n = 3). **B:** Protection towards glutamate (glut, 3 mM) toxicity mediated by gal-1 (10 µg/ml) was reduced by LY 294002 (10 µM). The experiment was performed three times independently. **C, D:** xCELLigence measurement of co-treatment of CM and LY 294002 (10 µM) showed different results during glutamate (glut, 3 mM) treatment. In two experiments the protection mediated by CM was slightly reduced (**C**). In two experiments no change in the protective properties of CM was observed (**D**) (n = 3).

3.2.15. Gel filtration separates CM into several protective fractions

To further determine proteins that contribute to the neuroprotective properties of CM, the medium was separated by gel filtration. The PrimeView 5.0 software detected protein peaks in several fractions (Figure 34 A) that were collected and tested in the HT-22 model system for neuroprotective properties. At least one fraction still provided neuroprotection towards glutamate-induced apoptosis in HT-22 neurons as detected by MTT measurements in three independent experiments (Figure 34 B) although some fractions also exposed slightly toxic effects.

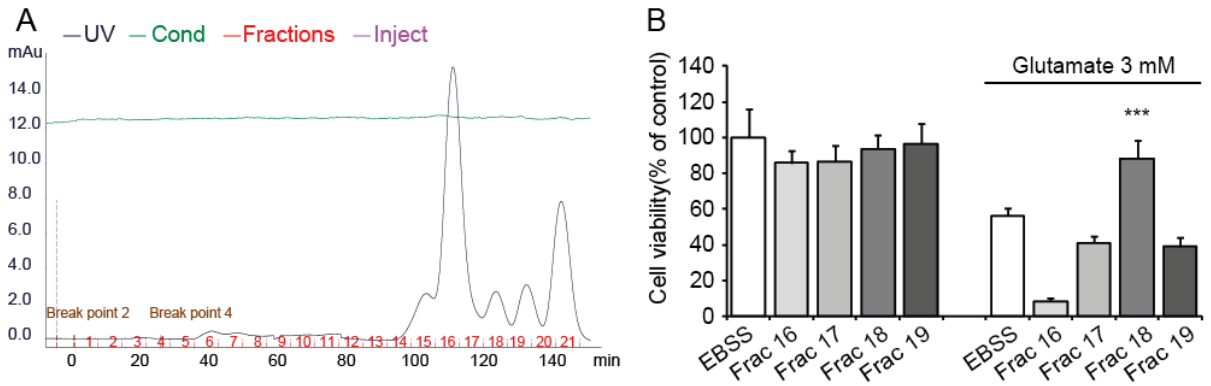

Figure 34: Gel filtration of CM.

A: CM was separated by gel filtration and several protein peaks could be detected by the PrimeView 5.0 software. **B:** Protective fraction as well as toxic fractions could be detected by MTT measurements in HT-22 cells undergoing glutamate-induced cell death (3 mM, 18 h). The graph is a representative example for three independent experiments. N = 6; *** $p < 0.001$ compared to glutamate-treated EBSS. Statistics were obtained using ANOVA, Scheffé test.

However, in MALDI-TOF analysis no proteins could be detected in any of these fractions. Further investigations are needed to clarify whether most of the proteins in the separated fractions were lost on the column and if protein amounts that were below the detection limit of MALDI-TOF analysis could still provide neuroprotection, or if technical problems during the MALDI-TOF measurements are responsible for this result.

3.2.16. Methods for CM concentration

For further investigations of CM in studies in vivo and also for clinical use it would be important to isolate the protective components of CM in a concentrated composition.

For that reason lyophilization of heated CM was assessed. The volume of the media was reduced to about one-tenth of the original volume and then tested in different dilutions in the HT-22 cell system. Both lyophilized CM as well as lyophilized EBSS control showed toxic effects (Figure 35 A). This was due to hyperosmolaric salt concentrations from the lyophilization of EBSS. Further, cell viability of HT-22 cells measured after the treatment with diluted lyophilized CM showed no significant difference to the same medium that was additionally exposed to glutamate, which indicates that the protective properties of CM were not lost during the lyophilization process. Thus, the next step was to combine the lyophilization with a former dialysis. The dialysed and lyophized CM showed no toxic effects, however, it failed to protect HT-22 cells against lethal glutamate concentrations (Figure 35 B). This result suggests that during dialysis protective substances are lost, probably by adsorption to the membrane.

A further attempt to concentrate CM was the use of size exclusion cut off filters. Heated CM was concentrated by a 3 kDa cut off filter to one-tenth of the original volume and tested in different dilutions to determine the efficacy of this concentration method. The concentrate prevented starvation of HT-22 cells in a 1:2 dilution and glutamate toxicity in a 1:6 dilution. However, 1:10 dilution, which represents the original volume failed to prevent cell death in HT-22 neurons (Figure 35 C). Non-concentrated, heated CM as a control failed to prevent HT-22 cells from glutamate-induced cell death already in a 1:4 dilution (data not shown). Thus, CM can be concentrated by cut off filtration, but then a lot of protective substances may be lost by adsorption to the membrane filter or by the loss of one or more cofactors that increase the neuroprotective potential of CM. To investigate whether NPC CM contents such a cofactor the concentrate of a 3 kDa cut off filtration was diluted with the 3 kDa filtrate instead of the EBSS buffer. Interestingly, the neuroprotective potential of the concentrate that was recombined with the filtrate showed significantly stronger neuroprotective effects against glutamate-induced cell death compared to the 3 kDa concentrate alone. Importantly, the 3 kDa filtrate showed no protective properties at the same dilution alone (Figure 35 D). This finding suggests an

additional cofactor with a molecular weight lower than 3 kDa that increases the neuroprotective potential of CM without providing neuroprotective effects by itself.

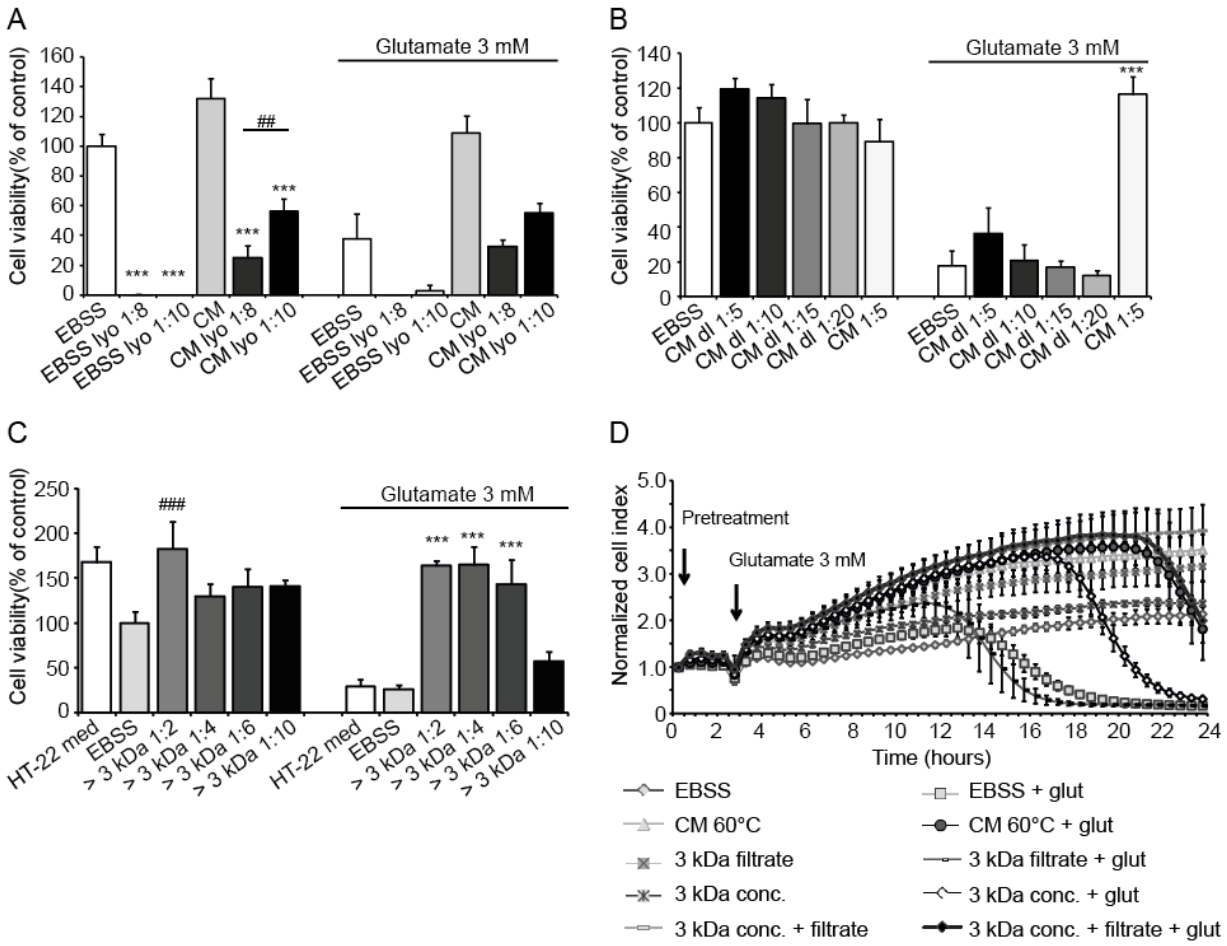

Figure 35: Attempts to concentrate CM.

A: CM and EBSS were concentrated by lyophilization (lyo) to one-tenth of the original volume. Afterwards, the concentrate was diluted with EBSS and tested in the HT-22 cell system. All dilutions showed toxic effects confirming the toxicity mediated by hyperosmolarity (n = 6). *** $p < 0.001$ compared to EBSS. **B:** CM was dialyzed and lyophylized (dl) to one-tenth of the original volume. The dilutions showed neither toxicity nor protective effects against glutamate-induced (3 mM, 15 h) cell death (n = 6). *** $p < 0.001$ compared to glutamate-treated EBSS. **C:** CM was concentrated by 3 kDa cut off filtration to one-tenth of its original volume. CM just protected HT-22 cells from glutamate damage (3 mM, 15 h) up to a 1:6 dilution. CM was protective against growth factor withdrawal in EBSS just up to a 1:2 dilution (n = 5). *** $p < 0.001$ compared to glutamate-treated EBSS; ## $p < 0.01$ compared to EBSS. **D:** All statistics were performed using ANOVA, Scheffé test. **D:** CM heated at 60°C was filtrated by a 3 kDa cut off filter. The fractions were tested separated and in combination with each other in a 1:2 dilution. Proliferation rate was monitored by the xCELLigence system. The combination of the 3 kDa concentrate and the filtrate showed comparable protection against glutamate-induced (3 mM, glut) cell death as undiluted heated CM without cut off filtration.

3.2.17. Stability of CM and cell lysates

For further investigations in vivo and also later clinical application and storage it is essential to know how stable the neuroprotective effect of CM is at room temperature and at body temperature. Since in vivo experiments using implantable mini-osmotic pumps as infusion system were planned CM heated at 60°C was stored at 37°C for 4 or 7 days to mimic in vivo conditions. The CM showed significant protective effects against glutamate-induced toxicity at all storage conditions without any detectable loss in potency (Figure 36 A). The protective effect against growth factor withdrawal was slightly decreased after 7 days in some experiments. This underlines the high potency and temperature stability of CM and makes it suitable for storage at room temperature and further studies in vivo.

In contrast, cell lysates of NPCs showed significant decreases of the neuroprotective effects against glutamate-mediated cell death after 4 and 7 days exposure to 37°C (Figure 36 B). Also, a protective effect against growth factor withdrawal could not be detected with the incubated NPC lysate.

Thus, these results show that CM is more stable towards storage at 37°C compared to cell lysate which makes CM from starving cells superior for further investigations.

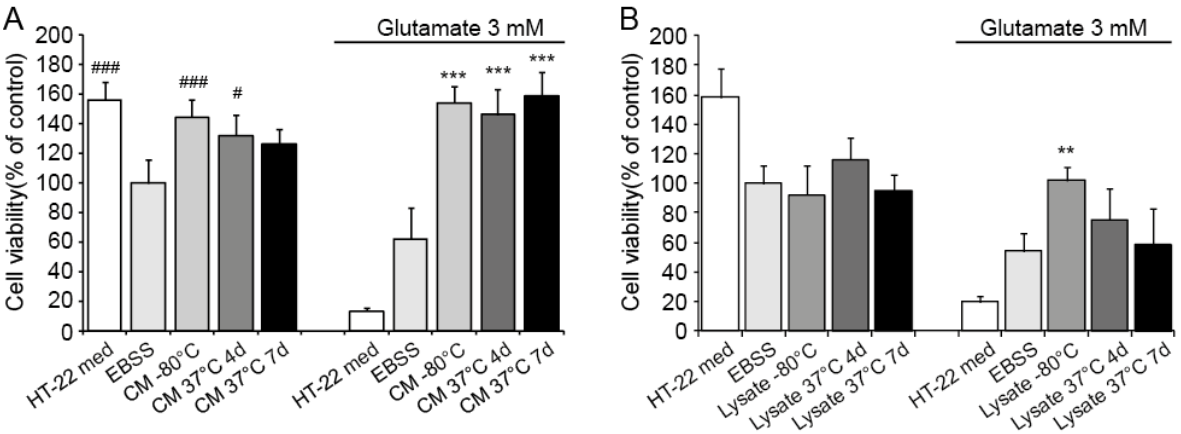

Figure 36: Stability of NPC CM and lysate.

A: CM was heated at 60°C for 10 minutes and afterwards stored at 37°C for 4 or 7 days. As control CM stored at -80°C was used. Afterwards, these CMs were used in the HT-22 model of glutamate-induced (3 mM, 19 h) toxicity (n = 7; *** $p < 0.001$ compared to glutamate-treated EBSS control; ### $p < 0.001$, # $p < 0.05$ compared to EBSS without glutamate; ANOVA, Scheffé test). **B:** NPCs were lysed for 120 seconds and afterwards, heated at 60°C for 10 minutes. Lysated NPCs showed reduced protective effect after 4 and 7 days at 37°C compared to CM kept at -80°C during this time (** $p < 0.01$; n = 6, ANOVA, Scheffé test).

3.2.18. Pre- versus post-treatment

Since CM is a possible therapeutic for application in the treatment of neurodegenerative diseases it is important to know if also a post-treatment with CM has neuroprotective capacities. For that reason a post-treatment with CM in the HT-22 model system was performed. NPC CM protected HT-22 cells from glutamate-induced cell death after 2, 4, 6, and 8 hours of glutamate treatment (Figure 37 A). When applied 10 hours after the onset of glutamate exposure, CM did not exert full protective effects, but still preserved a significant higher cell viability compared to glutamate-treated cells.

In contrast, when HT-22 neurons were pretreated with CM for several hours followed by washout and subsequent glutamate treatment, the cells were not protected from cell death (Figure 37 B).

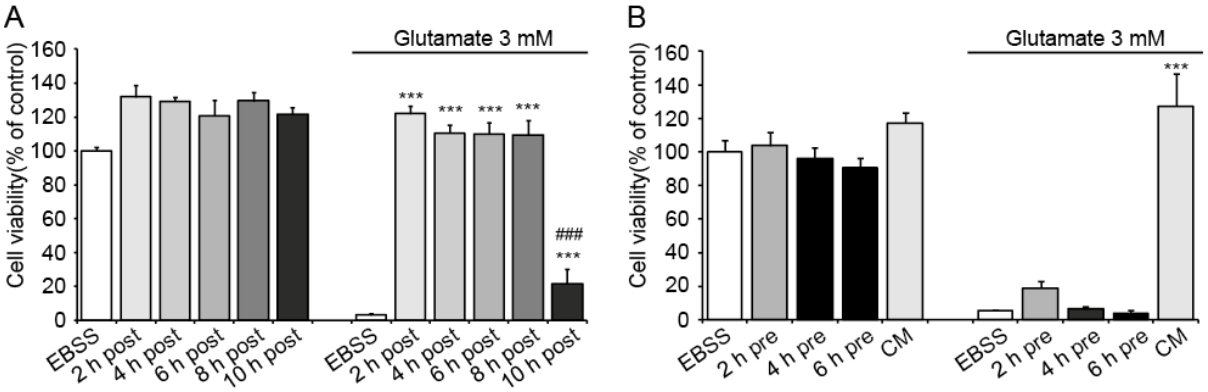

Figure 37: Pre- and post-treatment with CM.

A: HT-22 cells were treated with glutamate (3 mM, 22 h). CM was added at indicated time points after the glutamate addition. Until 8 hours post-treatment CM could prevent glutamate-induced cell death without any loss in potency (n = 8; *** $p < 0.001$ compared to glutamate-treated EBSS; ### $p < 0.001$ compared to 2, 4, 6, and 8 hours post-treatment; ANOVA, Scheffé test). **B:** Cells were pretreated with CM for indicated time points followed by a washout and subsequent glutamate (3 mM, 14 h) treatment. CM co-treated with glutamate was used as positive control (n = 8; *** $p < 0.001$ compared to glutamate-treated EBSS; ANOVA, Scheffé test).

4. Discussion

The data of this thesis demonstrate the potential of molecular and cellular preconditioning effects for attenuating neural cell damage induced by oxidative stress. At the molecular level many mechanisms for preconditioning converge at mitochondria, such as an increased production in ROS, opening of mitoK_{ATP} channels, or mitochondrial membrane depolarization. The data of the first part of this study provide strong evidence for a preconditioning effect by AIF gene silencing, which protects mitochondrial function and integrity in a paradigm of lethal oxidative stress in a neural cell line. Depletion of AIF preserved mitochondrial morphology, MMP and ATP levels after induction of oxidative stress in HT-22 cells, and this mitoprotective effect also significantly attenuated the secondary increase in lipid peroxidation, which was associated with mitochondrial damage and cell death in this model system (Tobaben et al., 2011). Preconditioning by AIF depletion was further associated with reduced complex I expression levels. Surprisingly, low doses of the complex I inhibitor rotenone also affected AIF expression levels and achieve protective effects against glutamate-induced cell death in the used model system similar to the effects observed after AIF silencing. These results suggest that AIF silencing provides protection against oxidative cell death at the level of mitochondria and not at the level of apoptotic DNA damage in the nucleus. Furthermore, these data indicate an association between AIF and complex I thereby regulating each other's stability.

In addition, preconditioning effects are known to be also mediated by intercellular communication in which cells protect neighboring cells e.g. by the transfer of protective substances (Brown, 2007). The ability of cellular communication in paradigms of lethal stress was used to generate CM from dying NPCs in the second part of the thesis. The investigations with this CM demonstrated strong neuroprotective effects against starvation and glutamate-induced cell death in HT-22 neurons. The neuroprotective effect of this CM was stable during storage at 37°C, specific for neural cell lines and consistent up to 8 hours after the onset of toxic glutamate exposure. Importantly, the findings provide evidence that cell death and lysis of the NPCs is necessary to mediate neuroprotection whereas many researchers link the neuroprotective effect of progenitor cell application to cell engraftment and neuronal differentiation (Uzun et al., 2010;Yamane et al., 2010).

Notably, heating CM to 60°C further increased the neuroprotective effects of NPC CM. Furthermore, this study identified proteins as the main mediators of neuroprotection in NPC CM and demonstrated that the strong neuroprotective potential of the medium is due to a broad mixture of several different substances, such as prdx-1 and gal-1. In addition, also the contribution of a low molecular weight cofactor to the neuroprotective potential of NPC CM was shown.

4.1. Importance of preconditioning and conditioning effects in neuronal cell survival as a therapeutic strategy

The present study shows clear evidence for the neuroprotective potential of preconditioning effects against otherwise lethal stress. The protective effects mediated by AIF deficiency or by dying cells, such as NPCs after growth factor withdrawal, clearly feature the exceptional ability of cells to change an intrinsic deficit into an advantage towards following stress situations.

The major goal of studying such mechanisms, which have evolved in different tissues to withstand injurious challenges, is to therapeutically exploit them by boosting or exogenously substituting neuroprotectants after e.g. acute nervous system insults. Furthermore, an aim of preconditioning research is to establish strategies that prevent patients against anticipated brain injuries, such as brain surgeries or in patients with a high risk to develop ischemic defects. For example, 20-30 % patients after subarachnoid haemorrhage have delayed neurological ischemic defects associated with vasospasm several days after the initial event (Dirnagl et al., 2009;Dirnagl and Meisel, 2008).

So far, there are several forms of preconditioning described in the literature. Pharmacological or chemical preconditioning against cerebral ischemia is mediated by compounds that interfere with the cellular respiratory chain or oxygen sensing thereby mimicking or inducing hypoxia. These substances can be inhibitors of the respiratory chain such as nitroproprionic acid (Riepe et al., 1997a), mitoK_{ATP} channel openers such as diazoxide (Prass et al., 2002), HIF inductors such as desferoxamine (Nagy et al., 2004), or modulators of the oxidative phosphorylation function such as acetylsalicylic acid (Riepe et al., 1997b). The data of this thesis demonstrate that preconditioning mediated by AIF depletion is due to an interaction with the respiratory

chain, which leads to higher tolerance against later oxidative stress stimuli of the mitochondria. This finding is underlined by similar neuroprotective effects found with the pharmacological complex I inhibitor rotenone.

Brief exposure to volatile anaesthetics, such as halothane, isoflurane or sevoflurane also results in a protected stage against ischemia long after they have been removed from the organism (Kapinya et al., 2002). The mechanisms behind anaesthetic induced delayed neuroprotection are similar to mechanisms identified as mediators from other forms of preconditioning, including e.g. the involvement of inducible nitric oxide synthase (iNOS) and K_{ATP} channels (Dirnagl and Meisel, 2008). Preconditioning with volatile anesthetics, which protects brain and heart in experimental models are already tested in clinical trials after the onset of cardiopulmonary bypass. For example, desflurane was shown to provide pharmacological preconditioning thereby reducing myocardial necrosis and improving the cardiac performance in the postoperative periods in coronary artery bypass graft surgery in a double-blinded, randomized, and placebo-controlled study (Meco et al., 2007).

Another interesting aspect for therapeutic application is “remote preconditioning” also called “preconditioning at a distance”. This means that brief preconditioning applied to one organ can also protect other organs. Dave et al. demonstrated that tolerance for ischemia can be induced in brain by remote preconditioning in a rat model of asphyxial cardiac arrest (ACA). Remote preconditioning was induced by tightening the upper two-thirds of both hind limbs using a tourniquet for 15 or 30 minutes two days before onset of the ACA. Remote preconditioned animals showed significant higher number of normal neurons compared to control groups seven days after resuscitation. The identities of the signaling pathways involved in the observed neuroprotection following remote preconditioning are not exactly known. However, researchers have demonstrated that pathways involving protein kinase C (PKC), iNOS, suppression of inflammatory pathways, prostaglandins, free radicals, the mitoK_{ATP} channels, and NF-κB are responsible for observed protective effects of remote preconditioning (Dave et al., 2006).

Also, ischemic postconditioning has been reported in the brain (Burda et al., 2006). Ischemic postconditioned rats show a prolonged phosphorylation of Akt, Erk, and p38MAPK in the cortex and the neuroprotective effect can be prevented by an

inhibition of PI3K (Pignataro et al., 2008). Postconditioning offers a new therapeutic strategy as it may be applied after the onset of an ischemic insult. It seems to be effective in protecting the human heart during coronary angioplasty (Staat et al., 2005), however, for practical reasons it is very unlikely to use postconditioning in stroke patients (Dirnagl and Meisel, 2008). Since NPC CM investigated in this study showed strong neuroprotective effects up to 8 hours post-treatment this could be a new method to use conditioning effects for therapeutic applications after the onset of a neural insult.

In clinical neurology and neurosurgery there is no established pre- or postconditioning treatment after cerebral insults available, to date. Clinical trials are needed to test the safety and efficacy of preconditioning strategies for protecting the brain against anticipated damage. A clinically used preconditioning stimulus must be subthreshold and should not cause any persistent damage. Thus, the therapeutic range of preconditioning is narrow (Dirnagl et al., 2009;Dirnagl and Meisel, 2008). Whether preconditioning mimetics, such as mild inhibition of mitochondrial respiration as it was found in this study by AIF gene silencing or by rotenone fall into this small range remains questionable. Tools for transient and specific inhibition of AIF and exact monitoring of the respiratory chain activity in vivo would be necessary to therapeutically use these targets.

However, the application of a CM, e.g. from apoptotic cells perfectly links the needed damaging insult that can be generated ex vivo with the resulting neuroprotective effect in vivo. Among other later discussed advantages when applying a defined composition instead of cells, such conditioning strategies can use the potential of cells to react to adverse environmental effects and are maybe superior to classical preconditioning.

Collectively, this study underlines the importance of research on the self-protecting mechanisms in the nervous system against oxidative stress and other neurological insults, to develop new strategies for the therapy of neurological diseases, where progressive neural damage and death causes the symptoms. In addition, it underlines the amazing adaptability of cells to their environment by which they ensure their survival.

4.2. Molecular preconditioning – neuroprotection mediated by AIF depletion

4.2.1. AIF deficiency mediates mitoprotection

The data presented in the first part of this thesis clearly indicated that neuroprotection mediated by AIF silencing occurs at the level of mitochondria, thereby mediating morphological and functional protection of these organelles. AIF depletion prevented mitochondrial morphology from glutamate-induced fragmentation and peri-nuclear accumulation. Overbalance in mitochondrial fragmentation is an early event in neurological diseases and acute brain injuries (Chan, 2004;Chen et al., 2003;Lin and Beal, 2006). The protection of the semi-tubular mitochondrial network in AIF-silenced cells suggests a protective effect upstream of mitochondrial membrane permeabilization.

At the functional level AIF-silencing preserved ATP levels, prevented MMP, and attenuated production of lipid peroxides towards otherwise lethal glutamate concentrations. Mitochondria are the so-called “powerhouse” supplying the cell with metabolic energy in form of ATP (Wallace, 2005). Thus, the conserved ATP levels and the preserved MMP under oxidative stress in AIF-silenced HT-22 neurons indicate intact functionality of the mitochondria and preservation of the energy supply of the cells. Additionally, a slight depolarization as detected in AIF-silenced neurons under normal culture conditions is often associated with preconditioning effects (Hisatomi et al., 2009;Orozco et al., 2006;Sedlic et al., 2010), and can be explained by the downregulation of complex I as discussed in chapter 4.2.2.. Such a slight depolarization of the MMP may cause a reduction of the electron transfer to molecular oxygen, thereby diminishing ROS production. In addition, it could reduce the uptake in mitochondrial calcium by the ca^{2+} uniporter or activate signaling cascades to induce cell survival programs and thus, lead to the observed neuroprotective effect (Sack, 2006). Therefore, these data indicate that the protective effect of AIF deficiency is mediated by a preconditioning effect, which has its initial point within the mitochondria.

This hypothesis is further supported by the preserved secondary increase in lipid peroxides in AIF-depleted cells, which demonstrates another proof for intact mitochondrial function and integrity. It is interesting to note that glutamate induces a

first increase in ROS formation before the onset of detectable cell death and a second strong increase in ROS when cellular damage becomes evident. The first increase seems to be attributed to the activation of 12/15-LOX whereas the second, higher increase is related to mitochondrial damage and the subsequent production of large amounts of ROS in the mitochondria (Tobaben et al., 2011).

The finding that AIF silencing provides protection against oxidative cell death at the level of mitochondria is additionally supported by former data that demonstrate that the detrimental nuclear changes and DNA fragmentation mediated by AIF in different models of neuronal cell death occur within a few minutes after AIF release from the mitochondria (Daugas et al., 2000) and very little AIF protein that is still present after AIF siRNA treatment or in Hq mice is able to induce PCD (Cregan et al., 2002;Daugas et al., 2000). These reports make it very unlikely that AIF knockdown should prevent from neuronal cell death just by sustained translocation to the nucleus.

Collectively, the present data of this thesis indicate that AIF downregulation mediates mitoprotection by a preconditioning effect caused within the mitochondria that increases the tolerance towards oxidative stress.

4.2.2. Preconditioning mediated by complex I inhibition

The present study demonstrate that the protective effect of AIF silencing is associated with reduced complex I expression levels in the HT-22 cell line. This finding is consistent with previous reports in Hq mice and other cell models for AIF depletion (Vahsen et al., 2004; Benit et al., 2008). Further, direct inhibition of complex I by the specific inhibitor rotenone in nM range decelerated mitochondrial damage after oxidative stress in HT-22 neurons and showed similar effects as obtained with AIF silencing. The protective effect mediated by low dose rotenone was also persistent when cells were pretreated with rotenone only, which indicated again a preconditioning effect. Furthermore, also rotenone slightly decreased the MMP, which confirmed an underlying mechanism of preconditioning. This depolarization can be explained by the mechanism of action of complex I as described in Figure 38. In the first step of the respiratory chain electrons are transferred from NADH (nicotinamide adenine dinucleotide) to the primary electron acceptor flavin mononucleotide (FMN). The electrons are further transferred through a chain of

conserved iron-sulphur (Fe-S) clusters, and finally to ubiquinone. The membrane spanning part of the enzyme lacks covalently bound prosthetic groups, but it is suggested to contain the proton translocating machinery by which protons are pumped from the matrix into the intermembrane space, thereby generating a proton gradient that is necessary for later ATP production by the oxidative phosphorylation. The transfer of two electrons from NADH to ubiquinone (Q) is coupled to the translocation of four (current consensus value) protons across the membrane, however, how the electron transfer is linked with the translocation of protons is still not fully understood (Efremov and Sazanov, 2011). Inhibition of complex I leads to a reduced proton gradient at the inner mitochondrial membrane and thus, can explain the depolarization mediated by rotenone and AIF depletion. Although AIF itself is not a part of complex I, a role of AIF in the biogenesis and/or maintenance of this polyprotein complex has been postulated (Vahsen et al., 2004). The data of this study indicate that also rotenone treatment alone slightly decreases AIF expression levels, which suggests a mutual stabilization of AIF and complex I thereby regulating neural survival towards oxidative stress. The fact that high doses of the complex I inhibitor rotenone lead to lethal stress is in accordance with a common link of AIF and mitochondrial complex I since mice that are completely depleted in AIF, are also no longer viable (Brown et al., 2006;Joza et al., 2001).

Complex I is part of a complex I/III/IV supercomplex (the so-called respirasome) which is essential for the stability/assembly of complex I as the major entry point of respiratory chain substrates. The mitochondrial complexes I (NADH dehydrogenase) and III (cytochrome c reductase) form a stable core respirasome to which complex IV (cytochrome c oxidase) can also bind (Schägger, 2001). Complex I is one of the largest known membrane proteins and consists of 45 protein subunits from which seven are encoded by the mitochondrial genome. The remaining subunits are encoded in the nucleus, translated in the cytosol and imported into the mitochondria (Dimauro and Rustin, 2009). Biochemical analyses postulate that the depletion of complex I in AIF-deficient cells derive from reduced expression of several of these nuclear encoded subunits (Vahsen et al., 2004).

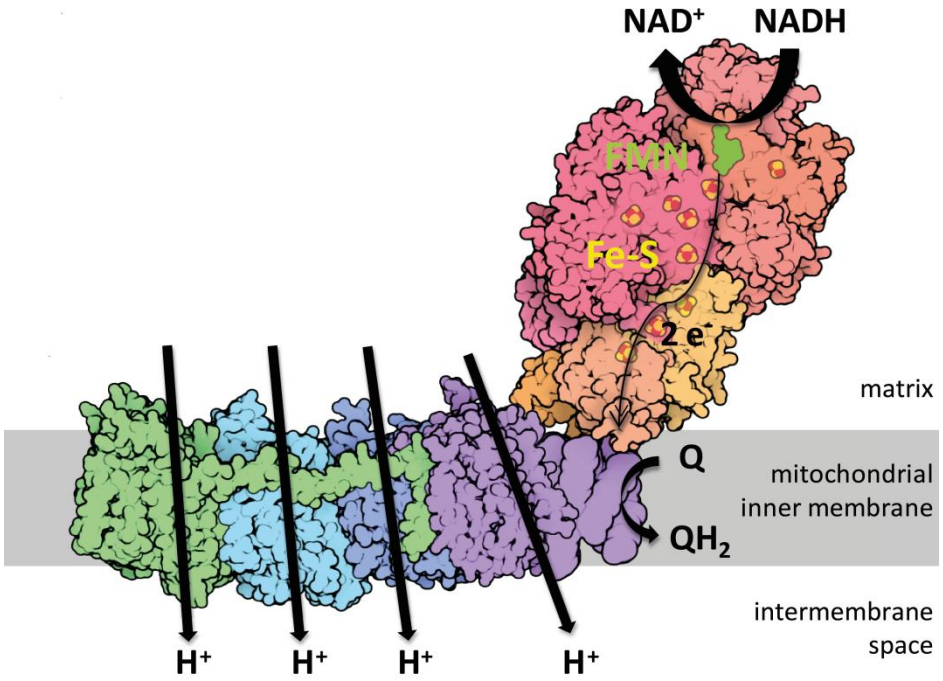

Figure 38: Proposed mechanism of complex I.

Complex I has a L-shaped structure with a hydrophobic and a hydrophilic arm. NADH transfers two electrons (e^-) to the first cofactor FMN (green) and then through a chain of Fe-S clusters (red and yellow spheres) to the ubiquinone binding site. This transfer is linked with the translocation of four protons across the membrane (modified from Efremov and Sazanov, 2011; www.rcsb.org).

There are controversial studies showing that neither AIF depletion nor its full deletion has major effects on the expression levels of respiratory chain subunits on the mRNA level in AIF-deficient ES and HeLa cells (Vahsen et al., 2004). However, another study reports a partial reduction on mRNA levels of respiratory chain subunits in muscle- and liver-specific AIF knockout mice (Pospisilik et al., 2007). Thus, AIF may regulate complex I levels by post-transcriptional mechanisms. Further investigations are needed to determine how exactly AIF is involved in the stability or the assembly of complex I and why this stabilization is mutual, i.e. affects also AIF stability as shown here using the complex I inhibitor rotenone.

It is established that inhibition of the respiratory chain can induce tolerance to e.g. focal cerebral ischemia (Wiegand et al., 1999). Since AIF plays a major role in intrinsic pathways of caspase-independent neuronal death in model systems of cerebral ischemia (Culmsee et al., 2005;Plesnila et al., 2004;Zhu et al., 2003;Zhu et al., 2007) a preconditioning effect mediated by complex I inhibition is feasible.

Preconditioning effects are often described to promote a small decrease in the efficiency of NADH oxidation by the respiratory chain, which leads to an increase in mitochondrial ROS formation followed by activation of mitoK_{ATP} channels (Busija et al., 2008;Dirnagl and Meisel, 2008;Ravati et al., 2000;Ravati et al., 2001). However, no increase in lipid peroxides was detected in AIF-depleted cells, and also pretreatment with the radical scavenger trolox did not change the effect of AIF siRNA in this study. This finding suggests that increased ROS production in AIF-silenced cells is not the major mechanism of the preconditioning effect. These data are in line with previous studies showing that ROS production under basal conditions or stimulated by complex I inhibitors were not different in mitochondria from Hq mouse brain compared to wildtype mitochondria (Chinta et al., 2009). In conclusion, AIF may not directly modulate ROS production in mitochondria. However, it would be of interest whether the mitoK_{ATP} channels system is affected during AIF depletion-mediated preconditioning to further confirm this hypothesis.

Collectively, the results provide strong evidence that AIF depletion is linked to a decrease in complex I expression level and respiratory chain activity resulting in a slight mitochondrial depolarization. These preconditioning effects lead to a stabilization of mitochondria and thus, to delayed cell death after the glutamate challenge and related induction of oxidative stress. In addition, the data indicate a mutual stabilization of AIF and mitochondrial complex I.

4.2.3. AMPK is not involved in the HT-22 model system

The data presented in this study suggest that neuroprotection mediated by AIF silencing is not due to changes in the activity of AMPK since protein levels of AMPK as well as p-AMPK remained unaffected by AIF siRNA. Further, co-treatment of AIF siRNA with an AMPK activator or inhibitor did not reduce the neuroprotective effect of AIF siRNA against glutamate-induced cell death. An involvement of AMPK would suggest also changes in the ATP levels since AMPK monitors energy production and energy expenditure and regulates its activation dependent on the AMP:ATP ratio (Weisova et al., 2011). In this study AIF-depleted HT-22 cells maintained their ATP levels under control conditions as well as under oxidative stress similar to cells treated with the complex I inhibitor rotenone. Thus, the slight inhibition of the respiratory chain seems not to have such a high impact on the ATP production that

could activate AMPK. Another explanation could be that the energy production is preserved otherwise, e.g. by changed metabolism with increased glycolysis independent of AMPK.

These results suggest that AMPK does not play a superior role in the regulation of cell survival mediated by AIF deficiency in the investigated model system.

However, the data of this thesis also show that variations in the AMPK activity affect cell survival rate in the HT-22 model system of glutamate-induced cell death in general. This is in line with reports from the literature that indicate an important role of AMPK for the regulation of neuronal cell death and survival is several other model systems. For example, Culmsee et al. demonstrated that AMPK is highly expressed in neurons in the developing rat brain and further, AMPK activation promotes neuronal survival in primary hippocampal neurons following glucose deprivation (Culmsee et al., 2000). In contrast, Venna et al. reported that ischemic preconditioning which leads to improved behavioral outcomes in a mice model of stroke was associated with an inhibition of AMPK. This neuroprotective effect was abolished by pharmacological activation of AMPK and also AMPK-α2 null mice that lack the catalytic isoform of AMPK failed to demonstrate a preconditioning response (Venna et al., 2012).

The contrary reports from the literature about how AMPK can mediate neuroprotection, as well as the findings in this study, showing that AMPK activation can mediate neuroprotection and neurotoxic effects may be explained by a recent study from Davila et al.. That study indicates that the effects of AMPK in the regulation of neuronal survival and cell death are strongly dependent on the duration and intensity of AMPK activation or inhibition. The authors demonstrate that AMPK mediates a two-step activation of forkhead box O3 (FOXO3), which generates a coherent feed-forward loop thereby determining excitotoxic cell fate. According to this hypothesis, short periods of AMPK activity allow p-AMPK to exert its pro-survival effects, whereas prolonged activation results in induction of cell death. The decision point is controlled by AKT-mediated dephosphorylation of FOXO3 in the first activation step. If the period of AMPK activation overcomes this delay of the first step, FOXO3 becomes activated in a second step, which results in Bim activation and apoptosis (Davila et al., 2012). Referring to this hypothesis, the performed

experiments in this thesis seem to be in an intermediate state of step one and two, in which activation of AMPK mediated by AICAR still provides neuroprotection against glutamate toxicity by its pro-survival functions, maintaining the cellular ATP levels, but also shows already slight toxic effects under control conditions (Figure 9 A).

For the activation of AMPK in HT-22 cells AICAR was used in the mM range. These high concentrations are necessary since AMPK activation is regulated by the ratio of AMP:ATP and AICAR acts by its metabolite AICAR-monophosphate (ZMP), which mimics AMP. ZMP activates AMPK by both allosteric activation and, more importantly, by promoting phosphorylation of the α-subunit (Thr^{172}) mediated by an upstream kinase complex. Phosphorylation of Thr^{172} produces at least 100-fold activation, so that it is quantitatively much more important than the allosteric activation that increases enzyme activity up to 5-fold (Towler and Hardie, 2007). The high concentrations of AICAR needed for the activation may also support unspecific effects. Furthermore, Guigas et al. demonstrated that AICAR inhibits cellular respiration by an AMPK-independent mechanism and thus, cellular effects mediated by AICAR are not necessarily caused by AMPK activation (Guigas et al., 2007).

Also, compound C used in this study may provide side effects next to its property as an inhibitor of AMPK. Its inhibitory effect results from reversible competition with ATP, but the exact mechanism of action is not further specified (Zhou et al., 2001). In addition, it has been reported that compound C does not exclusively inhibit AMPK but it also inhibits respiration and suppresses ROS generated by mitochondria (Emerling et al., 2007). Thus, other methods such as overexpression or siRNA approaches may offer more reliable tools for the investigations on AMPK. However, these efforts were not justified in this study since there was no hint for an involvement of AMPK in the mediation of AIF-depleted neuroprotection in the performed experiments.

4.2.4. AIF and its modulators as therapeutic targets

To date, direct inhibition of AIF by pharmacological compounds is not available. This is foremost attributable to the fact that apart from its apoptotic functions AIF also provides vital redox functions that are indispensable for cell life (Vahsen et al., 2004). The complete loss of AIF expression during embryogenesis leads to growth retardation and death during midgestation (Brown et al., 2006;Joza et al., 2001), and long-lasting downregulation of AIF results in progressing ataxia as found in Hq mice, which express just 20 % of AIF compared to wildtype mice. The ataxia manifests as a side-to-side, unsteady gait with a lateral tremor visible at rest. Moreover, progressive cerebellar cortical atrophy has been characterized in these mice, with an apoptotic loss of granule cells and a necrotic loss of Purkinje cells occurring subsequently. Further, the animals show retinal degradation resulting in blindness, growth retardation and weight loss. In addition, hemizygous males and homozygous females are afflicted with baldness (Benit et al., 2008;Klein et al., 2002). Apart from that, it has been reported that mice with muscle-specific loss of AIF develop severe dilated cardiomyopathy and skeletal muscle atrophy (Joza et al., 2005). Pathogenetic AIF mutations are also known to occur in humans causing muscular atrophy, neurological and psychomotoric abnormalities and progressive mitochondrial encephalomyopathy (Modjtahedi et al., 2010). All these adverse effects of permanent AIF defects lead to the conclusion that AIF is not a recommended direct target for the therapy of neurodegenerative diseases or acute brain injury, to date. However, development of tools that selectively target the pro-apoptotic function of AIF or that can downregulate AIF for a short time only could avoid the adverse effects of long-term inhibition and establish AIF as an interesting therapeutic target. So far, mechanisms of AIF release upstream of mitochondrial damage are suggested as potential targets for therapeutic strategies.

In the past years, different modulators of mitochondrial AIF release were identified, such as calpain I (Polster et al., 2005), the pro-apoptotic protein Bid (Grohm et al., 2010;Landshamer et al., 2008;Tobaben et al., 2011), and PARP-1 (Wang et al., 2009;Wang et al., 2011;Yu et al., 2002), that are of interest as indirect therapeutic targets of AIF. Polster et al. demonstrated that both precursor and mature forms of AIF are cleaved by calpain I near the amino terminus in vitro. This cleavage is essential for the release of AIF from the mitochondria and the subsequent induction

of chromatin condensation and cellular death (Polster et al., 2005). So far, several calpain inhibitors are in the focus of preclinical studies in animal models of ischemia and indicate neuroprotective potential (Bartus et al., 1994;Koumura et al., 2008;Markgraf et al., 1998). Another modulator of AIF release is the pro-apoptotic bcl-2 family member Bid. AIF translocation to the nucleus is preceded by increasing translocation of Bid to mitochondria, and peri-nuclear accumulation of Bid-loaded mitochondria in neurons (Landshamer et al., 2008). The inhibition of Bid by small molecule inhibitors, such as BI6C9 as a target for neurological disorders is subject of previous and ongoing studies (Culmsee et al., 2005;Grohm et al., 2010;Landshamer et al., 2008). In addition, PARP-1 activation, followed by increased PAR levels, is associated with the lethal release of AIF. Recent findings indicate that PAR binding to AIF's PAR-binding motif acts as the transducer that mediates AIF release from the mitochondria, allowing AIF to translocate to the nucleus. Therefore, also PARP-1 is an interesting therapeutic target and PARP-1 inhibition has been shown to reduce nuclear AIF translocation in a model of ischemic neuronal cell death (Culmsee et al., 2005). Also in an in vitro model of rat SCI pharmacological inhibition of PARP-1 showed histological protection and persistence of reflex activity (Nasrabady et al., 2011) and a further study demonstrated that prevention of PARP activation protected against both ROS-induced cells injury in vitro and 1-methyl-4-phenyl-1,2,3,6-tetrahydropyridine (MPTP)-induced nigrostriatal dopaminergic damage in an in vivo mouse model of PD (Iwashita et al., 2004).

Thus, all these regulators of mitochondrial damage and AIF release are validated as potential therapeutic targets in models of neuronal degeneration and death, and further highlight the importance for a deeper understanding of AIF and its mechanisms in regulating neuronal cell death and survival.

Taken together, the data of this thesis provide novel data showing a preconditioning effect of AIF silencing in mitochondria that includes mitochondrial complex I reduction, functional and morphological preservation of mitochondria, and prolonged cell survival after the glutamate challenge and related induction of oxidative stress. Both, targeting AIF release and its pro-apoptotic activation as well as mechanisms underlying AIF depletion-mediated preconditioning may be promising strategies of neuroprotection.

4.3. Molecular conditioning – life from dying NPCs

4.3.1. Life from death: cell death mediates neuroprotection

The second part of the present study provides evidence that cell death of NPCs mediates neuroprotection to surrounding neural cells under lethal stress. The results demonstrated that growth factor withdrawal of NPCs lead to caspase-dependent cell death. The induction of starvation could be prevented by the broad-spectrum caspase inhibitor Q-VD-OPh. CM of dying NPCs prevented hippocampal HT-22 neurons from glutamate-induced lethal stress and EBSS-induced starvation for several hours and even up to 8 hours after the toxic insult. Furthermore, CM also protected primary cortical neurons from glutamate toxicity (Neunteibl, personal communication). The finding that also HT-22 neurons themselves can mediate neuroprotective properties during starvation but not fibroblasts, indicated a specific effect for neural cell lines.

The rescue of NPCs from starvation by the caspase inhibitor Q-VD-OPh abolished the neuroprotective effect of CM and also cell lysates of NPCs mediated neuroprotection towards glutamate-treated HT-22 cells. These data suggest that only dying NPCs secrete a sufficient amount of substances that mediate protection in neighboring neurons. Since inhibitors of protein synthesis did not affect the generation of neuroprotective CM from dying NPC, the protective substances are likely already expressed in the healthy cells, and only their release increased after induction of apoptotic cellular stress. The proposed ability of apoptotic cells to provide signaling cues for their environment and to support surrounding cells has been also demonstrated in other settings, such as ß-cell mass regeneration (Bonner et al., 2010), inhibition of inflammation during wound healing (Li et al., 2010) and planarian regeneration (Pellettieri et al., 2010). The fact that the ability of apoptotic cells to rescue surrounding cells is already described in invertebrates indicates an evolutionarily conserved regeneration mechanism.

The finding that CM from dying stem cells provides neuroprotective effects is new and reflects conditions after stem/progenitor cell transplantation since the survival rate after stem/progenitor cell transplantation is very low (Chen et al., 2002;Menasche, 2005;Silva et al., 2005). In former studies, CM from various stem/progenitor cells was demonstrated to provide neuroprotection but none of these indicated that starvation or cell lysis was a crucial step for enhancing the protective

potential (Cho et al., 2012;Isele et al., 2007;Lim et al., 2008;Menasche, 2005;Scheibe et al., 2012). The data of this thesis indicate that the low survival rate after stem cell transplantation may be very important for the highly potent neuroprotective benefit in neurodegenerative diseases and acute brain injuries.

There are also some differences between NPC CM used in this study and CM from other stem cells reported in the literature. For example, Isele et al. demonstrated that BMSC CM attenuated staurosporine (STS) or amyloid-beta peptide-induced apoptosis in a concentration-dependent manner in primary embryonic rat neurons (Isele et al., 2007). This protective effect was abolished by a specific PI3K inhibitor. The data of this thesis demonstrate that inhibition of the PI3K pathway by the same inhibitor affect the neuroprotective effects only marginal, and indicate that there are more than just one pathway responsible for the neuroprotective benefit. Furthermore, the neuroprotective effect of BMSC CM was abolished by heating over 90°C (Isele et al., 2007) as also shown for NPC CM, but so far, nobody described an activation of the neuroprotective potential by moderate heat as it was done in this thesis.

The isolation of protection-mediating substances by aceton precipitation supported the conclusion that proteins are responsible for the observed neuroprotective effect. This hypothesis was further confirmed by pre-incubation of CM with a protease, which abolished the beneficial effect of CM. The spectrum of the proteins mediating neuroprotection could be even narrowed down by the results from the cut off filtrations. The results clearly indicated that the main mediators of neuroprotection in CM have a molecular size between 10 and 50 kDa. In experiments with cut off filters it should always be kept in mind that the separation of the fractions is not stringent, and the fractions can still contain proteins with a molecular weight around the size of the filter. Thus, it is conceivable that also substances with another molecular weight may contribute to or reinforce the potency of CM. Furthermore, the present data identified already two proteins, prdx-1 and gal-1, to participate in the mediation of the neuroprotective properties of NPC CM as discussed in chapter 4.3.3.1. and 4.3.3.2.. Importantly, the findings of this study clearly demonstrated the contribution of a cofactor to the neuroprotective effect that did not mediate protection alone but in combination with the broad mixture of CM as demonstrated by the separation of the fractions with the 3 kDa cut off filter.

Moreover, other components, such as miRNA, apoptotic bodies, or mitochondria, could cause further protective signals. It has been demonstrated that various miRNAs can have protective effects in models of neurodegenerative diseases, such as AD (Wang et al., 2008). The RNase that was applied to CM in the experiments of this thesis was able to cleave single stranded RNA. Thus, mature miRNA would have been also prone to digestion. However, the RNase treatment did not alter the neuroprotective effect of CM, which excluded RNA and miRNA as the main protective components of CM. Furthermore, apoptotic bodies have been demonstrated to enhance the differentiation of human endothelial progenitor cells in vitro (Hristov et al., 2004), but also isolation of apoptotic bodies from dying NPCs did not provide any neuroprotective benefit. This is in accordance with the fact that RNase did not affect the protective properties of CM since the described protective effects of apoptotic bodies are often linked with the delivery of miRNA (Zernecke et al., 2009).

Recently, it was reported that mitochondrial transfer from BMSCs protected against lung injuries (Prockop, 2012), but also isolated mitochondria from NPCs failed to protect HT-22 cells against glutamate-induced cell death. Furthermore, microvesicles can be excluded as mediators of neuroprotection since CM was filtrated through a 0.22 µm filter by default without losing protective properties.

The used CM mimics conditions after stem-cell based therapy that is currently investigated for the treatment of neurodegenerative diseases and acute brain injuries (Lindvall et al., 2004;Lindvall and Kokaia, 2006). Thus, CM from dying cells is an adequate model for the investigation of the mechanisms that mediate protective effects after stem/progenitor cell transplantation. Further, and most importantly, CM may offer an alternative to cell transplants in the treatment of degenerative diseases of the nervous system. In this way CM could overcome risks and limitations of the classical transplantation therapy as discussed in chapter 4.3.4..

4.3.2. Heat activation of CM

Interestingly, heat treatment at about 60°C significantly increased the neuroprotective potency of CM, and the neuroprotective effect of CM was only abolished at temperatures higher than 90°C. The finding, that also the aceton precipitate could be activated at 60°C indicates that the activation results from a protein. Enzymes and proteins typically function at temperatures below 60°C and denature if exposed to higher temperatures. The thermostability of proteins depends on a lot of various factors, such as amino acid composition, hydrophobic interactions, ion pairing, and hydrogen bonds within the protein. This stability can be improved by adjusting external environmental factors including cations, substrates, co-enzymes, and modulators (Ebrahimi et al., 2011). The performed experiments demonstrated that the proteins that are responsible for the neuroprotective effect of CM are heat stable up to 80°C. The identification of HSPs that are known to be activated through high temperatures, and the fact that recombinant gal-1 and prdx-1 are still active after heating at 60°C renders these proteins likely to contribute to the protective effect of CM.

One explanation for the increase in the neuroprotective potential could be the activation of proteins or enzymes by heat. The most prominent proteins that are known to be activated at higher temperatures are the HSPs. However, heat activation of these proteins is usually achieved at temperatures around 40-45°C (Romi et al., 2011). So far, there are no investigations of CM at higher temperatures described in the literature, most likely because temperatures as found for activation of the NPC CM in this thesis are considered to inactivate and denaturate most proteins. It is not described in the literature, for example whether HSPs are also activated at temperatures around 60°C as indicated for the NPC CM.

Another explanation for the increase in the neuroprotective potential of CM after incubation at high temperatures could be that inhibitory or toxic substances are inactivated, whereas the neuroprotective substances are more thermostable. For example, such a neurotoxic enzyme could be phospholipases A2 (PLA 2). It has been reported that PLA 2 activity in normal human serum was remarkably decreased by incubation at 55°C for only 5 minutes (Funatomi and Hatta, 1991), and also phospholipases from other organisms are described to lose their activity at about 60°C (Karray et al., 2012b). Furthermore, an inhibition of PLA 2 has been

demonstrated to provide direct neuroprotective effects in SY5Y neuronal cells in response to neurotoxic CM from differentiated HL-60 macrophages (Chen et al., 2012). These data support the hypothesis that heat activation of NPC CM may result from an inhibition of one or more enzymes that otherwise provide neurotoxic effects. In this case, CM would offer an advantage towards the direct application of stem cells since the particular protocol for CM production allows to get rid of toxic substances by heat incubation, whereas stem cells may release toxic components in the host tissue. Thus, identification of the neuroprotective components in CM which are heat stable is highly relevant for therapeutic aspects.

4.3.3. Neuroprotective components in the mixture of CM

4.3.3.1. Peroxiredoxins

MALDI-TOF analyses of CM detected different prdxs in all investigated protective samples. Prdxs are a family of small (22-27 kDA) non-seleno peroxidases with six mammalian isoforms. Their role as antioxidants results from their peroxidase activity that reduces and detoxifies hydrogen peroxide, peroxynitrite and a wide range of organic hydroperoxides.

Prdxs can be divided into three major subclasses, which are the typical 2-cysteine (2-Cys) prdxs (including prdx-1 to 4), atypical 2-Cys prdx (prdx-5), and 1-Cys prdx (prdx-6). All three groups share the same peroxidatic active-site structure and thus have the first step of peroxide reduction in common in which the peroxidatic cystein (Cys-SH) attacks the peroxide substrate and is oxidized to a cysteine sulfenic acid (Cys-SOH) (Wood et al., 2003).

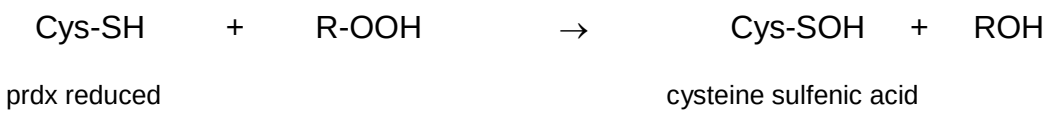

However, the typical and the atypical 2-Cys prdx contain two redox-active cysteins, whereas the 1-Cys prdx contains just one, and the second step of the reaction in which the cysteine sulfenic acid reacts back to the reduced prdx form distinguishes the three subclasses. Typical 2-Cys prdx are the largest class of prdxs and obligatory

forming homodimers containing two identical redox-active cysteins. In the second step of peroxide reduction the cysteine sulfenic acid from one subunit is attacked by the resolving cystein located in the C terminus of the other subunit to form a stable intersubunit disulfide bond. The catalytic cycle is closed by reduction of the disulfide bond through cell specific disulfide oxidoreductases, such as thioredoxin or tryparedoxin (Wood et al., 2003).

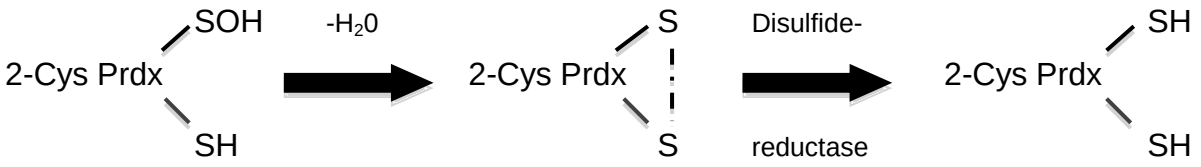

The atypical 2-Cys prdxs have the same mechanism as typical 2-Cys prdx, however, they are functionally monomeric so that the peroxidatic cytein and the corresponding resolving cystein are contained within the same polypeptide (Seo et al., 2000). In contrast, 1-Cys prdx conserves only one peroxidatic cysteine and it is presumably reduced by a thiol-containing reductant (Choi et al., 1998).

The physiological importance of prdxs is illustrated by their abundance as well as studies in knockout mice. For example, mice lacking prdx-1 develop severe haemolytic anemia, and are predisposed to certain cancers in the haematopoietic system. In addition, prdx-1 knockout mice have a 15 % reduction in lifespan (Neumann et al., 2003). Also, prdx-2 knockout mice develop a spontaneous phenotype of hemolytic anemia (Yang et al., 2008a), whereas prdx-6 knockout mice show exaggerated lipopolysaccharide (LPS)-induced acute lung injury and inflammation with increased oxidative stress, inflammatory responses, and matrix degradation (Yang et al., 2011).

In the CNS, prdxs are believed to act as free radical scavengers and are capable of protecting of a variety of cell types, including neurons, as reported in models of ischemic neuronal death in vitro, in overexpression models, and in neurodegenerative diseased tissue (Botia et al., 2008;Boulos et al., 2007;Fang et al., 2007;Hattori and Oikawa, 2007;Smith-Pearson et al., 2008).

The prdx isoform that was identified in all MALDI-TOF analyses was prdx-1. The finding that prdxs are released from NPCs under conditions of growth factor withdrawal was recently supported by the report that prdx-1, 2, 5, and 6 are secreted into brain tissue 12 hours after stroke onset and act outside of the cell. In that study, the extracellular prdxs, particular prdx-5 and 6, and, to a less degree, prdx-1 and 2, were associated with post-ischemic inflammation by the induction of cytokines and increased infarct volume. However, in many investigations the study did not further differentiate between effects mediated by the different prdx isoforms in further detail, and thus, it is possible that mainly prdx-5, which was not detected in CM, was responsible for the increased inflammation (Shichita et al., 2012).

The present study demonstrated that recombinant prdx-1 had neuroprotective effects in the HT-22 cell model system. However, the amount of released prdx-1 that was detected in CM in this study was in the nanomolar range whereas the recombinant protein was applied at micromolar concentrations to prevent glutamate-induced cell death in the HT-22 model system. Nevertheless, the reduced potency of CM after treatment with specific prdx-1 antibody demonstrated that prdx-1 was in any case an additive component that contributed to the neuroprotective effect of CM. It is possible that the human recombinant protein is not as potent as endogenous mouse prdx-1 in the model system of mouse cells. Further, it is conceivable that other components or cofactors in CM are able to activate the enzyme in a way that less prdx-1 is needed to provide neuroprotection.

There is also evidence from the literature that prdx-1 is able to mediate neuroprotective effects. Recently, lentiviral-mediated overexpression of prdx-1 has been demonstrated to protect against 6-hydroxydopamine-induced cell death in mouse dopaminergic neurons in vitro and in vivo (Hu et al., 2011). In addition to its role as an antioxidant enzyme, the neuroprotective effect of prdx-1 could be also due to an interaction with the apoptosis signal-regulating kinase 1 (ASK-1). Prdx-1 is described to interact with ASK-1 via the thioredoxin-binding domain thereby inhibiting the activation of ASK-1, which further results in the inhibition of downstream signaling cascades, such as the p38 pathway (Kim et al., 2008b).

Beyond that, prdx-1 expression has been reported to be increased in LPS-activated microglia which protects against H_2O_2 mediated microglial death also via inhibition of the p38 pathway (Kim et al., 2008a). The protection of microglia is a very interesting

aspect for neuroprotection in vivo since microglia are the main immune cells in the brain, and well established to be involved in neurodegenerative diseases. Beyond the neurotoxic effects of microglial activation by induction of an inflammatory state, microglia have been associated with neuroprotective effects, such as phagocytosis of dead neurons and clearance of debris (Polazzi and Monti, 2010). Thus, for in vivo application an effect of prdx-1 on microglia could also contribute to a neuroprotective effect.

The data of this thesis also demonstrated increased prdx-1 expression levels in HT-22 cells after the treatment with NPC CM. This could result either from exogenous prdx-1 that was taken up from the media, or from other signals mediated by CM that lead to an increase of endogenous prdx-1. An increase in endogenous prdx-1 levels could result from the transcription factor nuclear factor (erythroid-derived 2)-like 2 (Nrf-2). During oxidative stress, Nrf-2 can regulate the expression of genes whose protein products are involved in the detoxification of ROS, and it has been demonstrated that the prdx-1 gene is a target of Nrf-2 (Kim et al., 2007). To investigate whether endogenous prdx-1 in the HT-22 cell model system was increased by induction of Nrf-2, the PI3K inhibitor LY 294002 as an upstream regulator of Nrf-2 was used. Previous studies already demonstrated that it is possible to inhibit the Nrf-2-dependent induction of prdx-1 expression when targeting PI3K in SH-SY5Y cells (Nakaso et al., 2003). Inhibition of PI3K marginally affected the neuroprotective effects of CM. Therefore, an induction of endogenous prdx-1 by Nrf-2 only could play a minor role in the neuroprotection mediated by NPC CM in this study.

Taken together, the data of this thesis indicate that prdx-1 has the potential to mediate neuronal survival against glutamate-induced cell death in HT-22 neurons, and it seems to be one additive compound in the broad mixture of CM providing neuroprotective effects.

Other members of the prdx family, such as prdx-2 and 6 were also identified in some MALDI-TOF experiments in this study, and these may also enhance neuroprotection. For example, it was shown that prdx-2 protected against 6-hydroxydopamine-induced death of mouse dopaminergic neurons in vitro and in vivo. This neuroprotective effect of prdx-2 was mediated by inhibition of the ASK-1 pathway (Hu et al., 2011). In

addition, overexpression of prdx-2 in transgenic mice reveals in reduced brain injury and improves neurological recovery up to 3 weeks after transient focal cerebral ischemia compared to wildtype littermates (Gan et al., 2012).

For prdx-6, neuroprotective effects against hypoxia-induced retinal ganglion cell (RGC) damage have been described. RGCs exposed to hypoxia show reduced expression of prdx-6 which results in increased intracellular ROS levels and apoptotic cell death which can be prevented by overexpression of prdx-6 (Tulsawani et al., 2010). In another study, overexpression of prdx-6 was associated with protective effects against oxidative stress in primary cortical neurons that overexpress retinoic acid receptor-related orphan receptor α (RORα), a transcription factor that plays an essential role for the development of Purkinje cells (Boukhtouche et al., 2006).

Overall, there is clear evidence from the literature that prdxs have the ability to provide neuroprotection in vitro and in vivo. The data of this study indicate that prdxs, especially prdx-1, participate to the neuroprotective effects that CM provides against oxidative stress.

4.3.3.2. Galectin-1

Another interesting protein identified in CM by MALDI-TOF analyses in this study was gal-1. To date, there are 15 family members of the galectin protein family identified in mammals. They all have a conserved carbohydrate-recognition domain (CRD) of about 130 amino acids, which are responsible for β-galactoside binding. While some galectins contain only one CDR and are biologically active as monomers (gal-5, -7, and -10), as homodimers (gal-1, -2, and -11) or as oligomers (gal-3), others contain two CDRs (gal-4, -6, -8, -9, -12) (Camby et al., 2006).

Galectins are primarily localized in the cytosol, but they are also found in nuclei and intracellular plasma membrane. They exert functions inside of the cell where they regulate signal transduction independently of their lectin activity by protein-protein interactions. Galectins, however, can also be secreted and function outside of the cell which is mainly dependent on their lectin activity (Yang et al., 2008b). Gal-1 was the first protein of this family discovered in 1994 (Barondes et al., 1994). Gal-1 exists as a monomer (~14.5 kDa), as well as a homodimer (~29 kDa) in solutions. Both forms are able to bind to carbohydrates, however, the monomeric form with a lower level of

affinity. Furthermore, gal-1 can also exist in an oxidized form that lacks lectin activity (Camby et al., 2006).

Gal-1 has a lot of various biological functions including functions in the immune system, tumor formation, and the development of the neural system and muscle tissue. For example, in the immune system it contributes to the immunosuppressive activity of T regulatory cells, suppresses B-cell proliferation, and is involved in the activation of macrophages. It further favors tumor growth and migration, and participates in tumor cell evasion of immune response. In addition, it promotes cell differentiation in muscle cells (Yang et al., 2008b). All these functions are mediated by binding of gal-1 to various binding partners, such as carbohydrates, Ras, membrane glycoproteins, integrins, and several other proteins (Camby et al., 2006).

In neural and stem cells different properties of gal-1 have been described. It has been demonstrated that recombinant gal-1 promoted neurite outgrowth from a mouse olfactory neuron cell line (Puche and Key, 1995). The reduced form of gal-1 promotes proliferation of NSCs thereby interacting with β-1-integrin, which modulates cell adhesion (Sakaguchi et al., 2010). Thus, gal-1-null mice have fewer NPCs in the adult brain compared to their wildtype littermates (Sakaguchi et al., 2006). Also, an enhancement of axonal regeneration in peripheral nerves by the oxidized form of gal-1 has been described (Horie et al., 1999). Moreover, gal-1 inhibited glutamate toxicity in cerebellar cells (Lekishvili et al., 2006), and it has been further shown that oxidized gal-1 provided neuroprotection in a transgenic mouse model of ALS (Chang-Hong et al., 2005).

Recently, gal-1 was identified to be a pivotal regulator of microglial activation (Starossom et al., 2012). There are two different kinds of activation states in microglia. Classical activation, such as induced by LPS or interferon-γ, leads to a M1 phenotype that is associated with neurodegeneration, whereas alternative activation, such as induced by interleukin (IL)-4, results in a M2 phenotype that has been shown to be anti-inflammatory and neuroprotective. Starossom et al. found gal-1 to bind with a significantly higher affinity to M1-type microglia, which responds in a shift to the M2 state by downregulation of proinflammatory cytokines and iNOS expression, and by upregulation of typical M2 markers, such as arginase. This was mediated by binding of gal-1 to core 2 O-glycans decorating CD45 on microglial cells, resulting in retention of this glycoprotein on the plasma membrane and augmenting its

phosphatase activity. Further, gal-1 indirectly decreased neuronal loss through mechanisms involving p38MAPK-, CREB-, and NF-κB-dependent signaling pathways, which are activated upstream of the neurotoxic molecules tumor necrosis factor (TNF) and nitric oxide (NO) in the microglia (Starossom et al., 2012). The finding, that gal-1 shifts the neurodegenerative activation state of microglia into a neuroprotective state could play an important role for neuroprotective effects in vivo.

Collectively, there is evidence in the literature that both, the oxidized and the reduced form of gal-1, provide beneficial effects on neural cells.

In the model system of glutamate-induced apoptosis in HT-22 cells recombinant mouse gal-1 attenuated glutamate toxicity. In addition, the neuroprotective effect of CM was reduced by a specific antibody. The fact, that the reduction of the neuroprotective effect was not seen in all experiments can be due to inefficiency of the antibody. Further, it is not known, whether the inhibition by the antibody is competitive or reversible. Since an unspecific antibody did not affect the neuroprotective effects of CM, these experiments clearly demonstrated that gal-1 contributed to the neuroprotective effect of CM.

So far, there is only one study published demonstrating a contribution of gal-1 to neuroprotective effects observed after stem cell transplantation. Adult common marmosets were treated with human NSCs that were transfected by lentivirus with gal-1 nine days after contusive cervical SCI. The Gal-NSC-grafted animals showed a better performance on all the behavioral tests compared with the other control groups including their spontaneous motor activity, bar grip power, and performance on a treadmill test (Yamane et al., 2010). This clearly demonstrates the potential of gal-1 to provide beneficial effects after transplantation into the CNS in models of neuronal injury. However, very few is reported about the possible mechanisms behind this neuroprotective potential. There are several studies reporting that gal-1 influences the secretion and the receptors of growth factors that can mediate neuroprotection, for example, via the Akt signaling pathway. Former experiments in our laboratory demonstrated that NPC CM also leads to activation of Akt and Erk 1/2 in primary cortical neurons, which could suggest the involvement of growth factors (Neunteibl, Dolga, personal communication).

Hsieh et al. reported that gal-1 activates VEGFR-2 signaling by an direct interaction with the neuronal receptor neuropilin-1 (Hsieh et al., 2008). This mechanism is in line

with findings showing that transplanted stem cells mediate neuroprotective effects after stroke, such as recovery, inflammation, and vascular repair by secretion of VEGF (Horie et al., 2011). VEGF can be secreted and act in very low concentrations (pg/ml; Cho et al., 2012) so that it is conceivable that it is under the detection limit the MALDI-TOF measurements. Another interesting aspect in this context is that VEGF has been demonstrated to be heat stable when heating at 65°C for 5 minutes (Ferrara and Henzel, 1989) which is also found for the investigated CM in this study. Whether VEGFR stimulation or VEGF-mediated neuroprotective plays a role in the HT-22 cell model remains to be unknown. However, since VEGF is expected to mediate neuroprotective effects via the PI3K/Akt signaling pathway (Kilic et al., 2006) also this factor would presumably be an additional compound for the CM-mediated neuroprotection in HT-22 cells, if at all, since inhibition of PI3K marginally affected the neuroprotective potency of CM only as already described.

Another possible mechanism to provide neuroprotection by gal-1 is the induction of BDNF synthesis in the target cells. For example, Gal-1 enhanced BDNF synthesis in astrocytes which improved the functional outcome in rats following ischemia (Qu et al., 2010). However, BDNF was not able to provide neuroprotective effects in the applied HT-22 cell system leading to the conclusion, that gal-1 does not mediate neuroprotection of CM by stimulation of BDNF synthesis and release. This is in accordance with former reports showing that HT-22 cells do not express functional TrkB receptors and even after viral infection TrkB expressing HT-22 cells cannot be rescued from oxidative glutamate toxicity by BDNF but only from serum deprived cell death (Rössler et al., 2004). In primary cortical neurons BDNF is described to provide neuroprotection from glutamate-induced toxicity as well as from serum withdrawal (Hashimoto et al., 2002;Poser et al., 2003). Thus, BDNF production could still be a possible mechanism contributing to protective effects of gal-1 in CM in primary cortical neurons.

The data of this study suggest that gal-1 secreted by dying NPCs is able to contribute to the neuroprotective effect mediated by NPC CM, however, comparable to prdx-1 it may only play a minor role in the complex CM mixture.

4.3.3.3. Further possible neuroprotective components in NPC CM

In addition to prdxs and gal-1 there were also other proteins identified in NPC CM, which may provide neuroprotective effects.

Further possible candidate proteins for neuroprotection are members of the HSP family. The HSPs are separated into subfamilies according to their molecular weight. Under physiological conditions, HSPs are expressed at low levels, and they are induced by cellular stress, such as increased temperature, radiation, exposure to chemicals, oxidative stress, and various other pathological stimuli. Furthermore, they act as chaperone proteins and prevent protein misfolding and aggregation. In addition, it has been shown that recombinant HSPs can function as cytokines to induce production of proinflammatory cytokines and promote dendritic cell maturation (Romi et al., 2011;Wang et al., 2002).

The HSPs identified in NPC CM in this thesis were HSP 60, 70, and 90. There are several studies indicating that HSPs, especially HSP 70, provide neuroprotective effects in various models of neurodegenerative diseases and acute brain injury. For example, Liebelt et al. demonstrated that exercise preconditioning on a treadmill for several weeks before the onset of stroke in rats induced neuroprotection, which coincided with a significant upregulation of HSP 70 and p-Erk 1/2. These results were further associated with downregulated expression levels of Bax and AIF, while levels of Bcl-xL were upregulated in response to stroke after exercise (Liebelt et al., 2010).

Also in animal models of ALS HSP 70 is shown to be involved in neuroprotective mechanisms. For example, intraperitoneal injected recombinant human HSP 70 into G93A mutant SOD1 mice was effective at increasing lifespan, delaying symptom onset, preserving motor function, and prolonging motoneuronal survival (Gifondorwa et al., 2007).

Further, HSPs were shown to induce the production of IL-6 and TNF α and increase the phagocytosis and clearance of Aβ peptides in rat microglia. The mechanism of these activations by exogenous HSPs involved the NF-κB and p38MAPK pathways mediated by Toll-like receptor 4 activation. Thus, HSPs may serve a neuroprotective role by facilitating Aβ clearance and cytokine production (Kakimura et al., 2002). In another study Klucken et al. demonstrated that overexpression of HSP 70 reduced accumulation and toxicity of alpha-Synuclein, and also the alpha-Synuclein fibrillar

assembly was prevented by HSP 70 in mice (Huang et al., 2006;Klucken et al., 2004).

These examples clearly indicate that HSPs, especially HSP 70, have high potential to protect neural cells by intracellular as well as extracellular mechanisms. It has been demonstrated that HSP 70 can be released from several cells and taken up by other cells in a biologically active form, for example, in a model of human T98G glioma cells and differentiated LA-N-5 neuroblastoma cells as model for glia to neurons cell-cell communication (Guzhova et al., 2001;Hightower and Guidon, Jr., 1989;Tytell et al., 1986). In the present study, HSP 70 was identified in several MALDI-TOF analyses of NPC CM and, thus, it may contribute to the protective effects. However, all HSPs identified in CM have a higher molecular weight than 50 kDa while the main protective effects of CM were detected with fractions containing proteins at molecular weights between 10 and 50 kDa. An additional contributing effect of HSPs is, however, conceivable since separation by the cut off filters is not very stringent. In addition, it should be kept in mind that the investigation of separated CM fractions can also lead to misinterpretations since it is also conceivable that the potency of some compounds is strongly dependent on cofactors and interactions with other proteins. The separation of these interaction partners may lead to the abolishment of neuroprotective events since cofactors, such as identified in the 3 kDa cut off filtrate, get lost. Furthermore, the separation of CM is mostly associated with dilution effects as in the experiments performed by column gel filtration or adsorption effects when using size exclusion filters to fractionate the mixture.

In addition, MALDI-TOF analyses of NPC CM identified the eukaryotic elongation factors (eEF) 1 and 2. During elongation eEF 1 catalyzes the aminoacylated-transfer RNA delivery step, whereas eEF 2 acts as the translocase, allowing the ribosome to move down the mRNA one codon at a time (Sasikumar et al., 2012).

Marin et al. demonstrated that glutamate leads to a calcium-dependent phosphorylation of eEF 2 and they suggested that the resulting depression of protein translation represents a self-protecting mechanism against glutamate-induced neurotoxicity (Marin et al., 1997). Moreover, the kinase for eEF 2 regulates dendritic spine stability and synaptic structure by modulating dendritic BNDF synthesis (Verpelli et al., 2010), which may be a relevant mechanism for the neuroprotective effect of CM in primary cortical neurons.

The data of this study clearly demonstrated that there were several different modulators of cell survival in the mixture of CM, and additive effects of prdxs, gal-1 and also HSP 70 are very likely. Presumably, the interaction of several protein factors results in the highly potent neuroprotective composition of NPC CM. This hypothesis is further supported by the fact that neuronal loss and neurodegeneration in brain diseases are also not due to one single mechanism mediating neural cell death, but to multiple different mechanisms, including oxygen deficits, free radicals, products of lipid degradation, disrupted ionic homeostasis (e.g. calcium), altered neurotransmitter release (e.g. glutamate) and receptor function, inflammatory and immune changes, and apoptosis (Faden and Stoica, 2007;Yakovlev and Faden, 2004). Therefore, a therapy that combines synergistic effects of potent neuroprotectants with different modes of action directed against the main pathological mechanisms involved in neuronal cell death promises much higher therapeutic effects than drugs directed toward a single pathophysiological mechanism. Of course, such single targets can also inhibit cell death by reducing the barrier of factors that has to be overcome for cell death, or by prolonging the time window until executing damage, which can be used for regeneration. However, a combination therapy promises much more efficiency, and may lower risks for adverse effects as compared with prolonged high-dose therapy. One example for the higher efficiency of a combination therapy compared to the single application of the substances is the study of Culmsee et al., that demonstrates that combination therapy of the NMDA receptor antagonist memantine and the β_2-adrenoceptor agonist clenbuterol not only resulted in a further reduction of brain damage as compared with effects of the single components but also significantly extended the therapeutic window in a mouse model of permanent focal cerebral ischemia (Culmsee et al., 2004). Thus, CM promises to be a very efficient option for the treatment of neurological deficits.

4.3.4. Clinical implications of CM

The data of this thesis indicate that CM from dying NPCs may offer a highly potent therapeutic option for the treatment of diseases that are characterized by neural loss and degeneration.

There are several points that make CM an attractive alternative to direct stem/progenitor cell transplantation. Stem/progenitor cells are relatively easy to isolate and to expand, and thus, large amounts of CM can be produced easily in a short time. The activity of CM was found in this study to be improved by heating at 60°C. This process results not only in a higher efficacy of CM but also in high stability. NPC CM in this thesis was shown to mediate neuroprotection even after 7 days storage at 37°C without any loss of its potency. Due to this fact also continuous infusion of CM is possible which may increase the therapeutic benefit. For example, a continuous infusion of CM from human adipose stem cells was demonstrated to significantly improve functional and structural recovery in rats after MCAO (Cho et al., 2012).

Further advantages of CM compared to stem cell therapy are the setting of control standards and quality issues. CM could be standardized, e.g. to one protein that is identified to mediate neuroprotection. However, before such control standards can be introduced the exact composition of CM has to be clarified.

Since the exact mixture in CM is not yet known it is also conceivable that CM contains considerable amounts of toxic or counteracting substances. Therefore, CM needs to be examined for such potentially harmful factors, which then could be eliminated to further optimize CM for therapeutic applications. One possibility to get rid of such toxic substances could be the heating process at 60°C. Such toxic substances, that can be eliminated more easily from CM than from stem cells, could also include carcinogen components. An outgrowth of transformed cells in human MSC cultures (Scheibe et al., 2012;Wang et al., 2005) and similar characteristics in both stem cells and cancer stem cells (Ratajczak, 2005) have been reported. Thus, the risk of tumorigenicity induced by stem cell transplantation and also CM has to be studied very thoroughly. To date, there is one report of a human brain tumor derived from stem cell therapy. A 9-year old boy with ataxia telangiectasia was treated with intracerebellar and intrathecal injections of human fetal NSCs. Four years after the first injection a multifocal brain tumor of nonhost origin was diagnosed suggesting

that it was derived from the transplanted NSCs (Amariglio et al., 2009). The risk of tumor formation as a late effect of stem cell therapy is not only topic of discussion after transplantation into the brain but also discussed in other fields. For example, an increased risk for secondary tumor formation has been described for patients after allogenic hematopoietic stem cell transplantation (Gallagher and Forrest, 2007) and also iPS cells that are a promising tool for future stem cell therapy are known to have the potential for tumorigenicity, and thus, the generation of tumor-free iPSCs reaches more and more interest (Lin and Ying, 2013;Zhao et al., 2012). For that reason, it is highly important to ensure the safety of stem/progenitor cell transplantation, to identify risk factors, and to develop alternative therapy methods, such as the application of stem/progenitor cell CM that may overcome risks and limitations of classical stem cell therapy.

Another remaining question is the optimum route of delivery for CM. It has to be tested whether CM has to be applied directly into the brain or if also a peripheral application is possible. Several studies showed beneficial effects of intravenous injection of stem cells. For example, Chen et al. demonstrated that intravenously administered MSCs mediated recovery of somatosensory behavior and Neurological Severity Score in a rat model of stroke. Morphological analysis of the tissue indicated that MSCs are more likely to enter into damaged brain than into contralateral nonischemic brain (Chen et al., 2001). Another study from Jackson et al. directly compared different stem cell types and different routes of application, such as intracerebral or intravenous applications. Both BMSCs and epidermal neural crest stem cells (eNCSCs) were transplanted into the corpus callosum of rats lateral to an LPS inflammatory lesion or were injected intravenously. Both stem cell types showed significant homing potential to sites of inflammatory brain injury after intracerebral as well as after intravenous transplantation. However, only 8 % of the intravenously injected stem cells migrated to the lesion whereas more than 10 times of this number of stem cells reached the lesion site after intracranial administration (Jackson et al., 2010). The mechanisms responsible for stem cell migration into the brain after i.v. application are not yet fully understood. Inflammatory substances, such as IL-1β, TNF, and IL-6 originating from degenerating tissue may provide chemoattractant signals for stem cells, and the movement could be controlled in part through changes in expression of cell surface adhesion molecules. Further, disruption of the BBB may also facilitate selective entry of stem cells into brain lesion (Chen et al., 2001;Jackson

et al., 2010).
It would be necessary to investigate whether the observations of stem cell migration are also transferable for the substances providing neuroprotection in CM from stem/progenitor cells, or if the whole cells are needed to serve as a kind of shuttle for the neuroprotection-mediating compounds after intravenous injection.
Further, it is also necessary to develop an efficient and gently method to concentrate CM to guarantee an uncomplicated and efficient dosage for individual patients.

Of course, the neuroprotective benefit of CM as well as the safety, the reproducible generation, and the exact application of CM have to be tested extensively in vivo models before transferring the concept of CM application to clinical trials.

The data from this thesis indicate the benefit of NPC CM resulting from cell lysis during cell death. This implies the potential use of cell lysates instead of CM, since lysates are much easier generated than CM from dying cells. However, standardizing and controlling such a lysate, e.g. for the content of proteases, is also a major challenge. Furthermore, the lysate could not be activated by heat reliable, which is a great advantage of NPC CM. In addition, NPC lysate was less stable compared to NPC CM when stored at 37°C, and thus, cell lysates are unlikely suitable for continuous infusion or long-time storage.

Collectively, the results of this thesis indicate that CM from dying NPCs could be a viable and promising tool for the treatment of neurodegenerative insults, which could bypass several technical and clinical limitations of stem/progenitor cell transplantation.

5. Summary

Neuronal preconditioning describes a phenomenon that affords robust brain tolerance against neurodegenerative insults. This adaptive cytoprotection is a fundamental capability of living cells, allowing them to survive exposure to potentially recurrent stressors. The research of the molecular and cellular signaling during this self-protecting process is an important tool to develop novel strategies for the treatment of diseases that are characterized by neuronal cell death, which causes progressive loss of brain tissue and function after acute brain injury and in chronic neurodegenerative diseases.

The major aim of this study was to investigate preconditioning effects in a model of neuronal cell death on the molecular and cellular level. This issue was addressed in immortalized mouse hippocampal HT-22 neurons exposed to glutamate toxicity, which selectively induces oxidative stress through glutathione depletion.

The first part of the present study investigates, whether the neuroprotective effect mediated by the depletion of the pro-apoptotic protein AIF is attributed to mitochondrial preconditioning. AIF is a mitochondrial protein that mediates caspase-independent cell death after translocation into the nucleus by chromatin condensation and large-scale DNA fragmentation. The findings of this study demonstrate that AIF gene silencing protects mitochondrial function and integrity in a paradigm of lethal oxidative stress in the used neural cell line. Depletion of AIF preserved mitochondrial morphology, mitochondrial membrane potential, and ATP levels after induction of oxidative stress in HT-22 cells, and this mitoprotective effect also significantly attenuated the secondary increase in lipid peroxidation which was associated with mitochondrial damage and cell death in this model system. Furthermore, AIF depletion was associated with reduced complex I expression levels, and similar to protective effects achieved by low doses of the complex I inhibitor rotenone. These results suggest for the first time that AIF silencing provides protection against oxidative cell death at the level of mitochondria by preconditioning and not at the level of apoptotic DNA damage in the nucleus.

The second part of this thesis investigated conditioned medium (CM), which was generated by neural progenitor cells (NPCs) that undergo starvation-induced apoptosis after growth factor withdrawal. It is well established that transplantation of stem/progenitor cells to the brain improve abnormal motor behavior and memory

function in a broad spectrum of neurodegenerative diseases and after acute brain injury. However, stem cell-based therapy still holds many risks and unresolved issues regarding the mode of action and the optimal application. The validation of a CM from dying NPCs reflects the conditions after stem/progenitor cell injection since only very few cells survive after the transplantation. The findings of the present study clearly demonstrate that CM provides very potent, long-lasting, and stable neuroprotective effects that can even be further increased by heat activation. The data also indicate that cell lysis is essential for the generation of protective properties. Thus, the release of neuroprotective substances during the cell death of stem/progenitor cells seems to be a kind of cellular communication that protects neighboring cells and other tissues. Interestingly, a variety of proteins were identified as potential candidates that mediated the neuroprotective effect of CM, such as prdx-1 and gal-1. Further, the contribution of a low molecular weight cofactor was found. Thus, the results of these investigations are the basis for the development of a highly potent, standardized composition for the therapy of neurodegenerative diseases and acute brain injury.

In summary, the data from this thesis highlight the neuroprotective potential of preconditioning effects for the regulation of cell survival after neurodegenerative insults. In addition, they indicate the importance of understanding the underlying mechanisms to develop new strategies for the therapy of neurodegenerative diseases.

6. Zusammenfassung

Neuronale Präkonditionierung beschreibt ein Phänomen, bei dem es durch potentiell toxische Reize zu einer Toleranzentwicklung gegenüber neurodegenerativen Prozessen im Gehirn kommt. Diese Anpassungsfähigkeit der Zellen ist essentiell, um gegen spätere Stresseinwirkungen besser geschützt zu sein. Für die Entwicklung neuer Strategien bei der Behandlung von Erkrankungen, die durch neuronalen Zelltod und dem daraus resultierenden Verlust von funktionsfähigem Hirngewebe gekennzeichnet sind, ist es von größter Bedeutung, diesen Selbstschutz-mechanismus auf molekularer und zellulärer Ebene zu erforschen.

Das Ziel dieser Arbeit bestand darin, Effekte der Präkonditionierung sowohl auf molekularer Ebene, als auch auf zellulärer Ebene in einem Modell des neuronalen Zelltods zu untersuchen. Hierzu wurde eine neuronale hippocampale Zelllinie (HT-22 Zellen) verwendet, die dadurch gekennzeichnet ist, dass eine Schädigung mit Glutamat zu einem kontinuierlichen Abfall der intrazellulären Glutathionspiegel führt und somit oxidativen Stress induziert.

Der erste Teil der vorliegenden Arbeit beschäftigt sich mit der Fragestellung, ob ein durch AIF-Depletion vermittelter neuroprotektiver Effekt auf mitochondriale Präkonditionierung zurück zu führen ist. Das pro-apoptotische Protein AIF ist ein mitochondriales Protein, das Caspase-unabhängigen Zelltod vermitteln kann. Die Ergebnisse dieser Arbeit zeigen, dass eine Herunterregulierung von AIF im vorliegenden Modell sowohl die Funktionen als auch die Integrität der Mitochondrien schützt. Eine verringerte Expression von AIF bewahrte die mitochondriale Morphologie, das mitochondriale Membranpotential und die ATP-Spiegel der Zellen unter der Einwirkung von oxidativem Stress. Darüber hinaus verzögerte sich auch der späte Anstieg an Lipidperoxiden, der im Allgemeinen mit einer Schädigung der Mitochondrien und anschließendem Zelltod in diesem Zellmodell einher geht. Des Weiteren führte eine AIF-Depletion zu einer verringerten Expression des Komplex I der Atmungskette. Der Komplex I-Inhibitor Rotenon erzielte in niedriger Dosierung ähnlich protektive Effekte im untersuchten Zellsystem.

Diese Untersuchungen zeigten erstmalig, dass AIF-Depletion aufgrund mitochondrialer Präkonditionierungseffekte zum Schutz der Zelle gegen oxidativen

Stress führt und nicht, wie bislang angenommen auf einer verringerten DNA-Schädigung im Zellkern beruht.

Der zweite Teil der Arbeit beschäftigt sich mit der Untersuchung von konditioniertem Medium (CM), das nach Wachstumsfaktorentzug aus sterbenden neuralen Vorläuferzellen (NPCs) gewonnen wurde. Die Transplantation von Stammzellen und Vorläuferzellen ins Gehirn kann sowohl die motorischen Funktionen, als auch die Gedächtnisfunktion in einer Vielzahl von neurodegenerativen Erkrankungen, sowie nach Schädel-Hirn-Trauma und Schlaganfall verbessern. Jedoch beinhaltet die Stammzell-basierte Therapie noch sehr viele Risiken und offene Fragen bezüglich ihrer Wirkweise und der optimalen Anwendung. Die Entwicklung eines CMs von sterbenden NPCs spiegelt sehr gut die Bedingungen nach der Transplantation von Stammzellen wieder, da nur wenige Zellen diese Transplantation überleben und die meisten Zellen, während sie sterben, eine Vielzahl von Faktoren freisetzen. Die Ergebnisse der vorliegenden Studie zeigten, dass CM einen starken und lang andauernden neuroprotektiven Effekt vermittelt. Dieser Effekt konnte durch Hitzebehandlung des CMs noch verstärkt werden. Darüber hinaus zeigten die Daten, dass eine Lyse der NPCs notwendig ist, um einen protektiven Effekt zu erzielen. Vermutlich handelt es sich bei der beobachteten Protektion um Schutzsignale der sterbenden Zellen für die benachbarten Zellen und umliegendes Gewebe. Interessanterweise wurde eine Vielzahl von Proteinen im CM identifiziert, die für die Neuroprotektion verantwortlich zu sein scheinen, darunter auch Peroxiredoxin-1 und Galectin-1. Zusätzlich wurde die Beteiligung eines niedermolekularen Cofaktors an der Vermittlung des neuroprotektiven Effekts nachgewiesen. Die Ergebnisse dieser Untersuchungen bilden somit die Grundlage für die Entwicklung eines äußert potenten und standardisierbaren CMs, das für eine therapeutische Anwendung bei neurodegenerativen Erkrankungen, sowie anderen zerebralen Schädigungen vorstellbar ist.

Zusammenfassend zeigt diese Arbeit, wie effektiv Präkonditionierungseffekte für das Überleben neuronaler Zellen bei neurodegenerativen Ereignissen sind. Für die Entwicklung neuer Therapieoptionen ist es von größter Bedeutung, die zugrunde liegenden Mechanismen der protektiven Effekte durch molekulare und zelluläre Präkonditionierung zu entschlüsseln.

7. Abbreviations

ACA	Asphyxial cardiac arrest
AD	Alzheimer’s disease
AIF	Apoptosis inducing factor
ALS	Amyotrophic lateral sclerosis
AICAR	5-Amino-1-β-D-ribofuranosyl-imidazole-4-carboxamide
AMP	Adenosine monophosphate
AMPK	5' Adenosine monophosphate-activated protein kinase
ANOVA	Analysis of variance
Apaf-1	Apoptosis protease-activating factor-1
ASK-1	Apoptosis signal-regulating kinase 1
ATP	Adenosinetriphosphate
ATP 5A	ATP synthase
BBB	Blood brain barrier
BCA	Bicinchonic acid
Bcl-2	B-cell lymphoma-2
BDNF	Brain-derived neurotrophic factor
bFGF	basic Fibroblast growth factor
BMSC	Bone mesenchymal stem cells
BSA	Bovine serum albumin
BODIPY	4,4-Difluoro-5-(4- phenyl-1,3-butadienyl)-4-bora 3a,4a-diaza-sindacene-3-undecanoic acid
CAD	Caspase-activated deoxyribonuclease
CCCP	Carbonyl cyanide 3-chlorophenylhydrazone
CHX	Cycloheximide
CM	Conditioned medium
CNS	Central nervous system
CRD	Carbohydrate-recognition domain
Cx43	Connexin 43

Cyt C	Cytochrome C
DAPI	4',6-Diamidino-2-phenylindole
DMEM	Dulbecco's Modified Eagle Medium
DMSO	Dimethyl sulfoxide
DNA	Desoxyribonucleic acid
DTT	D,L-Dithiotreitol
EBSS	Earle's Balanced Salt Solution
EDTA	Ethylenediamine-tetra-acetic acid
EGTA	Ethylene glycol-bis(2-aminoethylether)-*N,N,N',N'*-tetraacetic acid
eEF 2	eukaryotic Elongation factor 2
EGF	Endothelian growth factor
EMA	European Medicines Agency
eNCSCs	Epidermal neural crest stem cells
Erk	Extracellular signal-regulated kinase
ESC	Embryonic stem cell
FACS	Fluorescence-activated cell sorting
FasL	Fas-ligand
FCS	Fetal calf serum
FDA	Food and Drug Administration
FGF	Fibroblast growth factor
FOXO3	Forkhead box O3
Gal-1	Galectin-1
Glut	Glutamate
Gpx 4	Glutathion peroxidase 4
GSH	Glutathione
IL	Interleukin
iNOS	inducible nitric oxide synthase
iPSC	induced pluripotent stem cell
HD	Huntington’s disease

HIF-1	Hypoxia-inducible factor 1
H_2O_2	Hydrogen peroxide
Hq	Harlequin
HRP	Horseradish peroxidase
HSP	Heat shock protein
LIF	Leukaemic inhibitory factor
12/15 LOX	12/15 Lipoxygenase
LPS	Lipopolysaccharide
LY 294002	2-(4-Morpholinyl)-8-phenyl-4H-1-benzopyran-4-one
MAPK	Mitogen-activated protein kinase
MEF	Mouse embryonic fibroblast
miRNA	microRNA
mitoK_{ATP}	Mitochondrial adenosine triphosphate-dependent potassium
MLS	Mitochondrial location sequences
MMP	Mitochondrial membrane potential
MnSOD	Manganese superoxide dismutase
MPTP	1-Methyl-4-phenyl-1,2,3,6-tetrahydropyridine
MSC	Mesenchymal stem cell
MTCO 1	Mitochondrially encoded cytochrome c oxidase 1
MTT	3-(4,5-Dimethylthiazol-2-yl)-2,5-diphenyltetrazolium bromide
NAD^+	Nicotinamide adenine dinucleotide
NADH	Nicotinamide adenine dinucleotide
NaOH	Sodium hydroxide
NDUFA-8	NADH dehydrogenase (ubiquinone) 1 alpha subcomplex 8
NEAA	Non-essential amino acids
NPC	Neural progenitor cell
Nrf-2	Nuclear factor (erythroid-derived 2)-like 2
NSC	Neural stem cell

NF-κB	Nuclear factor κB
NO	Nitric oxide
OGD	Oxygen-glucose deprivation
Omi/HtrA2	High temperature requirement protein A2
PAR	Poly(ADP-ribose)
PARP-1	Poly(ADP-ribose)polymerase 1
PBS	Phosphate buffered saline
PCD	Programmed cell death
PD	Parkinson's disease
PFA	Paraformaldehyde
PI3K	Phosphoinositide-3-kinase
PKC	Protein kinase C
PLA 2	Phospholipase A 2
Prdx	Peroxiredoxin
PVDF	Polyvinylidenfluorid
Q	Ubiquinone
QH_2	Ubiquinol
Q-VD-OPH	N-(2-Quinolyl)valyl-aspartyl-(2,6-difluorophenoxy) methyl ketone
RGC	Retinal ganglion cell
RORα	Receptor-related orphan receptor α
ROS	Reactive oxygen species
SCI	Spinal cord injury
Scr	Scrambled
SDHB	Succinate dehydrogenase complex, subunit B
SDS	Sodium dodecyl sulfate
SDS-PAGE	Sodium dodecyl sulfate polyacrylamide gel electrophoresis
SGZ	subgranular zone
SMAC/DIABLO	Second mitochondria – derived activator of caspase/direct IAP binding protein with low pI

SVZ	subventricular zone
TBE	Tris/borate/EDTA
TBI	Traumatic brain injury
tBid	truncated Bid
TBST	Tris-buffered solution with Tween 20
TEMED	Tetramethylenethylendiamin
TMRE	Tetramethylrhodamin ethal ester
TNF	Tumor necrosis factor
Trolox	6-Hydroxy-2,5,7,8-tetramethylchroman-2-carboxylic acid
UCP 2	Uncoupling protein 2
UQCRC 2	Ubiquinol-cytochrome c reductase core protein 2
VEGF	Vascular endothelial growth factor
xCT	glutamine-cystine antiporter
XIAP	X-chromosomal linked inhibitor of apoptosis
ZMP	AICAR-monophosphate

8. Attachment

	Accession Number	Peptide Count	Total Ion Score	Blast	n
1	P000022070|10481..18563 |X150812|MAUS_026728	11	678	vimentin	3
2	P000025562|10126..15853 |X171365|MAUS_011752	11	692	phosphoglycerate mutase 1	3
3	P000050959|11039..12925 |X170662|MAUS_029580	10	823	actin, cytoplasmic 1	3
4	P000024841|10204..71927 |X167120|MAUS_047126	9	556	clathrin heavy chain 1	2
5	P000021382|7754..13998| X146990|MAUS_004980	9	612	heterogeneous nuclear ribonucleoproteins A2/B1 isoform 2	3
6	P000049905|13972..15652 |X126642|MAUS_023944	7	445	Hsp90ab1 protein	3
7	P000021080|10090..41734 |X145184|MAUS_020849	7	565	14-3-3 protein epsilon	2
8	P000051665|14256..15439 |X186510|MAUS_034994	6	392	Eef2 protein	2
9	P000025352|10111..18938 |X170045|MAUS_004891	6	354	nestin	3
10	P000024506|10001..56355 |X165166|MAUS_020917	6	310	ATP-citrate synthase isoform 2	1
11	P000049063|10208..11951 |X127700|MAUS_017390	5	412	fructose-bisphosphate aldolase C	3
12	P000025266|10359..12260 |X169662|MAUS_059970	5	354	heat shock-related 70 kDa protein 2	3
13	P000024794|10233..14024 |X166888|MAUS_026864	5	255	78 kDa glucose-regulated protein precursor	2
14	P000018018|10907..19558 |X126344|MAUS_025980	4	372	60 kDa heat shock protein, mitochondrial	2
15	P000026091|10145..33559 |X174409|MAUS_051391	4	368	14-3-3 protein gamma	3
16	P000050150|11259..26246 |X150241|MAUS_025153	4	266	fatty acid synthase, isoform CRA_a	2
17	P000049393|10068..10738 |X173202|MAUS_020736	4	234	5',3'-nucleotidase, cytosolic	2
18	P000049887|10141..13142 |X127442|MAUS_023456	4	176	triosephosphate isomerase	3
19	P000049100|10156..11861 |X144739|MAUS_018293	3	256	profilin 1	2
20	P000052491|10112..53449 |X174110|MAUS_052397	3	186	ezrin	1
21	P000028168|10167..37010 |X186979|MAUS_021218	3	157	unnamed protein product**	2
22	P000021200|10058..20134 |X145952|MAUS_062380	3	126	tubulin beta-3 chain	2
23	P000027169|10057..20834 |X181030|MAUS_022234	3	397	mKIAA0098 protein	2
24	P000048462|9927..34091| X146372|MAUS_001924	3	267	ubiquitin-like modifier-activating enzyme 1 isoform 1	2

25	P000022728|10265..48819|X154656|MAUS_020361	3	227	mKIAA4025 protein	2
26	P000025576|10054..10446|X171437|MAUS_036964	3	226	histone H2A.1	3
27	P000024051|10098..78052|X162659|MAUS_054808	3	211	alpha-actinin-4	1
28	P000023811|18093..23788|X161063|MAUS_055762	3	202	elongation factor 1-delta isoform b and a	1
29	P000051382|23866..49452|X171377|MAUS_032050	3	191	radixin isoform b and a	2
30	P000020729|12290..20903|X143030|MAUS_071644	3	189	Eef1g protein	2
31	P000018185|10070..21870|X127342|MAUS_025613	3	171	mKIAA0002 protein	2
32	P000027703|10218..417953|X184343|MAUS_001424	3	170	staphylococcal nuclease domain-containing protein 1	2
33	P000017842|10105..15686|X125163|MAUS_020372	3	164	unnamed protein product***	1
34	P000023670|9343..21805|X160286|MAUS_034024	3	159	T-complex protein 1 subunit beta	1
35	P000049906|12179..13076|X126644|MAUS_023944	3	158	unnamed protein product*	3
36	P000020214|10028..37827|X139742|MAUS_036427	3	124	glucose-6-phosphate isomerase	2
37	P000022446|10050..26205|X152953|MAUS_030007	3	110	T-complex protein 1 subunit eta	1
38	P000023525|11427..21677|X159460|MAUS_019432	3	116	spliceosome RNA helicase Ddx39b	2
39	P000017827|18606..32227|X125077|MAUS_032294	2	230	pyruvate kinase isozymes M1/M2	3
40	P000022563|10037..14605|X153648|MAUS_022884	2	226	eukaryotic initiation factor 4A-II isoform c	2
41	P000019273|11820..23658|X134237|MAUS_028691	2	132	peroxiredoxin-1	3
42	P000023813|18093..23788|X161064|MAUS_055762	2	114	Eef1d protein	1
43	P000052885|10071..13417|X174586|MAUS_068220	2	123	galectin-1	3
44	P000022841|10671..15229|X155501|MAUS_060600	2	215	beta-enolase isoform 1	3
45	P000026814|10162..22559|X178937|MAUS_007739	2	202	T-complex protein 1 subunit delta	1
46	P000021882|10657..14323|X149735|MAUS_012848	2	201	40S ribosomal protein S5	1
47	P000022358|12325..18862|X152492|MAUS_037601	2	151	nucleoside diphosphate kinase A	2
48	P000018051|10145..13565|X126574|MAUS_027342	2	139	proliferating cell nuclear antigen	2
49	P000023615|10568..16711|X160009|MAUS_005566	2	135	tripartite motif protein 28	1
50	P000018324|10012..45563|X128172|MAUS_030662	2	120	importin-5	1
51	P000049450|19814..52139|X141334|MAUS_020929	2	116	116 kDa U5 small nuclear ribonucleoprotein component isoform b and a	1

52	P000051363|13015..31287|X128933|MAUS_031960	2	116	alanyl-tRNA synthetase, isoform CRA_a	2
53	P000023351|10064..25998|X158430|MAUS_024359	2	111	stress-70 protein, mitochondrial	2
54	P000050193|10116..14645|X133351|MAUS_025403	2	111	serine hydroxymethyltransferase, mitochondrial	2
55	P000051168|10572..27299|X124954|MAUS_030824	2	100	nucleobindin-1 isoform 2	1
56	P000051666|12663..13178|X186511|MAUS_034994	2	86	Eef2 protein	2
57	P000025173|16286..28220|X169131|MAUS_030934	2	75	ornithine aminotransferase, mitochondrial precursor	1
58	P000028300|15849..29542|X187842|MAUS_020608	2	60	unnamed protein product ****	1
59	P000052058|54375..85324|X137072|MAUS_040136	2	56	Abcc8 protein	1
60	P000052788|11093..11751|X133760|MAUS_062929	2	106	cofilin-2	2
61	P000020979|13650..14999|X144561|MAUS_045427	2	98	heterogeneous nuclear ribonucleoprotein H2	1
62	P000024530|11780..19301|X165293|MAUS_063229	2	85	L-lactate dehydrogenase A chain isoform 1	3
63	P000050306|10059..12827|X138058|MAUS_026202	1	84	tubulin alpha-4A chain	2
64	P000022341|4987..19276|X152343|MAUS_020321	1	81	malate dehydrogenase, cytoplasmic	2
65	P000027044|11348..15940|X180333|MAUS_031134	1	70	RNA binding motif protein, X-linked	1
66	P000048610|10070..11949|X180376|MAUS_003814	1	67	unnamed protein product #	2
67	P000051603|10079..19680|X160287|MAUS_034024	1	49	T-complex protein 1 subunit beta	2
68	P000027728|11792..17011|X184472|MAUS_033124	1	46	autophagy-related protein 9A	1
69	P000018585|18297..36323|X129808|MAUS_029767	1	45	calumenin isoform 2 precursor	2
70	P000052150|14007..14518|X184135|MAUS_041070	1	202	eukaryotic translation initiation factor 5A, isoform CRA_j	2
71	P000027720|10001..29781|X184437|MAUS_028478	1	143	clathrin light chain A isoform a	2
72	P000049171|10105..14953|X156572|MAUS_019179	1	142	malate dehydrogenase 2, NAD (mitochondrial), isoform CRA_a	2
73	P000018256|10051..19446|X127751|MAUS_026701	1	133	peroxiredoxin-6	1
74	P000021612|10095..170895|X148246|MAUS_059248	1	116	septin-9 isoform a	1
75	P000050901|31261..37899|X160534|MAUS_029309	1	103	SPARC-like protein 1 precursor	1
76	P000019044|10067..70923|X132733|MAUS_031996	1	92	amyloid beta (A4) precursor-like protein 2, isoform CRA_a	1
77	P000050653|40956..49939|X144926|MAUS_028426	1	90	RAD23b homolog (S. cerevisiae), isoform CRA_b	1
78	P000048814|21370..23494|X149919|MAUS_007564	1	80	Protein phosphatase 2 (formerly 2A), regulatory subunit A (PR 65), alpha isoform	1

79	P000023849|138851..197346|X161353|MAUS_01522	1	80	microtubule-associated protein 2 isoform 1	1
80	P000022723|10082..34315|X154628|MAUS_027193	1	76	apoptosis inhibitor 5	1
81	P000024990|10032..32892|X168014|MAUS_027694	1	73	ubiquitin-conjugating enzyme E2 variant 1	1
82	P000024886|10079..25200|X167431|MAUS_025487	1	73	unnamed protein product ##	1
83	P000022098|10031..14375|X150947|MAUS_030744	1	72	40S ribosomal protein S3	1
84	P000018086|10493..16824|X126792|MAUS_027613	1	72	eukaryotic translation initiation factor 6	1
85	P000020876|16150..26184|X143958|MAUS_003131	1	68	Platelet-activating factor acetylhydrolase, isoform 1b, alpha2 subunit	2
86	P000050727|10552..36224|X151778|MAUS_028693	1	68	nuclear autoantigenic sperm protein isoform 2	1
87	P000019422|94063..118926|X135040|MAUS_037921	1	64	Ddx60 protein	1
88	P000023062|23421..35730|X156697|MAUS_028656	1	63	CAP, adenylate cyclase-associated protein 1 (yeast), isoform CRA_a	1
89	P000028379|13763..29650|X188281|MAUS_025950	1	62	isocitrate dehydrogenase [NADP] cytoplasmic	1
90	P000028261|13795..26507|X187628|MAUS_001416	1	62	unnamed protein product ###	2
91	P000019757|31491..33092|X137005|MAUS_017466	1	58	differential display clone 8	1
92	P000026583|7873..12543|X177454|MAUS_042730	1	57	transcription elongation factor B polypeptide 1 isoform a	1
93	P000020021|8921..14148|X138532|MAUS_026817	1	56	adenylate kinase isoenzyme 1 isoform 1 and 2	1
94	P000024905|11351..27007|X167554|MAUS_032966	1	55	FK506 binding protein 1a	1
95	P000027584|10018..14299|X183530|MAUS_026926	1	55	peptidase (mitochondrial processing) alpha	1
96	P000026144|21788..28437|X174683|MAUS_024601	1	52	unnamed protein, Isoc2a protein	1
97	P000023329|11444..22540|X158255|MAUS_028964	1	52	protein DJ-1	1
98	P000025490|10227..43905|X170939|MAUS_028577	1	50	phospholipase A-2-activating protein	1
99	P000026153|32053..40277|X174766|MAUS_008206	1	47	LAG1 longevity assurance homolog 4	1
100	P000018440|11141..27236|X128960|MAUS_029716	1	47	transferrin receptor 2, isoform CRA_d	1
101	P000018700|10266..54945|X130521|MAUS_020698	1	46	chaperonin subunit 6b (zeta)	1
102	P000020601|10034..14008|X142106|MAUS_031807	1	95	6-phosphogluconolactonase	1
103	P000052151|12644..14518|X184127|MAUS_041070	1	61	eukaryotic translation initiation factor 5A, isoform CRA_j	1
104	P000024559|10621..14464|X165482|MAUS_005161	1	54	peroxiredoxin-2	1
105	P000051643|46982..147551|X153454|MAUS_034573	1	54	tyrosine-protein phosphatase non-receptor type 13	3

Attachment 1: MALDI-TOF analysis of CM, 10 kDa concentrate.

Proteins with a total ion score > 45 are listed; n = number of experiments containing the named protein out of three independent experiments, two runs each.
*pubmed data base also found heat-shock protein hsp86 and heat-shock protein hsp84 as significant alignment
** pubmed data base also found guanosine diphosphate (GDP) dissociation inhibitor 2, isoform CRA_b
*** pubmed database also found G protein beta subunit like as significant alignment
**** pubmed database also found Smc6 protein as significant alignment
# pubmed database also found calreticulin precursor as significant alignment
pubmed database also found 26S proteasome non-ATPase regulatory subunit 13 as significant alignment
pubmed database also found T-complex protein 1 subunit gamma as significant alignment.

	Accession Number	Peptide Count	Total Ion Score	Blast	n
1	P000049887|10141..13142 |X127442|MAUS_023456	11	893	triosephosphate isomerase	2
2	P000021382|7754..13998| X146990|MAUS_004980	9	702	heterogeneous nuclear ribonucleoproteins A2/B1 isoform 2	2
3	P000025352|10111..18938 |X170045|MAUS_004891	7	755	nestin	2
4	P000021019|10156..12512 |X144737|MAUS_018293	6	726	profilin-1	1
5	P000052885|10071..13417 |X174586|MAUS_068220	6	565	galectin-1	2
6	P000026632|10064..18153 |X177687|MAUS_027559	5	324	carbonic anhydrase 3	1
7	P000026934|10089..37671 |X179615|MAUS_039323	4	269	insulin-like growth factor-binding protein 2 precursor	2
8	P000025562|10126..15853 |X171365|MAUS_011752	4	245	phosphoglycerate mutase 1, unnamed protein product	1
9	P000023042|10105..21577 |X156567|MAUS_019179	3	359	malate dehydrogenase, mitochondrial precursor	1
10	P000018256|10051..19446 |X127751|MAUS_026701	3	214	peroxiredoxin-6	1
11	P000028443|16065..25048 |X188757|MAUS_028692	3	111	alcohol dehydrogenase [NADP+]	1
12	P000052788|11093..11751 |X133760|MAUS_062929	2	165	cofilin-2	2
13	P000020601|10034..14008 |X142106|MAUS_031807	2	103	6-phosphogluconolactonase	2
14	P000026451|11180..12320 |X176611|MAUS_025132	2	86	rho GDP-dissociation inhibitor 1	2
15	P000025619|10186..29074 |X171634|MAUS_007656	2	79	cAMP-regulated phosphoprotein 19 isoform 1	1
16	P000024559|10621..14464 |X165482|MAUS_005161	2	60	peroxiredoxin-2	1
17	P000026744|10033..11265 |X178434|MAUS_036504	2	225	14 kDa phosphohistidine phosphatase	1
18	P000027044|11348..15940 |X180333|MAUS_031134	2	207	RNA binding motif protein, X-linked	1
19	P000019273|11820..23658 |X134237|MAUS_028691	2	182	peroxiredoxin-1	2
20	P000020729|12290..20903 |X143030|MAUS_071644	2	170	Eef1g protein	1
21	P000052151|12644..14518 |X184127|MAUS_041070	2	168	eukaryotic translation initiation factor 5A, isoform CRA_j	1
22	P000022127|20166..42003 |X151103|MAUS_019961	2	160	lamina-associated polypeptide 2 isoform delta	1
23	P000028168|10167..37010 |X186979|MAUS_021218	2	147	guanosine diphosphate (GDP) dissociation inhibitor 2, isoform CRA_b and c	1
24	P000020999|10119..26981 |X144660|MAUS_036371	2	131	plasminogen activator inhibitor 1 RNA-binding protein isoform 3	1
25	P000022070|10481..18563 |X150812|MAUS_026728	2	120	vimentin, unnamed protein	1

26	P000026522|10089..36769|X177075|MAUS_028567	2	107	thioredoxin domain-containing protein 12 precursor	1
27	P000020979|13650..14999|X144561|MAUS_045427	2	104	heterogeneous nuclear ribonucleoprotein H2	1
28	P000049816|10037..11120|X153661|MAUS_022884	1	96	eukaryotic translation initiation factor 4A2, isoform CRA_e	1
29	P000022841|10671..15229|X155501|MAUS_060600	1	76	enolase 3, beta muscle, isoform CRA_a	1
30	P000022628|10124..21100|X154058|MAUS_030663	1	64	small acidic protein	1
31	P000021143|15292..17032|X145559|MAUS_030057	1	46	cellular nucleic acid binding protein, isoform CRA_d	1
32	P000025266|10359..12260|X169662|MAUS_059970	1	46	heat shock-related 70 kDa protein 2	1
33	P000026252|10001..22211|X175425|MAUS_005354	1	118	thioredoxin, mitochondrial precursor	1
34	P000028454|11635..18736|X188794|MAUS_041459	1	113	unnamed protein product ##	1
35	P000019800|10092..14855|X137236|MAUS_004035	1	106	glutathione S-transferase Mu 7	1
36	P000023849|138851..197346|X161353|MAUS_015222	1	103	microtubule-associated protein 2 isoform 1	2
37	P000023755|25947..39844|X160758|MAUS_018583	1	98	ras GTPase-activating protein-binding protein 1	1
38	P000050754|10031..24753|X121146|MAUS_028792	1	97	unnamed protein ###	1
39	P000049274|17720..19987|X153496|MAUS_020265	1	95	unnamed protein product*	1
40	P000023615|10568..16711|X160009|MAUS_005566	1	93	tripartite motif protein 28	1
41	P000027139|10177..22272|X180900|MAUS_017421	1	92	zinc finger protein 207 isoform 3	1
42	P000049950|10013..26131|X160634|MAUS_024165	1	76	hematological and neurological expressed 1-like protein	1
43	P000024242|23317..45487|X163695|MAUS_040028	1	76	ELAV-like protein 1	1
44	P000018497|10091..11013|X129298|MAUS_028843	1	71	SH3 domain-binding glutamic acid-rich-like protein 3	1
45	P000048657|14481..31915|X149553|MAUS_004789	1	70	dihydrolipoyllysine-residue succinyltransferase component of 2-oxoglutarate dehydroge	1
46	P000017842|10105..15686|X125163|MAUS_020372	1	69	unnamed protein product**	1
47	P000048624|10030..27024|X142457|MAUS_004207	1	66	sulfated glycoprotein 1 isoform E preproprotein	1
48	P000048921|16130..18081|X172408|MAUS_013698	1	63	astrocytic phosphoprotein PEA-15 isoform 2	1
49	P000022341|4987..19276|X152343|MAUS_020321	1	57	malate dehydrogenase, cytoplasmic	1
50	P000020713|33915..59863|X142921|MAUS_026867	1	48	GTPase-activating protein and VPS9 domain-containing protein 1	1
51	P000017718|10358..13038|X124382|MAUS_029328	1	49	Heterogeneous nuclear ribonucleoprotein D-like	1

52	P000048998|10001..59254|X149970|MAUS_015647	1	46	laminin subunit alpha-5 precursor	1
53	P000021881|10243..14334|X149727|MAUS_026694	1	45	unnamed protein product***	1

Attachment 2: MADLI-TOF analysis from CM containing proteins between 10 and 50 kDA.

Proteins with a total ion score > 45 are listed. n = number of experiments containing the named protein out of two independent experiments, two runs each.
pubmed database also found TAR DNA-binding protein 43 isoform 1 as significant alignment
pubmed database also found adenylate kinase 2, mitochondrial isoform b as significant alignment
* pubmed database also found small ubiquitin-related modifier 3 precursor as significant alignment
** pubmed database also found G protein beta subunit like as significant alignment
*** pubmed database also found methyltransferase-like protein 13 as significant alignment.

	Accession Number	Peptide Count	Total Ion Score	Blast
1	P000022070|10481..18563 |X150812|MAUS_026728	24	2142	vimentin, unnamed protein
2	P000025352|10111..18938 |X170045|MAUS_004891	13	1494	nestin
3	P000021382|7754..13998| X146990|MAUS_004980	13	1299	heterogeneous nuclear ribonucleoproteins A2/B1 isoform 2
4	P000018018|10907..19558 |X126344|MAUS_025980	5	746	60 kDa heat shock protein, mitochondrial
6	P000021080|10090..41734 |X145184|MAUS_020849	5	487	unnamed protein product
5	P000049063|10208..11951 |X127700|MAUS_017390	4	511	fructose-bisphosphate aldolase C
7	P000019273|11820..23658 |X134237|MAUS_028691	4	435	peroxiredoxin-1
8	P000051665|14256..15439 |X186510|MAUS_034994	4	402	Eef2 protein
9	P000025266|10359..12260 |X169662|MAUS_059970	4	373	heat shock-related 70 kDa protein 2
10	P000022358|12325..18862 |X152492|MAUS_037601	3	352	nucleoside diphosphate kinase A
11	P000024559|10621..14464 |X165482|MAUS_005161	3	347	peroxiredoxin-2
12	P000049887|10141..13142 |X127442|MAUS_023456	3	304	triosephosphate isomerase
16	P000026091|10145..33559 |X174409|MAUS_051391	3	189	14-3-3 protein gamma
24	P000020999|10119..26981 |X144660|MAUS_036371	3	162	plasminogen activator inhibitor 1 RNA-binding protein isoform 3
13	P000052150|14007..14518 |X184135|MAUS_041070	2	268	eukaryotic translation initiation factor 5A, isoform CRA_j
14	P000026451|11180..12320 |X176611|MAUS_025132	2	218	rho GDP-dissociation inhibitor 1
15	P000050901|31261..37899 |X160534|MAUS_029309	2	212	SPARC-like protein 1 precursor
19	P000023849|138851..19734 6|X161353|MAUS_01522 2	2	167	microtubule-associated protein 2 isoform 1
20	P000018561|11055..12743 |X129678|MAUS_031972	2	167	actin
21	P000018609|10131..29603 |X129995|MAUS_032366	2	164	tropomyosin alpha-1 chain isoform 5
22	P000050192|10767..14471 |X158955|MAUS_025381	2	164	protein canopy homolog 2 precursor
23	P000024794|10233..14024 |X166888|MAUS_026864	2	163	78 kDa glucose-regulated protein precursor
25	P000023351|10064..25998 |X158430|MAUS_024359	2	162	stress-70 protein, mitochondrial
26	P000052885|10071..13417 |X174586|MAUS_068220	2	154	galectin-1
31	P000020601|10034..14008 |X142106|MAUS_031807	2	111	6-phosphogluconolactonase

40	P000020539|15102..16662 |X141828|MAUS_026547	2	66	transgelin-2
41	P000022244|31246..60587 |X151691|MAUS_019894	2	66	sodium-dependent neutral amino acid transporter B(0)AT2
17	P000018256|10051..19446 |X127751|MAUS_026701	1	181	peroxiredoxin-6
18	P000027720|10001..29781 |X184437|MAUS_028478	1	175	clathrin light chain A isoform a
27	P000049100|10156..11861 |X144739|MAUS_018293	1	151	profilin 1
28	P000048410|12191..48337 |X168533|MAUS_001120	1	150	poly(rC) binding protein 3, isoform CRA_b
29	P000049705|84568..90210 |X126712|MAUS_022443	1	131	Myh9 protein
30	P000026252|10001..22211 |X175425|MAUS_005354	1	121	thioredoxin, mitochondrial precursor
32	P000027044|11348..15940 |X180333|MAUS_031134	1	108	RNA binding motif protein, X-linked
33	P000023329|11444..22540 |X158255|MAUS_028964	1	105	protein DJ-1
34	P000050754|10031..24753 |X121146|MAUS_028792	1	97	Unnamed protein***
35	P000048979|10078..13203 |X153786|MAUS_015092	1	94	endothelial differentiation-related factor 1
36	P000052754|16001..20459 |X186796|MAUS_062014	1	90	glia maturation factor-beta
37	P000049395|10113..23779 |X141606|MAUS_020737	1	76	hematological and neurological expressed 1 protein
38	P000051643|46982..14755 1|X153454|MAUS_034573	1	69	tyrosine-protein phosphatase non-receptor type 13
39	P000050653|40956..49939 |X144926|MAUS_028426	1	67	RAD23b homolog (S. cerevisiae), isoform CRA_b
42	P000018585|18297..36323 |X129808|MAUS_029767	1	65	calumenin isoform 2
43	P000022645|10044..16863 1|X154135|MAUS_027722	1	58	spermatogenesis-associated protein 5 isoform 2
44	P000049274|17720..19987 |X153496|MAUS_020265	1	63	Unnamed protein product*
45	P000026522|10089..36769 |X177075|MAUS_028567	1	62	thioredoxin domain-containing protein 12 precursor
46	P000024981|10082..33538 |X167954|MAUS_024740	1	61	DNA damage-binding protein 1
47	P000048921|16130..18081 |X172408|MAUS_013698	1	57	astrocytic phosphoprotein PEA-15 isoform 2
48	P000018229|10016..21244 |X127553|MAUS_071533	1	54	unnamed protein**
49	P000018477|12311..67294 |X129159|MAUS_009614	1	52	sarcosine dehydrogenase, mitochondrial precursor
50	P000028244|12672..22236 |X187481|MAUS_056917	1	51	signal-induced proliferation-associated protein 1
51	P000018497|10091..11013 |X129298|MAUS_028843	1	49	SH3 domain-binding glutamic acid-rich-like protein 3
52	P000017718|10358..13038 |X124382|MAUS_029328	1	49	Heterogeneous nuclear ribonucleoprotein D-like

53	P000022531|12780..15567 |X153420|MAUS_046879	1	46	immunity-related GTPase family M protein 1
54	P000027951|10175..25032 |X185764|MAUS_022683	1	49	Pla2g10 protein

Attachment 3: MALDI-TOF analysis from CM after heating at 60°C.

Proteins with a total ion score > 45 are listed. Data are given from one experiment with two runs.

* pubmed database also found mCG1036415 as significant alignment

** pubmed database also found small ubiquitin-related modifier 3 precursor as significant alignment

*** pubmed database also found adenylate kinase 2 as significant alignment, mitochondrial isoform b as significant alignment

	Accession Number	Peptide Count	Total Ion Score	Blast
1	P000050959|11039..12925 |X170662|MAUS_029580	3	138	A-X actin
2	P000023042|10105..21577 |X156567|MAUS_019179	2	124	malate dehydrogenase, mitochondrial precursor
3	P000049063|10208..11951 |X127700|MAUS_017390	2	120	fructose-bisphosphate aldolase C
4	P000017827|18606..32227 |X125077|MAUS_032294	2	111	pyruvate kinase isozymes M1/M2
5	P000025173|16286..28220 |X169131|MAUS_030934	2	90	ornithine aminotransferase, mitochondrial precursor
6	P000050193|10116..14645 |X133351|MAUS_025403	2	90	serine hydroxymethyltransferase, mitochondrial
7	P000021382|7754..13998| X146990|MAUS_004980	2	70	heterogeneous nuclear ribonucleoproteins A2/B1 isoform 2
8	P000025352|10111..18938 |X170045|MAUS_004891	1	99	nestin
9	P000018256|10051..19446 |X127751|MAUS_026701	1	76	peroxiredoxin-6
10	P000025576|10054..10446 |X171437|MAUS_036964	1	68	histone H2A.1
11	P000019800|10092..14855 |X137236|MAUS_004035	1	56	glutathione S-transferase Mu 7
12	P000023351|10064..25998 |X158430|MAUS_024359	1	51	kynureninase
13	P000017842|10105..15686 |X125163|MAUS_020372	1	49	unnamed protein product***
14	P000021200|10058..20134 |X145952|MAUS_062380	1	47	tubulin beta-3 chain
15	P000019600|10041..39229 |X136112|MAUS_039853	1	45	tripartite motif-containing protein 14
16	P000021143|15292..17032 |X145559|MAUS_030057	1	46	cellular nucleic acid binding protein, isoform CRA_d
17	P000049100|10156..11861 |X144739|MAUS_018293	1	46	profilin 1

Attachment 4: MALDI-TOF analysis of NPC lysate.

Proteins with a total ion score > 45 are listed Data are given from one experiment with two runs.

***pubmed database also found G protein beta subunit like as significant alignment.

	Accession Number	Peptide Count	Total Ion Score	Blast	n
1	P000021382|7754..13998|X146990|MAUS_004980	5	409	heterogeneous nuclear ribonucleoproteins A2/B1 isoform 2	3
2	P000019273|11820..23658|X134237|MAUS_028691	4	421	peroxiredoxin-1	3
3	P000050959|11039..12925|X170662|MAUS_029580	4	243	actin, cytoplasmic 1	2
4	P000022070|10481..18563|X150812|MAUS_026728	4	311	vimentin	3
5	P000018561|11055..12743|X129678|MAUS_031972	3	159	actin	1
6	P000021074|13694..16995|X145089|MAUS_070436	2	173	serpin H1 precursor	1
7	P000025266|10359..12260|X169662|MAUS_059970	2	115	heat shock-related 70 kDa protein 2	1
8	P000022841|10671..15229|X155501|MAUS_060600	2	65	enolase 3, beta muscle, isoform CRA_a	1
9	P000049887|10141..13142|X127442|MAUS_023456	2	72	triosephosphate isomerase	1
10	P000052788|11093..11751|X133760|MAUS_062929	1	83	cofilin-2	2
11	P000025577|5121..21089|X171447|MAUS_041126	1	72	eukaryotic translation initiation factor 5A, isoform CRA_j	2
12	P000052151|12644..14518|X184127|MAUS_041070	1	64	eukaryotic translation initiation factor 5A, isoform CRA_j	1
13	P000050043|10137..29012|X177775|MAUS_024640	1	60	phosphoserine aminotransferase isoform 1	1
14	P000017827|18606..32227|X125077|MAUS_032294	1	45	pyruvate kinase isozymes M1/M2	1
15	P000019759|10417..61808|X137002|MAUS_017466	1	79	TIMP-2	1
16	P000027720|10001..29781|X184437|MAUS_028478	1	55	clathrin light chain A isoform a	1
17	P000052885|10071..13417|X174586|MAUS_068220	1	60	galectin-1	2
18	P000051665|14256..15439|X186510|MAUS_034994	1	53	Eef2 protein	1
19	P000018203|10303..23041|X127436|MAUS_022658	1	116	transgelin-3	1
20	P000024530|11780..19301|X165293|MAUS_063229	1	95	L-lactate dehydrogenase A chain isoform 1	2
21	P000023813|18093..23788|X161064|MAUS_055762	1	75	Eef1d protein	1
22	P000019023|10120..25648|X132628|MAUS_022241	1	49	threonyl-tRNA synthetase, cytoplasmic	1

Attachment 5: MALDI-TOF analysis of HT-22-CM.

Proteins with a total ion score > 45 are listed; n = number of experiments containing the named protein out of three independent experiments, two runs each.

	Accession Number	Peptide Count	Total Ion Score	Blast
1	P000022070|10481..18563|X150812|MAUS_026728	3	133	vimentin
2	P000018561|11055..12743|X129678|MAUS_031972	2	123	actin, alpha skeletal muscle
3	P000050981|12265..13493|X184658|MAUS_029718	1	85	procollagen C-endopeptidase enhancer 1
4	P000020887|30213..69016|X143991|MAUS_064080	1	68	fibulin-2 isoform b
5	P000025538|10024..26993|X171220|MAUS_026005	1	45	ribulose-phosphate 3-epimerase
6	P000025852|10118..18033|X172882|MAUS_024650	1	45	solute carrier family 22 member 6

Attachment 6: MALDI-TOF analysis of SNL-CM.

Proteins with a total ion score > 45 are listed. Data are given from one experiment with two runs.

9. References

Amariglio, N. et al., 2009, Donor-derived brain tumor following neural stem cell transplantation in an ataxia telangiectasia patient: PLoS.Med., v. 6, no. 2, p. e1000029.

Bajgar, R., S. Seetharaman, A. J. Kowaltowski, K. D. Garlid, and P. Paucek, 2001, Identification and properties of a novel intracellular (mitochondrial) ATP-sensitive potassium channel in brain: J.Biol.Chem., v. 276, no. 36, p. 33369-33374.

Banerjee, S., D. Williamson, N. Habib, M. Gordon, and J. Chataway, 2011, Human stem cell therapy in ischaemic stroke: a review: Age Ageing, v. 40, no. 1, p. 7-13.

Bang, O. Y., J. S. Lee, P. H. Lee, and G. Lee, 2005, Autologous mesenchymal stem cell transplantation in stroke patients: Ann.Neurol., v. 57, no. 6, p. 874-882.

Barondes, S. H. et al., 1994, Galectins: a family of animal beta-galactoside-binding lectins: Cell, v. 76, no. 4, p. 597-598.

Barone, F. C., R. F. White, P. A. Spera, J. Ellison, R. W. Currie, X. Wang, and G. Z. Feuerstein, 1998, Ischemic preconditioning and brain tolerance: temporal histological and functional outcomes, protein synthesis requirement, and interleukin-1 receptor antagonist and early gene expression: Stroke, v. 29, no. 9, p. 1937-1950.

Bartus, R. T. et al., 1994, Calpain inhibitor AK295 protects neurons from focal brain ischemia. Effects of postocclusion intra-arterial administration: Stroke, v. 25, no. 11, p. 2265-2270.

Bedard, A., and A. Parent, 2004, Evidence of newly generated neurons in the human olfactory bulb: Brain Res.Dev.Brain Res., v. 151, no. 1-2, p. 159-168.

Benit, P., S. Goncalves, E. P. Dassa, J. J. Briere, and P. Rustin, 2008, The variability of the harlequin mouse phenotype resembles that of human mitochondrial-complex I-deficiency syndromes: PLoS.One., v. 3, no. 9, p. e3208.

Bloomfield, S. A., and B. Volgyi, 2009, The diverse functional roles and regulation of neuronal gap junctions in the retina: Nat.Rev.Neurosci., v. 10, no. 7, p. 495-506.

Bonner, C. et al., 2010, INS-1 cells undergoing caspase-dependent apoptosis enhance the regenerative capacity of neighboring cells: Diabetes, v. 59, no. 11, p. 2799-2808.

Botia, B. et al., 2008, Peroxiredoxin 2 is involved in the neuroprotective effects of PACAP in cultured cerebellar granule neurons: J.Mol.Neurosci., v. 36, no. 1-3, p. 61-72.

Boukhtouche, F., G. Vodjdani, C. I. Jarvis, J. Bakouche, B. Staels, J. Mallet, J. Mariani, Y. Lemaigre-Dubreuil, and B. Brugg, 2006, Human retinoic acid receptor-related orphan receptor alpha1 overexpression protects neurones against oxidative stress-induced apoptosis: J.Neurochem., v. 96, no. 6, p. 1778-1789.

Boulos, S., B. P. Meloni, P. G. Arthur, C. Bojarski, and N. W. Knuckey, 2007, Peroxiredoxin 2 overexpression protects cortical neuronal cultures from ischemic and oxidative injury but not glutamate excitotoxicity, whereas Cu/Zn superoxide dismutase 1 overexpression protects only against oxidative injury: J.Neurosci.Res., v. 85, no. 14, p. 3089-3097.

Brand, M. D., and T. C. Esteves, 2005, Physiological functions of the mitochondrial uncoupling proteins UCP2 and UCP3: Cell Metab, v. 2, no. 2, p. 85-93.

Brown, D., B. D. Yu, N. Joza, P. Benit, J. Meneses, M. Firpo, P. Rustin, J. M. Penninger, and G. R. Martin, 2006, Loss of Aif function causes cell death in the mouse embryo, but the temporal progression of patterning is normal: Proc.Natl.Acad.Sci.U.S.A, v. 103, no. 26, p. 9918-9923.

Brown, I. R., 2007, Heat shock proteins and protection of the nervous system: Ann.N.Y.Acad.Sci., v. 1113, p. 147-158.

Burda, J. et al., 2006, Delayed postconditionig initiates additive mechanism necessary for survival of selectively vulnerable neurons after transient ischemia in rat brain: Cell Mol.Neurobiol., v. 26, no. 7-8, p. 1141-1151.

Busija, D. W., T. Gaspar, F. Domoki, P. V. Katakam, and F. Bari, 2008, Mitochondrial-mediated suppression of ROS production upon exposure of neurons to lethal stress: mitochondrial targeted preconditioning: Adv.Drug Deliv.Rev., v. 60, no. 13-14, p. 1471-1477.

Cadet, J. L., and I. N. Krasnova, 2009, Cellular and molecular neurobiology of brain preconditioning: Mol.Neurobiol., v. 39, no. 1, p. 50-61.

Camby, I., M. M. Le, F. Lefranc, and R. Kiss, 2006, Galectin-1: a small protein with major functions: Glycobiology, v. 16, no. 11, p. 137R-157R.

Cande, C. et al., 2004, AIF and cyclophilin A cooperate in apoptosis-associated chromatinolysis: Oncogene, v. 23, no. 8, p. 1514-1521.

Carletti, B., F. Piemonte, and F. Rossi, 2011, Neuroprotection: the emerging concept of restorative neural stem cell biology for the treatment of neurodegenerative diseases: Curr.Neuropharmacol., v. 9, no. 2, p. 313-317.

Chan, P. H., 2004, Mitochondria and neuronal death/survival signaling pathways in cerebral ischemia: Neurochem.Res., v. 29, no. 11, p. 1943-1949.

Chang-Hong, R. et al., 2005, Neuroprotective effect of oxidized galectin-1 in a transgenic mouse model of amyotrophic lateral sclerosis: Exp.Neurol., v. 194, no. 1, p. 203-211.

Chen, H., S. A. Detmer, A. J. Ewald, E. E. Griffin, S. E. Fraser, and D. C. Chan, 2003, Mitofusins Mfn1 and Mfn2 coordinately regulate mitochondrial fusion and are essential for embryonic development: J.Cell Biol., v. 160, no. 2, p. 189-200.

Chen, J., Y. Li, L. Wang, Z. Zhang, D. Lu, M. Lu, and M. Chopp, 2001, Therapeutic benefit of intravenous administration of bone marrow stromal cells after cerebral ischemia in rats: Stroke, v. 32, no. 4, p. 1005-1011.

Chen, S., L. Yao, and T. J. Cunningham, 2012, Secreted phospholipase A2 involvement in neurodegeneration: differential testing of prosurvival and anti-inflammatory effects of enzyme inhibition: PLoS.One., v. 7, no. 6, p. e39257.

Chen, X., Y. Li, L. Wang, M. Katakowski, L. Zhang, J. Chen, Y. Xu, S. C. Gautam, and M. Chopp, 2002, Ischemic rat brain extracts induce human marrow stromal cell growth factor production: Neuropathology., v. 22, no. 4, p. 275-279.

Cheung, E. C. et al., 2006, Dissociating the dual roles of apoptosis-inducing factor in maintaining mitochondrial structure and apoptosis: EMBO J., v. 25, no. 17, p. 4061-4073.

Cheung, E. C., L. Melanson-Drapeau, S. P. Cregan, J. L. Vanderluit, K. L. Ferguson, W. C. McIntosh, D. S. Park, S. A. Bennett, and R. S. Slack, 2005, Apoptosis-inducing factor is a

key factor in neuronal cell death propagated by BAX-dependent and BAX-independent mechanisms: J.Neurosci., v. 25, no. 6, p. 1324-1334.

Chinta, S. J., A. Rane, N. Yadava, J. K. Andersen, D. G. Nicholls, and B. M. Polster, 2009, Reactive oxygen species regulation by AIF- and complex I-depleted brain mitochondria: Free Radic.Biol.Med., v. 46, no. 7, p. 939-947.

Cho, Y. J. et al., 2012, Therapeutic effects of human adipose stem cell-conditioned medium on stroke: J.Neurosci.Res., v. 90, no. 9, p. 1794-1802.

Choi, H. J., S. W. Kang, C. H. Yang, S. G. Rhee, and S. E. Ryu, 1998, Crystal structure of a novel human peroxidase enzyme at 2.0 A resolution: Nat.Struct.Biol., v. 5, no. 5, p. 400-406.

Correia, S. C., and P. I. Moreira, 2010, Hypoxia-inducible factor 1: a new hope to counteract neurodegeneration?: J.Neurochem., v. 112, no. 1, p. 1-12.

Correia, S. C., R. X. Santos, G. Perry, X. Zhu, P. I. Moreira, and M. A. Smith, 2010, Mitochondria: the missing link between preconditioning and neuroprotection: J.Alzheimers.Dis., v. 20 Suppl 2, p. S475-S485.

Cregan, S. P. et al., 2002, Apoptosis-inducing factor is involved in the regulation of caspase-independent neuronal cell death: J.Cell Biol., v. 158, no. 3, p. 507-517.

Culmsee, C., V. Junker, W. Kremers, S. Thal, N. Plesnila, and J. Krieglstein, 2004, Combination therapy in ischemic stroke: synergistic neuroprotective effects of memantine and clenbuterol: Stroke, v. 35, no. 5, p. 1197-1202.

Culmsee, C., C. Zhu, S. Landshamer, B. Becattini, E. Wagner, M. Pellecchia, K. Blomgren, and N. Plesnila, 2005, Apoptosis-inducing factor triggered by poly(ADP-ribose) polymerase and Bid mediates neuronal cell death after oxygen-glucose deprivation and focal cerebral ischemia: J.Neurosci., v. 25, no. 44, p. 10262-10272.

Curtis, M. A. et al., 2007, Human neuroblasts migrate to the olfactory bulb via a lateral ventricular extension: Science, v. 315, no. 5816, p. 1243-1249.

Daadi, M. M., A. L. Maag, and G. K. Steinberg, 2008, Adherent self-renewable human embryonic stem cell-derived neural stem cell line: functional engraftment in experimental stroke model: PLoS.One., v. 3, no. 2, p. e1644.

Daugas, E. et al., 2000, Mitochondrio-nuclear translocation of AIF in apoptosis and necrosis: FASEB J., v. 14, no. 5, p. 729-739.

Dave, K. R., I. Saul, R. Prado, R. Busto, and M. A. Perez-Pinzon, 2006, Remote organ ischemic preconditioning protect brain from ischemic damage following asphyxial cardiac arrest: Neurosci.Lett., v. 404, no. 1-2, p. 170-175.

David, K. K., S. A. Andrabi, T. M. Dawson, and V. L. Dawson, 2009, Parthanatos, a messenger of death: Front Biosci., v. 14, p. 1116-1128.

Davila, D., N. M. Connolly, H. Bonner, P. Weisova, H. Dussmann, C. G. Concannon, H. J. Huber, and J. H. Prehn, 2012, Two-step activation of FOXO3 by AMPK generates a coherent feed-forward loop determining excitotoxic cell fate: Cell Death.Differ., v. 19, no. 10, p. 1677-1688.

Delavallee, L., L. Cabon, P. Galan-Malo, H. K. Lorenzo, and S. A. Susin, 2011, AIF-mediated caspase-independent necroptosis: a new chance for targeted therapeutics: IUBMB.Life, v. 63, no. 4, p. 221-232.

Deli, M. A., C. S. Abraham, Y. Kataoka, and M. Niwa, 2005, Permeability studies on in vitro blood-brain barrier models: physiology, pathology, and pharmacology: Cell Mol.Neurobiol., v. 25, no. 1, p. 59-127.

Diano, S., R. T. Matthews, P. Patrylo, L. Yang, M. F. Beal, C. J. Barnstable, and T. L. Horvath, 2003, Uncoupling protein 2 prevents neuronal death including that occurring during seizures: a mechanism for preconditioning: Endocrinology, v. 144, no. 11, p. 5014-5021.

Diemert, S., A. M. Dolga, S. Tobaben, J. Grohm, S. Pfeifer, E. Oexler, and C. Culmsee, 2012, Impedance measurement for real time detection of neuronal cell death: J.Neurosci.Methods, v. 203, no. 1, p. 69-77.

Dimauro, S., and P. Rustin, 2009, A critical approach to the therapy of mitochondrial respiratory chain and oxidative phosphorylation diseases: Biochim.Biophys.Acta, v. 1792, no. 12, p. 1159-1167.

Dirnagl, U., K. Becker, and A. Meisel, 2009, Preconditioning and tolerance against cerebral ischaemia: from experimental strategies to clinical use: Lancet Neurol., v. 8, no. 4, p. 398-412.

Dirnagl, U., and A. Meisel, 2008, Endogenous neuroprotection: mitochondria as gateways to cerebral preconditioning?: Neuropharmacology, v. 55, no. 3, p. 334-344.

Duval, C., A. Negre-Salvayre, A. Dogilo, R. Salvayre, L. Penicaud, and L. Casteilla, 2002, Increased reactive oxygen species production with antisense oligonucleotides directed against uncoupling protein 2 in murine endothelial cells: Biochem.Cell Biol., v. 80, no. 6, p. 757-764.

Ebrahimi, M., A. Lakizadeh, P. gha-Golzadeh, E. Ebrahimie, and M. Ebrahimi, 2011, Prediction of thermostability from amino acid attributes by combination of clustering with attribute weighting: a new vista in engineering enzymes: PLoS.One., v. 6, no. 8, p. e23146.

Echtay, K. S., and M. D. Brand, 2007, 4-hydroxy-2-nonenal and uncoupling proteins: an approach for regulation of mitochondrial ROS production: Redox.Rep., v. 12, no. 1, p. 26-29.

Efremov, R. G., and L. A. Sazanov, 2011, Structure of the membrane domain of respiratory complex I: Nature, v. 476, no. 7361, p. 414-420.

Emerling, B. M., B. Viollet, K. V. Tormos, and N. S. Chandel, 2007, Compound C inhibits hypoxic activation of HIF-1 independent of AMPK: FEBS Lett., v. 581, no. 29, p. 5727-5731.

Eriksson, P. S., E. Perfilieva, T. Bjork-Eriksson, A. M. Alborn, C. Nordborg, D. A. Peterson, and F. H. Gage, 1998, Neurogenesis in the adult human hippocampus: Nat.Med., v. 4, no. 11, p. 1313-1317.

Faden, A. I., and B. Stoica, 2007, Neuroprotection: challenges and opportunities: Arch.Neurol., v. 64, no. 6, p. 794-800.

Fang, J., T. Nakamura, D. H. Cho, Z. Gu, and S. A. Lipton, 2007, S-nitrosylation of peroxiredoxin 2 promotes oxidative stress-induced neuronal cell death in Parkinson's disease: Proc.Natl.Acad.Sci.U.S.A, v. 104, no. 47, p. 18742-18747.

Farooqui, A. A., W. Y. Ong, and L. A. Horrocks, 2006, Inhibitors of brain phospholipase A2 activity: their neuropharmacological effects and therapeutic importance for the treatment of neurologic disorders: Pharmacol.Rev., v. 58, no. 3, p. 591-620.

Ferrara, N., and W. J. Henzel, 1989, Pituitary follicular cells secrete a novel heparin-binding growth factor specific for vascular endothelial cells: Biochem.Biophys.Res.Commun., v. 161, no. 2, p. 851-858.

Funatomi, H., and Y. Hatta, 1991, [Studies on heat stability of phospholipase A2 in human serum]: Nihon Shokakibyo Gakkai Zasshi, v. 88, no. 1, p. 71-76.

Gage, F. H., 2000, Mammalian neural stem cells: Science, v. 287, no. 5457, p. 1433-1438.

Gallagher, G., and D. L. Forrest, 2007, Second solid cancers after allogeneic hematopoietic stem cell transplantation: Cancer, v. 109, no. 1, p. 84-92.

Galluzzi, L., K. Blomgren, and G. Kroemer, 2009, Mitochondrial membrane permeabilization in neuronal injury: Nat.Rev.Neurosci., v. 10, no. 7, p. 481-494.

Galluzzi, L. et al., 2012, Molecular definitions of cell death subroutines: recommendations of the Nomenclature Committee on Cell Death 2012: Cell Death.Differ., v. 19, no. 1, p. 107-120.

Gan, Y. et al., 2012, Transgenic overexpression of peroxiredoxin-2 attenuates ischemic neuronal injury via suppression of a redox-sensitive pro-death signaling pathway: Antioxid.Redox.Signal., v. 17, no. 5, p. 719-732.

Gaspar, T., F. Domoki, L. Lenti, P. V. Katakam, J. A. Snipes, F. Bari, and D. W. Busija, 2009, Immediate neuronal preconditioning by NS1619: Brain Res., v. 1285, p. 196-207.

Gaspar, T., P. Katakam, J. A. Snipes, B. Kis, F. Domoki, F. Bari, and D. W. Busija, 2008, Delayed neuronal preconditioning by NS1619 is independent of calcium activated potassium channels: J.Neurochem., v. 105, no. 4, p. 1115-1128.

Gesuete, R., F. Orsini, E. R. Zanier, D. Albani, M. A. Deli, G. Bazzoni, and M. G. De Simoni, 2011, Glial cells drive preconditioning-induced blood-brain barrier protection: Stroke, v. 42, no. 5, p. 1445-1453.

Gidday, J. M., 2006, Cerebral preconditioning and ischaemic tolerance: Nat.Rev.Neurosci., v. 7, no. 6, p. 437-448.

Gifondorwa, D. J., M. B. Robinson, C. D. Hayes, A. R. Taylor, D. M. Prevette, R. W. Oppenheim, J. Caress, and C. E. Milligan, 2007, Exogenous delivery of heat shock protein 70 increases lifespan in a mouse model of amyotrophic lateral sclerosis: J.Neurosci., v. 27, no. 48, p. 13173-13180.

Götz, M., and W. B. Huttner, 2005, The cell biology of neurogenesis: Nat.Rev.Mol.Cell Biol., v. 6, no. 10, p. 777-788.

Grohm, J., N. Plesnila, and C. Culmsee, 2010, Bid mediates fission, membrane permeabilization and peri-nuclear accumulation of mitochondria as a prerequisite for oxidative neuronal cell death: Brain Behav.Immun., v. 24, no. 5, p. 831-838.

Guigas, B., N. Taleux, M. Foretz, D. Detaille, F. Andreelli, B. Viollet, and L. Hue, 2007, AMP-activated protein kinase-independent inhibition of hepatic mitochondrial oxidative phosphorylation by AICA riboside: Biochem.J., v. 404, no. 3, p. 499-507.

Guzhova, I., K. Kislyakova, O. Moskaliova, I. Fridlanskaya, M. Tytell, M. Cheetham, and B. Margulis, 2001, In vitro studies show that Hsp70 can be released by glia and that exogenous Hsp70 can enhance neuronal stress tolerance: Brain Res., v. 914, no. 1-2, p. 66-73.

Hashimoto, R., N. Takei, K. Shimazu, L. Christ, B. Lu, and D. M. Chuang, 2002, Lithium induces brain-derived neurotrophic factor and activates TrkB in rodent cortical neurons: an essential step for neuroprotection against glutamate excitotoxicity: Neuropharmacology, v. 43, no. 7, p. 1173-1179.

Hattori, F., and S. Oikawa, 2007, Peroxiredoxins in the central nervous system: Subcell.Biochem., v. 44, p. 357-374.

Hightower, L. E., and P. T. Guidon, Jr., 1989, Selective release from cultured mammalian cells of heat-shock (stress) proteins that resemble glia-axon transfer proteins: J.Cell Physiol, v. 138, no. 2, p. 257-266.

Hisatomi, T., T. Ishibashi, J. W. Miller, and G. Kroemer, 2009, Pharmacological inhibition of mitochondrial membrane permeabilization for neuroprotection: Exp.Neurol., v. 218, no. 2, p. 347-352.

Horie, H. et al., 1999, Galectin-1 regulates initial axonal growth in peripheral nerves after axotomy: J.Neurosci., v. 19, no. 22, p. 9964-9974.

Horie, N. et al., 2011, Transplanted stem cell-secreted vascular endothelial growth factor effects poststroke recovery, inflammation, and vascular repair: Stem Cells, v. 29, no. 2, p. 274-285.

Hristov, M., W. Erl, S. Linder, and P. C. Weber, 2004, Apoptotic bodies from endothelial cells enhance the number and initiate the differentiation of human endothelial progenitor cells in vitro: Blood, v. 104, no. 9, p. 2761-2766.

Hsieh, S. H., N. W. Ying, M. H. Wu, W. F. Chiang, C. L. Hsu, T. Y. Wong, Y. T. Jin, T. M. Hong, and Y. L. Chen, 2008, Galectin-1, a novel ligand of neuropilin-1, activates VEGFR-2 signaling and modulates the migration of vascular endothelial cells: Oncogene, v. 27, no. 26, p. 3746-3753.

Hu, X. et al., 2011, Peroxiredoxin-2 protects against 6-hydroxydopamine-induced dopaminergic neurodegeneration via attenuation of the apoptosis signal-regulating kinase (ASK1) signaling cascade: J.Neurosci., v. 31, no. 1, p. 247-261.

Hua, F., J. Ma, T. Ha, J. Kelley, D. L. Williams, R. L. Kao, J. H. Kalbfleisch, I. W. Browder, and C. Li, 2008, Preconditioning with a TLR2 specific ligand increases resistance to cerebral ischemia/reperfusion injury: J.Neuroimmunol., v. 199, no. 1-2, p. 75-82.

Huang, C., H. Cheng, S. Hao, H. Zhou, X. Zhang, J. Gao, Q. H. Sun, H. Hu, and C. C. Wang, 2006, Heat shock protein 70 inhibits alpha-synuclein fibril formation via interactions with diverse intermediates: J.Mol.Biol., v. 364, no. 3, p. 323-336.

Isele, N. B., H. S. Lee, S. Landshamer, A. Straube, C. S. Padovan, N. Plesnila, and C. Culmsee, 2007, Bone marrow stromal cells mediate protection through stimulation of PI3-K/Akt and MAPK signaling in neurons: Neurochem.Int., v. 50, no. 1, p. 243-250.

Iwashita, A., S. Yamazaki, K. Mihara, K. Hattori, H. Yamamoto, J. Ishida, N. Matsuoka, and S. Mutoh, 2004, Neuroprotective effects of a novel poly(ADP-ribose) polymerase-1 inhibitor, 2-[3-[4-(4-chlorophenyl)-1-piperazinyl] propyl]-4(3H)-quinazolinone (FR255595), in an in vitro

model of cell death and in mouse 1-methyl-4-phenyl-1,2,3,6-tetrahydropyridine model of Parkinson's disease: J.Pharmacol.Exp.Ther., v. 309, no. 3, p. 1067-1078.

Jackson, J. S., J. P. Golding, C. Chapon, W. A. Jones, and K. K. Bhakoo, 2010, Homing of stem cells to sites of inflammatory brain injury after intracerebral and intravenous administration: a longitudinal imaging study: Stem Cell Res.Ther., v. 1, no. 2, p. 17.

Jäderstad, J., H. Brismar, and E. Herlenius, 2010, Hypoxic preconditioning increases gap-junctional graft and host communication: Neuroreport, v. 21, no. 17, p. 1126-1132.

Janoff, A., 1964, Alterations in lysosomes (intracellular enzymes) during shock; effects of preconditioning (tolerance) and protective drugs: Int.Anesthesiol.Clin., v. 2, p. 251-269.

Joyce, N., G. Annett, L. Wirthlin, S. Olson, G. Bauer, and J. A. Nolta, 2010, Mesenchymal stem cells for the treatment of neurodegenerative disease: Regen.Med., v. 5, no. 6, p. 933-946.

Joza, N. et al., 2005, Muscle-specific loss of apoptosis-inducing factor leads to mitochondrial dysfunction, skeletal muscle atrophy, and dilated cardiomyopathy: Mol.Cell Biol., v. 25, no. 23, p. 10261-10272.

Joza, N. et al., 2001, Essential role of the mitochondrial apoptosis-inducing factor in programmed cell death: Nature, v. 410, no. 6828, p. 549-554.

Kakimura, J. et al., 2002, Microglial activation and amyloid-beta clearance induced by exogenous heat-shock proteins: FASEB J., v. 16, no. 6, p. 601-603.

Karray, A., A. Y. Ben, J. Boujelben, S. Amara, F. Carriere, Y. Gargouri, and S. Bezzine, 2012a, Drastic changes in the tissue-specific expression of secreted phospholipases A2 in chicken pulmonary disease: Biochimie, v. 94, no. 2, p. 451-460.

Karray, A., Y. Gargouri, R. Verger, and S. Bezzine, 2012b, Phospholipase A2 purification and characterization: a case study: Methods Mol.Biol., v. 861, p. 283-297.

Kerr, J. F., A. H. Wyllie, and A. R. Currie, 1972, Apoptosis: a basic biological phenomenon with wide-ranging implications in tissue kinetics: Br.J.Cancer, v. 26, no. 4, p. 239-257.

Kilic, E., U. Kilic, Y. Wang, C. L. Bassetti, H. H. Marti, and D. M. Hermann, 2006, The phosphatidylinositol-3 kinase/Akt pathway mediates VEGF's neuroprotective activity and induces blood brain barrier permeability after focal cerebral ischemia: FASEB J., v. 20, no. 8, p. 1185-1187.

Kim, S. U., and J. de Vellis, 2009, Stem cell-based cell therapy in neurological diseases: a review: J.Neurosci.Res., v. 87, no. 10, p. 2183-2200.

Kim, S. U. et al., 2008a, Peroxiredoxin I is an indicator of microglia activation and protects against hydrogen peroxide-mediated microglial death: Biol.Pharm.Bull., v. 31, no. 5, p. 820-825.

Kim, S. Y., T. J. Kim, and K. Y. Lee, 2008b, A novel function of peroxiredoxin 1 (Prx-1) in apoptosis signal-regulating kinase 1 (ASK1)-mediated signaling pathway: FEBS Lett., v. 582, no. 13, p. 1913-1918.

Kim, Y. J., J. Y. Ahn, P. Liang, C. Ip, Y. Zhang, and Y. M. Park, 2007, Human prx1 gene is a target of Nrf2 and is up-regulated by hypoxia/reoxygenation: implication to tumor biology: Cancer Res., v. 67, no. 2, p. 546-554.

Kim-Han, J. S., and L. L. Dugan, 2005, Mitochondrial uncoupling proteins in the central nervous system: Antioxid.Redox.Signal., v. 7, no. 9-10, p. 1173-1181.

Kirino, T., 2002, Ischemic tolerance: J.Cereb.Blood Flow Metab, v. 22, no. 11, p. 1283-1296.

Kis, B., K. Nagy, J. A. Snipes, N. C. Rajapakse, T. Horiguchi, G. J. Grover, and D. W. Busija, 2004, The mitochondrial K(ATP) channel opener BMS-191095 induces neuronal preconditioning: Neuroreport, v. 15, no. 2, p. 345-349.

Klein, J. A., C. M. Longo-Guess, M. P. Rossmann, K. L. Seburn, R. E. Hurd, W. N. Frankel, R. T. Bronson, and S. L. Ackerman, 2002, The harlequin mouse mutation downregulates apoptosis-inducing factor: Nature, v. 419, no. 6905, p. 367-374.

Klucken, J., Y. Shin, E. Masliah, B. T. Hyman, and P. J. McLean, 2004, Hsp70 Reduces alpha-Synuclein Aggregation and Toxicity: J.Biol.Chem., v. 279, no. 24, p. 25497-25502.

Koumura, A., Y. Nonaka, K. Hyakkoku, T. Oka, M. Shimazawa, I. Hozumi, T. Inuzuka, and H. Hara, 2008, A novel calpain inhibitor, ((1S)-1((((1S)-1-benzyl-3-cyclopropylamino-2,3-di-oxopropyl)amino)carbonyl)-3-met hylbutyl) carbamic acid 5-methoxy-3-oxapentyl ester, protects neuronal cells from cerebral ischemia-induced damage in mice: Neuroscience, v. 157, no. 2, p. 309-318.

Kuhn, H. G., J. Winkler, G. Kempermann, L. J. Thal, and F. H. Gage, 1997, Epidermal growth factor and fibroblast growth factor-2 have different effects on neural progenitors in the adult rat brain: J.Neurosci., v. 17, no. 15, p. 5820-5829.

Landshamer, S. et al., 2008, Bid-induced release of AIF from mitochondria causes immediate neuronal cell death: Cell Death.Differ., v. 15, no. 10, p. 1553-1563.

Lang, A. E., and A. M. Lozano, 1998a, Parkinson's disease. First of two parts: N.Engl.J.Med., v. 339, no. 15, p. 1044-1053.

Lang, A. E., and A. M. Lozano, 1998b, Parkinson's disease. Second of two parts: N.Engl.J.Med., v. 339, no. 16, p. 1130-1143.

Lee, J. S., J. M. Hong, G. J. Moon, P. H. Lee, Y. H. Ahn, and O. Y. Bang, 2010, A long-term follow-up study of intravenous autologous mesenchymal stem cell transplantation in patients with ischemic stroke: Stem Cells, v. 28, no. 6, p. 1099-1106.

Lekishvili, T., S. Hesketh, M. W. Brazier, and D. R. Brown, 2006, Mouse galectin-1 inhibits the toxicity of glutamate by modifying NR1 NMDA receptor expression: Eur.J.Neurosci., v. 24, no. 11, p. 3017-3025.

Li, F., Q. Huang, J. Chen, Y. Peng, D. R. Roop, J. S. Bedford, and C. Y. Li, 2010, Apoptotic cells activate the "phoenix rising" pathway to promote wound healing and tissue regeneration: Sci.Signal., v. 3, no. 110, p. ra13.

Li, Y., and M. Chopp, 2009, Marrow stromal cell transplantation in stroke and traumatic brain injury: Neurosci.Lett., v. 456, no. 3, p. 120-123.

Liebelt, B. et al., 2010, Exercise preconditioning reduces neuronal apoptosis in stroke by up-regulating heat shock protein-70 (heat shock protein-72) and extracellular-signal-regulated-kinase 1/2: Neuroscience, v. 166, no. 4, p. 1091-1100.

Lim, H. C. et al., 2008, Neuroprotective effect of neural stem cell-conditioned media in in vitro model of Huntington's disease: Neurosci.Lett., v. 435, no. 3, p. 175-180.

Lin, J. H. et al., 2008, A central role of connexin 43 in hypoxic preconditioning: J.Neurosci., v. 28, no. 3, p. 681-695.

Lin, M. T., and M. F. Beal, 2006, Mitochondrial dysfunction and oxidative stress in neurodegenerative diseases: Nature, v. 443, no. 7113, p. 787-795.

Lin, S. L., and S. Y. Ying, 2013, Mechanism and Method for Generating Tumor-Free iPS Cells Using Intronic MicroRNA miR-302 Induction: Methods Mol.Biol., v. 936, p. 295-312.

Lindvall, O., and Z. Kokaia, 2006, Stem cells for the treatment of neurological disorders: Nature, v. 441, no. 7097, p. 1094-1096.

Lindvall, O., and Z. Kokaia, 2011, Stem cell research in stroke: how far from the clinic?: Stroke, v. 42, no. 8, p. 2369-2375.

Lindvall, O., Z. Kokaia, and A. Martinez-Serrano, 2004, Stem cell therapy for human neurodegenerative disorders-how to make it work: Nat.Med., v. 10 Suppl, p. S42-S50.

Liu, J., P. Narasimhan, F. Yu, and P. H. Chan, 2005, Neuroprotection by hypoxic preconditioning involves oxidative stress-mediated expression of hypoxia-inducible factor and erythropoietin: Stroke, v. 36, no. 6, p. 1264-1269.

Liu, Y., D. A. Peterson, H. Kimura, and D. Schubert, 1997, Mechanism of cellular 3-(4,5-dimethylthiazol-2-yl)-2,5-diphenyltetrazolium bromide (MTT) reduction: J.Neurochem., v. 69, no. 2, p. 581-593.

Lledo, P. M., M. Alonso, and M. S. Grubb, 2006, Adult neurogenesis and functional plasticity in neuronal circuits: Nat.Rev.Neurosci., v. 7, no. 3, p. 179-193.

Lledo, P. M., and A. Saghatelyan, 2005, Integrating new neurons into the adult olfactory bulb: joining the network, life-death decisions, and the effects of sensory experience: Trends Neurosci., v. 28, no. 5, p. 248-254.

Mack, G. S., 2011, ReNeuron and StemCells get green light for neural stem cell trials: Nat.Biotechnol., v. 29, no. 2, p. 95-97.

Madhavan, L., V. Ourednik, and J. Ourednik, 2008, Neural stem/progenitor cells initiate the formation of cellular networks that provide neuroprotection by growth factor-modulated antioxidant expression: Stem Cells, v. 26, no. 1, p. 254-265.

Majno, G., and I. Joris, 1995, Apoptosis, oncosis, and necrosis. An overview of cell death: Am.J.Pathol., v. 146, no. 1, p. 3-15.

Marin, P., K. L. Nastiuk, N. Daniel, J. A. Girault, A. J. Czernik, J. Glowinski, A. C. Nairn, and J. Premont, 1997, Glutamate-dependent phosphorylation of elongation factor-2 and inhibition of protein synthesis in neurons: J.Neurosci., v. 17, no. 10, p. 3445-3454.

Markgraf, C. G., N. L. Velayo, M. P. Johnson, D. R. McCarty, S. Medhi, J. R. Koehl, P. A. Chmielewski, and M. D. Linnik, 1998, Six-hour window of opportunity for calpain inhibition in focal cerebral ischemia in rats: Stroke, v. 29, no. 1, p. 152-158.

Marshall, J., 1994, Clinical developments in cerebrovascular disease: J.Hist Neurosci., v. 3, no. 2, p. 115-118.

Masada, T., Y. Hua, G. Xi, S. R. Ennis, and R. F. Keep, 2001, Attenuation of ischemic brain edema and cerebrovascular injury after ischemic preconditioning in the rat: J.Cereb.Blood Flow Metab, v. 21, no. 1, p. 22-33.

Mattiasson, G. et al., 2003, Uncoupling protein-2 prevents neuronal death and diminishes brain dysfunction after stroke and brain trauma: Nat.Med., v. 9, no. 8, p. 1062-1068.

Mattson, M. P., 2000, Apoptosis in neurodegenerative disorders: Nat.Rev.Mol.Cell Biol., v. 1, no. 2, p. 120-129.

Meco, M., S. Cirri, C. Gallazzi, G. Magnani, and D. Cosseta, 2007, Desflurane preconditioning in coronary artery bypass graft surgery: a double-blinded, randomised and placebo-controlled study: Eur.J.Cardiothorac.Surg., v. 32, no. 2, p. 319-325.

Mehta, S. L., N. Manhas, and R. Raghubir, 2007, Molecular targets in cerebral ischemia for developing novel therapeutics: Brain Res.Rev., v. 54, no. 1, p. 34-66.

Menasche, P., 2005, Stem cells for clinical use in cardiovascular medicine: current limitations and future perspectives: Thromb.Haemost., v. 94, no. 4, p. 697-701.

Ming, G. L., and H. Song, 2011, Adult neurogenesis in the mammalian brain: significant answers and significant questions: Neuron, v. 70, no. 4, p. 687-702.

Mitrecic, D., C. Nicaise, L. Klimaschewski, S. Gajovic, D. Bohl, and R. Pochet, 2012, Genetically modified stem cells for the treatment of neurological diseases: Front Biosci.(Elite.Ed), v. 4, p. 1170-1181.

Modjtahedi, N., F. Giordanetto, and G. Kroemer, 2010, A human mitochondriopathy caused by AIF mutation: Cell Death.Differ., v. 17, no. 10, p. 1525-1528.

Montague, J. W., M. L. Gaido, C. Frye, and J. A. Cidlowski, 1994, A calcium-dependent nuclease from apoptotic rat thymocytes is homologous with cyclophilin. Recombinant cyclophilins A, B, and C have nuclease activity: J.Biol.Chem., v. 269, no. 29, p. 18877-18880.

Morimoto, B. H., and D. E. Koshland, Jr., 1990, Excitatory amino acid uptake and N-methyl-D-aspartate-mediated secretion in a neural cell line: Proc.Natl.Acad.Sci.U.S.A, v. 87, no. 9, p. 3518-3521.

Mu, Y., S. W. Lee, and F. H. Gage, 2010, Signaling in adult neurogenesis: Curr.Opin.Neurobiol., v. 20, no. 4, p. 416-423.

Murphy, T. H., M. Miyamoto, A. Sastre, R. L. Schnaar, and J. T. Coyle, 1989, Glutamate toxicity in a neuronal cell line involves inhibition of cystine transport leading to oxidative stress: Neuron, v. 2, no. 6, p. 1547-1558.

Nagy, K., B. Kis, N. C. Rajapakse, F. Bari, and D. W. Busija, 2004, Diazoxide preconditioning protects against neuronal cell death by attenuation of oxidative stress upon glutamate stimulation: J.Neurosci.Res., v. 76, no. 5, p. 697-704.

Nakaso, K., H. Yano, Y. Fukuhara, T. Takeshima, K. Wada-Isoe, and K. Nakashima, 2003, PI3K is a key molecule in the Nrf2-mediated regulation of antioxidative proteins by hemin in human neuroblastoma cells: FEBS Lett., v. 546, no. 2-3, p. 181-184.

Nasrabady, S. E., A. Kuzhandaivel, and A. Nistri, 2011, Studies of locomotor network neuroprotection by the selective poly(ADP-ribose) polymerase-1 inhibitor PJ-34 against excitotoxic injury to the rat spinal cord in vitro: Eur.J.Neurosci., v. 33, no. 12, p. 2216-2227.

Neumann, C. A. et al., 2003, Essential role for the peroxiredoxin Prdx1 in erythrocyte antioxidant defence and tumour suppression: Nature, v. 424, no. 6948, p. 561-565.

Noble, R. L., 1943, The development of resistance by rats and guinea pigs to amount of trauma usually fatal: Am.J.Physiol., v. 138, p. 346-356.

Onda, T., O. Honmou, K. Harada, K. Houkin, H. Hamada, and J. D. Kocsis, 2008, Therapeutic benefits by human mesenchymal stem cells (hMSCs) and Ang-1 gene-modified hMSCs after cerebral ischemia: J.Cereb.Blood Flow Metab, v. 28, no. 2, p. 329-340.

Oppenheim, R. W., 1991, Cell death during development of the nervous system: Annu.Rev.Neurosci., v. 14, p. 453-501.

Orozco, C., A. M. Garcia-de-Diego, E. Arias, J. M. Hernandez-Guijo, A. G. Garcia, M. Villarroya, and M. G. Lopez, 2006, Depolarization preconditioning produces cytoprotection against veratridine-induced chromaffin cell death: Eur.J.Pharmacol., v. 553, no. 1-3, p. 28-38.

Osato, K. et al., 2010, Apoptosis-inducing factor deficiency decreases the proliferation rate and protects the subventricular zone against ionizing radiation: Cell Death.Dis., v. 1, p. e84.

Otera, H., S. Ohsakaya, Z. Nagaura, N. Ishihara, and K. Mihara, 2005, Export of mitochondrial AIF in response to proapoptotic stimuli depends on processing at the intermembrane space: EMBO J., v. 24, no. 7, p. 1375-1386.

Öxler, E. M., A. Dolga, and C. Culmsee, 2012, AIF depletion provides neuroprotection through a preconditioning effect: Apoptosis..

Park, D. H., C. V. Borlongan, A. E. Willing, D. J. Eve, L. E. Cruz, C. D. Sanberg, Y. G. Chung, and P. R. Sanberg, 2009, Human umbilical cord blood cell grafts for brain ischemia: Cell Transplant., v. 18, no. 9, p. 985-998.

Parr, A. M., C. H. Tator, and A. Keating, 2007, Bone marrow-derived mesenchymal stromal cells for the repair of central nervous system injury: Bone Marrow Transplant., v. 40, no. 7, p. 609-619.

Pellettieri, J., P. Fitzgerald, S. Watanabe, J. Mancuso, D. R. Green, and A. A. Sanchez, 2010, Cell death and tissue remodeling in planarian regeneration: Dev.Biol., v. 338, no. 1, p. 76-85.

Petit, I., N. S. Kesner, R. Karry, O. Robicsek, E. Aberdam, F. J. Muller, D. Aberdam, and D. Ben-Shachar, 2012, Induced pluripotent stem cells from hair follicles as a cellular model for neurodevelopmental disorders: Stem Cell Res., v. 8, no. 1, p. 134-140.

Pignataro, G., R. Meller, K. Inoue, A. N. Ordonez, M. D. Ashley, Z. Xiong, R. Gala, and R. P. Simon, 2008, In vivo and in vitro characterization of a novel neuroprotective strategy for stroke: ischemic postconditioning: J.Cereb.Blood Flow Metab, v. 28, no. 2, p. 232-241.

Plaisant, F., A. Clippe, S. D. Vander, B. Knoops, and P. Gressens, 2003, Recombinant peroxiredoxin 5 protects against excitotoxic brain lesions in newborn mice: Free Radic.Biol.Med., v. 34, no. 7, p. 862-872.

Plesnila, N., C. Zhu, C. Culmsee, M. Groger, M. A. Moskowitz, and K. Blomgren, 2004, Nuclear translocation of apoptosis-inducing factor after focal cerebral ischemia: J.Cereb.Blood Flow Metab, v. 24, no. 4, p. 458-466.

Polazzi, E., and B. Monti, 2010, Microglia and neuroprotection: from in vitro studies to therapeutic applications: Prog.Neurobiol., v. 92, no. 3, p. 293-315.

Polster, B. M., G. Basanez, A. Etxebarria, J. M. Hardwick, and D. G. Nicholls, 2005, Calpain I induces cleavage and release of apoptosis-inducing factor from isolated mitochondria: J.Biol.Chem., v. 280, no. 8, p. 6447-6454.

Poser, S., S. Impey, Z. Xia, and D. R. Storm, 2003, Brain-derived neurotrophic factor protection of cortical neurons from serum withdrawal-induced apoptosis is inhibited by cAMP: J.Neurosci., v. 23, no. 11, p. 4420-4427.

Pospisilik, J. A. et al., 2007, Targeted deletion of AIF decreases mitochondrial oxidative phosphorylation and protects from obesity and diabetes: Cell, v. 131, no. 3, p. 476-491.

Prass, K., K. Ruscher, M. Karsch, N. Isaev, D. Megow, J. Priller, A. Scharff, U. Dirnagl, and A. Meisel, 2002, Desferrioxamine induces delayed tolerance against cerebral ischemia in vivo and in vitro: J.Cereb.Blood Flow Metab, v. 22, no. 5, p. 520-525.

Prockop, D. J., 2012, Mitochondria to the rescue: Nat.Med., v. 18, no. 5, p. 653-654.

Puche, A. C., and B. Key, 1995, Identification of cells expressing galectin-1, a galactose-binding receptor, in the rat olfactory system: J.Comp Neurol., v. 357, no. 4, p. 513-523.

Qu, W. S., Y. H. Wang, J. P. Wang, Y. X. Tang, Q. Zhang, D. S. Tian, Z. Y. Yu, M. J. Xie, and W. Wang, 2010, Galectin-1 enhances astrocytic BDNF production and improves functional outcome in rats following ischemia: Neurochem.Res., v. 35, no. 11, p. 1716-1724.

Ratajczak, M. Z., 2005, Cancer stem cells--normal stem cells "Jedi" that went over to the "dark side": Folia Histochem.Cytobiol., v. 43, no. 4, p. 175-181.

Ravati, A., B. Ahlemeyer, A. Becker, S. Klumpp, and J. Krieglstein, 2001, Preconditioning-induced neuroprotection is mediated by reactive oxygen species and activation of the transcription factor nuclear factor-kappaB: J.Neurochem., v. 78, no. 4, p. 909-919.

Ravati, A., B. Ahlemeyer, A. Becker, and J. Krieglstein, 2000, Preconditioning-induced neuroprotection is mediated by reactive oxygen species: Brain Res., v. 866, no. 1-2, p. 23-32.

Ray, J., and F. H. Gage, 2006, Differential properties of adult rat and mouse brain-derived neural stem/progenitor cells: Mol.Cell Neurosci., v. 31, no. 3, p. 560-573.

Riepe, M. W., F. Esclaire, K. Kasischke, S. Schreiber, H. Nakase, O. Kempski, A. C. Ludolph, U. Dirnagl, and J. Hugon, 1997a, Increased hypoxic tolerance by chemical inhibition of oxidative phosphorylation: "chemical preconditioning": J.Cereb.Blood Flow Metab, v. 17, no. 3, p. 257-264.

Riepe, M. W., K. Kasischke, and A. Raupach, 1997b, Acetylsalicylic acid increases tolerance against hypoxic and chemical hypoxia: Stroke, v. 28, no. 10, p. 2006-2011.

Robinson, M. B., J. L. Tidwell, T. Gould, A. R. Taylor, J. M. Newbern, J. Graves, M. Tytell, and C. E. Milligan, 2005, Extracellular heat shock protein 70: a critical component for motoneuron survival: J.Neurosci., v. 25, no. 42, p. 9735-9745.

Romi, F., G. Helgeland, and N. E. Gilhus, 2011, Heat-shock proteins in clinical neurology: Eur.Neurol., v. 66, no. 2, p. 65-69.

Ronnett, G. V., S. Ramamurthy, A. M. Kleman, L. E. Landree, and S. Aja, 2009, AMPK in the brain: its roles in energy balance and neuroprotection: J.Neurochem., v. 109 Suppl 1, p. 17-23.

Sack, M. N., 2006, Mitochondrial depolarization and the role of uncoupling proteins in ischemia tolerance: Cardiovasc.Res., v. 72, no. 2, p. 210-219.

Sagara, Y., R. Dargusch, D. Chambers, J. Davis, D. Schubert, and P. Maher, 1998, Cellular mechanisms of resistance to chronic oxidative stress: Free Radic.Biol.Med., v. 24, no. 9, p. 1375-1389.

Sakaguchi, M. et al., 2010, Regulation of adult neural progenitor cells by Galectin-1/beta1 Integrin interaction: J.Neurochem., v. 113, no. 6, p. 1516-1524.

Sakaguchi, M. et al., 2006, A carbohydrate-binding protein, Galectin-1, promotes proliferation of adult neural stem cells: Proc.Natl.Acad.Sci.U.S.A, v. 103, no. 18, p. 7112-7117.

Sasikumar, A. N., W. B. Perez, and T. G. Kinzy, 2012, The many roles of the eukaryotic elongation factor 1 complex: Wiley.Interdiscip.Rev.RNA., v. 3, no. 4, p. 543-555.

Schägger, H., 2001, Respiratory chain supercomplexes: IUBMB.Life, v. 52, no. 3-5, p. 119-128.

Scheibe, F., O. Klein, J. Klose, and J. Priller, 2012, Mesenchymal stromal cells rescue cortical neurons from apoptotic cell death in an in vitro model of cerebral ischemia: Cell Mol.Neurobiol., v. 32, no. 4, p. 567-576.

Sedlic, F., A. Sepac, D. Pravdic, A. K. Camara, M. Bienengraeber, A. K. Brzezinska, T. Wakatsuki, and Z. J. Bosnjak, 2010, Mitochondrial depolarization underlies delay in permeability transition by preconditioning with isoflurane: roles of ROS and Ca2+: Am.J.Physiol Cell Physiol, v. 299, no. 2, p. C506-C515.

Seo, M. S., S. W. Kang, K. Kim, I. C. Baines, T. H. Lee, and S. G. Rhee, 2000, Identification of a new type of mammalian peroxiredoxin that forms an intramolecular disulfide as a reaction intermediate: J.Biol.Chem., v. 275, no. 27, p. 20346-20354.

Shen, L. H., Y. Li, J. Chen, Y. Cui, C. Zhang, A. Kapke, M. Lu, S. Savant-Bhonsale, and M. Chopp, 2007, One-year follow-up after bone marrow stromal cell treatment in middle-aged female rats with stroke: Stroke, v. 38, no. 7, p. 2150-2156.

Shichita, T. et al., 2012, Peroxiredoxin family proteins are key initiators of post-ischemic inflammation in the brain: Nat.Med..

Silva, G. V. et al., 2005, Mesenchymal stem cells differentiate into an endothelial phenotype, enhance vascular density, and improve heart function in a canine chronic ischemia model: Circulation, v. 111, no. 2, p. 150-156.

Simerabet, M., E. Robin, I. Aristi, S. Adamczyk, B. Tavernier, B. Vallet, R. Bordet, and G. Lebuffe, 2008, Preconditioning by an in situ administration of hydrogen peroxide: involvement of reactive oxygen species and mitochondrial ATP-dependent potassium channel in a cerebral ischemia-reperfusion model: Brain Res., v. 1240, p. 177-184.

Slemmer, J. E. et al., 2008, Causal role of apoptosis-inducing factor for neuronal cell death following traumatic brain injury: Am.J.Pathol., v. 173, no. 6, p. 1795-1805.

Smith-Pearson, P. S., M. Kooshki, D. R. Spitz, L. B. Poole, W. Zhao, and M. E. Robbins, 2008, Decreasing peroxiredoxin II expression decreases glutathione, alters cell cycle distribution, and sensitizes glioma cells to ionizing radiation and H(2)O(2): Free Radic.Biol.Med., v. 45, no. 8, p. 1178-1189.

Staat, P. et al., 2005, Postconditioning the human heart: Circulation, v. 112, no. 14, p. 2143-2148.

Starossom, S. C. et al., 2012, Galectin-1 deactivates classically activated microglia and protects from inflammation-induced neurodegeneration: Immunity., v. 37, no. 2, p. 249-263.

Sun, K. H., P. Y. de, F. Vincent, and K. Shah, 2008, Deregulated Cdk5 promotes oxidative stress and mitochondrial dysfunction: J.Neurochem., v. 107, no. 1, p. 265-278.

Susin, S. A. et al., 1999, Molecular characterization of mitochondrial apoptosis-inducing factor: Nature, v. 397, no. 6718, p. 441-446.

Susin, S. A., N. Zamzami, M. Castedo, T. Hirsch, P. Marchetti, A. Macho, E. Daugas, M. Geuskens, and G. Kroemer, 1996, Bcl-2 inhibits the mitochondrial release of an apoptogenic protease: J.Exp.Med., v. 184, no. 4, p. 1331-1341.

Sutton, M. A., A. M. Taylor, H. T. Ito, A. Pham, and E. M. Schuman, 2007, Postsynaptic decoding of neural activity: eEF2 as a biochemical sensor coupling miniature synaptic transmission to local protein synthesis: Neuron, v. 55, no. 4, p. 648-661.

Takahashi, K., and S. Yamanaka, 2006, Induction of pluripotent stem cells from mouse embryonic and adult fibroblast cultures by defined factors: Cell, v. 126, no. 4, p. 663-676.

Tan, S., Y. Sagara, Y. Liu, P. Maher, and D. Schubert, 1998, The regulation of reactive oxygen species production during programmed cell death: J.Cell Biol., v. 141, no. 6, p. 1423-1432.

Tan, S., D. Schubert, and P. Maher, 2001, Oxytosis: A novel form of programmed cell death: Curr.Top.Med.Chem., v. 1, no. 6, p. 497-506.

Tang, X. Q., J. Q. Feng, J. Chen, P. X. Chen, J. L. Zhi, Y. Cui, R. X. Guo, and H. M. Yu, 2005, Protection of oxidative preconditioning against apoptosis induced by H2O2 in PC12 cells: mechanisms via MMP, ROS, and Bcl-2: Brain Res., v. 1057, no. 1-2, p. 57-64.

Temple, S., 2001a, Stem cell plasticity--building the brain of our dreams: Nat.Rev.Neurosci., v. 2, no. 7, p. 513-520.

Temple, S., 2001b, The development of neural stem cells: Nature, v. 414, no. 6859, p. 112-117.

Thomas, K. R., and M. R. Capecchi, 1987, Site-directed mutagenesis by gene targeting in mouse embryo-derived stem cells: Cell, v. 51, no. 3, p. 503-512.

Tobaben, S., J. Grohm, A. Seiler, M. Conrad, N. Plesnila, and C. Culmsee, 2011, Bid-mediated mitochondrial damage is a key mechanism in glutamate-induced oxidative stress and AIF-dependent cell death in immortalized HT-22 hippocampal neurons: Cell Death.Differ., v. 18, no. 2, p. 282-292.

Tretter, L., I. Sipos, and V. dam-Vizi, 2004, Initiation of neuronal damage by complex I deficiency and oxidative stress in Parkinson's disease: Neurochem.Res., v. 29, no. 3, p. 569-577.

Tulsawani, R., L. S. Kelly, N. Fatma, B. Chhunchha, E. Kubo, A. Kumar, and D. P. Singh, 2010, Neuroprotective effect of peroxiredoxin 6 against hypoxia-induced retinal ganglion cell damage: BMC.Neurosci., v. 11, p. 125.

Tytell, M., S. G. Greenberg, and R. J. Lasek, 1986, Heat shock-like protein is transferred from glia to axon: Brain Res., v. 363, no. 1, p. 161-164.

Uzun, G., D. Subhani, and S. Amor, 2010, Trophic factors and stem cells for promoting recovery in stroke: J.Vasc.Interv.Neurol., v. 3, no. 1, p. 3-12.

Vahsen, N. et al., 2004, AIF deficiency compromises oxidative phosphorylation: EMBO J., v. 23, no. 23, p. 4679-4689.

Vaux, D. L., and S. J. Korsmeyer, 1999, Cell death in development: Cell, v. 96, no. 2, p. 245-254.

Vendrame, M., J. Cassady, J. Newcomb, T. Butler, K. R. Pennypacker, T. Zigova, C. D. Sanberg, P. R. Sanberg, and A. E. Willing, 2004, Infusion of human umbilical cord blood cells in a rat model of stroke dose-dependently rescues behavioral deficits and reduces infarct volume: Stroke, v. 35, no. 10, p. 2390-2395.

Vendrame, M., C. Gemma, K. R. Pennypacker, P. C. Bickford, S. C. Davis, P. R. Sanberg, and A. E. Willing, 2006, Cord blood rescues stroke-induced changes in splenocyte phenotype and function: Exp.Neurol., v. 199, no. 1, p. 191-200.

Venna, V. R., J. Li, S. E. Benashski, S. Tarabishy, and L. D. McCullough, 2012, Preconditioning induces sustained neuroprotection by downregulation of adenosine 5'-monophosphate-activated protein kinase: Neuroscience, v. 201, p. 280-287.

Verpelli, C., G. Piccoli, A. Zanchi, F. Gardoni, K. Huang, D. Brambilla, L. M. Di, E. Battaglioli, and C. Sala, 2010, Synaptic activity controls dendritic spine morphology by modulating eEF2-dependent BDNF synthesis: J.Neurosci., v. 30, no. 17, p. 5830-5842.

Walker, J. M., 1994, The bicinchoninic acid (BCA) assay for protein quantitation: Methods Mol.Biol., v. 32, p. 5-8.

Walker, P. A., P. A. Letourneau, S. Bedi, S. K. Shah, F. Jimenez, and C. S. Jr, 2011, Progenitor cells as remote "bioreactors": neuroprotection via modulation of the systemic inflammatory response: World J.Stem Cells, v. 3, no. 2, p. 9-18.

Wallace, D. C., 2005, A mitochondrial paradigm of metabolic and degenerative diseases, aging, and cancer: a dawn for evolutionary medicine: Annu.Rev.Genet., v. 39, p. 359-407.

Wang, W. X., B. W. Rajeev, A. J. Stromberg, N. Ren, G. Tang, Q. Huang, I. Rigoutsos, and P. T. Nelson, 2008, The expression of microRNA miR-107 decreases early in Alzheimer's disease and may accelerate disease progression through regulation of beta-site amyloid precursor protein-cleaving enzyme 1: J.Neurosci., v. 28, no. 5, p. 1213-1223.

Wang, Y., V. L. Dawson, and T. M. Dawson, 2009, Poly(ADP-ribose) signals to mitochondrial AIF: a key event in parthanatos: Exp.Neurol., v. 218, no. 2, p. 193-202.

Wang, Y., D. L. Huso, J. Harrington, J. Kellner, D. K. Jeong, J. Turney, and I. K. McNiece, 2005, Outgrowth of a transformed cell population derived from normal human BM mesenchymal stem cell culture: Cytotherapy., v. 7, no. 6, p. 509-519.

Wang, Y., C. G. Kelly, M. Singh, E. G. McGowan, A. S. Carrara, L. A. Bergmeier, and T. Lehner, 2002, Stimulation of Th1-polarizing cytokines, C-C chemokines, maturation of dendritic cells, and adjuvant function by the peptide binding fragment of heat shock protein 70: J.Immunol., v. 169, no. 5, p. 2422-2429.

Wang, Y., N. S. Kim, J. F. Haince, H. C. Kang, K. K. David, S. A. Andrabi, G. G. Poirier, V. L. Dawson, and T. M. Dawson, 2011, Poly(ADP-ribose) (PAR) binding to apoptosis-inducing factor is critical for PAR polymerase-1-dependent cell death (parthanatos): Sci.Signal., v. 4, no. 167, p. ra20.

Weisova, P., D. Davila, L. P. Tuffy, M. W. Ward, C. G. Concannon, and J. H. Prehn, 2011, Role of 5'-adenosine monophosphate-activated protein kinase in cell survival and death responses in neurons: Antioxid.Redox.Signal., v. 14, no. 10, p. 1863-1876.

Wiegand, F. et al., 1999, Respiratory chain inhibition induces tolerance to focal cerebral ischemia: J.Cereb.Blood Flow Metab, v. 19, no. 11, p. 1229-1237.

Williams, R. L. et al., 1988, Myeloid leukaemia inhibitory factor maintains the developmental potential of embryonic stem cells: Nature, v. 336, no. 6200, p. 684-687.

Wood, Z. A., E. Schroder, H. J. Robin, and L. B. Poole, 2003, Structure, mechanism and regulation of peroxiredoxins: Trends Biochem.Sci., v. 28, no. 1, p. 32-40.

Xie, Z., J. Zhang, J. Wu, B. Viollet, and M. H. Zou, 2008, Upregulation of mitochondrial uncoupling protein-2 by the AMP-activated protein kinase in endothelial cells attenuates oxidative stress in diabetes: Diabetes, v. 57, no. 12, p. 3222-3230.

Xu, J., 2005, Preparation, culture, and immortalization of mouse embryonic fibroblasts: Curr.Protoc.Mol.Biol., v. Chapter 28, p. Unit.

Yakovlev, A. G., and A. I. Faden, 2004, Mechanisms of neural cell death: implications for development of neuroprotective treatment strategies: NeuroRx., v. 1, no. 1, p. 5-16.

Yamane, J. et al., 2010, Transplantation of galectin-1-expressing human neural stem cells into the injured spinal cord of adult common marmosets: J.Neurosci.Res., v. 88, no. 7, p. 1394-1405.

Yang, D. et al., 2011, Deletion of peroxiredoxin 6 potentiates lipopolysaccharide-induced acute lung injury in mice: Crit Care Med., v. 39, no. 4, p. 756-764.

Yang, H. Y. et al., 2008a, Gene expression profiling related to the enhanced erythropoiesis in mouse bone marrow cells: J.Cell Biochem., v. 104, no. 1, p. 295-303.

Yang, R. Y., G. A. Rabinovich, and F. T. Liu, 2008b, Galectins: structure, function and therapeutic potential: Expert.Rev.Mol.Med., v. 10, p. e17.

Ye, H. et al., 2002, DNA binding is required for the apoptogenic action of apoptosis inducing factor: Nat.Struct.Biol., v. 9, no. 9, p. 680-684.

Yu, S. W., H. Wang, M. F. Poitras, C. Coombs, W. J. Bowers, H. J. Federoff, G. G. Poirier, T. M. Dawson, and V. L. Dawson, 2002, Mediation of poly(ADP-ribose) polymerase-1-dependent cell death by apoptosis-inducing factor: Science, v. 297, no. 5579, p. 259-263.

Yu, S. W., Y. Wang, D. S. Frydenlund, O. P. Ottersen, V. L. Dawson, and T. M. Dawson, 2009, Outer mitochondrial membrane localization of apoptosis-inducing factor: mechanistic implications for release: ASN.Neuro., v. 1, no. 5.

Yuan, J., M. Lipinski, and A. Degterev, 2003, Diversity in the mechanisms of neuronal cell death: Neuron, v. 40, no. 2, p. 401-413.

Zernecke, A. et al., 2009, Delivery of microRNA-126 by apoptotic bodies induces CXCL12-dependent vascular protection: Sci.Signal., v. 2, no. 100, p. ra81.

Zhang, D. X., and D. D. Gutterman, 2007, Mitochondrial reactive oxygen species-mediated signaling in endothelial cells: Am.J.Physiol Heart Circ.Physiol, v. 292, no. 5, p. H2023-H2031.

Zhang, L., Y. Li, C. Zhang, M. Chopp, A. Gosiewska, and K. Hong, 2011, Delayed administration of human umbilical tissue-derived cells improved neurological functional recovery in a rodent model of focal ischemia: Stroke, v. 42, no. 5, p. 1437-1444.

Zhao, C., W. Deng, and F. H. Gage, 2008, Mechanisms and functional implications of adult neurogenesis: Cell, v. 132, no. 4, p. 645-660.

Zhao, Q., B. Lu, S. K. George, J. J. Yoo, and A. Atala, 2012, Safeguarding pluripotent stem cells for cell therapy with a non-viral, non-integrating episomal suicide construct: Biomaterials, v. 33, no. 29, p. 7261-7271.

Zhou, G. et al., 2001, Role of AMP-activated protein kinase in mechanism of metformin action: J.Clin.Invest., v. 108, p. 346-356.

Zhu, C., L. Qiu, X. Wang, U. Hallin, C. Cande, G. Kroemer, H. Hagberg, and K. Blomgren, 2003, Involvement of apoptosis-inducing factor in neuronal death after hypoxia-ischemia in the neonatal rat brain: J.Neurochem., v. 86, no. 2, p. 306-317.

Zhu, C. et al., 2007, Apoptosis-inducing factor is a major contributor to neuronal loss induced by neonatal cerebral hypoxia-ischemia: Cell Death.Differ., v. 14, no. 4, p. 775-784.

Zhu, J. M., Y. Y. Zhao, S. D. Chen, W. H. Zhang, L. Lou, and X. Jin, 2011, Functional recovery after transplantation of neural stem cells modified by brain-derived neurotrophic factor in rats with cerebral ischaemia: J.Int.Med.Res., v. 39, no. 2, p. 488-498.

Zong, W. X., and C. B. Thompson, 2006, Necrotic death as a cell fate: Genes Dev., v. 20, no. 1, p. 1-15.

10. Publications

10.1. Original papers

Öxler E.M., Dolga A. and Culmsee C. 2012. AIF depletion provides neuroprotection through a preconditioning effect. Apoptosis.

Diemert S., Dolga A.M., Tobaben S., Grohm J., Pfeifer S., **Oexler E.M.** and Culmsee C . 2012. Impedance measurement for real time detection of neuronal cell death. J Neurosci Methods 203: 69-77.

10.2. Poster presentations

Öxler E.M., Culmsee C. Neuroprotection mediated by AIF-deficiency - a preconditioning effect? DGPT Jahrestagung, 19.03.2012-22.03.2012, Dresden, Germany.

Oexler E.M., Dolga A.M., Culmsee C. AIF depletion provides neuroprotection through a preconditioning effect. Society for Neuroscience Annual Meeting, Neuroscience 2012, New Orleans, USA, 13.10.2012-17.10.2012.

Culmsee C., Pfeifer S., Dolga A.M., Blomgren K., **Öxler E.M.** Life from death: Apoptotic neural progenitor cells protect neurons against growth factor withdrawal and glutamate toxicity. Society for Neuroscience Annual Meeting, Neuroscience 2012, New Orleans, USA, 13.10.2012-17.10.2012.

Öxler E.M., Pfeifer S., Dolga A.M., Blomgren K., Culmsee C. “Phoenix rising”: The potential of apoptotic neural progenitor cells to provide neuroprotection. Fraunhofer Life Science Symposium, 29.11.2012-30.11.2012, Leipzig, Germany.

10.3. Patent

Patent No. 12166390.0 - 2107, Culmsee C. Blomgren K., Pfeifer S., **Öxler E.M.**, Sato Y., Zhu C., Stem cell derived composition for the treatment of acute injury and degenerative diseases, date of filing 02.05.2012.

11. Acknowledgements

First of all I would like to thank my supervisor Prof. Dr. Carsten Culmsee for giving me the opportunity to work as a PhD student in his lab where I had a great, unforgettable, and exciting time. He always had time for discussions and always guided me in the right direction just in the right time. Additionally, I greatly appreciate the chance he gave me to attend national and international meetings, and especially attending the workshop in Kyoto, which were unforgettable events that gained me insight into the current state of research combined with the great experience of socio-cultural circumstances. Thank you very much for this!

I would also like to thank all my colleagues, especially Amalia for her great support in paper preparation and submission and her constructive discussions. Thank you Sina for all the talks especially, on tough days and the help with the Äkta. Further, I would like to thank Svenja, Sebastian, and Julia for their patients and introduction into the lab work and the great events we had together. Thank also goes to Steffi, Anderson, Christina, Markus, and Sandra for the good time we had together inside and outside of the lab. Thank you Steffi and Markus for proof reading of my thesis. Further, I would like to thank the whole AG Culmsee for the good atmosphere in the lab. Special thank goes to Renate and Sandra, who introduced me into cell culture work, as well as to Katharina who always had a helping hand, whenever needed!

Thank you Emma for all the proof readings of manuscripts and all the support on bureaucratic affairs you managed together with Niki for me. Thank you both!

I also want to thank Jörg who had great ideas on the NPC project and who contributed a lot to its success!

I would also like to mention Prof. Dr. Klas Blomgren, who supported my NPC project and invited me to Sweden.

I also want to thank all the friends of mine that always supported me outside of the lab and got my minds to other thinks.

Great thanks go to my mother who always believed in me and supported me wherever possible. I also want to thank my brother for the great time we had together in Marburg. Without my family’s support I would never have been able to complete this thesis.

Finally, I thank Tobias who always was my rock in breaking waves. Thank you very much for all your daily support, for always finding the right words and for your appreciation for my work.

12. Curriculum vitae

Personal details

Date of birth: 02.11.1983

Place of birth: Donauwörth

Education and career

01/2010 – today	PhD thesis at the department of Pharmacology and Clinical Pharmacy, Philipps University of Marburg supervisor: Prof. Dr. Carsten Culmsee
12/2008-12/2009	Branch manager at Augusta Apotheke, Rain
12/2008	License as a pharmacist
05/2008-10/2008	Internship at Apotheke der Barmherzigen Brüder, Neuburg a.d. Donau
11/2007-04/2008	Internship at Merck KGaA, Darmstadt
08/2006-09/2006 11/2005-12/2005	Graduate assistance at the department of Pharmacology Toxicology, Univerity of Regensburg supervisor: Prof. Dr. Roland Seifert
10/2003-09/2007	Study of Pharmacy, University of Regensburg
08/1994-06/2003	Secondary school, Gymnasium Donauwörth
08/1990-07/1994	Elementary school, Johannes-Bayer-Volksschule, Rain